Proteomics reveal insights into TRPV1 function

Inaugural-Dissertation to obtain the academic degree
Doctor rerum naturalium (Dr. rer. Nat.)

Submitted to the Department of Biology, Chemistry and Pharmacy
of Freie Universität Berlin

by

Christina Hanack

December, 2013

This work was carried out in the period of July 2009 to December 2013 under the supervision of Prof. Jan Siemens at the Max-Delbrück Center for Molecular Medicine (MDC) in Berlin-Buch.

Date of PhD Defense: April 4, 2014

1st Reviewer: Prof. Dr. Constance Scharff
2nd Reviewer: Prof. Dr. Gary Lewin

Summary

Transient receptor potential (TRP) ion channels are important components of the somatosensory system, where they are involved in the detection of pain and temperature stimuli. Particularly, the capsaicin receptor TRPV1 plays a crucial role in the perception, transduction and modulation of thermal and inflammatory stimuli. By analogy to the first identified member of the TRP ion channel family in *Drosophila,* there is emerging evidence that mammalian TRP channels do not function as individual entities but rather depend on additional proteins that are necessary for their specific regulation and modulation.

Thus far, protein networks involving TRPV1 have not been sufficiently characterized. Therefore, this PhD work established a genetic and biochemical strategy to isolate TRPV1 protein complexes from transgenic mice expressing a tagged version of the receptor. Using high-resolution mass spectrometry, this work identified two putative interaction partners of TRPV1: the $GABA_B$ receptor from affinity purifications of the DRG and Vglut2 from sciatic nerve purifications.

TRPV1 showed overlapping distribution with both proteins in DRG neurons and the superficial layers of the dorsal horn of the spinal cord. A physical interaction was demonstrated by co-immunoprecipitation studies in sensory tissue preparations and heterologous cell systems.

Functionally, $GABA_B$ receptor activation was found to modulate TRPV1 sensitization *in vitro* and *in vivo* without affecting TRPV1 activity acutely. The specific $GABA_B$ agonist baclofen, reduced NGF-, bradykinin- and serotonin-induced sensitization of TRPV1 in cultured DRG neurons and at the level of the whole animal. In behavioral tests, thermal hyperalgesia was significantly decreased in mice co-injected with baclofen. This observation was absent in TRPV1 knockout animals. Thus, these data suggest that $GABA_B$ activation may result in modulation of the PLC/PKC signaling pathway, which is the common downstream signaling pathway of the three inflammatory substances tested. Interestingly, baclofen had no effect on prostaglandin-evoked thermal hyperalgesia, which is mainly mediated by activation of the cAMP/PKA pathway. In conclusion, the results highlight the contribution of $GABA_B$ receptors to peripheral analgesia and may provide a novel strategy to

interfere with TRPV1 sensitization during inflammatory pain. The detailed mechanism underlying the observed effect has to still be elucidated.

Mass spectrometry analysis also identified Vglut2 as a candidate protein. Analysis of the interaction between TRPV1 and Vglut2 demonstrated that a fraction of TRPV1 might be present on a Vglut2-containing vesicular pool as shown by subcellular fractionation of the spinal cord and immunoisolations of Vglut2 - and TRPV1-containing synaptic vesicles. The question of whether TRPV1 plays a role in loading vesicles with glutamate was addressed but did not provide conclusive results. Thus, there remain unsolved questions about the presence and function of TRPV1 channels in synaptic vesicles. Further work is needed to understand its functional association with Vglut2 and putative contribution to glutamatergic synaptic transmission.

Zusammenfassung

Rezeptoren der TRP (Transient Receptor Potential) Familie von Ionenkanälen spielen eine zentrale Rolle bei der Reizwahrnehmung und Reizweiterleitung im somatosensorischen Nervensystem. Insbesondere das Familienmitglied TRPV1 nimmt eine bedeutende Funktion in der Schmerz- und Temperaturwahrnehmung ein. Analog zu den TRP Kanälen in der Phototransduktionskaskade von *Drosophila* geht man davon aus, dass TRP Kanalproteine bei Säugern Komponenten eines Multiprotein-Komplexes sind, die nur innerhalb diesem spezifisch und effizient funktionieren. Proteine, die mit TRPV1 spezifisch in einem Komplex assoziiert sind, sind noch nicht ausreichend charakterisiert worden. Ziel der Doktorarbeit war daher die Isolierung und Untersuchung von TRPV1 Proteinkomplexen in Mäusen, um die Funktionsweise des Rezeptors besser zu verstehen. Dazu wurde eine Proteomik-Methode entwickelt, die ermöglichte, den Rezeptor aus nativem sensorischen Gewebe transgener Mäuse zu isolieren. Durch massenspektrometrische Analyse von TRPV1-Aufreinigungen aus den DRG und dem Ischias-Nerv konnten spezifisch und signifikant angereicherte Proteine identifiziert werden. Zwei Proteine, $GABA_{B1a}$ und Vglut2, wurden ausgewählt, um ihre Bedeutung für die Funktionsweise von TRPV1 mittels Expressions- und biochemischen Analysen sowie funktionellen Studien zu verdeutlichen.

TRPV1 kolokalisierte mit dem $GABA_B$ Rezeptor in DRG Neuronen und in den Laminae I und II im dorsalen Rückenmark. Eine physische Interaktion wurde durch Ko-Immunopräzipitation in DRG Neuronen sowie heterologen Zell Expressionssystemen gezeigt. Auf funktioneller Ebene reduzierte der spezifische $GABA_B$ Agonist, Baclofen, die Sensitivierung von TRPV1 nach Applikation inflammatorischer Substanzen wie NGF, Bradykinin und Serotonin *in vitro* und *in vivo,* während Baclofen keinen Effekt auf akute Aktivierung von TRPV1 hatte. In Verhaltensexperimenten verminderte Baclofen die Entstehung von NGF-, Bradykinin- und Serotonin-induzierter thermaler Hypersensibilität. Diese Ergebnisse zeigen, dass $GABA_B$ Aktivierung möglicherweise die PLC/PKC-Signalkaskade moduliert, welche den drei inflammatorischen Substanzen zugrunde liegt, und damit die Sensitivierung von TRPV1 inhibiert.

Interessanterweise konnte der schmerzlindernde Effekt nicht nach Prostaglandin-induzierter thermaler Hyperalgesie beobachtet werden, welche auf Aktivierung des cAMP/PKA-Signalwegs basiert. In Folgeexperimenten muss noch untersucht werden, welcher Mechanismus der Inhibition der TRPV1 Sensitivierung durch Baclofen zugrunde liegt. Zusammenfassend unterstreichen die Ergebnisse die Funktion von $GABA_B$ Rezeptoren im peripheren Nervensystem und heben zusätzlich $GABA_B$ Rezeptoren als potentielle Kandidaten für die Schmerztherapie hervor.

Die massenspektrometrische Analyse von TRPV1-Aufreinigungen aus dem Ischias-Nerv identifizierte Vglut2 als potentiellen Interaktionspartner. Die Charakterisierung der Assoziation von TRPV1 und Vglut2 zeigte, dass beide Proteine in DRG Neuronen, im dorsalen Rückenmark sowie in transfizierten F11 Zellen kolokalisieren. Des Weiteren wurde mittels subzellulärer Fraktionierung des Rückenmarks und Immunoisolationen ersichtlich, dass eine Subpopulation von TRPV1 Molekülen in Vglut2 positiven synaptischen Vesikeln enthalten ist. Die Funktion des Rezeptors auf diesen Vesikeln wurde durch Glutamat-Uptake-Experimente versucht zu erörtern, führte jedoch zu keinem Ergebnis. Somit bleibt die Frage nach einer Funktion offen. Zukünftige Experimente müssen zeigen, ob und wie TRPV1 und Vglut2 funktionell assoziiert sind und welche Rolle TRPV1 in der glutamatergen synaptischen Transmission einnimmt.

Abbreviations

AC	Adenylylcyclase
AKAP	A kinase anchoring protein
AMPA	α-amino-3-hydroxy-5-methyl-4-isoxazolepropionic acid
ANOVA	Analysis if variance
ATP	Adenosine triphosphate
BAC	Bacterial artificial chromosome
BK-2	Bradykinin receptor 2
BSA	Bovine serum albumin
CaMKII	Calcium calmodulin-dependent protein kinase II
cAMP	Cyclic adenosine monophosphate
Cap	Capsaicin
CCI	Chronic constriction injury
cDNA	Complementary DNA
CFA	Complete Freund´s Adjuvant
CGRP	Calcitonin gene-related peptide
CNS	Central nervous system
Co-IP	Co-immunoprecipitation
Ctrl	Control
DAG	Diacylglycerol
DMEM	Dulbecco's modified Eagle's medium
DNA	Deoxyribonucleic acid
dNTP	Deoxynucleotidetriphosphate
DOG	2-deoxygalactose
DRG	Dorsal root ganglion
E. coli	Escherichia coli
EGFP	Enhanced green fluorescent protein
EPSP	Excitatory postsynaptic potential
FCCP	Carbonyl cyanide 4-(trifluoromethoxy)phenylhydrazone
GABA	Gamma Aminobutyric Acid
galK	Galactokinase
Gensat	Gene expression atlas of the central nervous system
GFP	Green fluorescent protein
GPCR	G-protein coupled receptor
HCN	Hyperpolarization-activated cyclic nucleotide-gated channel
HEK 293	Human embryonic kidney cells 293
HEPES	4-2hydroxyethyl-1-piperazineethanesulfonic acid
I-RTX	5'Iodoresiniferatoxin
IB4	Isolectin B4
InaD	Inactivation no afterpotential D
IP	Immunoprecipiation
IP3	Inositol triphosphate
IPSP	Inhibitory postsynaptic potential
LB	Luria-Bertani

LP1	Crude membrane fraction
LP2	Synaptic vesicle fraction
LS0	Hypo-osmotically shocked synaptosomes
LS1	Supernatant containing synaptic vesicles
LTP	Long-term potentiation
MiliQ	Ultrafiltrated water (from MiliQ-Plus water system, Millipore)
mRNA	Messenger ribonucleic acid
MS	Mass spectrometry
n	Number
n.s.	Not significant
NGF	Nerve growth factor
NMDA	N-methyl-D-asparate
Nomp-C	No-mechano-potential C
o/n	Over night
P1	Nuclear pellet
P2	Crude synaptosomal fraction
PBS	Phosphate buffered saline
PCR	Polymerase chain reaction
PFA	Paraformaldehyde
PGE2	Prostaglandin E2
pH	potentiumhydrogenii
PI3 kinase	Phosphatidylinositide 3-kinase
PIP2	Phosphatidylinositol bisphosphate
PIRT	Phosphoinisotide interacting regulator of TRP
PKA	Protein kinase A
PKC	Protein kinase C
PLA	Proximity Ligation Assay
PLC	Phospholipase C
PNS	Peripheral nervous system
PVD	Polyvinylidene fluoride
RNA	Ribonucleic acid
RNase	Ribonuclease
RT	Room temperature
RTX	Resiniferatoxin
SDS	Sodium dodecyl sulphate
SF-tag	Strep-Flag-tag
SP	Substance P
Src	Proto-oncogene tyrosine-protein kinase Src
TBS	Tris-buffered saline
TE	Tris-EDTA
TG	Trigeminal ganglion
TM	Transmembrane domain
TrkA	Neurotraophic tyrosine kinase receptor type 1
TRP	Transient receptor potential
TRPV1	Transient receptor potential Vanilloid 1
VGAT	Vesicular GABA transporter

VGLUT	Vesicular Glutamate transporter
VR1	Vanilloid receptor 1
WT	Wild type

Units

°C	degrees Celsius
bp	base pairs
d	days
g	gram
h	hour
kb	kilobase
kDa	kilodalton
l	liter
M	molar
min	minute
ml	milliliter
mM	millimolar
ng	nanogram
nm	nanometer
rpm	Revolutions per minute
s	second
µg	microgram

Table of Contents

1. Introduction

1.1. The primary afferent nociceptor

1.1.1. Anatomy of the pain pathway

Primary afferent neurons provide sensory innervation to the skin, muscles, joints, fascia, bones and viscera and convey this information to the central nervous system. They comprise specialized neurons that detect mechanical, chemical and thermal stimuli. Those neurons that respond to tissue damage (intense mechanical, thermal or noxious chemical stimuli) express specialized proteins in their peripheral terminals capable of pain transduction and have been termed nociceptors. The nociceptive system is a protective mechanism for alerting the body of danger from potential tissue damage. The cell bodies of the primary afferents are located in the dorsal root ganglia (DRG) or trigeminal ganglia (TG). The DRG are located lateral to the spinal cord in the vertebral column. DRG neurons are pseudounipolar with an axon that sends an efferent branch to target peripheral tissues like the skin and muscle and a central afferent branch that targets the spinal cord or medulla (Woolf and Ma, 2007) (Fig. 1). All nociceptive information is relayed to laminae I, II and V of the dorsal horn of the spinal cord (Bráz et al., 2005) (Fig. 1). The trigeminal ganglion is analogous to the DRG of the spinal cord and is responsible for innervation of the face.

When primary afferent neurons are activated by a sensory stimulus, they transduce the stimulus into electrical currents, which propagate down the axon in the form of an action potential. The propagation of electric activity is mediated by voltage gated ion channels, which transmit the information centrally to the dorsal horn via neurotransmitter release at the presynaptic terminal. Glutamate is the predominant neurotransmitter of all nociceptors. From there on, the signals are processed centrally to the thalamus and brainstem; they terminate in cortical structures such as the somatosensory cortex, the cingulate and insular cortices and the amygdala (Hunt and Mantyh, 2001; Basbaum et al., 2009).

1.1.2. Primary sensory neuron subtypes

Somatosensory primary afferent neurons are categorized into three main groups based on anatomical and functional criteria: Aβ, Aδ and C fibers (Julius and Basbaum, 2001). Cell bodies with the largest diameters give rise to myelinated, rapidly conducting Aβ fibers, so called mechanoreceptors. These neurons detect innocuous stimuli such as touch and pressure applied to skin, muscle and joints. By contrast, small- and medium-diameter cell bodies give rise to most of the damage-sensing nociceptors, including unmyelinated, slowly conducting C fibers and thinly myelinated, more rapidly conducting Aδ-fibers. Based on their speed of transmission, Aδ fibers and C fibers are thought to mediate well-localized "first" or fast pain and poorly localized slow or "second" pain, respectively (Basbaum et al., 2009).

Nociceptors express a variety of different molecular markers, ion channels and receptors, and can be subdivided into two broad classes: based on the presence or absence of the receptor for plant isolectin (Snider and McMahon, 1998; Stucky and Lewin, 1999) they are referred to as IB4+ (nonpeptidergic) and IB4- (peptidergic) nociceptors. Peptidergic nociceptors express the neuropeptides Substance P (SP) and calcitonin gene-related peptide (CGRP) as well as the TrkA neurotrophin receptor for nerve growth factor (NGF) which is required for nociceptor survival (Silos-Santiago et al., 1995; Zylka et al., 2005). This group of fibers projects to the outermost region of the dorsal horn (lamina I and outer lamina II) (Fig. 1). In contrast, nonpeptidergic nociceptors lack neuropeptides but express the GDNF receptor ret (Molliver et al., 1997). They project to the inner lamina II of the dorsal horn that contains primarily local spinal interneurons (Molliver et al., 1995) (Fig. 1). Although both subtypes initially require NGF during development, their adult phenotypes differ due to the downregulation and loss of TrkA receptors on the nonpeptidergic nociceptors (Molliver et al., 1997). Due to their different molecular diversity and central innervation patterns these two subpopulations have been proposed to play different roles in the transduction of noxious stimuli (Snider and McMahon, 1998; Stucky and Lewin, 1999; Cavanaugh et al., 2009). While nonpeptidergic afferents contribute to mechanical pain behaviors (Wu et al., 2004; Bráz et al., 2005), the peptidergic neurons that express the heat and capsaicin receptor TRPV1 are essential for behaviors evoked by noxious heat and inflammation (Stucky and Lewin, 1999; Marmigère and Ernfors, 2007; Cavanaugh et al., 2009).

In addition to these profound neurochemical and anatomical differences, nociceptors show further functional distinctions. They can be characterized based on their sensory modality or modalities, such as heat, cold, mechanical, chemical or silent. The majority, however, is polymodal, because they detect more than one nociceptive modality (Perl, 2007; Lawson et al., 2008).

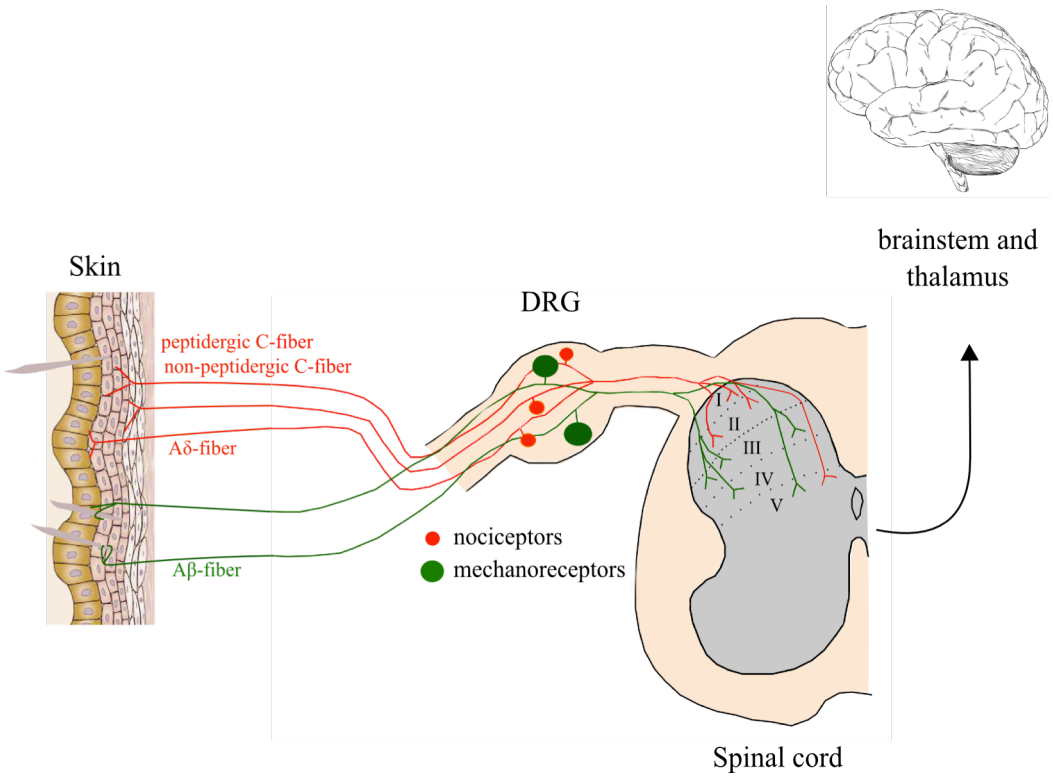

Figure 1: Schematic representation of the pain pathway.

The skin is innervated by primary afferents that sense noxious stimuli such as hot/cold temperature, mechanical force or chemical irritants. The sensory information is transmitted along the axon of the primary afferent to its soma, located in the DRG, and then further to the central terminals in the dorsal horn of the spinal cord. Here the input is conveyed via ascending nociceptive pathways to higher brain centers. Modified from Lumpkin and Caterina, 2007

1.2. Mammalian TRP channels

TRP channels were first discovered in the *Drosophila* visual system, where Cosens and Manning found a mutation that they called *trp* (for transient receptor potential), because it showed a transient instead of sustained response to prolonged light (Cosens and Manning, 1969). *Trp* mutant flies appeared blind in optomotor behavioural tests (Minke et al., 1975). The responsible gene was cloned and found to encode a calcium-selective channel (Montell and Rubin, 1989; Hardie and Minke, 1992). Subsequently, several channels with sequence similarity to *Drosophila* TRP were identified in a

number of different species and these channels are collectively known as TRP channels (Voets et al., 2005). They constitute a large family with a wide range of physiological functions and many channels have a key role in sensory transduction processes (Montell, 2005). For instance, yeast use a TRP channel to respond to hypertonicity (Denis and Cyert, 2002; Zhou et al., 2003). Nematodes use TRP channels at the tip of their noses to sense and avoid noxious chemical (de Bono et al., 2002). Mammals use TRP channels for taste, hot and cold temperatures, and pain. Thus, TRP channels play a critical role in response to all major classes of external stimuli. Importantly, TRP channels can respond to multiple stimuli and thereby serve as polymodal signal detectors. This allows them to act as multifunctional sensors in a cell's immediate environment (Tominaga et al., 1998; Bautista et al., 2006).

Since the discovery of *Drosophila* TRP, the search for mammalian homologs has resulted in the identification of > 30 *trp*-related genes in mice and 27 in humans (Voets et al., 2005). Mammalian TRP channels have been classified into 7 subfamilies based on sequence homology (Fig. 2): TRPC (Canonical), TRPV (Vanilloid), TRPM (Melastatin), TRPP (Polycystin), TRPML (Mucolipin), TRPA (Ankyrin) and TRPN.

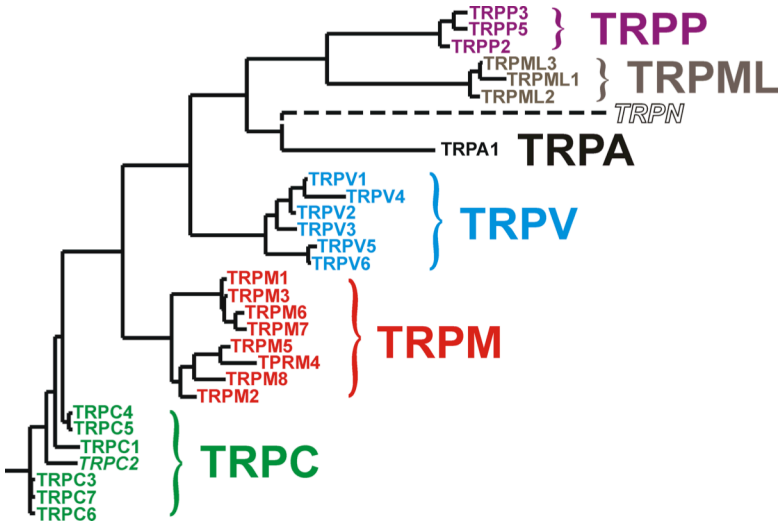

Figure 2: Phylogenetic tree of the seven TRP channel family members

The family of TRP channels is divided into seven different groups based on sequence similarity. TRPC (classical or canonical), TRPV (vanilloid), TRPM (melastatin), TRPP (polycystin), TRPML (mucolipin), TRPA (ankyrin) and TRPN (no mechanoreceptor potential, Nomp-C). Adapted from Nilius and Mahieu, 2006

The TRPC family comprises the closest homologs to *Drosophila* TRP channels. TRPVs are named after the first identified member, vanilloid receptor 1 (now

TRPV1). TRPVs 1-4 are all heat-activated channels, with TRPV1 (43°C) and TRPV2 (52°C) being noxious heat sensors and TRPV3 (33°C) and TRPV4 (25°-34°C) responding to warm temperatures (Benham et al., 2002; Gunthorpe et al., 2002; Lee and Caterina, 2005). TRPV5 and 6 are very different from the other TRPV members. They are the only TRP channels that are highly selective for calcium ions and they are both tightly regulated by calcium (Vennekens et al., 2000; 2001; Yue et al., 2001). Of the TRPM family, TRPM8 is particularly interesting because it is activated by physical cooling and menthol (Bautista et al., 2007; Colburn et al., 2007; Dhaka et al., 2007). The TRPP and TRPML families are not yet substantially characterized, but are becoming increasingly interesting because of their involvement in several human diseases such as polycystic kidney disease and mucolipidosis type IV (Nilius et al., 2007; Qamar et al., 2007; Hsu et al., 2007; Dong et al., 2008). TRPA has only one family member, TRPA1, a nociceptive channel characterized by the presence of about 17 ankyrin repeats. The TRPN subfamily is named after the "NO-mechano-potential C" (Nomp-C) channel in *C. elegans* (Walker et al., 2000; Sidi et al., 2003). So far, the only TRPN family member identified in vertebrates is from zebrafish (Sidi et al., 2003).

TRP channels have a predicted structure that relates them to the superfamily of voltage gated potassium channels (Clapham et al., 2003; Flockerzi, 2007). Due to the lack of accurate X-ray crystallography data providing a three-dimensional structure of an entire TRP channel, most data concerning domain composition comes from structure/function relationship studies. TRP channels are made up of four subunits, each with six transmembrane segments and intracellular N- and C-terminal domains (Benham et al., 2002; Owsianik et al., 2006; Gaudet, 2008). The cytosolic domains are variable in length and often contain a variety of domains and motifs such as ankyrin repeats, coiled-coil domains, lipid-interaction domains, phosphorylation sites and calmodulin or inositol triposphate (IP_3) binding sites (Clapham et al., 2003; Flockerzi, 2007). Currently, the ankyrin repeat stretch of TRPV channels is the only domain for which high-resolution crystallographic data have been obtained (Jin et al., 2006; Gaudet, 2009). It is thought that the four subunits assemble as homo-and/or heterotetramers to form functional channels. Many channels preferentially homo-tetramerize (e.g. TRPV1, TRPV2, TRPV3, and TRPV4), however, the formation of heteromultimeric channels between members of the same subfamily (e.g. TRPC1 with TRPC4 and TRPC5 or TRPV1 with TRPV2 and TRPV3) or different subfamilies (e.g.

TRPA1 with TRPV1) has been reported (Hellwig et al., 2005; Schaefer, 2005; Lepage and Boulay, 2007; Salas et al., 2009). Heteromerization enlarges the functional diversity of TRP channels, although little is known about whether and how TRP channels change subunit composition in response to environmental stimuli.

1.3. TRPV1

TRPV1 was isolated from a rodent DRG cDNA library using a calcium influx assay (Caterina et al., 1997) and is probably the most studied and best characterized TRP channel. The gene was initially named Vanilloid receptor 1 (VR1) because it was activated by the vanilloid and hot chili pepper active ingredient, capsaicin, which gives chili peppers their piquancy and burning sensation. VR1 was later renamed according to the new taxonomy of TRP ion channels (Montell et al., 2002; Clapham et al., 2003). TRPV1 was the first thermally gated cation channel to be discovered in nociceptors. Activation of TRPV1 results in an influx of Ca^{2+} and other cations like Na^{+}, K^{+} and Mg^{2+} (Caterina et al., 1997). The influx of cations induces cellular depolarization and subsequent release of neuropeptides, mainly Substance P and CGRP, which play a central role in the development of neurogenic inflammation and transduction of neuronal impulses (Tominaga, 2007).

1.3.1. Molecular structure of TRPV1

Similar to other TRP ion channels, TRPV1 has six transmembrane domains and a hydrophobic pore region between the fifth and sixth segment (Fig. 3) (Caterina et al., 1997; Kedei et al., 2001). The N-terminus contains six ankyrin repeats. These are repetitions of 33-residue motifs and serve as important protein-protein interaction platforms for intra- and intercellular associations. The crystal structure of these repeats has revealed an important ATP/Calmodulin binding site that is essential for effective desensitization of the receptor (Lishko et al., 2007) (Fig. 3). The C-terminus has been proposed to serve as a determinant of subunit tetramerisation and to contribute to important aspects of channel function (García-Sanz et al., 2007). TRPV1 subunits preferentially assemble into homomeric complexes (Hellwig et al., 2005). When expressed alone in heterologous cell expression systems, the electrophysiological properties of TRPV1 are identical to those of native TRPV1 in DRG neurons (Cesare and McNaughton, 1996; Caterina et al., 1997; Gunthorpe et al.,

2002; Premkumar et al., 2002), suggesting that it forms homotetramers *in vivo*. However, TRPV1 can also form heterotetramers with other TRPV channels such as TRPV2 and TRPV3 in a subset of DRG neurons (Liapi and Wood, 2005; Smith et al., 2002; Rutter et al., 2005; Hellwig et al., 2005).

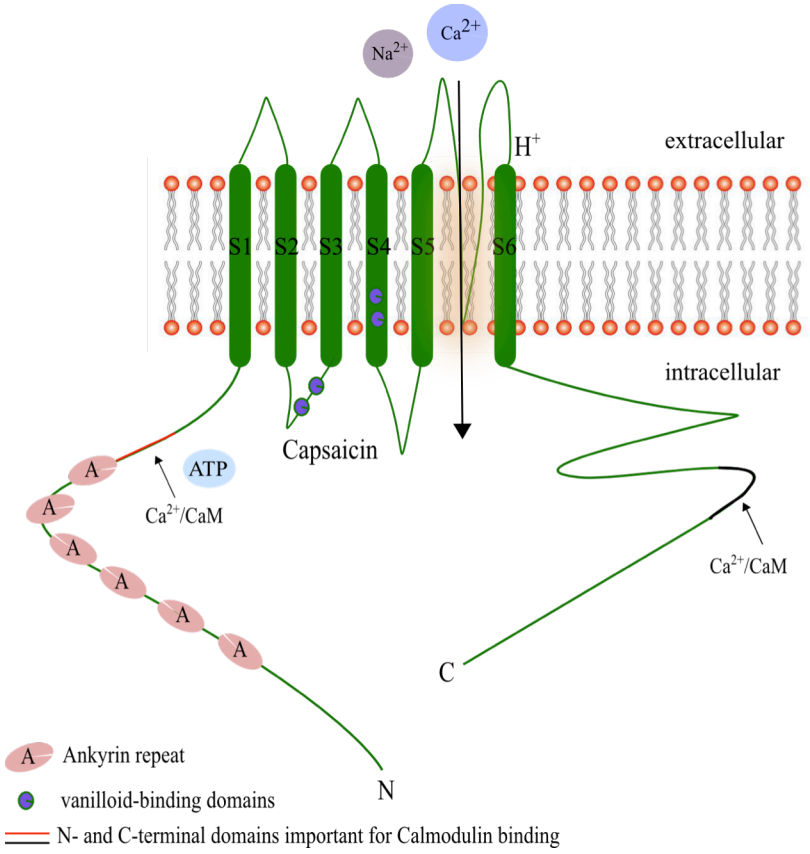

Figure 3: TRPV1 topology

TRPV1 has six transmembrane domains flanked by two intracellulular domains and a pore loop between the fifth and sixth transmembrane-spanning regions. The influx of cations such as Ca^{2+} and Na^{+} through the channel results in depolarization of the cell. The N-terminus contains six ankyrin repeats that are important for protein-protein interactions. Ca/CaM binding sites are located at both the N- and C-termini. Capsaicin binding sites are depicted. At least four subunits assemble to form a functional channel. Heteromerization with other TRPV1 members has been reported.

1.3.2. TRPV1 expression and localization

TRPV1 is found in multiple cell types but it is most prevalent in sensory neurons. It is mainly expressed in a subset of neurons in the dorsal root ganglia and trigeminal ganglia (Helliwell et al., 1998). Within DRG neurons, TRPV1 expression is almost exclusively restricted to small- to medium-sized neurons which comprise both unmyelinated C-fibers and thinly myelinated Aδ-fibers. While the majority of TRPV1

containing neurons expresses the peptidergic markers CGRP and Substance P as well as the TrkA receptor, a subset also co-localizes with the lectin IB4 (Guo et al., 1999; Dinh et al., 2003; Hwang and Valtschanoff, 2003). TRPV1 is also found in most cells of the nodose ganglia (Helliwell et al., 1998; Michael and Priestley, 1999) which innervate the viscera of the thorax and abdomen. Peripheral TRPV1 positive terminals are located in the sciatic nerve as well as in non-neuronal tissues, such as layers of skin epidermis (Denda et al., 2001; Inoue et al., 2002; Lee and Caterina, 2005; Denda and Tsutsumi, 2011), gastric epithelial cells (Kato et al., 2003; Ward et al., 2003), urinary bladder (Avelino et al., 2002), airways (Kollarik and Undem, 2004) and cardiovasculature (Peng and Li, 2010; Thilo et al., 2010). Within the spinal cord TRPV1 is mainly found on peptidergic afferents (lamina I, IIo) of nociceptors that make synaptic contact with projection neurons in the dorsal horn (Cavanaugh et al., 2011a). Activation of central terminal TRPV1 by capsaicin results in an increase of synaptic glutamate release (Yang et al., 1998; Ferrini et al., 2007). Interestingly, TRPV1 has also been proposed to have function in synaptic physiology in multiple brain areas, including solitary tract nucleus and trigeminal nucleus (Peters et al., 2011; Andresen et al., 2012), both of which receive afferent signals via vagal, glossopharyngeal and facial nerves. Moreover, TRPV1 expression was reported in the hippocampus, hypothalamus, thalamus, substantia nigra and striatum (Roberts et al., 2004; Tóth et al., 2005; Gibson et al., 2008; Maccarrone et al., 2008; Musella et al., 2009; Cavanaugh et al., 2011b), albeit at much lower levels than in the DRG. There is disagreement as to the extent and localization of TRPV1 expression in the brain because it was originally believed that TRPV1 had only limited expression in the central nervous system. However, hypothalamic expression helps to explain the hypothermia that is caused upon injection of capsaicin into the hypothalamus (Szolcsányi et al., 1971). Furthermore, it was described that TRPV1 might be able to induce long-term changes in physiological circuit behavior during learning because TRPV1 deficient mice exhibit impaired hippocampal long-term potentiation, resulting in reduced anxiety and conditioned fear (Marsch et al., 2007; Gibson et al., 2008). Despite accumulating data about TRPV1 functions in CNS processes, the complete picture as to what extent TRPV1 is expressed and plays functional roles in the central nervous system is still a matter of debate and has yet to be fully understood.

1.3.3. Endogenous Activation of TRPV1

TRPV1 is an exceptional ion channel because it functions as a polymodal receptor displaying a dynamic threshold of activation. Until now, TRPV1 is the only known receptor for vanilloids like capsaicin, a highly lipophilic substance that can easily cross the plasma membrane. Other plant-derived chemicals activating TRPV1 include resiniferatoxin (RTX) (a strong irritant and potent capsaicin analog from cactus *Euphorbia resinifera*), piperine (the pungent compound in black peppers) (McNamara et al., 2005), camphor (an extract from *cinnamommum camphora*) (Xu et al., 2005), gingerol (ginger) (Dedov et al., 2002) and eugenol (clove oil) (Yang et al., 2003). Both, capsaicin and RTX, induce a dose-dependent influx of calcium ions in cultured sensory neurons. TRPV1 can also be activated by synthetic ligands, such as Ovanil, which is commonly used as a pharmacological tool to modulate channel function. In addition, the receptor is activated by numerous other chemicals including endogenous arachidonic-acid related compounds (arachidonoyl ethanolamide, 12,15-(S)-hydroperoxyeicosatetraenoic acid, leukotriene B4) (Trevisani et al., 2002), anandamide (endocannabinoids) (Zygmunt et al., 1999), allicin (garlic) (Macpherson et al., 2005) and venoms from cnidarians and spiders (Cuypers et al., 2006; Siemens et al., 2006; Bohlen et al., 2010).

More importantly, TRPV1 was the first temperature-sensitive TRP channel to be identified because of its activation by noxious heat (> 42°C) (Tominaga et al., 1998). Single-channel openings recorded in excised membrane patches expressing TRPV1 suggested that TRPV1 is directly gated by heat and that the channel is, itself, a heat sensor. The temperature sensor domain must be present in the channel (Grandl et al., 2010; Kim et al., 2013) as TRPV1 is intrinsically heat sensitive (Cao et al., 2013). The distal half of the C-terminus was reported to convey thermal sensitivity to the channel (Brauchi et al., 2006). Last but not least, TRPV1 is activated by acidic conditions (pH < 6.5) (Tominaga et al., 1998). An acidic pH is characteristic for inflamed tissue and induces a shift in thermal threshold activation from > 42°C to ambient temperatures (20°C) (Montell et al., 2002) (see also next chapter).

1.3.4. The role of TRPV1 in inflammatory pain

Once tissue has been injured mechanically, by heat or by chemical irritants, inflammatory mediators are released from damaged and non-neural cells (i.e. mast

cells, macrophages, fibroblasts, platelets) residing within or migrating into the injured area. This creates an "inflammatory soup" that is rich in cytokines, growth factors, neurotransmitters, peptides, kinins, purines, extracellular protons, and amines (Hunt and Mantyh, 2001) (Fig. 4). Each of these factors can sensitize nociceptors by interacting with specific cell-surface receptors expressed by these neurons. Sensitization decreases the activation threshold of nociceptors, which become thereby responsive to low-intensity thermal and mechanical stimuli (peripheral sensitization). As a result of this, previously innocuous stimuli are perceived as painful (allodynia), and previously noxious stimuli become more intensely painful (hyperalgesia).

TRPV1 clearly plays a central role in the sensitization of nociceptors and in the development of thermal hyperalgesia, arguably the best described functional feature of the capsaicin receptor in the literature. TRPV1 deficient mice display drastically reduced sensitization of nociceptors and thermal hyperalgesia is essentially abolished in these animals (Caterina et al., 2000; Davis et al., 2000). TRPV1 knockout mice do not develop thermal hypersensitivity in response to an acute hind-paw injection of pro-inflammatory agents (bradykinin, Complete Freund's Adjuvant (CFA), capsaicin, NGF) (Davis et al., 2000; Chuang et al., 2001). Termini of TRPV1 positive neurons are also sites of release for various pro-inflammatory neuropeptides, such as Substance P, CGRP and ATP, which in turn facilitate the production of inflammatory mediators and initiate the process of neurogenic inflammation leading to vasodilation and plasma extravasation (Geppetti et al., 2008). These inflammatory mediators change neuronal excitability either by direct interaction with TRPV1 (e.g. protons, adenosine triphosphate, lipids) or indirectly by binding to metabotropic receptors (e. g. NGF and bradykinin) (Woolf and Salter 2000; Julius, 2013) (see also next chapter) (Fig. 4). Moreover, inflammation causes up-regulation of TRPV1 protein expression levels; this is observed in several inflammatory human disease conditions such as rheumatoid arthritis, irritable bowel syndrome, vulvodynia and mastalgia (for review see (Nilius et al., 2007; Szallasi et al., 2007; White et al., 2011)). As a result of the increased peripheral activation associated with inflammation, neurons in the dorsal horn of the spinal cord undergo long-term changes in their physiological properties (central sensitization). For this reason, TRPV1 is an attractive pharmacological target for the development of anti-inflammatory drugs.

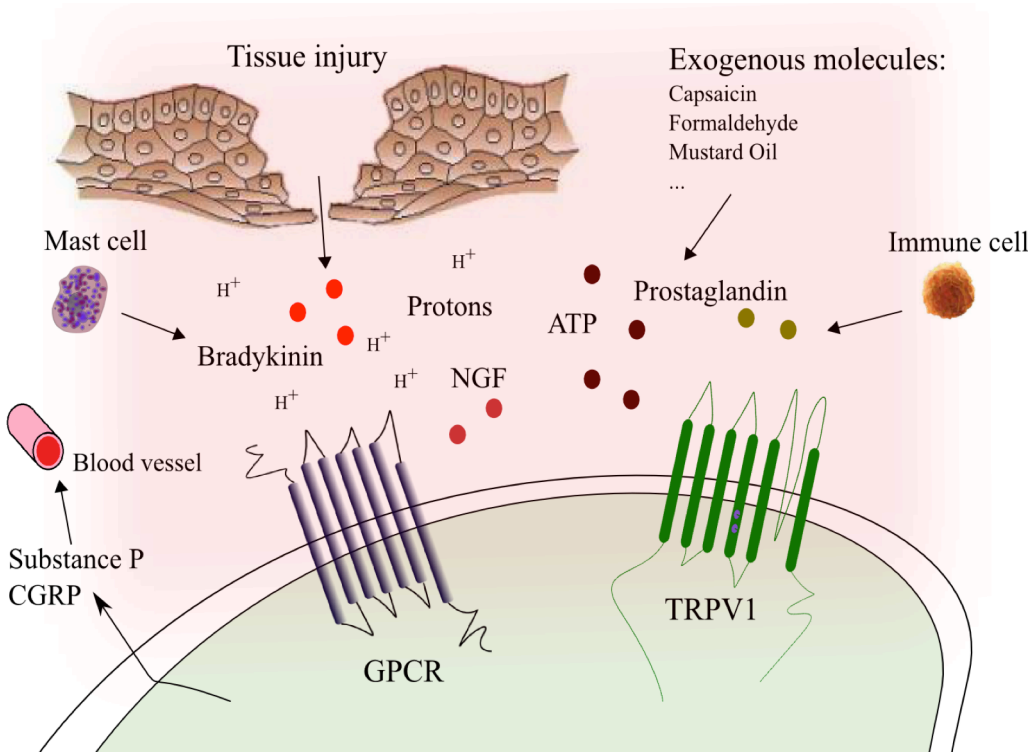

Figure 4: Sensitization of TRPV1 by inflammatory mediators.

Damaged tissue and inflammatory cells release chemical mediators that alter the excitability of nociceptors by lowering their depolarisation threshold. TRPV1 plays a major role in mediating this effect. Components of the "inflammatory soup" include, for instance, bradykinin, prostaglandins, protons, ATP and NGF, which can directly or indirectly sensitize TRPV1. Sensitization also facilitates immunogenic inflammation whereby release of substance P and CGRP induces vasodilation and plasma extravasation. Modified from Marchand et al., 2005

1.3.5. Inflammatory mediators modulating TRPV1

As already mentioned, TRPV1 can either be directly activated by inflammatory mediators or it can be modulated by the actions of protein kinases, phosphatases and lipid messengers. Many inflammatory agents bind to G-protein coupled receptors which signal to PKC and PKA to sensitize TRPV1. In general, protein kinase-dependent phosphorylation causes sensitization (PKA, PKC) whereas dephosphorylation by protein phosphatases promotes desensitization. Phosphorylation increases the channel's open probability (mediated by PKCε) or induces recruitment of new channels to the plasma membrane (mediated by Src kinase) (Jin et al., 2004). TRPV1 has a variety of phosphorylation sites and is regulated by three major kinases. PKC phosphorylates residues S502, T704, S744, S800 and S820 (Bhave et al., 2002; Premkumar et al., 2004), resulting in a potentiation of capsaicin- or proton-evoked responses and in a reduction of the thermal threshold for TRPV1 activation. PKA

phosphorylates TRPV1 at six residues, of which only S116 is important for modulation (Bhave et al., 2002; Vlachová et al., 2003). Furthermore, CaMKII controls TRPV1 activity through phosphorylation of Ser 502 and Thr 704 and thereby regulates capsaicin binding (Jung et al., 2004).

1.3.5.1. Protons

One of the main responses to injury is tissue acidosis, which occurs during ischemia or inflammation (Bevan and Geppetti, 1994). The extent of associated pain correlates very well with the magnitude of acidification (Reeh and Steen, 1996). Under acidic conditions, the excitability of nociceptors is increased even at normal body temperature (Jordt et al., 2000) because extracellular protons can potentiate the response of TRPV1 through direct activation. Mutational studies have shown that acidification to pH < 6.0 directly activates TRPV1 by protonating a glutamate (Glu648) adjacent to the pore region. This leads to opening of the channel at ambient temperature. Thus, protons act primarily by increasing the probability of channel opening (Tominaga et al., 1998; Baumann and Martenson, 2000). Milder acidification protonates Glu600 (located in a putative extracellular domain) (Jordt et al., 2000), and this enhances activation of TRPV1 by other stimuli without directly activating the channel. Moreover, protons can also permeate the channel pore in the presence from an acidic extracellular milieu, leading to a substantial intracellular acidification (Hellwig et al., 2004; Vulcu et al., 2004).

1.3.5.2. Bradykinin

Bradykinin is an inflammatory peptide that is secreted after tissue injury or noxious stimulation and as such, it is a major contributor to the inflammatory response. TRPV1 contributes to sensitization by bradykinin because thermal hypersensitivity in response to intraplantar injection is abolished in TRPV1 deficient mice as compared to wild type mice (Bauer et al., 1992; Ferreira et al., 1993; Chuang et al., 2001). Furthermore, bradykinin application to cultured DRG neurons induces enhancement of heat-induced currents and bradykinin-evoked action potentials are reduced by the TRPV1 antagonist capsazepine (Dray et al., 1992; Dray and Perkins, 1993; Cesare and McNaughton, 1996; Chuang et al., 2001; Couture et al., 2001; Liang et al., 2001). Bradykinin-evoked thermal hyperalgesia is mediated by binding to G-protein-coupled receptors (bradykinin receptor 2; BK_2). This stimulates phospholipase C (PLC)-

catalyzed hydrolysis of phospho-inositol phosphate 2 (PIP_2) into inositol-phosphate 3 (IP_3) and diacylglycerol (DAG). IP_3 and DAG activate protein kinase C (PKC), which directly phosphorylates TRPV1 preferentially at serine residues 502 and 800 (Fig. 5) (Numazaki et al., 2002; Bhave et al., 2003), leading to a potentiation of TRPV1 activity by noxious stimuli. PKC signaling plays a central role in bradykinin-evoked thermal hyperalgesia because application of bradykinin induces translocation of PKC to the plasma membrane (Chuang et al., 2001; Moriyama et al., 2005; Huang et al., 2006; Wang et al., 2008).

1.3.5.3. NGF

NGF is a member of the neurotrophin family and is important for nociceptor development and survival. NGF is synthesized and secreted by a variety of tissues including schwann cells located within sensory ganglia and end-target tissues of nociceptive terminals (keratinocytes, epidermal fibroblasts). NGF is a mediator of inflammatory pain because it is upregulated during inflammation or after injury. Acute hind paw injection of NGF produces a fast and sustained hypersensitivity to noxious thermal stimulation (Lewin et al., 1993). NGF mediated thermal hyperalgesia is a result of TRPV1 sensitization because it potentiates TRPV1 activity and leads to an increase of TRPV1 channels on the plasma membrane (Ji et al., 2002; Bron et al., 2003; Zhang et al., 2005; Stein et al., 2006). The latter includes transferring functional TRPV1 from intracellular pools to the membrane as well as up-regulation of the expression level of TRPV1. As a consequence, the number of capsaicin sensitive neurons is increased and the response of neurons to heat and capsaicin enhanced (Ji et al., 2002; Amaya et al., 2004; Breese et al., 2005). NGF interacts with two types of receptors: tyrosine kinase receptor A (TrkA) and pan-neurotrophin p75 (p75). Hyperalgesia is mainly mediated through TrkA receptors: Activation stimulates PI3 kinase, which in turn activates Src kinase. Src kinase phosphorylates TRPV1 at a single tyrosine residue (Y199) leading to trafficking of TRPV1 to the plasma membrane (Fig. 5) (Zhang et al., 2005).

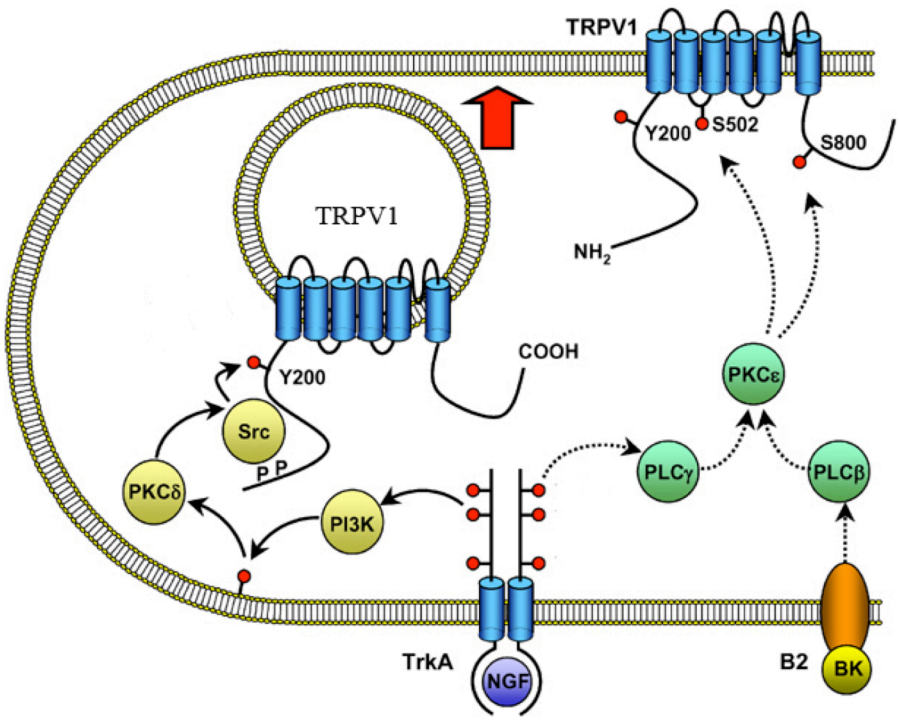

Figure 5: Sensitization of TRPV1 by NGF and bradykinin

NGF and bradykinin are inflammatory mediators that sensitize TRPV1. NGF activation of TrkA receptors induces trafficking of TRPV1 to the plasma membrane: Binding to TrkA stimulates PI3 kinase, with Src kinase being activated downstream of PI3 kinase. Src Kinase phosphorylates TRPV1 at Y199, leading to trafficking and insertion of TRPV1 into the plasma membrane. A second sensitization mechanism is the PLC/PKC signaling pathway. Bradykinin activates PLC, which catalyzes breakdown of PIP_2, which in turn activates PKC leading to phosphorylation of TRPV1 at S502 and S800 and enhanced gating of the channel. Adapted from Huang et al., 2006

1.3.5.4. ATP

ATP is released from injured cells and produces pain by directly activating nociceptors. While P2X receptors have been implicated in the induction of pain, P2Y receptors have been linked to TRPV1 sensitization. In TRPV1 knockout mice, ATP fails to induce thermal hyperalgesia (Moriyama et al., 2003; Tominaga et al., 2004; Malin et al., 2008). Patch clamp experiments confirmed that extracellular ATP enhances TRPV1-dependent capsaicin and proton-evoked responses and leads to a reduced temperature threshold for TRPV1 activation (Tominaga et al., 2001). These potentiating effects of ATP on TRPV1 activity are abolished upon application of PKC inhibitors, implicating activation of PKC via a PLCβ-coupled cascade as a possible mechanism (Tominaga et al., 2001; Moriyama et al., 2003; Tominaga et al., 2004).

1.3.5.5. Phosphoinositide lipids

TRPV1 is regulated by Phosphatidylinositol 4,5-bisphosphate (PIP_2), which was originally proposed to constitute the common mechanism for bradykinin- and NGF-mediated sensitization of TRPV1. According to the PLC-model of hyperalgesia (Stein et al., 2006), phosphoinositides inhibit TRPV1 by interacting with positively charged amino acid residues located within the C-terminal domain. Disruption of this interaction through PLC-mediated PIP_2 hydrolysis contributes to channel sensitization by releasing TRPV1 from tonic inhibition (Chuang et al., 2001; Prescott and Julius, 2003). Moreover, removal of the PIP_2 binding cassette in the C-terminal domain ablates the sensitizing effect of NGF. However, this model has been challenged by studies that support a role for PIP_2 as an essential cofactor of TRPV1 that exerts negative or positive effects on thermal and chemical sensitivity depending on stimulus intensity (Lukacs et al., 2007; Rohacs, 2007; Klein et al., 2008; Ufret-Vincenty et al., 2011). More recently, Cao *et al*. reconstituted functional TRPV1 in liposomes and showed that TRPV1 displayed both intrinsic heat and chemical sensitivity in the absence of phosphoinositides (Cao et al., 2013). This argues against a requirement for PIP_2 as an obligate cofactor. Addition of PIP_2 to their system rather supports a role for PIP_2 as a negative regulator for TRPV1 because it caused a rightward shift in the channel's thermal or chemical activation threshold (Cao et al., 2013).

1.4. Other molecular components of the nociceptive system

The neuronal subtypes in the DRG express a variety of different ion channels and receptors, which contribute to pain sensation and enable cells to undergo significant changes in their excitability in response to altered environmental conditions (Waxman et al., 2000). Members of other ion channel families such as $Na_v1.8$, $Ca_v2.2$ or ASICs (Acid sensing ion channels) are involved in damage sensing and pathological pain. Among the TRP family, TRPA1 is clearly another exceptional ion channel because it senses a plethora of noxious stimuli in the environment and endogenous molecules release in injured tissues. It is activated by a variety of irritating chemical compounds such as those found in mustard oil, garlic, cinnamon oil, gas exhaust and formalin (Bandell et al., 2004; Jordt et al., 2004; Macpherson et al., 2005; Bautista et al., 2006; McNamara et al., 2007), all of which induce a burning sensation.

Various neuromodulators and neurotransmitters that process the sensory information further add to the diversity of nociceptors (Fürst, 1999) and provide a specific

response to diverse types of stimuli (Cavanaugh et al., 2009). Most primary afferents are glutamatergic and DRG neurons release glutamate to activate second-order spinal cord neurons. The discovery of Vesicular Glutamate Transporters (VGLUTs) enabled the characterization of specific glutamatergic neuronal subpopulations involved in pain sensation.

1.4.1. Vesicular Glutamate Transporters are important for pain signaling

Glutamate is the major excitatory neurotransmitter in the mammalian CNS. In presynaptic terminals glutamate is stored in synaptic vesicles and released by exocytosis. The transport of glutamate from the cytosol into synaptic vesicles is mediated by Vesicular Glutamate Transporters, of which three distinct subtypes (VGLUTs 1-3) have been identified in mammals. Anatomical studies have established that they are expressed by mostly nonoverlapping and functionally distinct populations of glutamatergic neurons. Mice heterozygous for Vglut1 do not show any pain-related behavioral changes, which may be related to the fact that Vglut1 is largely expressed in nonnocicpetive neurons terminating in laminae III/IV and II_i of the spinal cord (Brumosvsky et al., 2007; Leo et al., 2009). In contrast, Vglut2 is expressed by the majority of Aδ and C-fibers, including peptidergic and IB4-binding unmyelinated C-fibers that innervate laminae I and II (Landry et al., 2004; Brumovsky et al., 2007) (Fig. 6). Importantly, studies using mice lacking Vglut2 selectively in nociceptors established an important role for this transporter in acute and inflammatory pain signaling (Scherrer et al., 2010; Lagerström et al., 2010; Liu et al., 2010; Rogoz et al., 2012). Vglut2 positive neurons also show high overlap with TRPV1 expressing neurons (Liu et al., 2010) and it was shown that Vglut2 plays a crucial role in thermal pain (Lagerström et al., 2010. Vglut3 localizes in a small subset of DRG C-low threshold mechanoreceptors (Seal et al., 2009) and has been shown to be involved in auditory function and mechanical pain sensation (Seal et al., 2008).

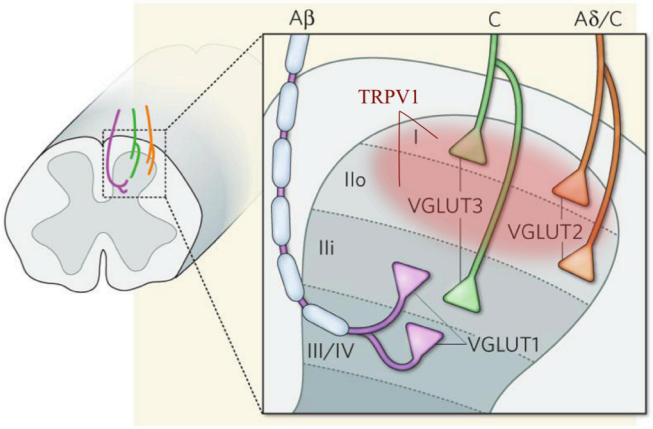

Figure 6: Termination of glutamatergic sensory afferents in the dorsal horn spinal cord

Nociceptive neurons are glutamatergic and use the family of VGLUTs to package glutamate into vesicles at the presynapse. While Vglut1 is expressed by mechanosensitive Aβ fibers terminating in lamina III/IV and II_i, Vglut2 is expressed by nociceptive Aδ fibres and C fibres terminating in laminae I and II and thus overlaps with TRPV1. Vglut3 is expressed by mechanosensitive fibers that terminate at the lamina II/III border and in lamina I. Modified from Drew and MacDermott, 2009

1.4.2. GABAergic pathways as a means to control pain

Nociceptor terminals make synaptic connections with a neuronal network composed of projection neurons as well as excitatory and inhibitory interneurons. GABA (Gamma-Aminobutyric Acid) is the main inhibitory neurotransmitter in the nervous system and exerts its function through ionotropic $GABA_A$ and metabotropic (G-protein coupled) $GABA_B$ receptors. $GABA_B$ receptors are highly concentrated in the superficial layers of the dorsal horn spinal cord, predominantly on afferent terminals of small- and medium-sized sensory neurons located in the DRG (Towers et al., 2000; Calver et al., 2000; Charles et al., 2001). Their activation produces analgesia by the inhibition of presynaptic neurotransmitter release as well as by the inhibition of postsynaptic responses (Sokal and Chapman, 2003; Ataka et al., 2000). In fact, $GABA_B$ knockout mice exhibit pronounced heat and mechanical hyperalgesia (Schuler et al., 2001; Gassmann et al., 2004), indicating that a lack of $GABA_B$ leads to an increased central hyperexcitability of spinal nociceptive pathways. Therefore, $GABA_B$ receptors represent targets for pharmacologically manipulating inhibitory drive to treat chronic pain (Pinto et al., 2008; Zeilhofer et al., 2009; Laffray et al., 2012).

1.5. *Drosophila* TRP channels form macromolecular protein complexes

An emerging hypothesis is that members of the TRP channel family associate in supramolecular assemblies composed of multiple signaling components. The existence of a TRP channel-containing protein complex was first shown in *Drosophila* photoreceptors (Montell, 1999). The central protein in this assembly is InaD (inactivation no afterpotential D), a scaffold composed of five PDZ protein interaction motifs (Tsunoda et al., 1997) (Fig.7). InaD binds directly to at least seven proteins that function in phototransduction. The three core proteins of this complex are TRP (Shieh and Zhu, 1996; Huber et al., 1996b; 1998), PLC (NORPA) (Chevesich et al., 1997), and an eye-specific protein kinase C (Huber et al., 1996a; Xu et al., 1998), which appear to be constitutively bound to InaD (Chevesich et al., 1997; Tsunoda et al., 1997). Co-immunoprecipitation studies have indicated that two other TRP homologues, TRP-like (TRPL) (Phillips et al., 1992; Niemeyer et al., 1996) and TRPγ (Xu et al., 2000), form heteromers with TRP and each other. TRP serves as an important anchor that targets the entire InaD protein complex to its appropriate localization within the cell (Chevesich et al., 1997; Li and Montell, 2000). This was shown using *Drosophila* mutants in which different constituents of the INAD complex were genetically removed and the TRP and InaD binding domains deleted (van Huizen et al., 1998; Li and Montell, 2000). At least four other proteins dynamically associate with InaD and are required for rapid and efficient phototransduction. These include the major rhodopsin (RH1), the second transduction channel, TRPL, the NINAC protein (a myosin III linking the complex to the cytoskeleton), and calmodulin (Xu et al., 1998; Wes et al., 1999).

The organization of signaling proteins into a multi-protein complex provides the basis for an efficient transduction cascade and regulation of calcium entry through the TRP channel. The signalplex brings signaling components into close proximity, thus promoting specificity and increasing the rate of signaling. Because almost all TRP channels contain multiple putative protein-protein interaction platforms, it is likely that they may be similarly organized in multi-protein complexes and have important functions as anchors that localize multiple signal transduction elements. Thus far, it has been reported that members of the mammalian TRPC channels, TRPC4 and TRPC5, associate in macromolecular complexes similar to the *Drosophila* signalplex (Tang et al., 2000). PDZ-binding motifs in the C-terminus of TRP channels have been

implicated in the control of plasma membrane localization (Mery et al., 2002; Palmada et al., 2005; Song et al., 2005), however, so far there is only limited evidence for an involvement of PDZ proteins in the control of TRP channel activity.

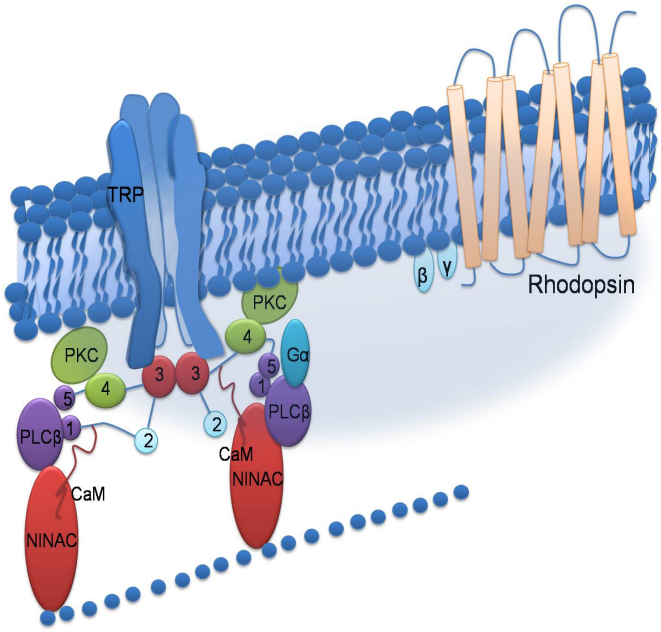

Figure 7: The InaD signaling complex

Key elements of the *Drosophila* phototransduction cascade are assembled into a multimolecular complex by the scaffolding protein, InaD. The InaD protein contains 5 PDZ domains (1-5). TRP serves as an anchor that localizes the protein complex to its appropriate site within the cell. Modified from Hardie and Raghu, 2001

1.6. Identification of TRPV1 protein complex components using proteomics

There is growing evidence that ion channels and receptors do not function as individual proteins; instead, they are often associated with other proteins in a complex or network inside a cell. This encompasses proteins that are either directly or indirectly associated with the receptor. Associated proteins can drastically influence the properties of the receptor by modulating its function or affecting downstream signaling pathways. Thus, their activity strongly depends on their molecular environment (Schulte et al., 2011). For many years the knowledge about such protein environments was quite limited. Up until now, technical challenges such as poor solubilization of receptors, small amounts of source material and a lack of sensitive protein analysis techniques have hindered the isolation of protein complexes from native tissue. However, recent advances in functional proteomics have allowed development of an experimental workflow that combines affinity purification of

readily solubilized protein complexes with quantitative high-resolution mass spectrometry (Schulte et al., 2011). This approach has been quite successful because it preserves the integrity of the protein complex during its isolation from native tissue. Specific enrichment of the target protein is achieved by affinity purification using antibodies directed against the endogenous protein or epitope tagged proteins. In recent years, comprehensive investigations of ion channels and their associated proteins have been performed for a variety of receptors including Ca_v channels (Müller et al., 2010), AMPA-type glutamate receptors (Schwenk et al., 2009; 2012), $GABA_B$ receptors (Schwenk et al., 2010) and HCN channels (Zolles et al., 2009). This shows that proteomic approaches are able to reveal novel accessory subunits of channels and provide important insights into channel-mediated signaling pathways. So far, no experimental approach has enabled a comprehensive access to the molecular environment of TRPV1 channels. Therefore this thesis work aimed at isolating and identifying TRPV1 protein complex components to understand TRPV1 regulation and function.

1.6.1. Known protein interaction partners of TRPV1

A few studies have implicated that TRPV1 is coupled to downstream signaling elements through a multi-protein complex composed of proteins that directly or indirectly bind to the receptor. For instance, TRPV1 was shown to interact with tubulin (Goswami et al., 2004; 2006), TRPV2 (Liapi and Wood, 2005; Rutter et al., 2005; Hellwig et al., 2005), snapin and synaptotagmin IX (Morenilla-Palao et al., 2004). Three more examples are given below.

1.6.1.1. Calmodulin and ATP

Calmodulin is a calcium-binding protein and is required for TRPV1 desensitization (Tominaga and Tominaga, 2005), caused by an increase in intracellular calcium. Desensitization is an important mechanism for dampening TRPV1 responsiveness so that pain-producing conditions do not permanently activate the channel and do not overload the cell with toxic levels of calcium. Calmodulin has been shown to bind to the C- and N-terminus of TRPV1 (Fig. 3) (Numazaki et al., 2003; Rosenbaum et al., 2004) in a calcium-dependent manner. In addition, the Gaudet lab showed that calmodulin controls desensitization by displacing an ATP from a multi-ligand binding

site within the intracellular N-terminus (Lishko et al., 2007) (Fig. 3). According to their model, one molecule of ATP is present in a nucleotide-binding pocket within the TRPV1 ankyrin fold. ATP binding occludes calmodulin and thus prevents inappropriate desensitization. However, upon TRPV1 activation, calcium permeates the channel, binds to and activates calmodulin. Activated calmodulin then displaces ATP and downregulates channel function. Therefore, ATP and calmodulin compete for the same binding pocket and the effectiveness of these interactions determines the extent of channel desensitization (Lishko et al., 2007).

1.6.1.2. AKAP 79/150

A-Kinase Anchorin Proteins (AKAP) are scaffolding proteins that organize multi-protein complexes and recruit protein kinases A and C to key phosphorylation sites on many different receptors. Biochemical studies identified the plasma membrane localized isoform AKAP79/150 protein as an important link for sensitization of TRPV1. AKAP has binding sites for these kinases and TRPV1, thus forming a signaling complex that promotes rapid phosphorylation of critical sites on TRPV1 (Schnizler et al., 2008; Zhang et al., 2008). Genetic deletion of AKAP79 reduces PKC-mediated hyperalgesia in mice (Jeske et al., 2009). AKAP binds to a region in the C-terminus of TRPV1 (Btesh et al., 2013). If binding is prevented, sensitization by bradykinin and PGE_2 is abrogated, therefore AKAP is critical for heat hyperalgesia (Zhang et al., 2008; Btesh et al., 2013; Fischer et al., 2013).

1.6.1.3. PIRT

Pirt (Phosphoinositide interacting regulator of TRP) is a membrane protein and predominantly expressed in small and medium sized DRG neurons. It is implicated in nociception and itch signaling pathways (Patel et al., 2011). Pirt knockout mice show less severe but similar phenotypes as TRPV1 knockout mice. Cultured DRG neurons from these mice show decreased noxious heat and capsaicin evoked currents. Furthermore, Pirt positively regulates TRPV1 activity, as expression of Pirt in Hek293 cells enhances TRPV1 mediated currents. Co-immunoprecipitation assays in Hek cells and binding studies revealed that the C-terminus of Pirt binds TRPV1 and several phosphoinositides, including PIP_2 (Kim et al., 2008). Since TRPV1 does not contain a PIP_2 binding site, it was hypothesized that Pirt acts as a PIP_2 sensor that in turn regulates TRPV1 activity (Kim et al., 2008). However, this study is controversial

as a later study showed that Pirt is not required for potentiation of TRPV1 by PIP_2; instead, the proximal C-terminal region of TRPV1 directly interacts with PIP_2, making it a strong candidate for mediating regulation of the channel (Ufret-Vincenty et al., 2011). Thus the exact role of Pirt for TRPV1 function remains to be determined.

2. Aims of thesis

This thesis aimed at establishing a genetic and biochemical strategy to purify TRPV1 receptors from native sensory tissue and to analyze identified complex components for their effects on TRPV1 function. Most ion channels and receptors associate in dynamic supramolecular assemblies composed of multiple signaling components that are important for their efficient function. Thus far, protein networks involving TRPV1 have not been sufficiently characterized. Therefore, TRPV1 protein complexes were isolated from transgenic mice expressing an SF-tagged version of the receptor and analyzed by mass spectrometry to learn more about protein constituents surrounding TRPV1 and to identify putative direct interaction partners.

Based on the genetic elements of the TRPV1 BAC it was possible to drive SF-TRPV1 expression in cells that natively express the receptor. SF-TRPV1 BAC mice were characterized functionally and at the protein level. After optimization of the purification procedure *in vitro* and *in vivo*, TRPV1 receptors were affinity purified from the DRG and sciatic nerve and subjected to mass spectrometry analysis. One candidate protein from each tissue was selected and its association with TRPV1 validated and characterized.

The specific aims of this thesis were:

- Generation of SF-tagged TRPV1 constructs
- Generation of BAC transgenic mice expressing SF-TRPV1 in sensory neurons that natively express TRPV1
- Confirmation of accurate expression and functionality of SF-TRPV1 in the BAC transgenic mice
- Affinity purification of SF-TRPV1 from native sensory tissue
- Identification of putative protein interaction partners by mass spectrometry (MS) analysis
- Validation and characterization of the association of two candidate proteins with TRPV1 by immunohistochemical and biochemical means
- Functional analysis of the interaction by calcium imaging and mouse behavioral assays

3. Materials and Methods

3.1. General chemicals

Name	Supplier
[3,4-3H]-L-Glutamic acid	Hartmann Analytic GmbH, Braunschweig, Germany
5'Iodoresiniferatoxin	Tocris bioscience, Bristol, United Kingdom
Acetic acid	Carl Roth GmbH & Co. KG, Karlsruhe, Germany
Adenosine 5′-triphosphate (ATP)	Sigma-Aldrich Chemie GmbH, Schnelldorf, Germany
Agarose	Biozym Scientific GmbH, Oldendorf, Germany
AMG 9810	Tocris bioscience, Bristol, United Kingdom
Ammonium acetate	Carl Roth GmbH & Co. KG, Karlsruhe, Germany
Ammonium sulfate	Carl Roth GmbH & Co. KG, Karlsruhe, Germany
Ampicilin	Carl Roth GmbH & Co. KG, Karlsruhe, Germany
(R)-Baclofen	Tocris Bioscience, Bristol, United Kingdom
BCA Protein assay reagent A	Thermo Scientific, Pittsburgh, PA, USA
Bradykinin	Sigma-Aldrich Chemie GmbH, Schnelldorf, Germany
Beta-Glycerophosphate disodium salt	Sigma-Aldrich Chemie GmbH, Schnelldorf, Germany
Beta-Mercaptoethanol	Carl Roth GmbH & Co. KG, Karlsruhe, Germany
Bicine	Sigma-Aldrich Chemie GmbH, Schnelldorf, Germany
Bis-Tris	Carl Roth GmbH & Co. KG, Karlsruhe, Germany
Bovine serum albumin (BSA)	Sigma-Aldrich Chemie GmbH, Schnelldorf, Germany
Bromophenol blue	Carl Roth GmbH & Co. KG, Karlsruhe, Germany
Calcium chloride	Merck KgaA, Darmstadt, Germany
Capsaicin	Sigma-Aldrich Chemie GmbH, Schnelldorf, Germany
Chloroform	Carl Roth GmbH & Co. KG, Karlsruhe, Germany
Cinnamaldehyde	Sigma-Aldrich Chemie GmbH, Schnelldorf, Germany
Complete Protease Inhibitor Cocktail	Roche Pharma AG, Grenzach-Wyhlen, Germany
Copper (II) sulfate penta hydrate	Merck KgaA, Darmstadt, Germany
DMEM	Invitrogen GmbH (Gibco), Karlsruhe, Germany
Desthiobiotin	IBA GmbH, Göttingen, Germany
Dimethyl sulfoxide (DMSO)	Carl Roth GmbH & Co. KG, Karlsruhe, Germany
dNTP	New England Biolabs, Frankfurt am Main, Germany
Donkey serum	Invitrogen GmbH (Gibco), Karlsruhe, Germany
Dithiothreitol (DTT)	Carl Roth GmbH & Co. KG, Karlsruhe, Germany
EDTA	Carl Roth GmbH & Co. KG, Karlsruhe, Germany
EGTA	Carl Roth GmbH & Co. KG, Karlsruhe, Germany
Ethanol	Carl Roth GmbH & Co. KG, Karlsruhe, Germany
Ethidium bromide	Carl Roth GmbH & Co. KG, Karlsruhe, Germany
FBS (fetal bovine serum)	Invitrogen GmbH (Gibco), Karlsruhe, Germany
FCCP	Sigma-Aldrich Chemie GmbH, Schnelldorf, Germany
Flag Peptide	Sigma-Aldrich Chemie GmbH, Schnelldorf, Germany

Formaldehyde 37%	Sigma-Aldrich Chemie GmbH, Schnelldorf, Germany
Fura2	Invitrogen GmbH (Gibco), Karlsruhe, Germany
Glycerol	Carl Roth GmbH & Co. KG, Karlsruhe, Germany
Glycine	Carl Roth GmbH & Co. KG, Karlsruhe, Germany
Goat serum	Invitrogen GmbH (Gibco), Karlsruhe, Germany
Hepes	Carl Roth GmbH & Co. KG, Karlsruhe, Germany
Immu-Mount	Thermo Scientific, Pittsburgh, PA, USA
Isoflurane	Abbot Laboratories
Isopropanol	Carl Roth GmbH & Co. KG, Karlsruhe, Germany
Ketavet 10%	WDT eG, Garbsen, Germany
L-Glutamate	Sigma-Aldrich Chemie GmbH, Schnelldorf, Germany
Lipofectamine 2000	Invitrogen GmbH (Gibco), Karlsruhe, Germany
Magnesium chloride	Carl Roth GmbH & Co. KG, Karlsruhe, Germany
Menthol	Sigma-Aldrich Chemie GmbH, Schnelldorf, Germany
Methanol	Carl Roth GmbH & Co. KG, Karlsruhe, Germany
Milk powder	Carl Roth GmbH & Co. KG, Karlsruhe, Germany
MOPS	Carl Roth GmbH & Co. KG, Karlsruhe, Germany
Mustard oil	Sigma-Aldrich Chemie GmbH, Schnelldorf, Germany
n-Dodecyl β-D-maltoside (DDM)	Glycon Biochemicals GmbH, Luckenwalde, Germany
Sodium orthovanadate	Sigma-Aldrich Chemie GmbH, Schnelldorf, Germany
Paraformaldehyde	Sigma-Aldrich Chemie GmbH, Schnelldorf, Germany
Phenol	Carl Roth GmbH & Co. KG, Karlsruhe, Germany
Phenylmethylsulfonfluoride (PMSF)	Carl Roth GmbH & Co. KG, Karlsruhe, Germany
Pluronic acid F-127	Invitrogen GmbH (Gibco), Karlsruhe, Germany
Poly-D Lysine hydro-bromide	Sigma-Aldrich Chemie GmbH, Schnelldorf, Germany
Potassium Chloride	Carl Roth GmbH & Co. KG, Karlsruhe, Germany
Potassium gluconate	Sigma-Aldrich Chemie GmbH, Schnelldorf, Germany
Prostaglandin E_2	Sigma-Aldrich Chemie GmbH, Schnelldorf, Germany
Quick Start™ Bradford Dye Reagent	BioRad GmbH, Munich, Germany
RNase-free water	Ambion (Life Technologies), Karlsruhe, Germany
Rompun® (2% Xylazin)	Bayer Vital GmbH, Leverkusen, Germany
Serotonin hydrochloride	Sigma-Aldrich Chemie GmbH, Schnelldorf, Germany
Sodium acetate	Carl Roth GmbH & Co. KG, Karlsruhe, Germany
Sodium azide	Sigma-Aldrich Chemie GmbH, Schnelldorf, Germany
Sodium chloride	Carl Roth GmbH & Co. KG, Karlsruhe, Germany
Sodium dodecyl sulfate	Sigma-Aldrich Chemie GmbH, Schnelldorf, Germany
Sodium fluoride	Sigma-Aldrich Chemie GmbH, Schnelldorf, Germany
Sodium hydroxide	Carl Roth GmbH & Co. KG, Karlsruhe, Germany
Sodium-tricitrat-dihydrate	Carl Roth GmbH & Co. KG, Karlsruhe, Germany
Sucrose	Sigma-Aldrich Chemie GmbH, Schnelldorf, Germany
Tetracyline	Sigma-Aldrich Chemie GmbH, Schnelldorf, Germany
Tissue Tek	Sakura Finetek GmbH, Staufen, Germany
Triethanolamine	Carl Roth GmbH & Co. KG, Karlsruhe, Germany

Tris base	Carl Roth GmbH & Co. KG, Karlsruhe, Germany
Tris-Hydrochloride	Carl Roth GmbH & Co. KG, Karlsruhe, Germany
Triton-X-100	Sigma-Aldrich Chemie GmbH, Schnelldorf, Germany
Trizol	Ambion (Life Technologies), Karlsruhe, Germany
Trypsin-EDTA (0.25 %)	Invitrogen GmbH (Gibco), Karlsruhe, Germany
Tween-20	Carl Roth GmbH & Co. KG, Karlsruhe, Germany
Urea	Carl Roth GmbH & Co. KG, Karlsruhe, Germany
Yeast extract	Becton, Dickinson and Company, Sparks, MD, USA

3.2. Composition of prepared buffers and solutions

All buffers and solutions were prepared using Type I water (MQ) with a resistivity of 18 Mohm-cm produced with a Barnstead E-pure water purification system.

Name	**Composition**
10x PBS (pH 7.0)	80 g/l NaCl, 2.4 g/l KH_2PO_4, 2 g/l KCl, 14.4 g/l Na_2HPO_4
1x TBST	150 mM NaCl, 50 mM Tris-Cl, pH 7.4, 0.1% Tween
20x Mops SDS Running Buffer	50 mM Mops, 50 mM Tris base, 0.1% SDS, 1 mM EDTA
20x Transfer Buffer	25 mM Bicine, 25mM Bis-Tris (free base), 1 mM EDTA
50 x TAE	242g/l Tris Base, 5.71% (v/v) Glacial acetic acid, 0.05 M EDTA pH 8.0
6x loading dye	0.2 % Xylene cyanol, 0.2 % Bromphenolblue, 30 % Glycerol
6x Sample Buffer (Laemmli)	0.35 M Tris-HCl, pH 6.8, 30% Glycerol, 10% SDS, 0.06 % bromophenol blue
Blocking Solution (IH)	1% BSA, 3% Goat/Donkey Serum, 0.1% Triton X-100 in PBS
Blocking Solution (WB)	5% milk powder in 1xTBST
Buffer A (Immunoisolation)	5% BSA, 2 mM EDTA in PBS
Duolink Wash Buffer A	0.01 M Tris, 0.15 M NaCl, 0.05% Tween 20, pH 7.4
Duolink Wash Buffer B	0.2 M Tris, 0.1 M NaCl, pH 7.4
Homogenization buffer (Subcellular fractionation)	0.32 M Sucrose, 4 mM Hepes-KOH, pH 7.4
Homogenization buffer (Tissue IPs)	0.32 M Sucrose, 30 mM Tris-Cl, pH 7.4

KGC3 Buffer (Glutamate uptake)	150 mM potassium gluconate, 20 mM Pipes, 4 mM EGTA, 2 mM Na-ATP, 2,871 mM $MgCL_2$ (1 mM free Mg^{2+})
Lysis Buffer (II, Fractionation)	10 mM Hepes-KOH, pH 7.4 in ddH_20
Paraformaldehyde 4%	4% paraformaldehyde in 1 x PBS, with 0.2 M Na_2H_2PO4 pH 7.4
Ponceau S Solution	0.1% Ponceau, 5% Acetic acid
Ringer (2 Ca^{2+})	140 mM NaCl, 5 mM KCl, 2mM $MgCl_2*6H_20$, 2 mM $CaCl_2*2H_20$, 10 mM Glucose, 10 mM Hepes
RIPA Buffer	50 mM Tris-HCl, pH 7.4, 150 mM NaCl, 1% NP-40, 0.5% sodium deoxycholate, 0.1% SDS
Solubilization buffer	30 mM Tris-Cl, pH 7.4, 150 mM NaCl, 10% Glycerol, 0.1-0.5% DDM, 0.1 mM $CaCl_2$, 1 mM $MgCl_2$, 2 mM KCl
Tail lysis buffer for Genotyping	200 mM NaCl, 100 mM Tris-HCl pH 8.5, 5 mM EDTA. 0.5 % SDS, 100 µg/ml Proteinase K
TE-buffer	10 mM Tris-HCl pH 8.0, 1 mM EDTA pH 8.0

(IH = Immunohistochemistry, WB = Western Blot, II = Immunoisolation)

3.3. Enzymes and molecular weight markers

Name	Source
Restriction enzymes	New England Biolabs GmbH, Frankfurt, Germany
Taq DNA Polymerase	New England Biolabs GmbH, Frankfurt, Germany
Phusion Polymerase	New England Biolabs GmbH, Frankfurt, Germany
Reverse Transcriptase	Invitrogen GmbH, Karlsruhe, Germany
T4 Ligase	New England Biolabs GmbH, Frankfurt, Germany
Antartic Phosphatase	New England Biolabs GmbH, Frankfurt, Germany
Proteinase K (20 mg/ml)	Carl Roth GmbH & Co. KG, Karlsruhe, Germany
1 kb plus ladder	New England Biolabs GmbH, Frankfurt, Germany
100 bp ladder	New England Biolabs GmbH, Frankfurt, Germany
PageRuler Protein ladder	Thermo Scientific, Schwerte, Germany

3.4. Bacteria strains

Strain	Genotype
E. coli DH10 beta	F^- endA1 recA1 galE15 galK16 nupG rpsL ΔlacX74 Φ80lacZΔM15 araD139 Δ(ara,leu)7697 mcrA Δ(mrr-hsdRMS-mcrBC) λ^-
E. coli SW102	F- mcrA Δ (mrr-hsdRMS-mcrBC) Φ80dlacZ M15 ΔlacX74 deoR recA1 endA1 araD139 Δ(ara, leu) 7649 galU galK rspL nupG [λcI857 (cro-bioA) <> tet]

3.5. Cell lines

Cell line	Description
Hek293	Human embryonic kidney 293 cells
F11	Hybrid of a rat embryonic dorsal root ganglion (DRG) and mouse neuroblastoma cell line N18TG2

3.6. Culture Media

Medium	Composition
LB Medium	10 % Tryptone, 5 % Yeast extract, 10 % NaCl, adjusted to pH 7.0
Mammalian cell culture medium	10 % FBS in DMEM
Ham's F12 Medium	10% FBS, 1xHAT in F12-Medium
Mouse DRG culture medium	500 µl MEM Vitamins (100x), 5 ml Goat serum, 500 µl P/S, 500 µl Uridine (3.5mg/ml)/5-Fluoro-2 deoxyuridine (1.5mg/ml) in 50 ml F12-Medium

3.7. Oligonucleotides

All oligonucleotides used were obtained from Eurofins MWG Operon. They were designed to be between 20 and 35 bp in length to ensure specific binding to the template. Furthermore, the melting temperature (Tm) of primers used within one reaction was chosen to be similar to ascertain optimal annealing temperature suitable for both primers.

Name	Sequence (5' → 3')	Usage
SF-TRPV1 BAC F6	TGACAAGAAGAGCGTGGAGGGG	Genotyping
SF-TRPV1 BAC R6	AGCTGACGGTGATGATAGGGCAGG	Genotyping
Vglut2 ER1 Fwd	AAGAATTCGCCACCATGGAGTCGGTAAAACAAAGGAT	Cloning
Vglut2 Not1 Rev	AAGCGGCCGCTTATGAATAATCATCTCGGTCCTTATAG	Cloning
$GABA_{B1}$ ERI Fwd	AAGAATTCGCCACCATGCTGCTGCTGCTGCTGGTGC	Cloning
$GABA_{B1}$ NotI Rev	AAGCGGCCGCTCACTTGTAAAGCAAATGTACTC	Cloning
$Gaba_{B2}$ Rev	AAGCGGCCGCCTACAGGCCCGAGACCATG	Cloning
$Gaba_{B2}$ Fwd	AAGAATTCGCCACCATGGCTTCCCCGCCGAGCTCC	Cloning
TRPV1 Kpn1 Fwd	GGTACCAAGAGAAATGGGCTAGCTTAGACTCGG	Cloning
TRPV1 Not1 Rev	AAGCGGCCGCTCATTTCTCCCCTGGGGCC	Cloning
Tag Sal1 Fwd	AAAGTCGACGCCACCATGGATTATAAAGATGATG	Cloning
Tag Kpn1 Rev	AAGGATCCTCCTTTCTCGAACTGCGGGTG	Cloning
Vglut2 wt fwd	CGAGAATTGCCTCTGATG CTGTGAGAG G	Genotyping
Vglut2 wt/ko rev1	CAAGCCTTCCTCTTTCAGTGG	Genotyping
Vglut2 TG R	CGCAAGCCCGGTGCCTGA	Genotyping

3.8. Plasmid vector backbones

Name	Company
pBlueScript	Stratagene
pCS2+	Addgene Inc.
pCDNA3.1(-)	Invitrogen
EGFP c1	Clonetech

3.9. Kits

Purpose	Kit	Supplier
Protein detection	Amersham™ ECL plus WB detection kit	GE Healthcare
Protein detection	Super Signal West Dura	Thermo Scientific
Gel extraction	QIAquick® gel extraction kit	Qiagen, Hilden, Germany
DNA purification	QIAprep® spin miniprep kit	Qiagen, Hilden, Germany
DNA purification	HighSpeed® Plasmid Midi kit	Qiagen, Hilden, Germany
DNA purification	EndoFree® Plasmid maxi kit	Qiagen, Hilden, Germany

3.10. Antibodies

3.10.1. Primary Antibodies

Name	Dilution	Supplier
Flag M2, monoclonal, ms	1:1000 (IHC, ICC, WB)	Sigma-Aldrich 3165
$GABA_{B1}$, polyclonal, gp	1:1000 (IHC, ICC, WB)	Chemicon 2256
$GABA_{B2}$, polyclonal, gp	1:1000 (IHC, ICC, WB)	Chemicon 5394
NMDA, monoclonal, ms	1:5000 (WB)	Synaptic Systems 114001
Strep546, monoclonal, ms	1:200 (IHC, ICC)	IBA GmbH 2-1540-005
Strepmap classic, monoclonal, ms	1:1000 (WB)	IBA GmbH 2-1507-001
Synaptogyrin-1, polyclonal, rb	1:10000 (WB)	Synaptic Systems 103002
Synaptophysin, monoclonal, ms	1:30000 (WB)	Synaptic Systems 101011
TRPV1, polyclonal, gt	1:5000 (WB)	Santa Cruz sc-12498
TRPV1, polyclonal, gp	1:2000 (IHC, ICC, WB)	David Julius group
TRPV1, polyclonal, rb	1:2000 (IHC, ICC)	David Julius group
Vgat, polyconal, rb	1:200 (ICC), 1:10000 (WB)	Synaptic Systems 131002
Vglut2, monoclonal, ms	1:200 (ICC)	Millipore MAB5504
Vglut2, monoclonal, ms	0,5 µg [1]	Synaptic Systems 135411
Vglut2, polyclonal, rb	1:200 (ICC), 1:10000 (WB)	Synaptic Systems

(IHC= Immunohistochemistry, ICC = Immunocytochemistry, WB= Western Blot,
II= Immunoisolation, ms = mouse, gp = guinea pig, gt = goat, rb = rabbit)
[1] amount of antibody/10^7 Beads (Pan-Mouse-IgG).

3.10.2. Secondary Antibodies

Name	Dilution	Supplier
Goat anti-mouse-HRP	1:20000	Jackson ImmunoResearch, UK
Goat anti-guinea pig-HRP	1:20000	Jackson ImmunoResearch, UK
Goat anti-rabbit-HRP	1:20000	Jackson ImmunoResearch, UK
Rabbit anti-goat-HRP	1:20000	Jackson ImmunoResearch, UK
Alexa Fluor® 488 goat α-Mouse IgG	1:1000	Invitrogen GmbH (Molecular probes), Germany
Alexa Fluor® 555 goat α-Mouse IgG	1:1000	Invitrogen GmbH (Molecular probes), Germany
Alexa Fluor® 555 goat α-rabbit IgG	1:1000	Invitrogen GmbH (Molecular probes), Germany
Alexa Fluor® 488 donkey α-Rabbit IgG	1:1000	Invitrogen GmbH (Molecular probes), Germany
Alexa Fluor® 555 donkey α-Goat IgG	1:1000	Invitrogen GmbH (Molecular probes), Germany
Alexa Fluor® 488 donkey α-Goat IgG	1:1000	Invitrogen GmbH (Molecular probes), Germany
Alexa Fluor® 488 goat α-guinea pig IgG	1:1000	Invitrogen GmbH (Molecular probes), Germany

3.11. Beads for protein purification

Name	Supplier
Anti-Flag affinity gel	Sigma-Aldrich Chemie GmbH, Schnelldorf, Germany
Anti-Flag M2 magnetic beads	Sigma-Aldrich Chemie GmbH, Schnelldorf, Germany
Dynabeads Pan mouse IgG	Invitrogen GmbH (Gibco), Karlsruhe, Germany
Strep-tactin superflow	IBA GmbH, Göttingen, Germany

3.12. Equipment

Molecular Biology

Name	Supplier
Sorvall 250 ml dryspin tubes 03069	Thermo Scientific, Schwerte, Germany
C1000^{TM} Thermal Cycler	BioRad GmbH, Munich, Germany
Centrifuge 5417 R	Eppendorf, Cologne, Germany
Centrifuge 5804 R	Eppendorf, Cologne, Germany
Gel documentation	Chemidoc BioRad, Munich, Germany
Microwave	Daewoo KOR-8605, Germany
OWL Easycast^{TM} B2	Thermo Scientific, Schwerte, Germany
Power Source 250V	VWR, Darmstadt, Germany
Rotor SLA-3000 Super-Lite	Thermo Scientific, Schwerte, Germany
Sorvall Rotor SS34	Thermo Scientific, Schwerte, Germany
Sorvall RC 6+ Centrifuge	Thermo Scientific, Schwerte, Germany
Nanodrop ND-1000	Peqlab Biotechnology GmbH, Erlangen, Germany
Thermomixer	Eppendorf, Cologne, Germany
GenePulser xCell	BioRad GmbH, Munich, Germany

Cell culture

Cell incubator	Binder GmbH, Germany
Laminar flow hood	BDK, Germany
Cell culture plates and dishes	CellStar, Greiner Bio-one, Germany

Biochemistry

Centrifuge, Maxima Ultracentrifuge	Beckman Coulter GmbH, Krefeld, Germany
Film processor apparatus	Fuji, Japan
Dissection Microscope	Olympus SZ61
Douncers and glass homogenizers	Various suppliers
DynaMag^{TM}-2	Invitrogen GmbH (Gibco), Karlsruhe, Germany
Microscope Lamp KL 1500 LCD	Schott, KL 1500 LCD, Germany
Needles, 23G and 27G	Braun Melsungen AG, Germany
Plate Reader Infinite M2000	Tecan Group Ltd., Germany
Sorvall Rotor TH 641	Thermo Scientific, Schwerte, Germany
Rotor TLA 100.3	Beckman Coulter GmbH, Krefeld, Germany
Rotor TLA 100.4	Beckman Coulter GmbH, Krefeld, Germany
Rotor TLA 120.1	Beckman Coulter GmbH, Krefeld, Germany
Scanner CanoScan Lide 200	Canon, Germany
Scintillation counter	Tri-Carb3110 Perkin Elmer
Sonifier	Branson (Emerson technologies GmbH), Germany
WX Ultra 80 Centrifuge	Sorvall WX Ultra Series, Thermo Electron Corp.
X-cell *SureLock TM* mini cell system	Invitrogen GmbH (Gibco), Karlsruhe, Germany

3.13. Animals

All animals were housed with ad libitum access to food and water in rooms air conditioned at 22-23°C with constant temperatures under a 12/12 hours light/dark cycle. All procedures were in accordance with ethical guidelines laid down by the local governing body. Wild type C57Bl/6 mice were obtained from Charles River laboratory and used for breeding and backcrossing. Vglut2 heterozygous mice were obtained from Dr. Christian Rosenmund. TRPV1 knockout mice were obtained from Dr. David Julius.

3.14. Molecular Biology

Standard molecular cloning methods were performed according to Sambrook and Russel (2001).

3.14.1. Agarose Gel Electrophoresis

Agarose gel electrophoresis can be used to separate and analyze molecules by their molecular weight. It was performed to analyze PCR and *in vitro* transcription products. Depending on the expected fragment size the DNA samples were loaded onto a 1 % - 1.5 % gel prepared in 1x TAE buffer. Ethidium bromide was added to the gel to facilitate visualisation of the DNA fragments under UV light. 1 kb or 100 bp ladders were used as a DNA standard. For permanent documentation, gels were photographed using a ChemicDoc (BioRad).

3.14.2. Amplification of DNA fragments by PCR

PCR is a rapid procedure for *in vitro* amplification of a DNA sequence by using specific oligonucleotide primers and a thermostable DNA polymerase. Repetitive cycles of template denaturation, primer annealing and extension of annealed primers result in an exponential amplification of the DNA fragment. The reaction mix was prepared on ice, adding the polymerase last and was composed of 1.5 µl DNA template, 1.25 µl 10x Coral load PCR buffer (Qiagen), 0.25 µl of 10mM dNTPs (Qiagen), 0.625 µl F-primer (10 µM), 0.625 µl R-primer (10 µM) and 0.15 µl of Taq DNA polymerase (NEB) in a volume of 12.5 µl. All PCRs were carried out in the PCR C1000^{TM} thermal cycler (BioRad). Finally, PCR products were analyzed on 1-1.5 % agarose gels.

3.14.3. Restriction digest

DNA was digested using endonucleases (New England Biolabs) that cut DNA at specific restriction sites. Therefore, 1 µl of the restriction enzyme and 3 µl of the required restriction buffer were added to an appropriate amount of DNA (~ 0.5 µg). The final volume was adjusted to 30 µl with DNase-free water. The digest was incubated for 1 hour at the temperature required for the restriction enzyme. For molecular cloning the amount of DNA was increased (5-10 µg), depending on the expected fragment sizes.

3.14.4. Gel purification of DNA

The QIAquick® gel extraction kit (Qiagen, Germany) was used to isolate and purify enzyme digested or PCR-amplified plasmid DNA after agarose gel electrophoresis. The bands of interest were cut out of a 1% agarose gel under UV light and liquefied in 600 µl QC buffer at 55°C for 10 min. The extraction was performed according to the manual and the DNA was eluted in 30 µl of TE buffer.

3.14.5. Vector dephosphorylation

During ligation, DNA ligase catalyzes the formation of a phosphodiester bond between adjacent nucleotides only if one nucleotide contains a 5'-phosphate group and the other a 3'-hydroxyl group. Recircularization of plasmid DNA can therefore be minimized by removing the 5' phosphates from both ends of the linear DNA with Phosphatase to decrease vector background after transformation. It was carried out in a total volume of 30 µl using 10x buffer and 1 µl of the Antarctic phosphatase. The samples were incubated at 37°C for 30 min.

3.14.6. Ligation

DNA fragments can be rejoined by ligation. In terms of molar ratios 3-6 times more insert than vector was used. Each ligation was set up in a volume of 10 µl containing 1 µl of T4 DNA ligase and 1 x T4 ligation buffer. The ligations were incubated at 16°C over night (o/n).

3.14.7. Transformation

DNA was transformed into bacteria using electroporation. Therefore, cells were thawed on ice and mixed with 1 µl of the ligation reaction. After 1 min incubation on ice the suspension was electroporated (Voltage 1.8 KV, Capacitance 25 µV, Resistance 200) using a GenePulser xCell (BioRad). Afterwards the cells were washed out with 1mL of SOC medium and incubated at 37°C for 1 h with horizontal shaking. Finally, several dilutions were spread on agar plates containing the appropriate antibiotic. Incubation took place in a 37°C room o/n.

3.14.8. Plasmid DNA extraction

Plasmid DNA extraction was carried out using the Miniprep kit (Qiagen). All steps were done according to the manual. For isolating larger amounts of plasmid DNA from overnight cultures the Plasmid Maxiprep Kit (Qiagen) was used. The isolation was performed according to the manual.

3.14.9. Phenol-Chloroform Extraction

Phenol-Chloroform extraction was used to purify DNA. An equal volume of phenol/chloroform was added to the DNA sample and mixed thoroughly. After the samples were centrifuged at 12,000 rpm for 2-3 min, the upper phase containing the DNA was carefully transferred into a new tube. An equal volume of chloroform was added to remove remaining traces of protein and phenol. After another centrifugation the collected upper phase was precipitated with ammonium acetate and ethanol to increase DNA concentration.

3.14.10. Sequencing

DNA sequencing was carried out by Eurofins MWG Operon. For double-stranded plasmid-DNA 80ng/µl of DNA was mixed with 10 pmol/µl of sequencing-primer.

3.14.11. Extraction of DNA from mouse tails for genotype analysis

For genotyping the tissue was digested in tail lysis buffer with Proteinase K (50µg/ml) at 55°C over night. Following heat inactivation for 10 min at 90°C, 300 µl of MiliQ water were added to the sample. 1.5 µl of this sample was used in a PCR reaction.

3.14.12. Reverse Transcription-PCR (RT-PCR)

Reverse Transcription was performed to generate cDNA from DRG in order to amplify the genes of Vglut2 and Vglut1. Therefore, lumbar and thoracal DRGs were dissected from wild type mice and immediately collected in 1 ml of ice cold Trizol. Tissue was destructed mechanically using glass homogenizers and incubated at room temperature (RT) for 5 min to allow the dissociation of nucleic acids. All of the

following steps were carried out at 4°C. After addition of 200 µl Chloroform the samples were incubated for 2-3 min at RT and centrifuged at 16000 x g for 5 min. The upper phase containing the RNA was collected in a fresh tube and 500 µl Isopropanol was added. The samples were incubated on ice for 10 min to allow precipitation of nucleic acids. After a 10 min centrifugation at 16000 x g the obtained pellet was washed twice with 75 % RNase-free ethanol, centrifuged and finally resuspended in 20 µl of RNase-free water. The purity of the RNA content was determined spectrophotometrically.

RNA was reverse transcribed using the SuperScriptTM III Reverse transcriptase kit (Invitrogen). Briefly, 1 µg total RNA was mixed with 1µl oligo (dT) (50 µM) and 1µl dNTP mix (10 mM). This reaction was heated to 65°C for 5 min and incubated on ice for 1 min. After addition of 1µl SuperScriptTM III Reverse Transcriptase, 1µl 0.1 M DTT and 2µl First-Strand Buffer the reaction was incubated at 50°C for 60 min. This step was followed by heating at 70°C for 15 min to inactivate the reaction. The cDNA was then used as a template for gene amplification in a PCR.

3.15. Generation of SF-TRPV1 BAC transgenic mice

BAC transgenic mice were generated that express a tagged version of TRPV1 only in sensory neurons that natively express the receptor. Therefore, the Strep-Flag (SF)-tag (provided by Dr. Glöckner) was inserted into a mouse BAC clone (RP23-390G23, Imagene) encoding the TRPV1 gene and one neighboring gene (ItgAE and TRPV3) on each side. The SF-tag was inserted behind the start codon of the TRPV1 gene using *galK*-based positive-negative selection as described by Warming *et al.* (Warming et al., 2005). This selection procedure allows BACs to be manipulated without the introduction of selectable markers at the modification site. It uses a bacterial strain (*E. coli* SW102) containing the λ prophage recombineering system. This strain is defective in using galactose as a carbon source due to the deletion of the galactokinase gene (*galK*) from the galactose operon. Fig. 8 shows an overview of the *galK* selection procedure. The selection scheme is a two-step system:

1) A positive selection step: targeting the BAC with the *galK* cassette containing homology to a defined position within the BAC. In brief, the *galK* cassette was PCR-amplified from the pGalK plasmid with homology arms added to the primers. The homology arms ensure the correct positional integration of the SF-tag behind the start codon of TRPV1. Prior to transformation, the bacteria

were heated to 42°C for 15 min to activate expression of the recombination genes from the λ *pL* promoter. Electroporation (V=1.75 kV, R = 200 Ω, C = 25 µF) of the *galK* cassette into the BAC and subsequent growth of the bacteria (*E. coli* SW102, *galK* defective) at 32°C on minimal plates containing chloramphenicol and galactose as the carbon source to maintain the BAC led to insertion of the galK cassette. Bacteria become therefore phenotypically *galK* positive.

2) A negative selection step: replacement of the *galK* cassette by the sequence of the SF-tag through a second homologous recombination event. The insertion was achieved by selection for the loss of *galK* in the presence of 2-deoxy-galactose (DOG) on minimal plates containing DOG and glycerol as the sole carbon source. DOG is harmless unless phosphorylated by functional *galK*. Phosphorylation of DOG by galactokinase turns DOG into a nonmetabolizable intermediate that is toxic to the cells. Only bacteria that incorporated the SF-tag sequence and use glycerol survive.

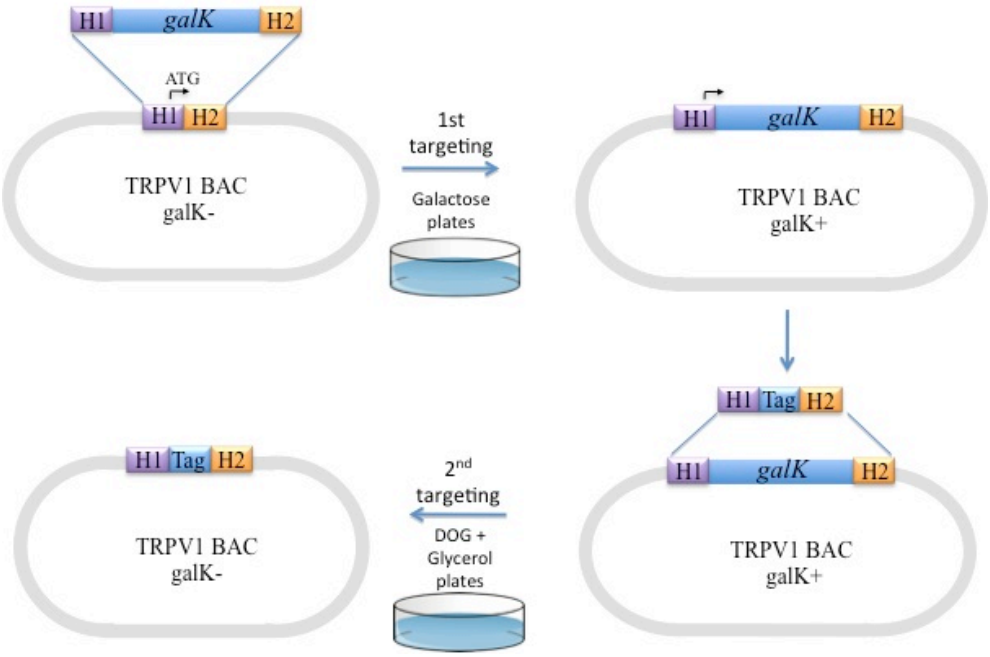

Figure 8: Overview of the *galK* selection procedure

GalK based recombineering is composed of two targeting events: 1) targeting the galk cassette to a defined region on the BAC and 2) removal of the galk cassette by replacement by the SF-tag sequence. Modified from Warming et al., 2005

Modified BAC clones were analysed by restriction digests (EcoRI and SpeI) and PCR to verify BAC integrity. The SF-tag was PCR amplified from the BAC and sent for sequencing to ensure that the tag was in frame with the start codon of TRPV1. In

addition, Pulse field gel electrophoresis was performed to verify the correct size of the BAC. Finally, one modified BAC clone was purified by ultracentrifugation as described in 3.15.1.

3.15.1. BAC DNA purification for transgenesis

All steps of BAC DNA isolation and ultracentrifugation were performed according to the gensat protocol (www.Gensat.org). The extracted BAC DNA was purified by ultracentrifugation in a CsCl gradient. Ultracentrifugation was performed for 20 h at 18°C at 360000 x g using a Ti90 rotor (Beckman). The bottom band was isolated with a syringe, five times extracted with NaCl saturated butanol, precipitated and dissolved in 30 µl TE. The BAC DNA was then linearized with 4 µl of I-SceI in a final volume of 100 µl and dialyzed for at least 4 hours against the injection buffer. BAC DNA (2 ng/µl) was injected into the fertilized oocytes of BDF/BL6 mice.

3.16. Vectors

3.16.1. SF-TRPV1

SF-TRPV1 was generated encoding the Strep-Flag (SF)-tag (provided by Dr. Gloeckner) fused to the N-terminus of TRPV1. Therefore, TRPV1 was PCR amplified from a pCDNA3 plasmid with primers carrying a KpnI and Not1 site and subcloned into the pCRII-Topo vector (Invitrogen). The start codon was thereby removed. The SF-Tag was PCR amplified with primers carrying a SalI and KpnI site and inserted into the pCR-II-Topo vector. Subsequently, both modified Topo vectors were cut using the respective enzymes and ligated in frame into the mammalian pCS2+ expression vector.

3.16.2. Vglut2 and Vglut1

The cDNAs corresponding to the open reading frame of mouse Vglut2 and Vglut1, respectively, were amplified by PCR from a cDNA that was generated from mouse DRG. Primers for Vglut2 and Vglut1 were engineered to contain EcoRI and NotI restriction sites to facilitate cloning into the mammalian expression vector pCDNA3.1 (Invitrogen).

3.16.3. $GABA_{B1}$ and $GABA_{B2}$

The cDNAs for $GABA_{B1}$ and $GABA_{B2}$ were obtained from Imagene (# 6401243, 6816977) and PCR amplified using primers containing EcoRI and NotI restriction sites. After subcloning into the TOPO TA vector (Invitrogen), both genes were cut out using the respective restriction enzymes and ligated into pCDNA3.1 expression vectors.

3.17. Cell culture

3.17.1. Cell culture of Hek293 and F11 cells

Cells were maintained in a humidified atmosphere at 5% CO_2 and 37°C. Hek293 cells were grown in DMEM medium supplemented with 10% Fetal Bovine Serum (FBS) and penicillin/streptomycin. F11 cells were cultured in Ham's 12 Medium supplemented with 10% FBS and 1xHAT. Cells were passaged every 3-4 days after reaching 80-90 % confluence by washing with 5 ml 1 x PBS and trypsinizing with 1 ml 0.25 % Trypsin-EDTA for 2 min. Digestion was stopped by adding 7 ml medium, and 1 ml of cells was seeded in a new culture dish with 10 ml medium. For transient transfection, Lipofectamine 2000 (Invitrogen) and serum-free optimum (Invitrogen) were used according to the manufacturer's instructions. For immunostaining, the cell number after trypsinization was determined by counting eight squares (0.1 mm^3 volume each) in a Neubauer hematocytometer, calculating the mean and multiplying it with dilution factor and with 104 to obtain the number of cells per ml. Subsequently, 5 x 104 cells per well were seeded on Poly-D-Lysine (100 µg/ml in PBS) coated glass coverslips (13 mm) in a 12well plate.

3.17.2. Primary DRG culture

DRG were quickly dissected and collected in ice-cold DRG medium. Subsequently, the DRG were incubated in 1 mg/ml Collagenase IV (Gibco) at 37°C for 30 min to dissociate the tissue. After removal of the supernatant and washing with PBS, the DRG were incubated in 0.05 % trypsin (Gibco) in PBS at 37°C for 15 min. The trypsin was removed and the cells were resuspended in 1 ml of DRG medium. After gentle titruation the DRG were loaded onto a 2 ml BSA pillow and centrifuged at

250xg for 5 min to separate the myelin and debris. The resulting cell pellet was resuspended in 50 µl fresh DRG medium and plated onto Poly-D-lysine (100 µg/ml) and laminin (10 µg/ml) coated coverslips. The cells were flooded with medium 30 min after plating.

3.17.3. Immunocytochemistry of cultured F11 cells

For immunostaining of cultured F11 cells, cells were grown on Poly-D-Lysine (100 µg/ml) coated coverslips and fixed with 2% PFA for 10 min at 4°C. Following three washing steps in 1 ml PBS for 5 min each, cells were blocked for 1 h in PBS/1 % BSA/3 % goat or donkey serum. In order to allow intracellular access of the antibodies, the blocking solution also contained 0.1% Triton X-100. Subsequently, the coverslips were incubated in a wet chamber in 50 µl primary antibody solution over night at 4°C. After washing two times with 1 ml PBS for 10 min, the coverslips were incubated with secondary antibody solution for 1 h at RT. Finally, following three washing steps with 1 ml PBS, the coverslips were mounted to objective slides in a drop of ImmuMount.

3.17.4. Proximity Ligation Assay (PLA) on cultured F11 and DRG neurons

Cultured F11 cells or DRG neurons, respectively, were grown on Poly-D-Lysine (100 µg/ml) coated coverslips and fixed with 2% PFA for 10 min at 4°C. Following three washing steps in 1 ml PBS, cells were blocked in PBS/1 % BSA/3 % goat serum/0.1 % Triton for 1 hour at RT. Afterwards, the cells were incubated in primary antibody solution (mouse anti-Vglut2, rabbit anti-TRPV1) for 1 h at RT. Following two PBS washes, cells were incubated with the PLA probes (rabbit plus PLA, mouse minus PLA) (1:5 in blocking solution) in pre-heated humidity chambers at 37°C for 1 hour. This was followed by two washing steps in washing buffer A and incubation of the cells in the ligation solution for 30 min at 37°C. After washing the cells with washing buffer A, they were incubated in the amplification solution for 100 min at 37°C. Subsequently, cells were washed twice in washing buffer B for 10 min and mounted to objective slides in a drop of ImmuMount.

3.18. Biochemistry

3.18.1. Protein purification from heterologous cell expression systems

Proteins were purified from transiently transfected Hek293 or F11 cells grown in 6-well plates or 10 cm dishes. After quick washing of the cells with ice cold PBS, they were resuspended in solubilization buffer including 1 mM PMSF, 1xEDTA-free Protease inhibitors cocktail, 5 mM NaF, 1 mM NaOV, 20 mM β-Glycerophosphate. Cells were left for 20 min at 4°C to rotate to ensure complete lysis. Cell debris and nuclei were spun down at 17000 x g at 4°C. Solubilized protein was incubated with the respective affinity resin for 2 hours on a rotating wheel at 4°C. After washing the beads three times with 1 ml of washing buffer (30 mM Tris, pH 7.4, 150 mM NaCl, 0.1 mM $CaCl_2$, 1 mM $MgCl_2$, 2 mM KCl, 10% glycerol, 0.5% DDM) proteins were eluted with 2x Laemmli buffer.

3.18.2. Protein purification from mouse tissue

DRG, sciatic nerve and spinal cords from BAC transgenic SF-TRPV1 and wild type control mice were quickly dissected and snap frozen in liquid nitrogen. All procedures were carried out at 4°C. The tissue was homogenized in cold homogenization buffer (0.32 M sucrose, 30 mM Tris-Cl pH 7.4, 1x EDTA-free protease inhibitor cocktail, 1 mM PMSF, 5 mM NaF, 1 mM NaOV, 20 mM β-Glycerophosphate) using a glass-teflon homogenizer for 10 min. This was followed by a low speed spin at 250 x g for 10 min to remove the nuclear fraction and cell debris. The supernatant was cleared by ultracentrifugation in a TLA 100.3 rotor (200000 x g for 50 min) to yield crude cytosol and the plasma membrane fraction. Plasma membrane enriched protein fractions were solubilized at 4°C for 1 hour using solubilisation buffer including 1 mM PMSF, 1x EDTA-free protease inhibitor cocktail, 5 mM NaF, 1 mM NaOV, and 20 mM β-Glycerophosphate. Unsolubilized material was removed by centrifugation (10 min at 17000 x g). 1 mg/ml of solubilisates were incubated for 2 hours at 4°C with 50 µl of Flag or Strep beads. After three washing steps, bound proteins were eluted with either 6 M Urea/2 M Thiourea (for mass spectrometry analysis), 2x Laemmli buffer (Western Blot analysis) or the Flag peptide (200 µg/ml) (Western

Blot analysis), respectively. Eluates were analyzed by western blots or silver stained gels.

3.18.3. Determination of protein concentration by Bradford

The Bio-Rad Protein Assay, based on the method of Bradford, is an accurate procedure for determining concentration of solubilized protein. It involves the addition of an acidic dye to protein solution, and subsequent measurement at 595 nm with a microplate reader. Comparison to a BSA standard curve provides a relative measurement of protein concentration.

3.18.4. Mass spectrometry

Proteins were affinity purified as described in 3.18.2 and proceeded to in-solution digestion followed by LC-MS/MS analysis. Mass spectrometry was performed in collaboration with Dr. Marie-Luise Kirchner from Matthias Selbach's group. In brief, protein eluates were reduced for 30 min at RT in 10 mM dithiothreitol solution followed by alkylation for 20 min by 55 mM iodacetamide in the dark at RT. The endoproteinase LysC (Wako, Japan) was added following a protein:enzyme ratio of 50:1 and incubated for 4h at RT. After dilution of the sample with 4x digestion buffer (50 mM ammonium bi-carbonate in water (pH 8.0)), sequence grade modified trypsin (Promega) was added (same protein:enzyme ratio as for LysC) and digested over night. Finally, trypsin and Lys-C activity were quenched by acidification of the reaction mixtures with TFA to pH ~2. Afterwards, peptides were extracted and desalted using StageTips (Rappsilber et al., 2003). Peptide mixtures were separated by reversed phase chromatography using the EASY-nLC system (Thermo Scientific) on in-house manufactured 20 cm fritless silica microcolumns with an inner diameter of 75 µm. Columns were packed with ReproSil-Pur C18-AQ 3 µm resin (Dr. Maisch GmbH). Peptides were separated on a 8-60% acetonitrile gradient (214 min) with 0.5% formic acid at a nanoflow rate of 200 nl/min. Eluting peptides were directly ionized by electrospray ionization and transferred into a Q Exactive mass spectrometer (Thermo Scientific). Mass spectrometry was performed in the data dependent positive mode with one full scan (m/z range = 300-1,700; R = 70,000; target value: 3 x 106; maximum injection time = 120 ms). The 10 most intense ions with a charge state greater than one were selected (R = 35,000, target value = 5 x 105;

isolation window = 4 m/z; maximum injection time = 120 ms). Dynamic exclusion for selected precursor ions was set to 30s.

3.18.4.1. Data Analysis

MS/MS data were analyzed by MaxQuant software v1.2.2.5 as described (Cox et al., 2011). The internal Andromeda search engine was used to search MS/MS spectra against a decoy *mus musculus* UniProt database (MOUSE.2012-06) containing forward and reverse sequences. The search included variable modifications of methionine oxidation and N-terminal acetylation, and fixed modification of carbamidomethyl cysteine. Minimal peptide length was set to six amino acids and a maximum of two missed cleavages was allowed. The false discovery rate (FDR) was set to 0.01 for peptide and protein identifications. If the identified peptide sequence set of one protein was equal to or contained another protein's peptide set, these two proteins were grouped together and the proteins were not counted as independent hits. Label-free quantitation (LFQ) was performed in MaxQuant as described (Hubner et al., 2010). Unique and razor peptides were considered for quantification with a minimum ratio count of 1. Retention times were recalibrated based on the built-in nonlinear time-rescaling algorithm. MS/MS identifications were transferred between LC-MS/MS runs with the “Match between runs” option in which the maximal retention time window was set to 2 min. For every peptide, corresponding total signals from multiple runs were compared to determine peptide ratios. Median values of all peptide ratios of one protein then represent a robust estimate of the protein ratio. LFQ intensity values were logarithmized and missing values were imputed with random numbers from a normal distribution, whose mean and standard deviation were chosen to best simulate low abundance values below the noise level (width = 0.3; shift = 1.8). SF-TRPV1 pull-down (antibody specific) samples and wild type control samples were selected as individual groups of 3 technical replicates each; significantly enriched proteins were determined by a volcano plot-based strategy, combining standard two-sample t-test p-values with ratio information. Significance corresponding to an FDR of 1 was determined by a permutation-based method (Tusher et al., 2001).

3.18.4.2. Mass spectrometry with Logopharm GmbH

One mass spectrometry run was carried out by Logopharm GmbH, Freiburg. Therefore, affinity purified protein isolates were eluted with 2x Laemmli buffer. After addition of 1 M DTT, the samples were separated on a SDS-Gel and silverstained (without crosslinker). The gel was divided into two fractions and subjected to in-gel digestion as described (Pandey and Mann, 2000). This was followed by liquid chromatography-tandem mass spectrometry using a high-resolution hybrid-Mass spectrometer (LTQ Orbitrab XL, Thermo Scientific) coupled to a nano-HPLC-System (UltiMate 3000, Dionex). Analysis was performed by Logopharm GmbH.

3.18.5. SDS-PAGE and Western Blot

Protein samples (5-15 µg per lane) were analyzed by discontinuous SDS-PAGE (sodium dodecyl sulfate-polyacrylamide gel electrophoresis) by separation in 4-12% polyacrylamide gel according to their molecular weight using the Xcell SureLock™ mini-cell system (Invitrogen). Laemmli sample buffer (6x) and β-mercaptoethanol as a reducing agent were added to all samples prior to loading. Afterwards, the gel was removed from the chamber and used for Western blotting. Western blotting is the process of transferring proteins from a polyacrylamide gel to a membrane where they are fixed and can be detected by specific antibodies. Before use, Immobilon polyvinylidene fluoride (PVDF) membranes (Roche) were soaked in methanol for 1 min. The transfer was carried out in semi-wet conditions with 1x NuPAGE® transfer buffer for 60 min at 35 V. Afterwards, the membrane was blocked in 5 % milk powder in TBS-T for 1h at RT. Subsequently, the membrane was incubated in primary antibody prepared in blocking solution at 4°C o/n. Following three washing steps with TBS-T, the membrane was incubated with an HRP (horse radish peroxidase) secondary antibody (1:20000 in blocking solution) for 1 h. Horseradish peroxidase catalyzes the oxidation of hydrogen peroxide to 3-aminophthalate via several intermediates, which leads to emission of low intensity light that can be enhanced by certain chemicals up to 1000-fold, thereby simplifying detection and increasing the sensitivity of the reaction (enhanced chemiluminescence (ECL). Following three washing steps, the signal of bound antibody was detected using the ECL plus western blotting detection system (GE Healthcare, Germany), which generates a chemifluorescent signal at 440 nm that can be detected on a fluorescence

imager as well as on film. The membrane was exposed to a CL-X Posure™ film (Thermo Scientific, Germany) for 1-30 min to detect the chemiluminescence. The films were developed in a film processor apparatus (Fuji, Japan).

3.18.6. Silverstaining

Silverstaining is a rapid method to silver stain proteins in polyacrylamide gels. The SilverQuest Silver Staining Kit (Invitrogen) was used and is based on the chemical reduction of silver ions to metallic silver on a protein band. All steps were done according to the manual.

3.18.7. Subcellular fractionation of the spinal cord

Subcellular fractionation of the spinal cord was carried out as originally described by Huttner et al., 1983 (Huttner et al., 1983). Briefly, mouse or rat spinal cords were freshly dissected and homogenized in ice-cold buffer (320 mM sucrose, 4 mM HEPES/KOH, pH 7.4, 1 mM PMSF, and 1 µg/ml protease inhibitor cocktail) and centrifuged for 10 min at 4°C and 1300 × *g* using a TLA 100.4 rotor. The resulting supernatant 1 (S1) was centrifuged at 14000 × *g* for 15 min, yielding a synaptosome-containing pellet (P2). The synaptosomes were hypo-osmotically shocked by diluting them 1:10 in lysis buffer (10 mM HEPES/KOH, pH 7.4, 1 mM PMSF, and 1 µg/ml protease inhibitor cocktail) and mechanically disrupted using a Teflon-glass homogenizer. These lysed synaptosomes (LS0) were used for immunoisolation. Glutamate uptake experiments were performed with the crude synaptic vesicle fraction (LP2) prepared from LS0 by centrifugation at 30000 x g for 20 min and subsequent centrifugation of LS1 at 300000 x g for 30 min at 4°C.

3.18.8. Immunoisolation

As starting material for immunoisolation, synaptosomes from adult mouse spinal cords were prepared. Superparamagnetic beads (Dynabeads Pan Mouse IgG, Invitrogen) were incubated for 2 h at 4°C in coating buffer (PBS, pH 7.4, 0.1 % BSA) supplemented with 1 µg of IgG per 10^7 beads of the primary mouse antibodies directed against Flag or Vglut2. The coated beads were washed three times in coating buffer and then incubated overnight at 4°C with the LS0 fraction suspended in

incubation buffer (PBS, pH 7.4, 2 mM EDTA, and 5 % BSA) at a ratio of 200 µg of protein to 1.4×10^7 beads. Vesicles bound to beads were washed three times in coating buffer, followed by two washes in PBS, and finally dissolved in 2x Laemmli buffer. Beads without primary antibodies were subjected to the same procedure and used as control for nonspecifically bound material.

3.18.9. Glutamate Uptake of enriched synaptic vesicle fractions

[^{3}H]Glutamate uptake was performed using synaptic vesicle preparations as described in 3.18.7. Uptake was started by adding 49.5 µm K-glutamate and 0.5 µm [^{3}H] glutamate to synaptic vesicles. Nonspecific uptake was estimated using the protonophore FCCP, which dissipates the proton gradient. Uptake was stopped after 10 min at 25°C by adding ice-cold KGC buffer. Nonbound radioactivity was removed by centrifugation at 435000 × *g* for 10 min, and the pellets were washed three times. Radioactivity was measured by liquid scintillation counting.

3.19. *In vivo* analyses

3.19.1. Thermal nociception

Thermal latency was determined using the Plantar test (Ugo Basile). This method was originally described by Hargreaves (Hargreaves et al., 1988). Therefore the animals were placed in a preheated (30°C) plexiglas chamber (15 cm diameter, 22.5 cm in height) and were allowed to habituate for 30 min prior to testing. For thermal stimulation the radiant heat source was focused onto the plantar surface of the hind paw. The withdrawal latency in response to the stimulus was determined manually. Each paw was tested 5 times. Cutoff latency to avoid tissue damage was 20 seconds.
Hyperalgesia was induced by subcutaneous injection of NGF (2 µg/site), bradykinin (20 nmol/site), serotonin (100 nmol/site) or prostaglandin E_2 (1 nmol/site) into the plantar surface of both mouse hind paws. Baclofen was injected 30 min prior to injection of these substances into one paw. 0.9 % Saline injection instead of baclofen served as a negative control.

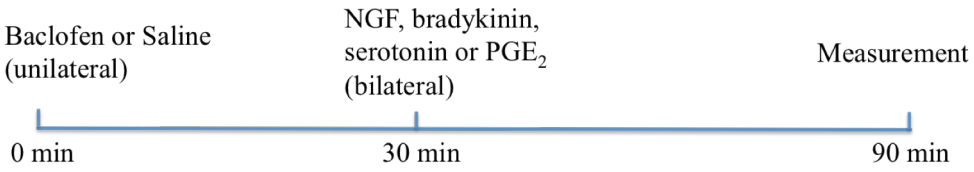

3.19.2. Chronic Constriction Injury

The chronic constriction injury (CCI) model (Bennett and Xie, 1988) was used to induce neuropathic pain. The surgery was performed under isoflurane anesthesia. Following sterilization procedures, a 5-mm incision was made below the pelvis. The biceps femoris and the gluteus superficialis were separated, and the sciatic nerve was exposed. Three loose ligations were tied around the nerve. Following homeostasis, the wound was sutured. Mice were submitted to Hargreaves' Test 5 days post surgery. The stimulus was applied to both the ipsilateral and contralateral hind paw.

3.19.3. Perfusion of animals

Intracardiac perfusion of mice was carried out under deep anesthesia 10 min after i.p. injection of ketamine/xylazine mix (260 mg/kg and 20 mg/kg, respectively). The absence of paw reflex was confirmed and the thoracic cage was opened by cutting along an oval shape starting from the sternum. A 27 gauge injection needle was placed into the left ventricle of the heart, followed by a small incision in the right ventricle. Mice were then perfused with 5 ml ice-cold 1 x PBS, followed by 10 ml 4 % PFA. Lumbar spinal cord and DRG were removed, post-fixed for 1 h in the same fixative and cryo-protected over night in 30 % sucrose in PBS.

3.19.4. Immunohistochemistry

Frontal sections of 10 or 20 µm (DRG and spinal cord, respectively) were cut and air dried on adhesion object slides and stored at –80°C. After the sections were defrozen and washed with PBS, the slides were blocked with 3% goat serum, 1% BSA and 0.1% TritonX in PBS for 1 hour. This was followed by an overnight incubation with primary antibodies in 1% blocking solution at 4°C. After rinsing in PBS, the sections were incubated with secondary antibodies in blocking solution for 1h at RT. The

tissue sections were washed with PBS to remove excess serum and mounted with ImmuMount. Pictures were taken on a Zeiss LSM 710 confocal microscope.

3.20. Calcium Imaging

Transiently transfected Hek293 cells or cultured DRG neurons were subjected to microscopic fluorescent calcium imaging. Therefore, cells were cultured on Poly-D-Lysine (100 µg/ml) and Laminin (10 µg/ml) coated coverslips. The next day, cells were loaded with 5µM of the calcium reporter dye Fura-2AM for 1h at RT. Glass coverslips were inserted into a recording chamber that was mounted on an inverted microscope (Axiovert 200, Zeiss) equipped with a fluorescence-optimized 10x Zeiss UplanApo (10×/0.75) objective. Cells were excited intermittently every 3 seconds at wavelengths of 340 nm and 380 nm (Lambda DG4, Sutter Instrument Company). Emitted light was captured at 510 nm and detected via a Snap CCD EZ camera. Imaging data were acquired using the MetaFluor software (Molecular Device, USA). Offline Analysis was carried out using Excel and GraphPad. The first 10 seconds of acquisition were averaged and used to normalize the 340/380 fluorescence ratio. At the end of every measurement, the viability and neuronal phenotype of the cells was verified by stimulation with a depolarizing buffer containing 100 mM KCl, 45 mM NaCl, 2 mM $CaCl_2$, 1 mM $MgCl_2$, 10 mM HEPES and 5 mM Glucose. The solutions were adjusted to pH 7.4 with NaOH/HCl and to 310 Osmol with sucrose.

3.21. Statistical Analyses

Analysis was performed with Prism software using the Student's t test for paired comparisons, unless indicated otherwise. All results are presented as mean ± SEM.
P values < 0.05 were considered statistically significant.

4. Results

Ion channel mediated signaling is thought to result from multiple protein-protein interactions, which are transient or stable in nature and occur in the molecular environment of the ion channel proteins. The present knowledge on protein complexes involving TRPV1 receptors is still rather limited. This PhD thesis established a genetic and biochemical strategy to purify TRPV1 receptors and associated proteins from native sensory tissue. Subsequent mass spectrometry identified several candidate proteins from which two proteins were chosen and further characterized to verify and study their functional association with TRPV1. This provided new information about TRPV1 mediated signaling and function.

4.1. Affinity tag selection

Numerous methods have been developed over the years for isolating protein complexes. Biochemical co-purification of protein interaction partners coupled to sensitive MS analysis (functional proteomics) is the current method of choice and has been implemented in ion channel research (Schulte et al., 2011). Due to the lack of good antisera directed against TRPV1, a tagged version of TRPV1 was generated. A combination of a Flag-tag and two moieties of the StrepII-tag (= SF-tag) seemed to be optimal for the isolation of TRPV1 receptor complexes. This small tag (4.6 kDa) is a novel derivative of the original TAP-tag designed by Gloeckner and colleagues (Gloeckner et al., 2009a; 2009b) and was shown to result in better biochemical purification of protein complexes than the classical version of the tag (Collins and Choudhary, 2008). Since TRP channels are not inserted into the plasma membrane via signal peptide-mediated ER translocation, the SF-tag was directly fused to the N-terminus of TRPV1 (Fig. 9).

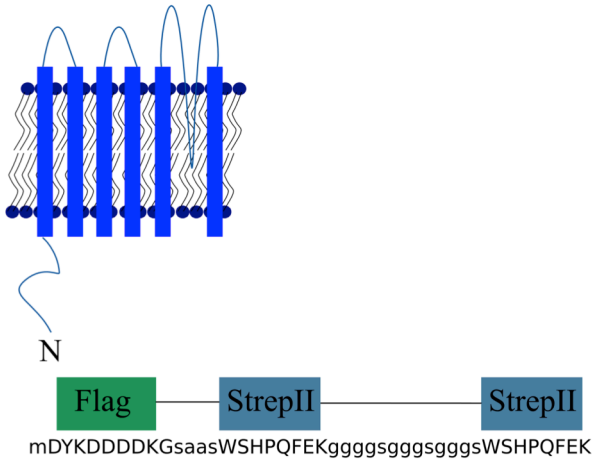

Figure 9: Amino Acid Sequence of the SF-tag

The SF-tag (4.6 kDa) consists of a Flag tag and a tandem StrepII tag. It was fused to the N-terminus of TRPV1.

4.2. SF-tagged TRPV1 can be stably expressed in heterologous cellular systems and is functional

The prerequisite of an affinity tag is that it is compatible with TRP channel function, gating and folding and that it should not sterically hinder potential TRP interaction partners. Expression and functionality of SF-tagged TRPV1 was assessed by western blot and calcium imaging in cultured Hek293 cells (Fig.10). Hek293 cells transfected with a construct encoding SF-TRPV1 were lysed and analyzed by western blot by probing with an antibody recognizing the Flag epitope (Fig. 10A). SF-TRPV1 was stably expressed and had the expected size (100 kDa). Untransfected Hek cells were used as a negative control and did not show any band (Fig. 10A). Next, Hek cells transiently transfected with SF-TRPV1 and untagged TRPV1 as a negative control, respectively, were subjected to microscopic fluorescent calcium imaging. Activation of the receptor was assessed using 1 µM capsaicin, the specific TRPV1 agonist. Elevated calcium concentrations were measured by an increased ratio of Fura-2 emission at 340 versus 380 nm wavelength excitation. Fig. 10B and C shows that similar responses were observed for tagged and untagged receptors, indicating that the SF-tag does not interfere with TRPV1 function.

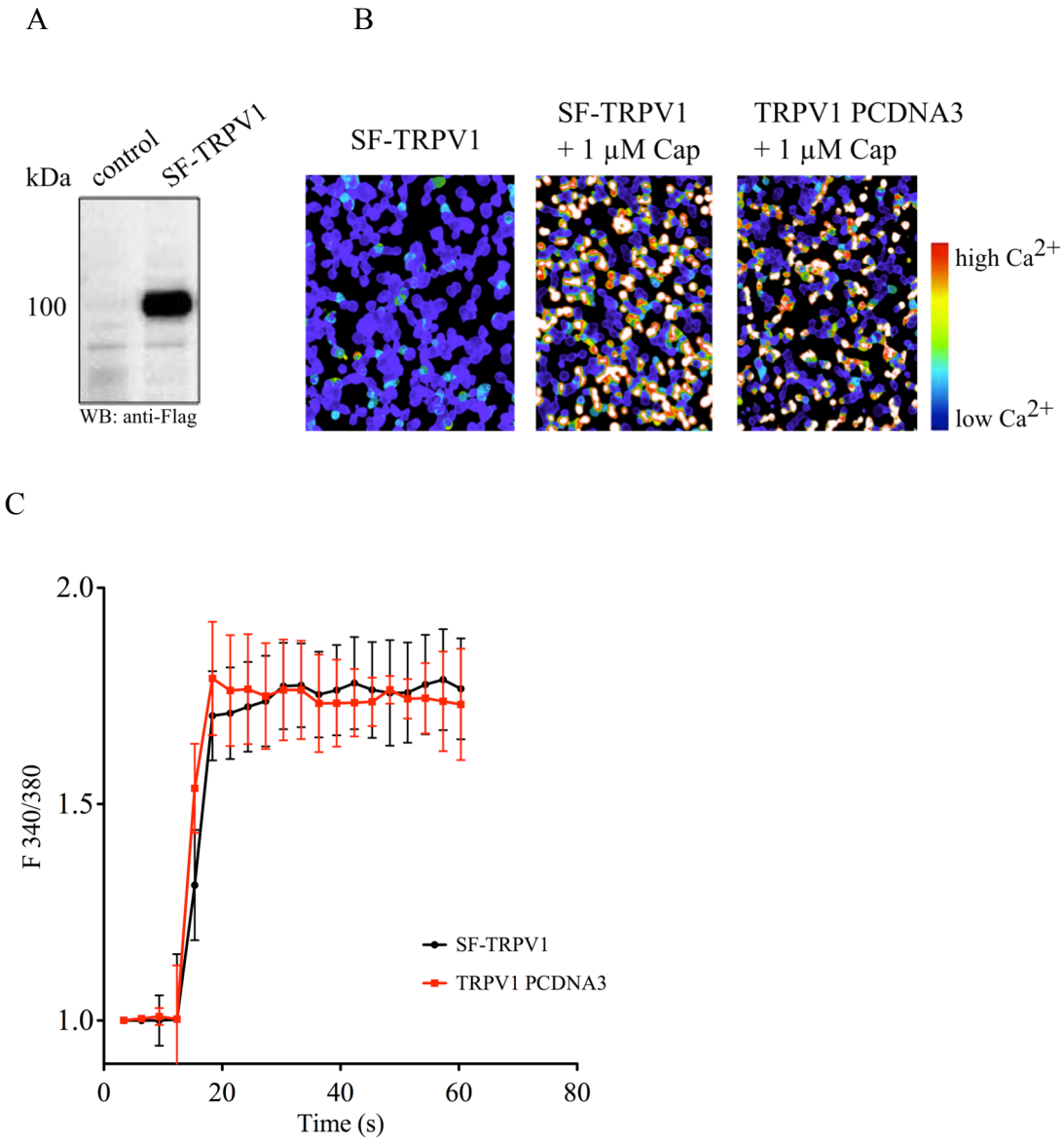

Figure 10: Functionality of SF-tagged TRPV1

(A) Western blot of Hek293 cells transfected with SF-tagged TRPV1 and probed with an antibody against the Flag tag. Control (untransfected Hek cells)

(B) Calcium imaging of Hek293 cells transfected with SF-tagged TRPV1 and wild type TRPV1, respectively. Cells were challenged with 1 µM capsaicin. Elevated calcium levels lead to an increased ratio of Fura-2 emission (indicated by the color bar). Similar responses were observed for tagged and untagged TRPV1.

(C) Time course of fluorescence ratios of Hek293 cells transfected with SF-TRPV1 or untagged TRPV1 during application with 1 µM capsaicin. SF-TRPV1 transfected cells show a similar activation to capsaicin as the untagged TRPV1 transfected cells. N=4

4.3. Generation of BAC transgenic SF-TRPV1 mice

In order to purify TRPV1 from native sensory tissue, BAC (Bacterial Artificial Chromosome) transgenic mice were generated that express SF-tagged TRPV1 in cells that natively express the receptor. The mice were generated with the help of Jana

Rossius as well as Katja Becker and Boris Jerchow from the MDC Transgenic Core Facility. BAC transgenesis allows the precise targeting of a transgene into the genomic locus of the BAC via homologous recombination. BACs are ideal for generating transgenic mice because the insert size may allow expression of a gene under the control of its own regulatory elements, mimicking the endogenous expression pattern. Fig. 11 shows a diagram of the BAC containing the TRPV1 genomic locus and the integration site of the sequence for the SF-tag. The BAC (RP23-390G23) encodes the TRPV1 genomic sequence and one neighbouring gene (ItgAe and TRPV3) on each side. This ensures the presence of all the regulatory elements needed to drive correct expression of TRPV1. The SF-tag was inserted behind the start codon of the TRPV1 gene (Fig. 11, 12A) using positive/negative GalK selection (Warming et al., 2005) as described in 3.15. Modified clones were analyzed by PCR and restriction digestion to ensure integrity of the BAC. Pulse Field Gel Electrophoresis further provided information about the correct size of the BAC (217 kb). In addition, the SF-tag was PCR amplified from the modified BAC and sequenced to ensure that it was in frame with the start codon of TRPV1.

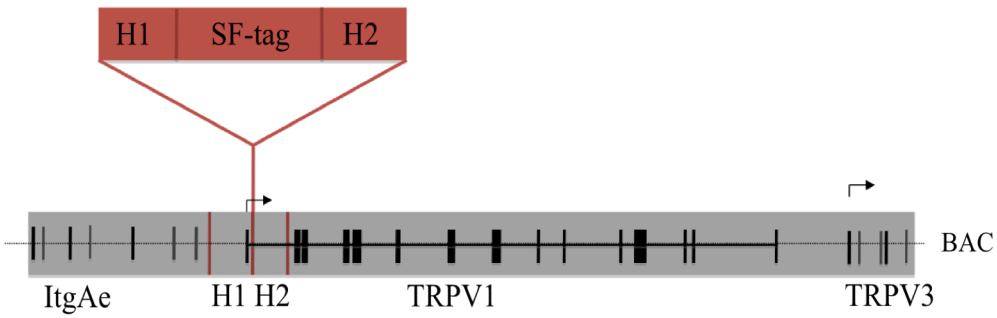

Figure 11: Schematic representation of the TRPV1 BAC and the integration site of the SF-tag
The BAC contains the TRPV1 genomic sequence and neighbouring genes ItgAe and TRPV3. The SF-tag, flanked by two homology arms, was inserted behind the start codon of TRPV1; H1and H2= homology arm 1 and 2; black bars represent exons; arrows = start codons

4.3.1. Screening of BAC transgenic founder lines

Following BAC injection into fertilized oocytes from BDF/BL6J mice, 42 transgenic founders were obtained. PCR analysis with primers (F6 and R6, Fig. 12A) amplifying the SF-tag sequence revealed that 15 of these mice were positive for the SF-tag (Fig. 12A, C). Southern blot analysis with a 5' probe further confirmed the correct integration of the TRPV1 BAC for 8 out of the 15 founders. In every line two bands were obtained,

the larger one (13.6 kb) representing the endogenous wild type band and the smaller one (8.4 kb) corresponding to the number of BAC copies integrated into the genome (Fig.12B). Of the 15 founders, 7 were crossed with C75/Bl6 mice for colony expansion. Two lines were discarded due to lack of expression of SF-TRPV1 as assessed by immunohistochemistry of DRG neurons with antibodies against the SF-tag.

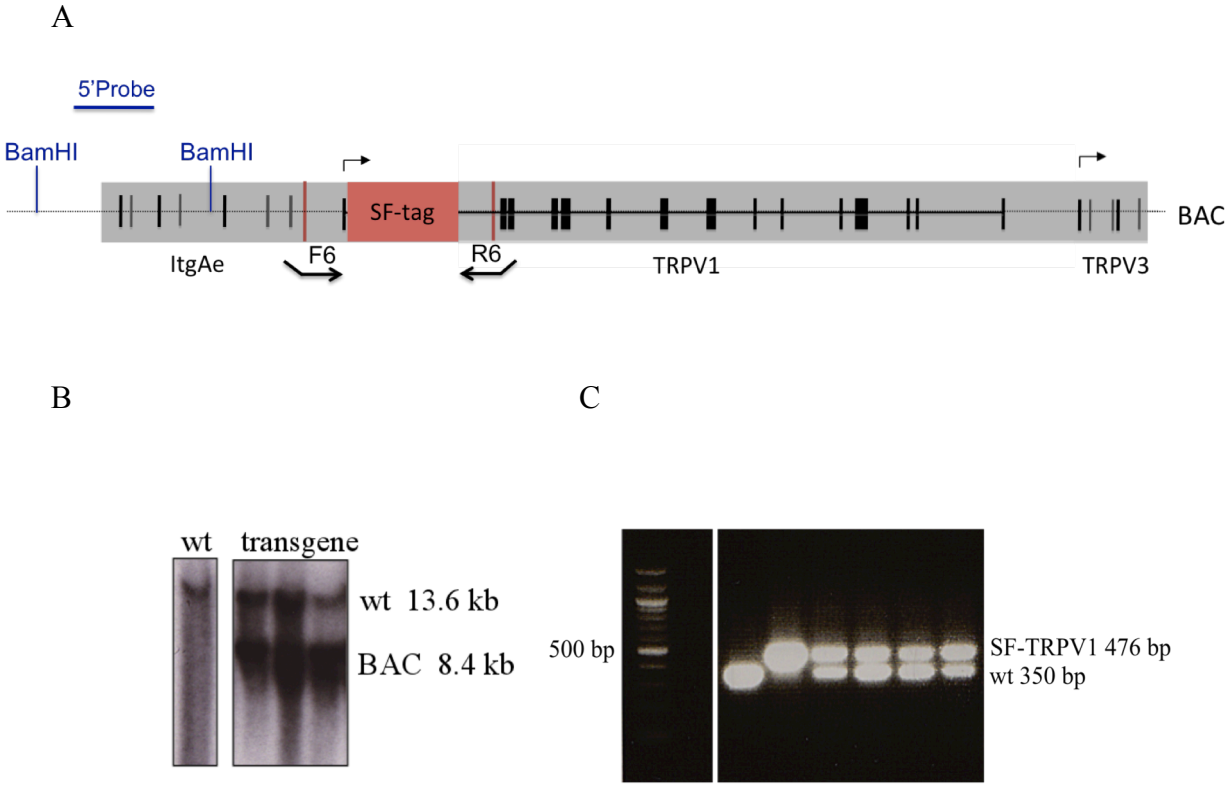

Figure 12: Analysis of SF-tagged TRPV1 BAC transgenic founders

(A) Schematic representation of the modified BAC and location of the 5'Probe for southern blot analysis as well as PCR primers F6 and R6 for genotyping
(B) Analysis of founders by southern blot with the 5'probe. Wild type band = 13.6 kb, TRPV1 BAC = 8.4 kb. The strength of the BAC band is indicative of the number of BAC copies integrated into the genome
(C) PCR analysis of founders with primers F6 and R6. Mice positive for the BAC have an additional 476 bp band

As the founders express variable protein levels of SF-TRPV1 due to integration of different numbers of BAC copies, it was decided to expand one founder line that highly overexpresses SF-TRPV1 and a second one that expresses SF-TRPV1 in comparable amounts as the endogenous receptor. Fig. 13 shows a western blot of soluble fractions prepared from the DRG of these two founders compared to solubilisates from wild type DRG. Probing with an antibody recognizing the N-terminus of TRPV1 showed that endogenous TRPV1 runs at 95 kDa. Soluble fractions of SF-TRPV1 BAC mice have an additional 100 kDa band due to expression of the tagged version of the receptor. The

SF-TRPV1 band is very strong in the overexpressing founder whereas it is comparable to native TRPV1 in the lower-expressing founder (Fig. 13). An antibody against β-actin was used to indicate equal loading.

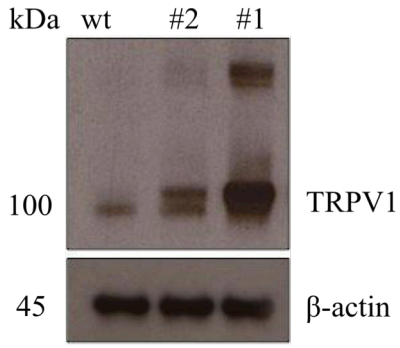

Figure 13: Comparison of TRPV1 protein expression level in DRG

Soluble fractions from DRG isolated from wild type and the two SF-TRPV1 BAC founder lines (#1 and 2) were probed with an antibody against TRPV1. Endogenous TRPV1 runs at 95 kDa. Solubilisates from SF-TRPV1 mice show an additional band at 100 kDa. The low expressing founder (#2) expresses SF-TRPV1 in a similar amount as the wild type whereas the higher expressing founder (#1) highly overexpresses SF-TRPV1. β-actin was used as a loading control

4.4. SF-tagged TRPV1 exhibits wild type localization

TRPV1 receptor expression is restricted to small-and medium-sized DRG neurons and to primary afferents terminating in laminae I and II_o in the dorsal horn of the spinal cord. Specific expression and localization of SF-TRPV1 in the BAC transgenic mice was assessed by immunohistochemistry. Therefore, DRG sections were prepared from these mice and stained with antibodies directed against the Flag tag and endogenous TRPV1. Fig. 14A shows that SF-TRPV1 is expressed in small-and medium-sized neurons and overlaps with wild type TRPV1. DRG sections from wild type animals not expressing SF-tagged TRPV1 served as a negative control and did not show any specific labelling (Fig. 14A). The specificity of the antibodies was confirmed by labeling only with secondary antibodies (see appendix). Furthermore, SF-TRPV1 is expressed in laminae I and II of the dorsal horn of the spinal cord as shown by staining with an antibody against the Strep tag (Fig. 14B). The overlap with endogenous TRPV1 indicates that SF-TRPV1 is correctly transported into the central nervous system. SF-TRPV1 is also detected in the cornea, which is densely innervated by sensory fibers expressing TRPV1, indicating that it is also transported into the periphery (Fig. 14C).

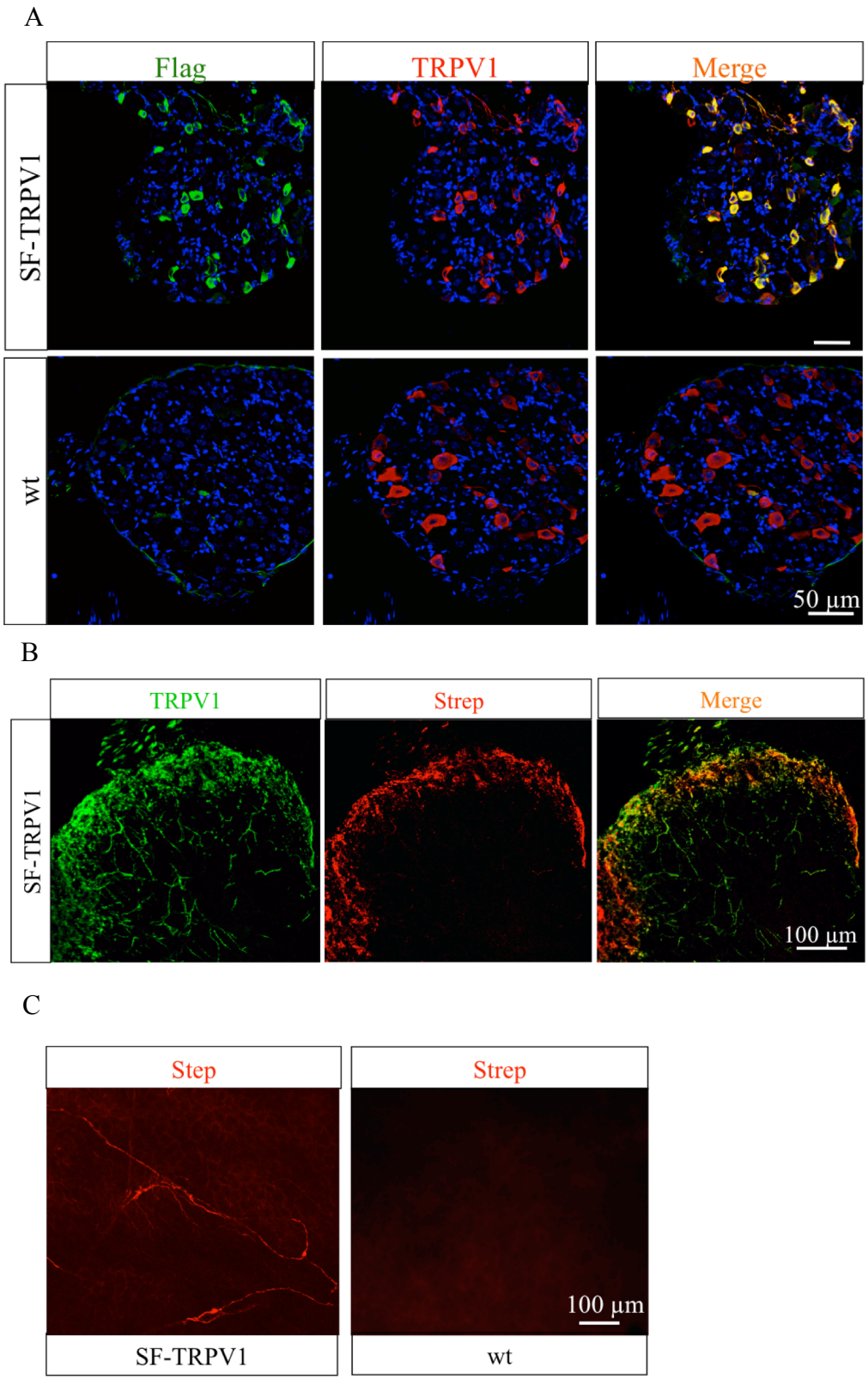

Figure 14: SF-tagged TRPV1 channels show wild type localization

Immunohistochemical analysis of SF-TRPV1 expression in adult DRG (A), lumbar dorsal horn spinal cord (B) and cornea (C) with antibodies recognizing the SF-tag (Flag or Strep). TRPV1 is selectively expressed in sensory neurons expressing native TRPV1. It is transported into the central nervous system and into the periphery.

4.5. SF-TRPV1 is functional in the BAC transgenic mice

Crossing the BAC transgenic SF-TRPV1 mice onto the TRPV1 knockout background (SF-TRPV1$^{V1-/-}$) allowed validation of the functionality of SF-TRPV1 *in vivo* as these mice only express the tagged version of TRPV1. Primary DRG cultures were prepared from these mice and subjected to calcium imaging. The DRG were challenged with 1 µM capsaicin to activate TRPV1 expressing neurons. This was followed by challenge with a high potassium solution to select all excitable neurons. 42.7 % of excitable neurons of the SF-TRPV1 knockout mice were responsive to capsaicin (Fig. 15A, B) as quantified with MetaFluor software. Similarly, 41 % of excitable DRG neurons isolated from TRPV1 +/+ mice responded to capsaicin. DRG neurons isolated from TRPV1 knockout mice served as a negative control and did not show any activation after capsaicin application. These results show that SF-TRPV1 is functional in these mice and responds to capsaicin in a similar range as wild type TRPV1.

A

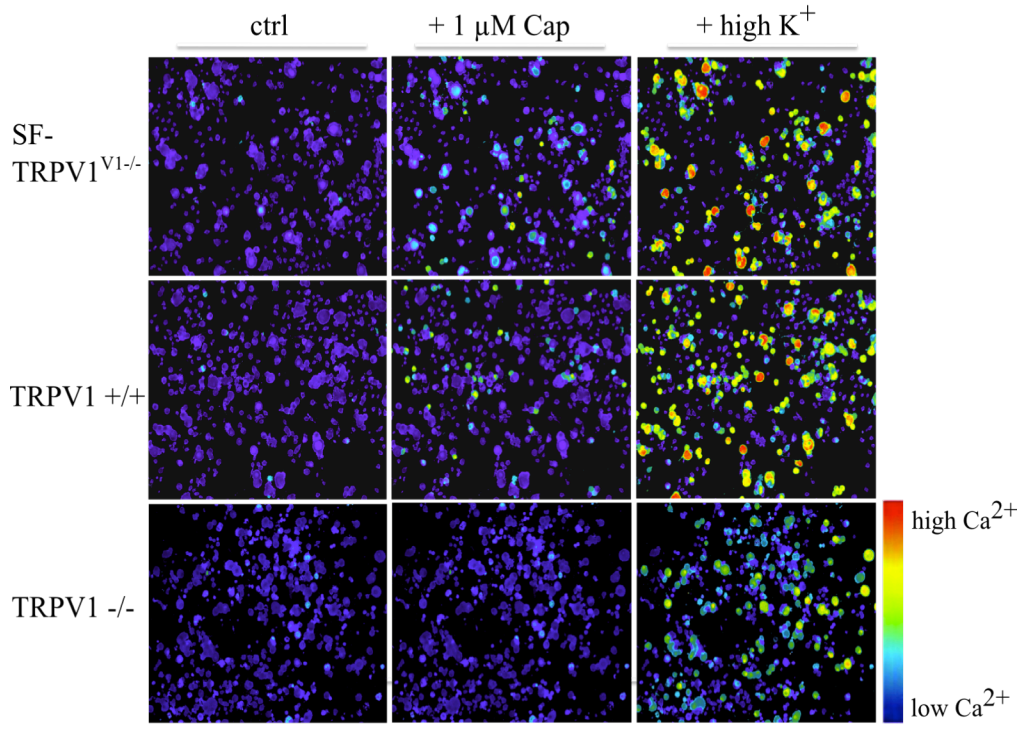

B

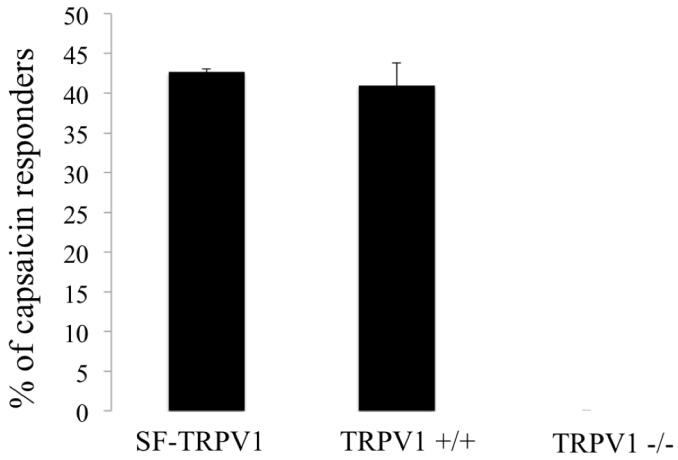

Figure 15: SF-TRPV1 is functional *in vivo*

(A) Calcium imaging of DRG neurons isolated from SF-TRPV1 BAC transgenic, TRPV1 +/+ and TRPV1 -/- mice. Neurons were challenged with 1 µM capsaicin to activate TRPV1 positive cells. Capsaicin responsive neurons were normalized to their response to high potassium.

(B) Quantification of (A). Bar graphs represent capsaicin responders (in %) of DRG neurons isolated from SF-TRPV1, TRPV1 +/+ and TRPV1 -/- mice. No difference was observed between tagged and untagged TRPV1 expressing DRG neurons.
Calcium imaging data were analyzed with MetaFluor Software

4.6. Behavioral analysis of BAC transgenic SF-TRPV1 mice

It is possible that the BAC transgenic mice are more sensitive to thermal pain due to overexpression of TRPV1. Therefore, the two SF-TRPV1 BAC founders (low and high expresser) were subjected to the Hargreaves' test to assess their thermal pain threshold. Fig. 16A shows the withdrawal latencies of the ipsilateral and contralateral paws to acute thermal pain stimuli of the two founders compared to wild type and TRPV1 knockout animals. No significant difference was observed between the different genotypes, indicating that SF-TRPV1 BAC transgenic mice show normal behavioral responses to acute thermal pain. TRPV1 receptors play a critical role in the development of thermal hyperalgesia during inflammatory and neuropathic pain. To assess the behavioral responses of these mice under a chronic pain condition, neuropathic pain was induced in these mice using the chronic constriction injury (CCI) model (Bennett and Xie, 1988). As Fig. 16B shows, the thermal latencies of the high expressing SF-TRPV1 BAC transgenic mouse are much more decreased in response to the heat stimulus as compared to the low expresser and wild type mice. The same was observed with SF-TRPV1 BAC mice (high expresser) crossed onto the TRPV1 knockout background (SF-TRPV1$^{V1-/-}$), indicating that SF-TRPV1 can be sensitized and rescues the phenotype of the knockout. Furthermore, these animals

show an increased sensitivity to the heat stimulus also in the contralateral paw, suggesting that the over expresser can be much more sensitized than wild type mice due to higher TRPV1 expression levels.

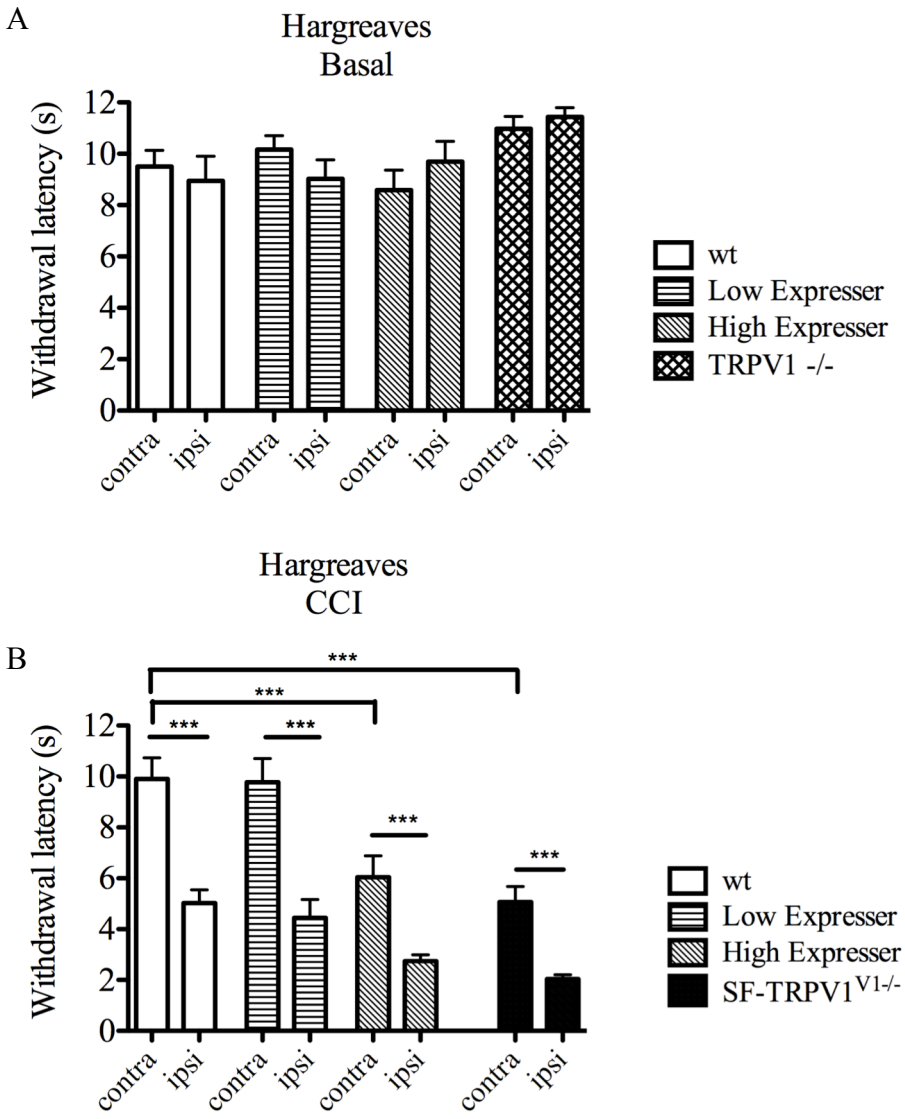

Figure 16: Analysis of thermal pain sensitivity under basal and neuropathic pain conditions

(A) Acute thermal pain sensitivity of wild type, SF-TRPV1 BAC and TRPV1 -/- mice was assessed using the Hargreaves' Test as described in 3.19.1. Bar graphs show the mean latencies of ipsilateral and contralateral paw withdrawal upon radiant heat. No significant differences were observed between the four genotypes. N=6, n.s, t-test

(B) Mean withdrawal latencies to heat stimulation during neuropathic pain induced by the CCI model in the ipsilateral paw. The sensitivity to thermal pain was significantly increased in the ipsilateral paw compared to the control paw. The high expresser and SF-TRPV1$^{V1-/-}$ were much more sensitive to the heat stimulus in both hind paws as compared to wild type mice and the low expresser. N=6, $p<0.001$, t-test

4.7. Optimization of TRPV1 purification for mass spectrometry

TRPV1 receptors were purified from sensory tissue with the aim of identifying protein interaction partners through mass spectrometry analysis. Therefore, a purification protocol had to be established which allowed the extraction of the target protein from native source material under conditions preserving its association with other proteins. Fig. 17 shows an overview of the purification protocol from sensory tissue. The purification for the identification of protein interactions includes 1) tissue preparation, 2) enrichment for membrane proteins, 3) solubilisation of protein complexes with gentle detergents, 3) affinity purification of target protein with affinity resin, 4) mass spectrometric analysis of trypsin-digested peptide fragments (nano-LC-MS/MS) and 5) protein identification through database search and subsequent confirmation and functional analysis of identified protein interactions.

Because membrane proteins are difficult to isolate with standard biochemical methods without interfering with their structure, the purification procedure was first optimized *in vitro* using transfected Hek293 cells. This was followed by establishing and optimizing the experimental conditions for the purification of TRPV1 from native tissue.

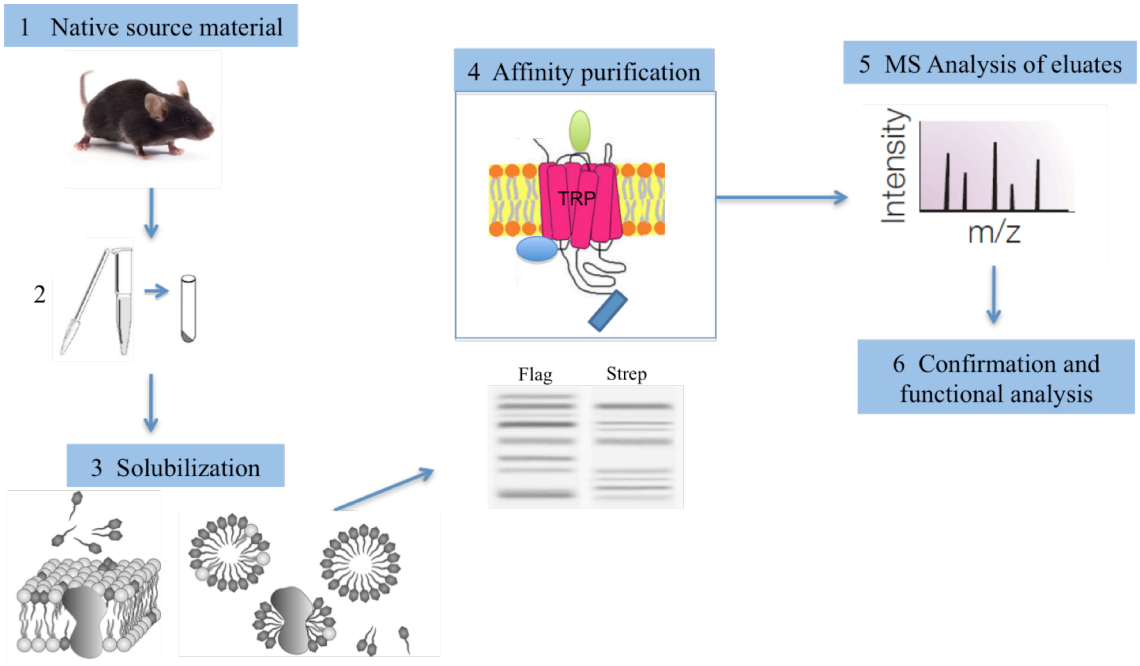

Figure 17: Overview of TRPV1 purification strategy
The purification of TRPV1 receptors consists of (1) the preparation of native source material, (2) enrichment for membrane proteins, (3) extraction of membrane proteins, (4) affinity purification and (5) subsequent mass spectrometry analysis. Identified interaction partners are further confirmed by biochemical and functional assays (6).

4.7.1. Preparation of source material

The first step in isolating proteins is the preparation of the source material. For TRPV1 purification, the DRG, spinal cord and sciatic nerve were isolated from BAC transgenic SF-TRPV1 and wild type mice not expressing SF-TRPV1 as a negative control. Efficient homogenization was achieved by using specialized devices for small amounts of material. Because some organelles, such as ribosomes and mitochondria, contain highly abundant proteins that tend to enhance background, plasma membrane enriched protein fractions, that were partially depleted of cytosol, nuclei and mitochondria, were prepared by differential centrifugation as described in 3.18.2.

4.7.2. Extraction of target protein

Solubilization is a critical step due to the required use of detergent. It has a large impact on the proteomics approach because not only the target ion channel but also associated partner proteins must be efficiently solubilized. It is also important to achieve a good balance between preserving the integrity of the protein complex and maintaining sufficiently stringent conditions to eliminate nonspecific binders.
Therefore, TRPV1 purification was first tested in transfected Hek293 cells using different types of detergents in different concentrations. Fig. 18 shows a silver stained gel of TRPV1 elutions after Flag affinity purification using buffers containing different detergents. Even though TRPV1 can be purified using all of the detergents tested except for 0.5% Chaps, n-Dodecyl β-D-maltoside (DDM) met the requirements best due to its mild properties. DDM is a nonionic detergent that is commonly used for the isolation of hydrophobic membrane proteins and is able to preserve protein activity better than other common detergents, including NP-40, Chaps and Octyl-beta-glucoside (Luche et al., 2003). Importantly, its non-ionic nature makes it compatible with mass spectrometry. Using less stringent detergent conditions for TRPV1 solubilisation and immunoprecipitation was likely to effectively maintain the structural integrity of the target protein and to allow the recovery of more labile protein complexes.

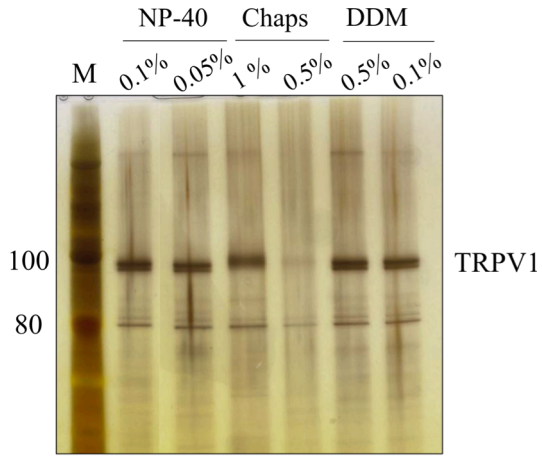

Figure 18: Comparison of detergent conditions for the isolation of TRPV1

Detergents used in the solubilisation and pull-down of TRPV1 from transfected Hek293 cells are indicated. Due to its mild properties, 0.1% DDM was chosen for the purifications of TRPV1

4.7.3. Choice of affinity resin for capture and elution of TRPV1

The SF-tag allowed the use of either Flag or Strep affinity resins for the TRPV1 enrichment. For Flag-tag based affinity purifications solubilized protein was incubated with Anti-Flag M2 magnetic beads. The target protein was eluted using either 2x Laemmli buffer, the Flag peptide (100 µg/ml), or 6 M Urea /2 M Thio-Urea. For Strep affinity purifications solubilized protein was incubated with the Streptactin matrix and eluted with Desthiobiotin. Fig. 19 shows that TRPV1 could be purified from Hek293 cells transfected with SF-TRPV1 using both Strep and Flag affinity purifications (Fig. 19A). This indicates that the SF-tag is accessible by the affinity resin. Furthermore, TRPV1 is detectable on silver stained gels (Fig. 19B), indicating that the purification is efficient and results in sufficient protein yield. Untransfected Hek293 cells were used as a negative control and did not show any band on the western blot or the silvergel. The yield of eluted TRPV1 protein was similar in both pull-downs, although Flag beads show more efficient TRPV1 depletion. The best experimental conditions were achieved by eluting with 6 M Urea/2 M Thio-Urea because it was efficient and enabled subsequent tryptic in-solution digests when samples were processed for mass spectrometry.

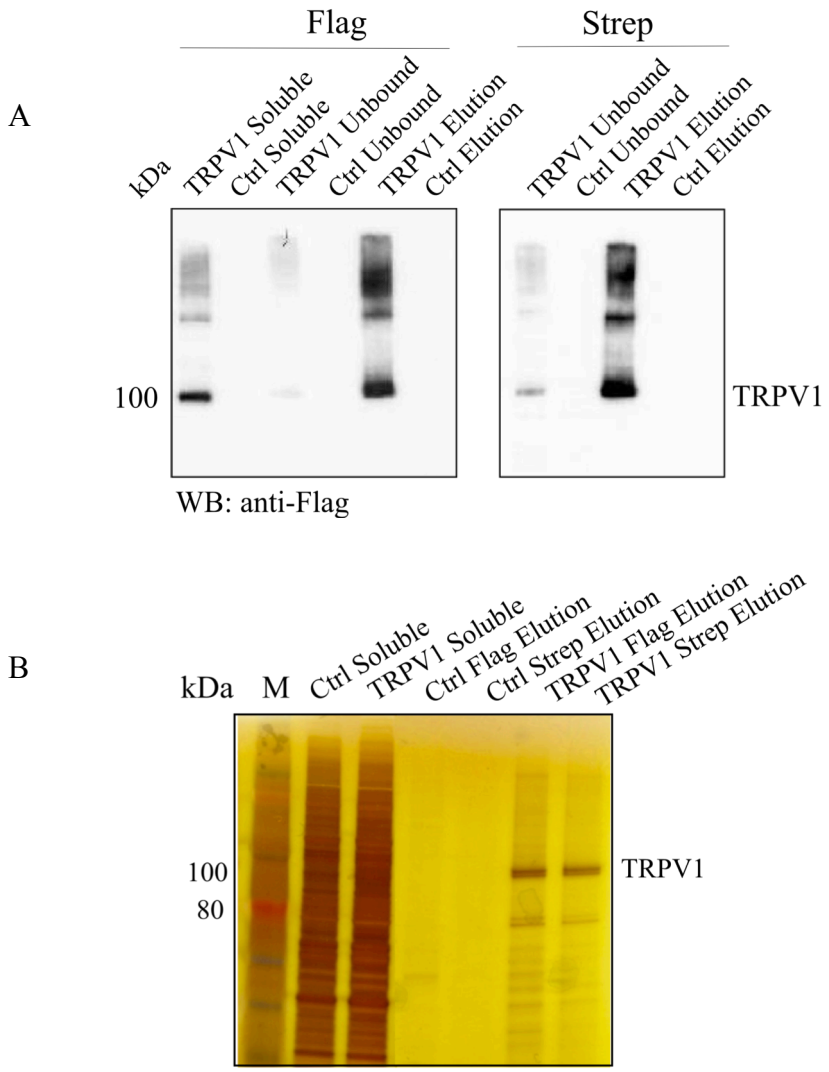

Figure 19: Flag and Strep affinity purification of TRPV1 from Hek293 cells

(A) Flag (left) and Strep (right) affinity purification from Hek293 cells expressing SF-TRPV1. Protein was eluted using the Flag peptide (Flag IP) or desthiobiotin (Strep IP), respectively. TRPV1 was detected in both pull-downs.
(B) Silver stained gel of purified TRPV1 fractions using Flag and Strep affinity resin, respectively. TRPV1 was efficiently purified in both pull-downs.
Soluble (Solubilized protein), unbound (flow-through), ctrl (untransfected Hek cells as negative control)

4.8. Purification of TRPV1 receptors from native sensory tissue

Following the optimization of the purification of TRPV1 from heterologous cell systems, the next step was to establish the experimental conditions for the isolation of TRPV1 from native tissue of the BAC transgenic SF-TRPV1 mice. Therefore, plasma membrane enriched fractions were solubilized with 0.5% DDM containing solubilization buffer and 1 mg/ml solubilized protein and affinity purified using Strep or Flag affinity resin, respectively. Fig. 20A and B show western blots of a Flag and

Strep affinity purification of TRPV1 from the DRG of BAC transgenic SF-TRPV1 and wild type control mice as a negative control. The unbound fraction indicates that the Flag-tag based affinity purification depleted TRPV1 much better in comparison with the Strep IP, as already seen in the pulldowns from Hek293 cells (Fig. 19A).
Fig. 20C shows that affinity purifications recovered heteromeric TRPV1 channels composed of SF-TRPV1 and wild type TRPV1, as revealed by the 100 and 105 kDa band (arrows) in the eluate.

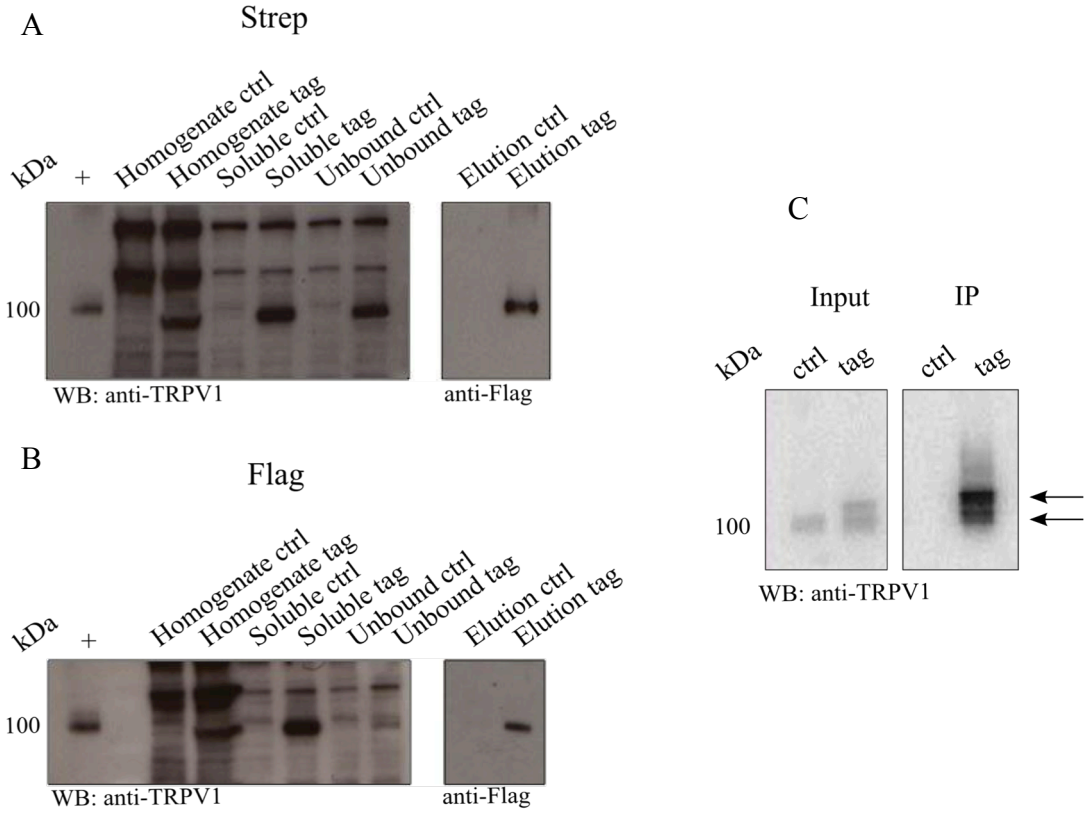

Figure 20: Affinity purification of TRPV1 from the DRG

Western blots of affinity purifications of TRPV1 using Strep (A) and Flag (B) affinity resin, respectively. TRPV1 can be pulled down using both resins, however, Flag affinity purifications show better TRPV1 depletion. Due to nonspecific labelling by the Flag M2 antibody in the first three fractions (homogenate, soluble and unbound), a TRPV1 antibody was used. The elution was blotted using the M2 Flag antibody. (C) Recovery of heteromeric TRPV1 channels composed of endogenous and tagged receptors, as indicated by the two arrows.
+ (positive control: TRPV1 elution from Hek293 cells), Soluble (Solubilized protein), unbound (flow-through), ctrl (wild type tissue), tag (tissue from SF-TRPV1 mouse)

Moreover, TRPV1 could also be efficiently solubilized and purified from the sciatic nerve and the spinal cord (Fig. 21A), indicating that TRPV1 can be purified from compartments within the peripheral and central nervous system.
Importantly, the receptor could be detected in purified fractions by silver staining (Fig.

21B, arrow), which indicates that it was present in sufficient quantity for subsequent mass spectrometry analysis. While there were certainly background bands due to the abundance of proteins in complex tissue samples, there were additional bands that do not appear in the controls (Fig. 21B).

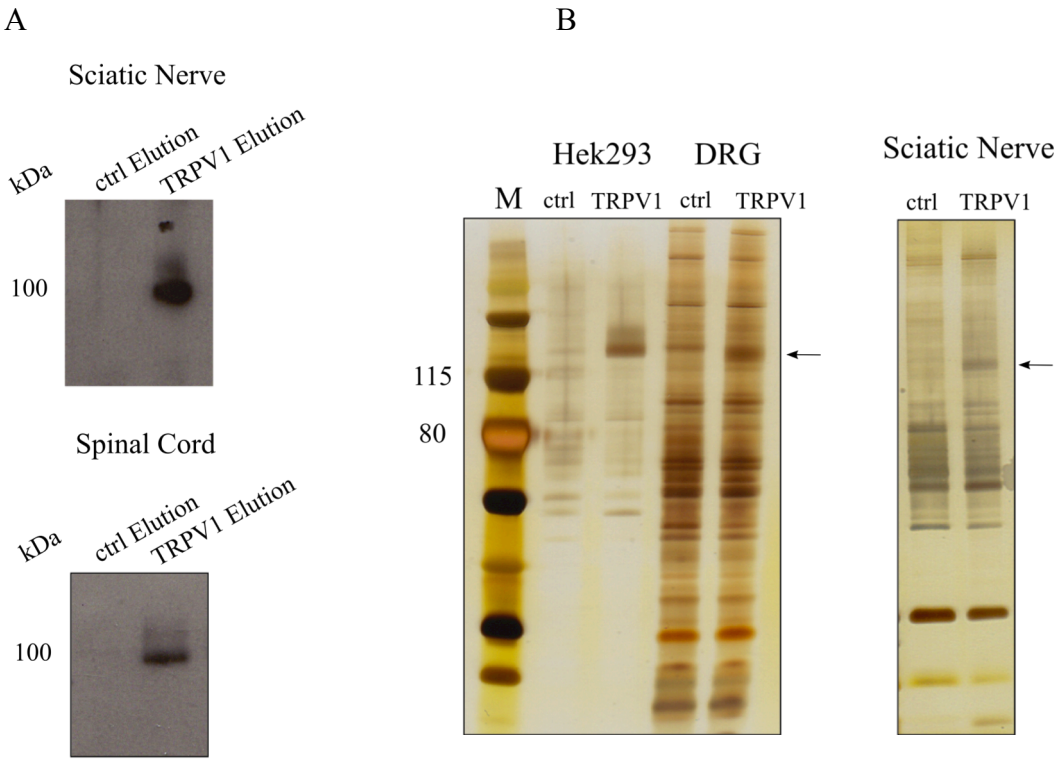

Figure 21: TRPV1 can be purified in sufficient quantity from sensory tissue

(A) Western blot of Flag affinity purification of TRPV1 from the sciatic nerve and spinal cord. Shown are the elutions of purified TRPV1 from the BAC transgenic SF-TRPV1 and wild type control mice

(B) Silver stained gel of purified fractions of TRPV1 from the DRG and sciatic nerve of BAC transgenic SF-TRPV1 and wild type control mice. The arrow indicates TRPV1. Ctrl= wildtype mouse, + tag mouse

4.9. Identification of TRPV1 binding proteins in sensory tissue using mass spectrometry based proteomic approach

In order to identify TRPV1 receptor binding proteins, Flag tag-based affinity purification from solubilized DRG and sciatic nerve membrane fractions was used. Wild type tissue, not expressing the Flag tagged protein, served as a negative control. Samples were analyzed by different mass spectrometry facilities (LOGOPHARM GmbH, Freiburg, and MDC core facility) or processed in collaboration with Dr. Marieluise Kirchner (Matthias Selbach group, MDC). Each sample was prepared in

triplicate, allowing statistical t-test analysis. Affinity purified fractions of proteins were analyzed by high-performance high-resolution mass spectrometry (LC-MS/MS), providing protein identifications and relative abundance within the sample. For data quantification and evaluation, MaxQuant and Perseus software were used. Thereby, pull-downs from the SF-tagged TRPV1 expressing sample were compared to pull-downs from the untagged wild type control sample. TRPV1 was detected in the MS runs as the most abundant protein, confirming efficient affinity purification of the bait protein. TRPV1 binding proteins were defined by level of enrichment over control and p-value from student t-test. Fig. 22 shows a volcano plot of a representative experiment using DRG tissue with the observed fold changes over control against the negative logarithmic p-values of the t-tests. The significance line corresponds to the desired False Discovery Rate (FDR) for interactors and is set customarily in Perseus to be <0.05. This line is used to define true interactors. Background binding proteins have a ratio close to 1:1 and are located close to the vertical 0-line. Proteins with a high fold change and high P-value, such as the bait protein TRPV1, are considered as significantly enriched over control and are potential interactors of TRPV1 (upper right corner). The fraction of proteins with negative fold change values (upper left corner, green area) represents false positive hits, since the rate of specific binding to control samples is usually low. However, pull-downs from heterogeneous tissue samples are generally more complex and contain many proteins that nonspecifically bind to the affinity resin. For this reason, the number of proteins found in the control sample is relatively high. Proteins that were previously identified to interact with TRPV1, such as TRPV2 and calmodulin, were found as specific TRPV1 binders in the experiments (Numbers 1 and 2 in Fig. 22), validating the efficiency and specificity of the approach to isolate and identify TRPV1 interacting proteins. Three additional proteins were robustly found in all pull-down experiments; Reep5 (Number 3 in Fig. 22), S100-A10 (Number 4 in Fig. 22) and CD9 antigen were previously identified in a yeast-two-hybrid screen (Siemens lab, unpublished data), demonstrating that interactors can be efficiently detected using complementary approaches. As the DRG contain the somata of the primary afferents, proteins important for synthesis (i.e. ribosomal) were highly abundant in DRG pull-downs (see complete list of identified proteins in appendix), and were annotated as unspecific binders. Pull-downs from the sciatic nerve identified many proteins involved in transport (i.e. vesicular proteins, trafficking and cytoskeletal proteins) (see complete list of identified proteins in appendix), which is

plausible for this type of tissue. Tab. 1 lists a selection of candidate proteins that were identified as significant hits from a representative MS run following Flag affinity purification from the DRG and the sciatic nerve categorized according to their primary function. The selected proteins had a log2 fold change value > 2 and were thus considered significant. Moreover, they were robustly identified as specifically enriched in different MS experiments.

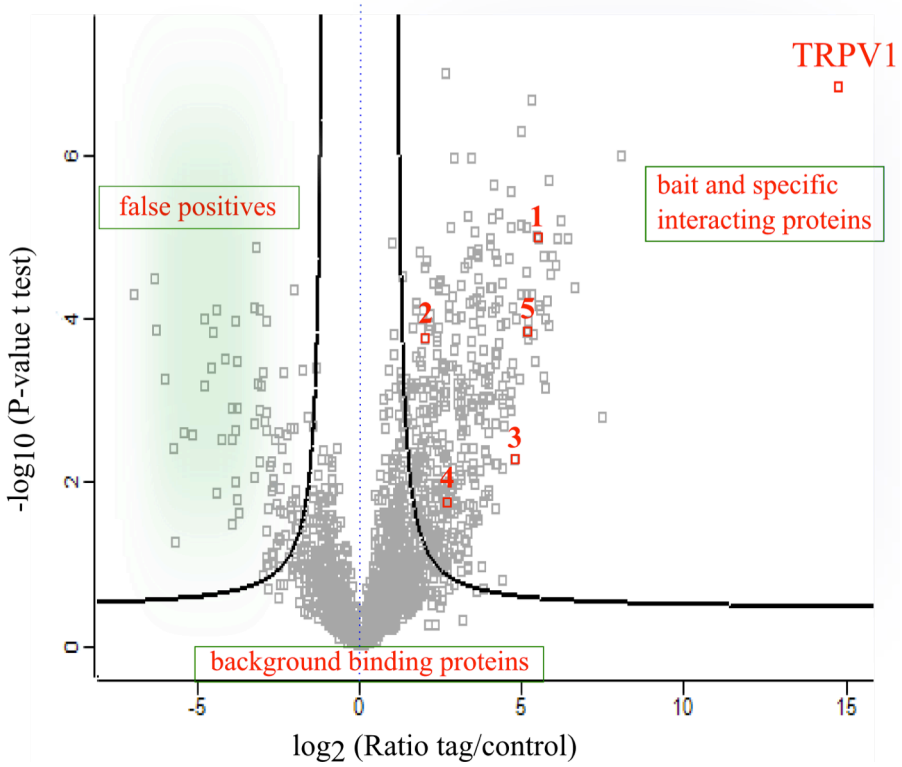

Figure 22: Determination of interaction partners by volcano plot

Logarithmic ratios (fold changes) are plotted against the negative logarithmic p-value of the t test (significance). Background binding proteins have a ratio close to 1:1 and are located close to the vertical 0-line. Proteins located in the right corner are considered interactors because of high abundance and significance. Proteins in the left corner are considered false positives because they are not expected to be more abundant in the pulldown of the control sample. TRPV1 is the most abundant protein detected. Numbers 1-5 are selected proteins that were significantly detected in each MS run. 1= TRPV2, 2 = calmodulin, 3 = S100-A10, 4 = reep5, 5 = $GABA_{B1a}$

Two candidate proteins, $GABA_{B1a}$ from the DRG (Number 5 in Fig. 22) and Vglut2 from the sciatic nerve, were selected for verification based on their abundance and significance but also based on their physiological relevance in the pain pathway and potential connection with TRPV1 based on literature research. In addition, these two proteins were identified as highly significant hits by Logopharm GmbH.

Protein Name	Uniprot ID	DRG ratio Flag/wt control	Sciatic Nerve ratio Flag/wt control
Ion channels/Transporters			
TRPV2	Q9WTR1	5.7	/
GABA type B receptor unit 1a	Q9WV18	5.8	/
Signaling			
A-kinase anchor protein 12	Q9WTQ5	2.6	/
Calcium binding			
Calmodulin	P62204	2.5	0.8
S100-A13	P97352	5.3	1.8
S100-A10	P08207	2.3	1.2
Trafficking			
Reep5	Q60870,	3.4	/
Vesicle-trafficking protein SEC22b	O08547	5.7	/
Synaptic Vesicle			
Vesicular Glutamate Transporter 2	Q8BLE7	/	2.2
Cytoskeleton			
Microtubule associated protein 2	P20357	/	2.8
Others			
CD9 antigen	P40240	2.7	6.4
Membrane-associated progesterone receptor component 1	Q55022	3.2	/
Calnexin	P35564	5.2	/

Tab.1: Results of mass spectrometric analysis of TRPV1 Flag tag-based affinity purifications from DRG and sciatic nerve.
The table lists a selection of identified proteins with log2 fold change values >2 of a representative MS run. Note that calmodulin, S100-A13 and A10 were significant in the DRG pull-down but not in the pull-down from the sciatic nerve in this experiment. Proteins are categorized according to their primary function. $GABA_{B1a}$ and Vglut2 were selected for verification because of their significant enrichment and additional identification by Logopharm GmbH.

5. Verification and characterization of the two candidate proteins

Two candidate proteins were chosen for further analysis because they were highly abundant and specific in the mass spectrometry analysis and appeared relevant for TRPV1 function based on literature research. These two proteins were cloned and further characterized to elucidate their association with TRPV1. The verification of a potential interaction is important because the interaction may be indirect via a common interaction partner or it may simply be nonphysiological. It is therefore crucial to verify the binding by additional methods, for example co-immunoprecipitation and co-localization studies in heterologous cell systems and tissue sections using confocal microscopy. As proteomic data provide no direct information regarding protein function, it is also important to validate the functional role of the newly identified interaction partners and their association with TRPV1, particularly in native cells.

The first section of this chapter will describe the verification of the $GABA_{B1a}$ subunit as a potential candidate protein. $GABA_{B1a}$ is a splice variant of the $GABA_{B1}$ subunit that is predominantly expressed in DRG neurons. It was specifically enriched in Flag affinity purifications of TRPV1 from the DRG. $GABA_B$ receptors play a central role in the pain pathway, though their contribution to peripheral nociception has to still be elucidated.

The second section will describe the characterization of a potential interaction between TRPV1 and the Vesicular Glutamate Transporter 2 (Vglut2), which was specifically enriched in Flag affinity purifications of TRPV1 from the sciatic nerve. Vglut2 arose interest because previous studies reported overlapping distribution of TRPV1 and Vglut2 and mice lacking Vglut2 only in nociceptors are phenotypically very similar to TRPV1 deficient mice.

5.1. Verification of the $GABA_B$ receptor as a potential TRPV1 interaction partner

$GABA_B$ is a heterodimeric receptor, composed of two subunits named $GABA_{B1}$ and $_{B2}$ (Kaupmann et al., 1997; Jones et al., 1998; Kuner et al., 1999). Both subunits display a classical GPCR topology: an extracellular N-terminal domain, seven transmembrane helices and an intracellular C-terminus (Fig. 23A). While $GABA_{B1}$ is responsible for ligand binding, $GABA_{B2}$ is responsible for G-protein coupling (Galvez et al., 2001; Margeta-Mitrovic et al., 2001a; 2001b). Both subunits have to be present to form a functional receptor. At least two isoforms of the $GABA_{B1}$ subunit exist (1a and 1b) that differ by the presence of a pair of sushi domains in the N-terminal domain (Kaupmann et al., 1997).

$GABA_B$ receptors predominantly mediate their effects via G protein signaling ($G_{i\alpha}$ and $G_{o\alpha}$) (Fig. 23B). Presynaptic $GABA_B$ receptors inhibit the release of a number of different neurotransmitters, mainly by reducing calcium influx through voltage-gated P/Q and N-type Ca^{2+} channels. Postsynaptic $GABA_B$ receptors couple to a specific type of K^+ channel, the inwardly rectifying $K_{ir}3$ channels (GIRK) (Misgeld et al., 1995; Kaupmann et al., 1998), which induces K^+ efflux, hyperpolarization of the neuron and neuronal inhibition. In addition, $GABA_B$ receptors negatively couple to adenylyl cyclase (AC) via $G_{i\alpha}$ and $G_{o\alpha}$ proteins (Nishikawa et al., 1997), which results in decreased levels of presynaptic cAMP and kinase activity within the cell.

A

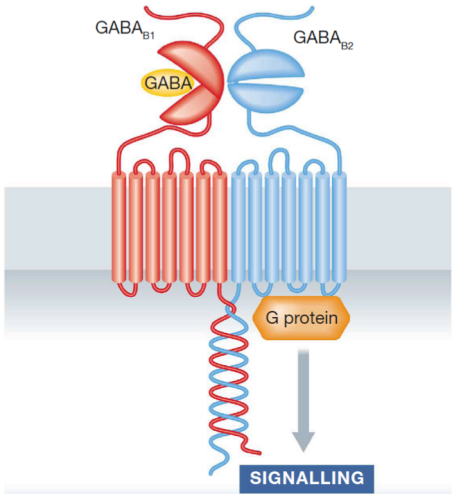

B

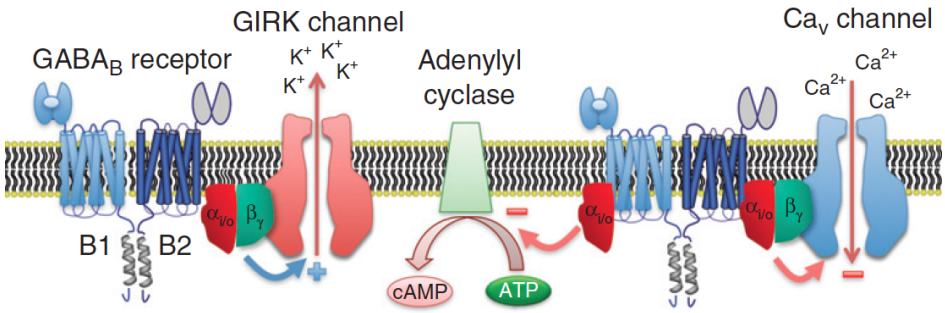

Figure 23: GABA$_B$ receptor structure and activation-mediated effects

(A) Functional GABA$_B$ receptors are heterodimers formed by a GABA$_{B1}$ and $_{B2}$ subunit. Each subunit has extracellular N-termini, 7 TM helices and intracellular C-termini. Functional receptors heterodimerize via a C-terminal coiled-coil domain. While GABA$_{B1}$ binds agonists, GABA$_{B2}$ is important for G-protein coupling and trafficking of the receptor to the plasma membrane. Adapted from Benke and Zeilhofer, 2012

(B) Activation of the receptor stimulates G-protein (Gi/o) dissociation of the Gα and Gβγ dimer. The Gαi/o subunit inhibits adenylyl cyclase while the Gβγ dimer modulates Ca$_v$ or GIRK channels, resulting in neuronal inhibition. Adapted from Padgett and Slesinger, 2010

5.1.1. GABA$_{B1}$ and GABA$_{B2}$ co-localize with TRPV1 in DRG neurons

Co-localization is defined as the presence of two different molecules residing at the same physical location in a cell. If proteins interact *in vivo* they are expected to display overlapping distribution within a cell. In the DRG, the GABA$_{B1}$ subunit, predominantly the splice variant 1a, and GABA$_{B2}$ are expressed in Aδ and C fibers. (Towers et al., 2000; Charles et al., 2001). To investigate whether TRPV1 and the GABA$_B$ receptor co-localize in the same neurons, immunohistochemistry of DRG sections was carried out using antibodies against TRPV1 and GABA$_{B1}$ or GABA$_{B2}$, respectively. Fig. 24A shows that all cells expressing TRPV1 are also positive for both GABA$_B$ subunits. Furthermore, immunolabeling was performed on cultured DRG neurons with antibodies against TRPV1 and GABA$_{B1}$ or GABA$_{B2}$, respectively. Fig. 24B shows co-expression of TRPV1 with GABA$_{B1}$ and GABA$_{B2}$ at the plasma membrane. Staining of DRG neurons with a secondary antibody confirmed labeling specificity (see appendix).

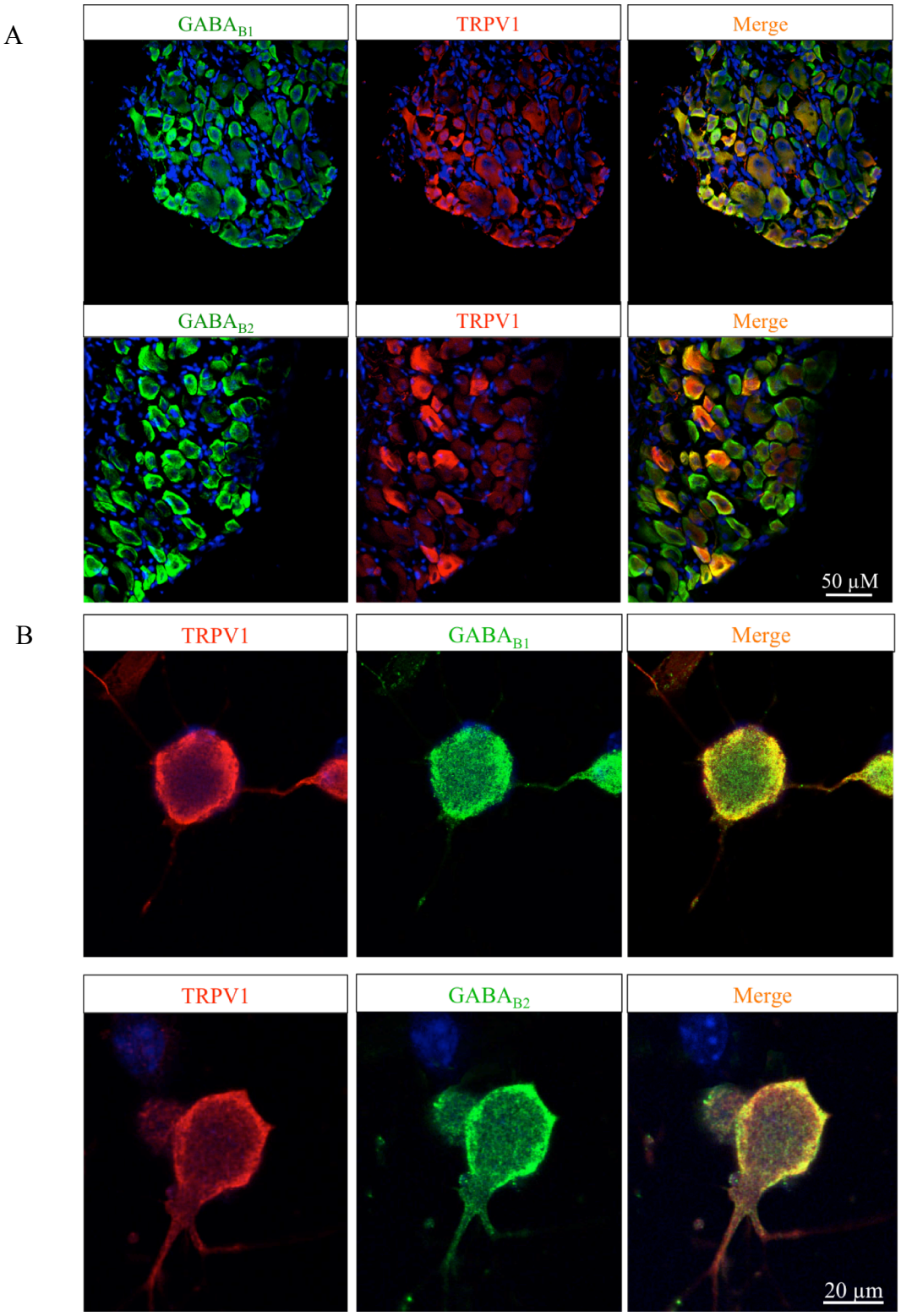

Figure 24: Immunohistochemical analysis of TRPV1 and GABA$_B$ receptor subunits in DRG neurons

(A) Co-staining of TRPV1 and GABA$_{B1}$ or GABA$_{B2}$ in DRG sections was observed in all TRPV1 positive cells. Scale bar = 50 µM

(B) Co-localization of TRPV1 and GABA$_{B1}$ or GABA$_{B2}$ was observed at the plasma membrane of cultured DRG neurons. Scale bar = 20 µM.

5.1.2. $GABA_{B1}$ and $GABA_{B2}$ co-localize with TRPV1 in the dorsal horn of the spinal cord

The presence of $GABA_B$ receptors in laminae I-III of the dorsal horn in the spinal cord provides the anatomical basis for analgesic effects of the $GABA_B$ specific agonist, baclofen (Towers et al., 2000; Engle et al., 2005). To investigate whether TRPV1 and the $GABA_B$ receptor co-localize in the spinal cord, immunohistochemistry on cryosections of the spinal cord was performed with antibodies against TRPV1 and $GABA_{B1}$ or $GABA_{B2}$, respectively. Fig. 25 shows co-localization of TRPV1 with $GABA_{B1}$ and $GABA_{B2}$ in the superficial layers. As reported by other groups, $GABA_{B1a}$ was densely localized throughout the superficial laminae, whereas $GABA_{B2}$ was also found in deeper laminae.

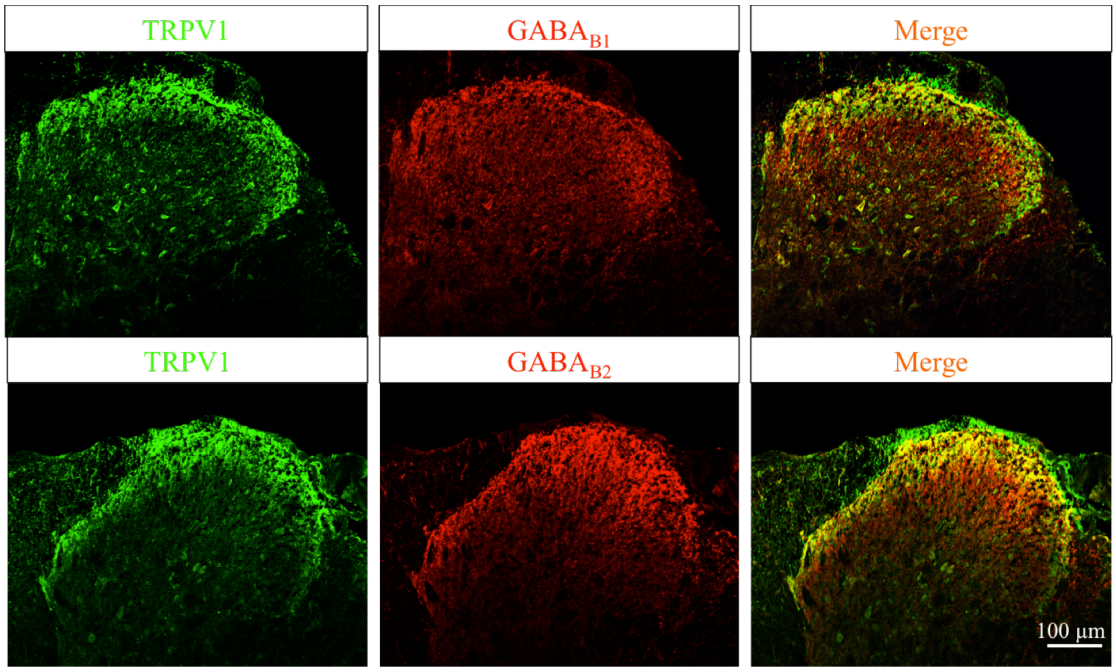

Figure 25: Co-labeling of endogenous TRPV1 and $GABA_B$ receptor subunits in the dorsal spinal cord
Co-staining of TRPV1 and $GABA_{B1}$ or $GABA_{B2}$ was detected in the superficial laminae of the dorsal horn spinal cord. Note that $GABA_{B1}$ expression was restricted to the more superficial layers than $GABA_{B2}$. Scale bar = 100 µm

5.1.3. The $GABA_B$ receptor co-immunoprecipitates with TRPV1

Many protein-protein interactions remain intact when a cell is lysed under non-denaturing conditions. Thus, if the target protein is immunoprecipitated, then its partner protein, which is stably associated with it, may co-precipitate and be detectable in the resulting pelleted material. Co-immunoprecipitation (Co-IP) is most

commonly used to verify whether two proteins of interest interact. Fig. 26 shows a western blot of a Flag IP of TRPV1 from the DRG of BAC transgenic SF-TRPV1 and wild type control mice with antibodies recognizing TRPV1 and $GABA_{B1}$. Complementary to the mass spectrometry results, $GABA_{B1}$ could be detected in purified TRPV1 fractions, indicative of a stable interaction.

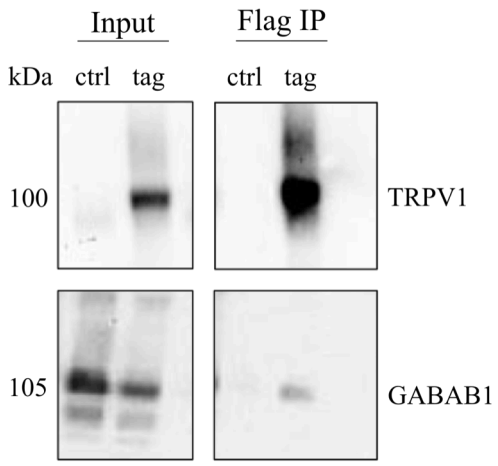

Figure 26: $GABA_{B1}$ co-purifies with TRPV1 from the DRG

Western Blot of a Flag IP of TRPV1 from the DRG with antibodies against TRPV1 and $GABA_{B1}$. $GABA_{B1}$ was detected in the elution of the tagged but not the control sample.
Legend: ctrl (wild type control tissue), tag (SF-TRPV1 tissue)

To investigate whether TRPV1 and the $GABA_B$ receptor physically interact in heterologous cell systems, co-immunoprecipitation experiments were performed in Hek293 cells. Hek293 cells were transiently transfected with plasmids encoding SF-TRPV1, $GABA_{B1}$ and $GABA_{B2}$, respectively. Cells were harvested, solubilized and subjected to immunoprecipitation with Flag magnetic beads. Hek cells transfected individually with TRPV1, $GABA_{B1}$ or $GABA_{B2}$, respectively, were used as negative controls. Western blot analysis revealed that both $GABA_{B1}$ (Fig. 27A) and $GABA_{B2}$ (Fig. 27B) robustly co-immunoprecipitate with TRPV1 from Hek293 cells co-expressing TRPV1. In the individual transfections, $GABA_{B1}$ or $GABA_{B2}$ subunits were not detected in the elutions, indicative of no nonspecific binding to the affinity resin.

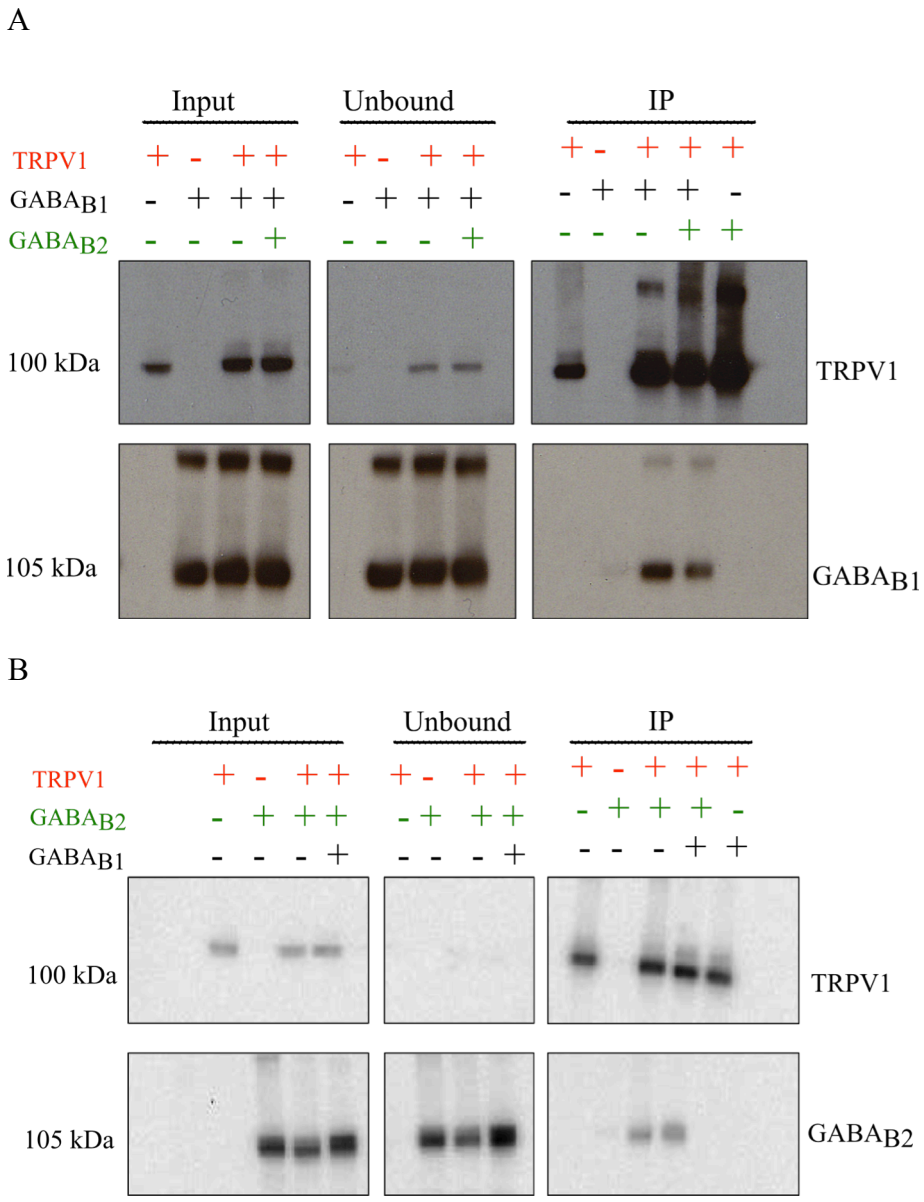

Figure 27: $GABA_{B1}$ and $GABA_{B2}$ co-immunoprecipitate with TRPV1 from Hek293 cells

(A) Co-immunoprecipitation of $GABA_{B1}$ with TRPV1. Hek293 cells were transiently transfected with SF-TRPV1 and vectors expressing $GABA_{B1}$ or $GABA_{B2}$ and subjected to immunoprecipitation (IP) with Flag magnetic beads. This was followed by immunoblotting with antibodies as indicated.

(B) Co-immunoprecipitation of $GABA_{B2}$ with TRPV1. Immunoprecipitation was performed as in (A) followed by immunoblotting with antibodies as indicated.
$GABA_B$ receptor immunoreactivity was also observed as higher molecular weight oligomers

5.1.4. Effect of baclofen on TRPV1 function in DRG neurons

To analyze the functional association between TRPV1 and $GABA_B$ receptors, the effect of baclofen, a $GABA_B$ specific agonist, was tested by calcium imaging of TRPV1 expressing DRG neurons. Preliminary results obtained from

electrophysiological recordings (performed by Dr. Mirko Moroni) on DRG neurons indicated that application of baclofen (100 µM) neither elicits currents *per se* nor affects TRPV1 currents when co-applied with capsaicin (100 nM) or low pH (pH 5). It was then tested whether baclofen has an effect on TRPV1 expressing neurons upon induction of an inflammatory condition. NGF is an inflammatory mediator that sensitizes TRPV1 receptors and potentiates its activity. DRG neurons were cultured and subjected to calcium imaging. Because TRPV1 quickly desensitizes, DRG neurons were stimulated with a multi-pulse protocol, which aims at reaching steady-state desensitization of TRPV1 receptors prior to NGF (100 ng/ml) application. The neurons were stimulated with five pulses of 100 nM capsaicin, followed by NGF application and a further capsaicin pulse. This was followed by a high potassium solution to select the neuronal population. Fig. 28A shows the normalized fluorescence ratios plotted over time. It shows that the response of the neurons increased upon the 6th capsaicin stimulus due to either the relief from desensitization of TRPV1 receptors or due to the presence of newly translocated TRPV1 receptors to the plasma membrane caused by the NGF cascade. When the same protocol is applied, pre-incubating the neurons with 100 µM baclofen, the response to the 6th capsaicin stimulus is decreased (Fig. 28B).

A

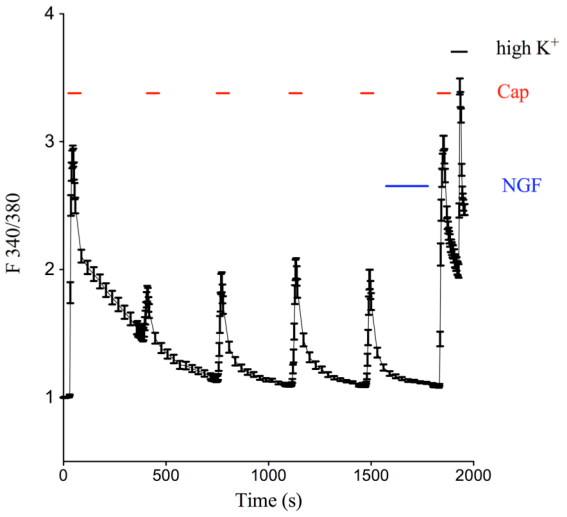

B

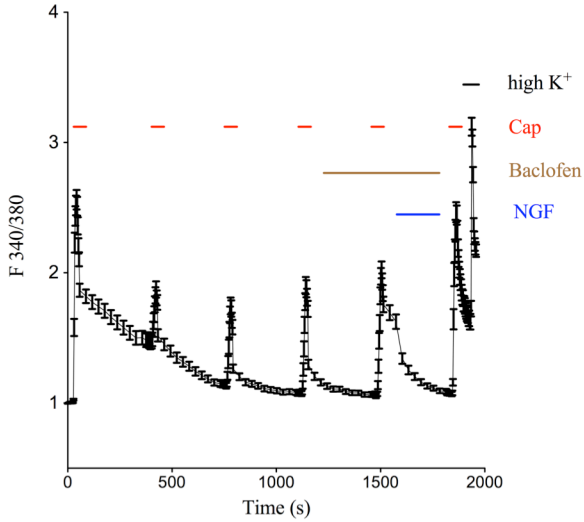

C

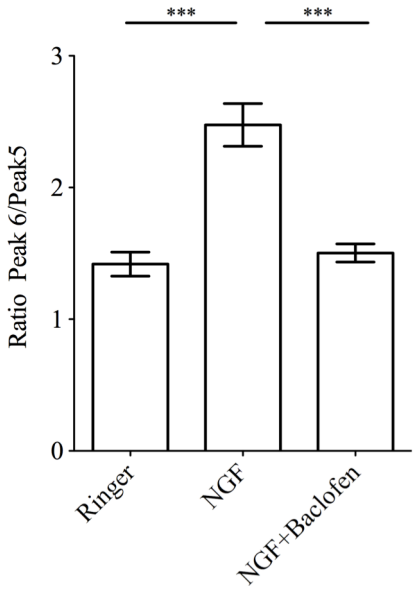

Figure 28: Effect of baclofen on NGF treated TRPV1 expressing neurons

Calcium imaging of cultured DRG neurons challenged with a multi-pulse capsaicin stimulation protocol

(A) DRG neurons were treated with NGF prior to capsaicin stimulation. The graph shows the averaged fluorescence ratios over time. The response of the neurons increased after the 6th capsaicin stimulus

(B) DRG neurons were pre-incubated with baclofen prior to NGF application. In this case, the response of the neurons to the 6th capsaicin stimulus was decreased

(C) Summary of (A) and (B). The graph represents the ratio between peaks 6 and 5 (after and before NGF application) in the presence or absence of baclofen. Cells treated with ringer solution were used as a negative control. N=250, Unpaired t-test, p-value < 0.001
Graphs adapted with permission from Dr. Mirko Moroni

5.1.5. Baclofen reduces NGF-induced thermal hypersensitivity

It has long been described that intraplantar or systemic injection of NGF into rodents induces a rapid hypersensitivity to thermal pain (Lewin et al., 1993). To investigate the effect of baclofen on NGF-induced thermal hypersensitivity, C57Bl6 mice were subjected to Hargreaves' Test after intraplantar injection of baclofen and NGF. In the Hargreaves' Test a radiant heat source is directed to the mouse hind paw and the latency until paw withdrawal is scored (Hargreaves et al., 1988). This test can be used to determine the responses to noxious thermal stimuli. Fig. 29 shows the mean withdrawal latencies for each paw (ipsilateral and contralateral). Basal withdrawal latencies were measured one day before application of the drugs (white bars in Fig. 29A, B, C). Because $GABA_B$ receptors act via G-protein coupling and have a slower onset, baclofen was administered unilaterally 30 min before NGF injection into both

hindpaws. Data were collected 60 minutes after NGF injection. Fig. 29A shows that intraplantar baclofen administration into the ipsilateral paw reduced the magnitude of thermal hypersensitivity as these mice displayed longer latencies compared to the control paw that received saline instead of baclofen. Mice that received bilateral NGF injection with no baclofen, developed thermal hypersensitivity in both paws (middle bars, Fig. 29A). Unilateral baclofen injection produced no antinociceptive effect in the contralateral paw, indicating that baclofen did not act outside of the paw. TRPV1 knockout mice do not develop thermal hyperalgesia upon NGF injection (Davis et al., 2000) and thus served as a negative control (Fig. 29B).

Furthermore, sole administration of baclofen did not produce any difference in the response to the heat stimulus, indicating that baclofen does not decrease pain responses *per se* (Fig. 29C).

A

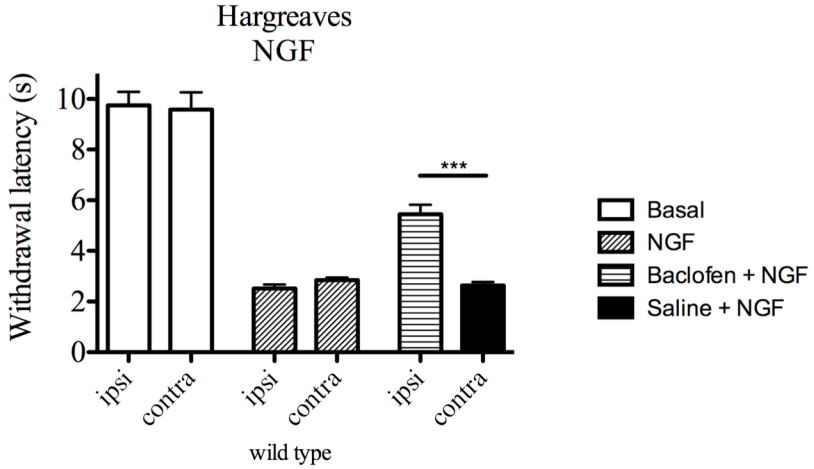

B

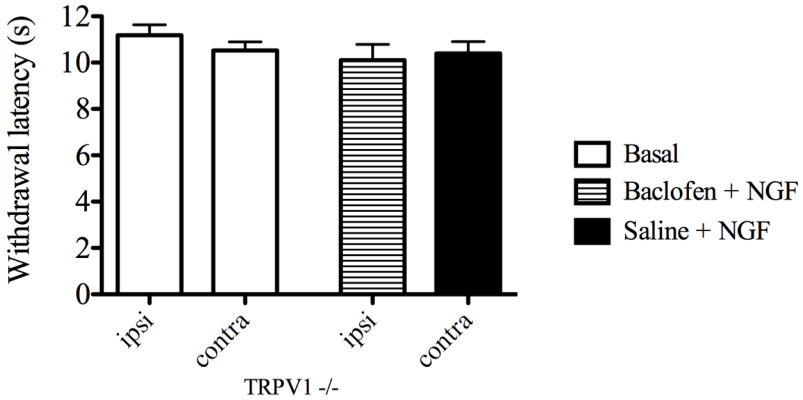

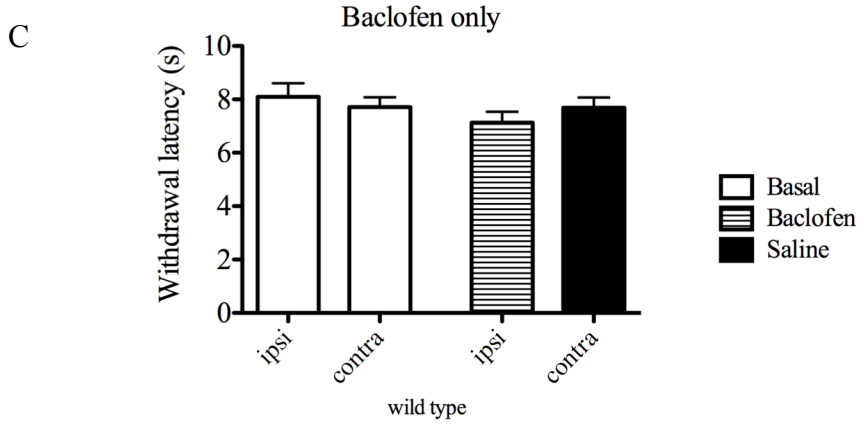

Figure 29: NGF-induced thermal pain sensitivity is decreased after baclofen administration

(A) Responses to thermal stimuli were measured with the Hargreaves apparatus as described in 3.19.1. NGF (2 µg/paw) was injected into both hind paws 30 min after unilateral administration of baclofen (3 µg/paw). Bar graphs show the mean latencies of paw withdrawal upon radiant heat. Basal withdrawal latencies were measured one day before application of the drugs (white bars). Baclofen decreased thermal pain sensitivity in the ipsilateral paw as compared to the control paw that received only NGF injection. N=6, $p<0.001$, t-test

(B) Mean withdrawal latencies to heat stimulation in TRPV1 -/- mice treated as in (A). NGF and baclofen injection did not have any effect. N=6

(C) Sole administration of baclofen into the hind paw did not produce any effect. Mice received baclofen injections and were subjected to Hargreaves's Test as in (A). Withdrawal latencies to thermal stimuli did not change. N=6, $p>0.05$, t-test

5.1.6. Effect of baclofen on bradykinin- and serotonin-induced hyperalgesia

To test whether the baclofen effect is specific to the NGF cascade, two other inflammatory mediators were used to induce inflammatory pain. Bradykinin and serotonin both sensitize TRPV1 via activation of the PLC-signaling pathway leading to potentiation of TRPV1 activity (Fig. 5) (Chuang et al., 2001; Ohta et al., 2006). Calcium imaging of cultured DRG neurons was performed as described in 5.1.4. Neurons were stimulated with multiple pulses of capsaicin, followed by incubation with bradykinin (10 nM) or serotonin (100 µM), respectively, and a further capsaicin pulse. Fig. 30A shows the averaged ratios between peaks 6 and 5 (after and before bradykinin or serotonin stimulation) in the presence or absence of baclofen. As observed with NGF (Fig. 28), the response of the neurons to the 6th capsaicin pulse decreased in the presence of baclofen (Fig. 30A).

At the behavioural level, the same experimental paradigm was used as with NGF: prior to bradykinin or serotonin injection into both hind paws, baclofen was

administered unilaterally into the hind paw. Fig. 30B shows that intraplantar baclofen administration in the ipsilateral paw also antagonized the hyperalgesic effect of bradykinin in wild type mice, while the contralateral paw was not affected. The same effect was observed after serotonin-evoked hyperalgesia (Fig. 30C). TRPV1 knockout mice were again used as negative controls and did not show any behavioral changes. This demonstrates that the baclofen effect is not due to NGF-mediated trafficking of TRPV1 to the plasma membrane, but instead baclofen might affect the PLC/PKC-signaling cascade, thereby interfering either with PIP_2 hydrolysis or with phosphorylation of TRPV1.

A

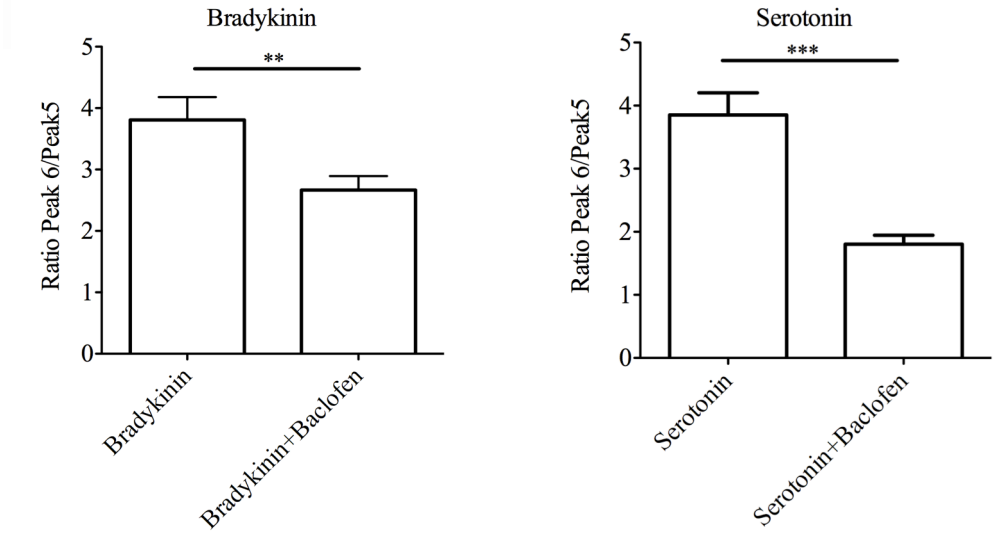

B

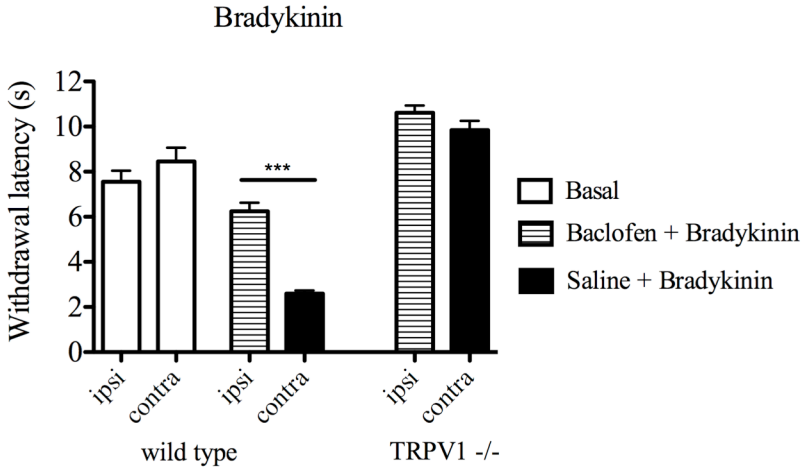

C

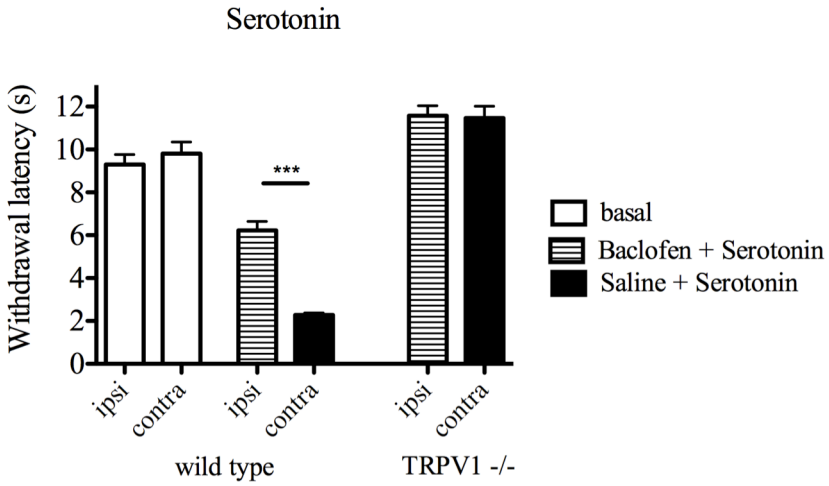

Figure 30: Effect of baclofen on bradykinin- and serotonin- induced thermal hypersensitivity

(A) Calcium imaging of cultured DRG neurons. Graph represents the ratio between peaks 6 and 5 (after and before bradykinin or serotonin application) in the presence or absence of baclofen. When neurons were pre-incubated with baclofen, the response to the 6th stimulus with 10 nM bradykinin (left graph) or 100 µM serotonin (right graph) was decreased. N=180 (bradykinin), N=142 (serotonin), Unpaired t-test, p-value < 0.05. Graphs adapted with permission from Dr. Mirko Moroni

(B) Bradykinin (20 nM/paw) was injected into both hind paws 30 min after unilateral administration of baclofen (3 µg/paw). Responses to thermal stimuli were measured with the Hargreaves apparatus as described in 3.19.1. Bar graphs show the mean latency of paw withdrawal upon radiant heat. Baclofen decreased thermal pain sensitivity as compared to the control paw that only received bradykinin injection. N=6, p<0.001, t-test

(C) Serotonin (100 nM/paw) was injected into both hind paws 30 min after unilateral administration of baclofen (3 µg/paw). Responses to thermal stimuli were measured as in (B). Bar graphs show the mean latency of paw withdrawal upon radiant heat. Baclofen decreased thermal pain sensitivity as compared to the control paw that only received serotonin injection. N=6, p<0.001, t-test

5.1.7. Effect of baclofen on prostaglandin-induced hyperalgesia

Another proinflammatory mediator that is released from damaged tissue is prostaglandin E_2 (PGE_2), which mediates TRPV1 potentiation via a PKA-signaling pathway (Smith et al., 2000; Gu et al., 2003). To address the question whether the observed baclofen effect is restricted to the PLC/PKC signaling cascade, PGE_2 was bilaterally injected into the hindpaw following unilateral baclofen administration. Fig. 31 shows that intraplantar baclofen into the ipsilateral paw had no effect on PGE_2-induced thermal hyperalgesia. These data suggest that baclofen diminishes TRPV1 sensitization through the PLC/PKC signaling pathway.

To summarize the results of this chapter, TRPV1 showed overlapping expression with both $GABA_B$ subunits in DRG neurons and the spinal cord as well as physical co-association in Flag pull-downs from the DRG and transfected Hek293 cells. Interestingly, $GABA_B$ receptor activation was shown to modulate TRPV1 sensitization *in vitro* and *in vivo* without affecting TRPV1 activity acutely. The specific $GABA_B$ agonist, baclofen, reduced NGF-, bradykinin- and serotonin-induced sensitization of TRPV1 while no effect was observed with PGE_2, indicating that $GABA_B$ activation might result in modulation of the PLC/PKC signaling pathway.

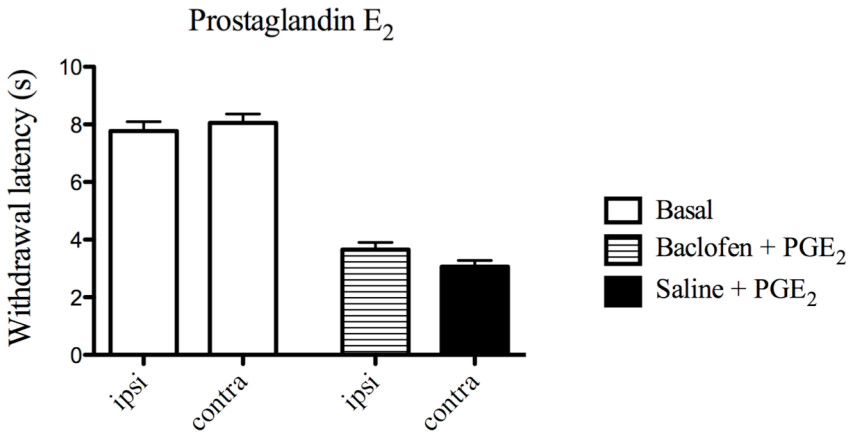

Figure 31: Baclofen has no effect on PGE_2-induced thermal hyperalgesia

PGE_2 (1 nM/paw) was injected into both hind paws 30 min after unilateral administration of baclofen (3 µg/paw). Responses to thermal stimuli were measured with the Hargreaves apparatus. Bar graphs show the mean latency of paw withdrawal upon radiant heat. Baclofen had no effect on thermal pain sensitivity. N=6, $p>0.05$, t-test

5.2. The Vesicular Glutamate Transporter 2 as a putative partner protein of TRPV1

Mass spectrometry analysis revealed that the Vesicular Glutamate Transporter 2 (Vglut2) was specifically and with high abundance enriched in Flag affinity purifications from the sciatic nerve. To analyze and confirm a potential interaction between Vglut2 and TRPV1, co-localization, co-immunoprecipitation assays and functional analyses were carried out.

5.2.1. TRPV1 co-localizes with Vglut2 vesicles in cultured F11 cells

Co-localization was assessed by immunocytochemistry of F11 cells transiently transfected with plasmids encoding TRPV1 and Vglut2. F11 cells are derived from a fusion between mouse embryonic neuroblastoma and rat dorsal root ganglion neurons and therefore resembles the native environment of these two proteins. Fig. 32A shows co-labeling using antibodies against TRPV1 and Vglut2. TRPV1 shows a punctate staining pattern at the plasma membrane and cell processes. A large fraction of TRPV1 puncta resides in Vglut2 positive vesicles at the plasma membrane and along the processes. Vglut2 has been shown to co-exist with the Vesicular GABA Transporter (VGAT) in subtypes of GABAergic and glutamatergic terminals to modulate vesicular content and fine-tune synaptic plasticity (Herzog et al., 2006; Zander et al., 2010). Analogously, co-expression of TRPV1 and Vgat was also found in F11 cells that were transiently transfected with both plasmids (Fig. 32B).

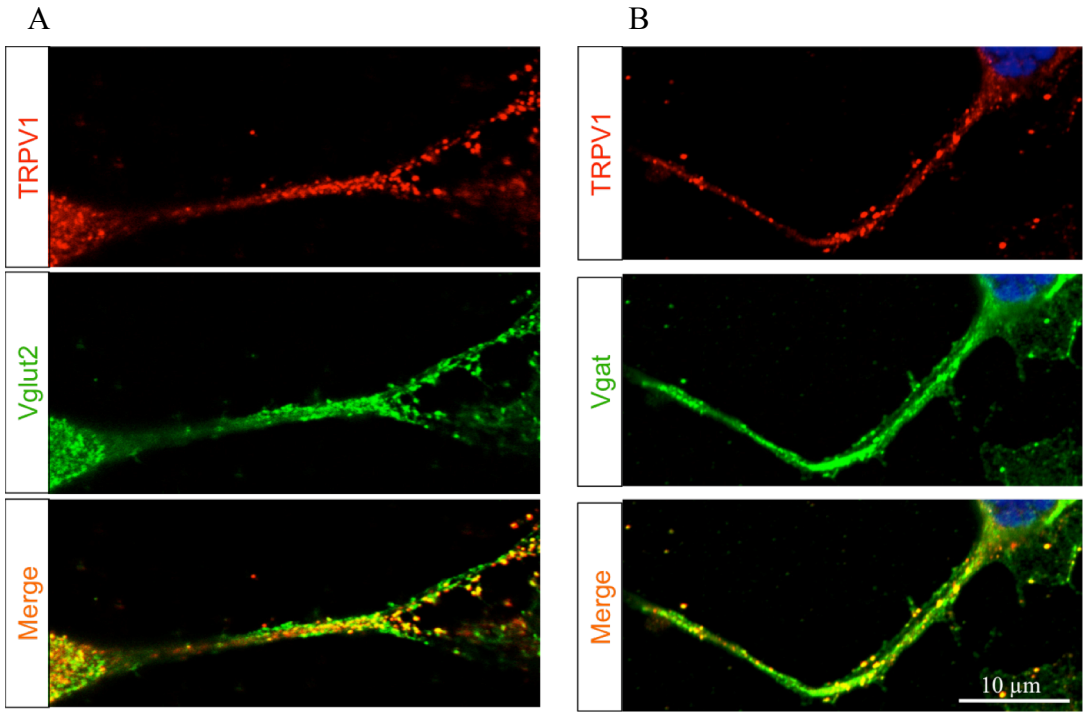

Figure 32: TRPV1 and Vglut2 co-localize in transfected F11 cells

(A) F11 cells were transiently transfected with plasmids encoding TRPV1 and Vglut2 and stained with the corresponding antibodies. Co-localization was observed at the plasma membrane and along the processes.
(B) TRPV1 co-localizes with VGAT in transfected F11 cells. Scale bar = 10 µm

5.2.2. Detection of protein interaction using a Proximity Ligation Assay

The immunostaining results of transiently transfected F11 cells indicate that TRPV1 and Vglut2 are co-localized. However, overexpression may cause proteins to become incorrectly localized. Therefore, localization of the endogenous proteins must be studied. However, a problem with detection of endogenous Vglut2 is that it is not sufficiently highly expressed in DRG neurons. To investigate whether TRPV1 and Vglut2 interact endogenously, the Proximity Ligation Assay (PLA) was used which enables visualization of low abundance endogenous protein-protein interactions. Primary DRG neurons were cultured and stained with antibodies recognizing TRPV1 and Vglut2. Species-specific secondary antibodies, called PLA probes, were bound to the primary antibodies. Each PLA probe has a short DNA strand attached to it; when two proteins are in close proximity, the DNA strands can interact by the addition of two circle-forming fluorescently labeled oligonucleotides, which are then ligated and amplified via subsequent rolling circle amplification using a polymerase. The

hundredfold amplification of the signal produced by PLA results in a high fluorescence signal and makes this method very sensitive.

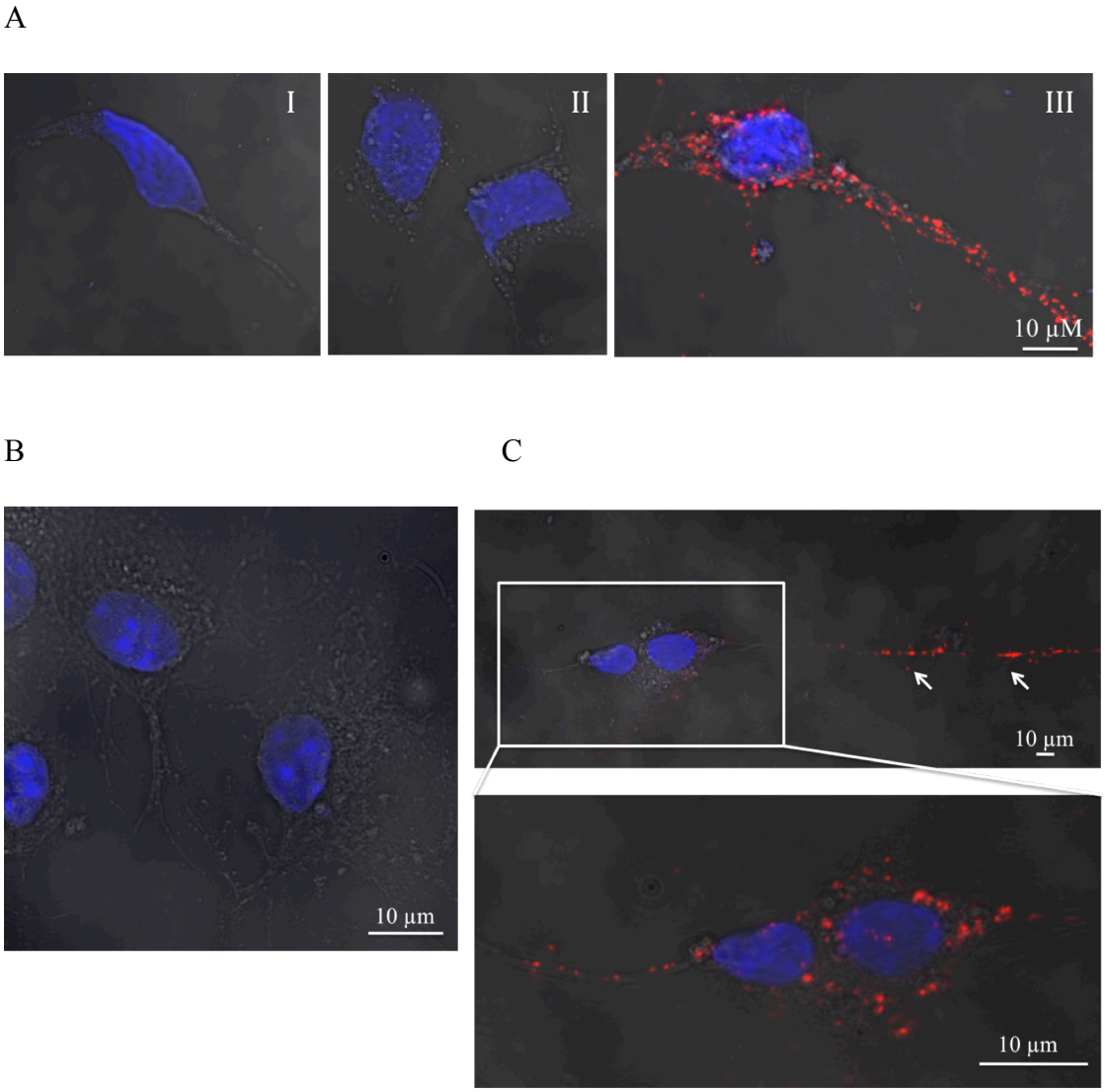

Figure 33: Endogenous labeling of TRPV1 and Vglut2 in DRG neurons using the Proximity Ligation Assay

(A) F11 cells were transiently transfected with plasmids encoding TRPV1 (I), Vglut2 (II) or TRPV1 plus Vglut2 (III) and stained according to the PLA protocol as described in 3.17.4. Fluorescence was observed only in cells that were transfected with both plasmids (III). No fluorescence was detected in the individually transfected cells (I and II).

(B) Staining DRG neurons only with the PLA probes, without prior incubation with primary antibodies, did not result in any fluorescence.

(C) DRG neurons were stained with primary antibodies against TRPV1 and Vglut2, which was followed by the PLA staining procedure as in (A). Box represents enlarged view of fluorescence observed at the plasma membrane. Fluorescence was also detected at the neurites (arrows).

Fig. 33 shows the endogenous interaction of TRPV1 and Vglut2 in cultured DRG neurons labeled with the PLA kit. Labeling was observed both at the plasma

membrane (Fig. 33C, enlarged view) and along neurites (Fig. 33C, arrow). As a negative control, cells were processed through the PLA protocol but without incubation with primary antibodies and did not show any labeling (Fig. 33B). In addition, F11 cells transiently transfected with either Vglut2 or TRPV1 alone were labeled with the PLA protocol and additionally confirmed the specificity of the PLA probes (Fig. 33A). While individually transfected cells did not show any labeling (Fig. 33A I, II), cells transfected with both plasmids showed a strong PLA labeling. These results indicate that TRPV1 and Vglut2 are physically associated in DRG neurons at the endogenous level.

5.2.3. Vglut2 co-immunoprecipitates with TRPV1 from transfected F11 cells

To examine whether TRPV1 and Vglut2 are physically associated in heterologous cell systems, co-immunoprecipitation experiments were performed in F11 cells. The cells were transiently transfected with plasmids encoding SF-TRPV1 and Vglut2. Western Blot analysis using antibodies recognizing SF-TRPV1 and Vglut2 following capture with Flag magnetic beads detected both proteins (Fig. 34A). Immunoblotting was carried out using antibodies recognizing TRPV1 and Vglut2. Cells that were individually transfected with only TRPV1 or Vglut2 served as controls. In the single transfections, Vglut2 was not detected in the elution, indicating no nonspecific binding to the beads. Importantly, co-assembly of TRPV1 and Vglut2 was confirmed by “reverse immunoprecipitation” using an antibody directed against Vglut2 in F11 cells solubilized under the same conditions as above (Fig. 34B). These results indicate that TRPV1 and Vglut2 physically interact in F11 cells.

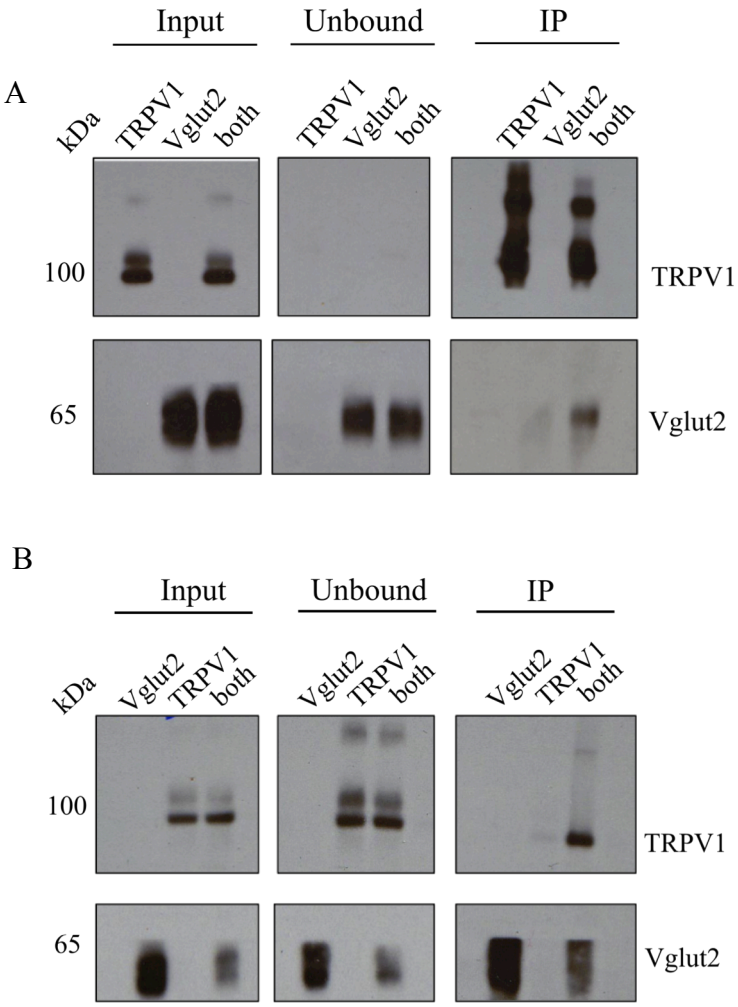

Figure 34: Co-immunoprecipitation of Vglut2 and TRPV1 from transfected F11 cells

(A) F11 cells were transfected with the following combinations: TRPV1 or Vglut2 alone and TRPV1 plus Vglut2. Cells were subjected to immunoprecipitation using Flag magnetic beads. Vglut2 co-immunoprecipitates with TRPV1.

(B) F11 cells were transfected with the same combinations of plasmids as in (A) and subjected to Reverse IP using an antibody directed against Vglut2. TRPV1 was detected in the Vglut2 pull-down. Input (soluble fraction), unbound (flow-through)

5.2.4. Vglut2 co-immunoprecipitates with TRPV1 from the sciatic nerve

TRPV1 purifications from mouse tissue were performed using solubilization buffer with 0.1% DDM as a detergent due to its mild properties and because it preserves protein activity. However, the mild solubilization conditions make it possible to pull down incompletely solubilized membrane sheets and intact vesicles instead of solubilized protein complexes. To rule out the possibility that the high abundance of Vglut2 is due to the low concentration of detergent in the purification procedure, TRPV1 was Flag affinity purified from the sciatic nerve of BAC transgenic SF-

TRPV1 mice using more stringent detergents for solubilization including 1% DDM, 1% Triton and RIPA buffer. Elutions were analyzed by subsequent mass spectrometry. Tab. 2 lists under which solubilization conditions selected synaptic vesicle proteins were still detected. While most vesicular proteins could not be detected using harsher conditions, Vglut2 was still specifically enriched in all conditions tested. Fig. 35 shows a western blot of a pull-down of SF-TRPV1 from sciatic nerve comparing two detergent conditions, 0.1% DDM and RIPA buffer. Antibodies were used as indicated. These results further indicate that TRPV1 and Vglut2 are directly associated because RIPA buffer disrupts vesicular membranes.

Name	0.1% DDM	1% DDM	1% Triton	RIPA
TRPV1	+	+	+	+
Vglut2	+	+	+	+
Synaptobrevin-2	+	+	+	-
Snap-25	+	-	-	-
Synaptophysin	+	-	-	-
Synaptogyrin-3	+	-	-	-
Snapin	+	-	-	-
Synaptojanin-1	+	-	-	-
V-ATPase	+	-	+	-
Synaptotagmin-14	+	+	+	-

Tab. 2: Comparison of selected synaptic vesicle proteins detected in MS runs using different detergents for the purification of TRPV1 from sciatic nerve.
TRPV1 is detected in all purifications. Vglut2 co-purified in all conditions tested. Most other synaptic vesicle proteins only co-purified with 0.1% DDM.

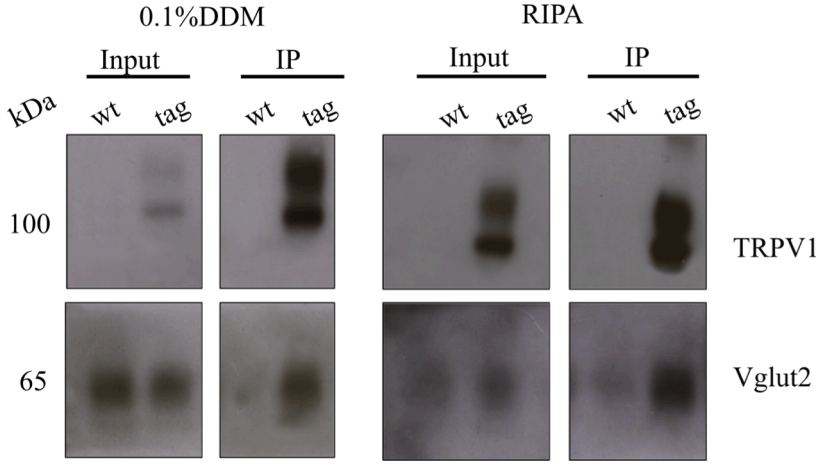

Figure 35: Comparison of Flag affinity purifications of TRPV1 from sciatic nerve
Flag affinity purification of TRPV1 from sciatic nerve of SF-TRPV1 BAC transgenic mice. Wild type mice were used as a negative control. Purifications were performed using 0.1% DDM or RIPA buffer. The relative yield of TRPV1 was larger in the more stringent (RIPA buffer) condition. Vglut2 co-purifies in both conditions. A faint Vglut2 band was observed in the control sample due to nonspecific binding to the affinity resin possibly due to heterogeneity of tissue samples.

5.2.5. TRPV1 localizes in membrane and synaptic vesicle compartments

TRPV1 has long been described to be expressed at the plasma membrane where it allows primarily calcium influx into the cell upon activation. However, since the co-immunoprecipitation and co-localization assays with Vglut2 suggest that these two proteins are physically associated, the next step was to test whether TRPV1 is present in purified synaptic vesicle fractions isolated from mouse spinal cord. Therefore, subcellular fractionation of mouse spinal cords was carried out to enrich for synaptic vesicle proteins through several differential centrifugation steps. The subcellular fractionation procedure was based on established methods (Huttner et al., 1983; Varoqui et al., 2001). The purification can be divided into 5 steps: 1) homogenization of the spinal cord (H), 2) low speed centrifugation to obtain a crude nuclear pellet (P1), 3) differential centrifugation of the cleared homogenate to obtain a crude synaptosomal fraction (P2), 4) hypo-osmotic lysis of the synaptosomes to release synaptic vesicles (LS0), 5) separation of crude membranes (LP1) and synaptic vesicles by centrifugation (LP2) and 6) isolation of synaptic membranes by sucrose gradient centrifugation (SM). The fractionation was carried out using SF-TRPV1, wild type and TRPV1 -/- mice. Fig. 36A shows a western blot of the different fractions with antibodies against TRPV1, synaptic vesicle proteins (Vglut2, Synaptophysin) and synaptic membranes (NMDA). Vglut2 and synaptophysin show a specific enrichment in the synaptic vesicle fraction. The postsynaptic NMDA receptor was found enriched in LP1 and synaptic membrane fraction and decreased in the synaptic vesicle fraction. TRPV1, both wild type and SF-TRPV1 (Fig. 36A, B), were detected in both crude synaptic vesicle and synaptic membrane compartments. No TRPV1 signal was detected in tissue samples from the TRPV1 -/- mice (Fig. 36C). A faint NMDA signal was also observed in the LP2 fraction of the wild type sample in Fig. 36B, possibly due to carry-over from the previous fractionation step.

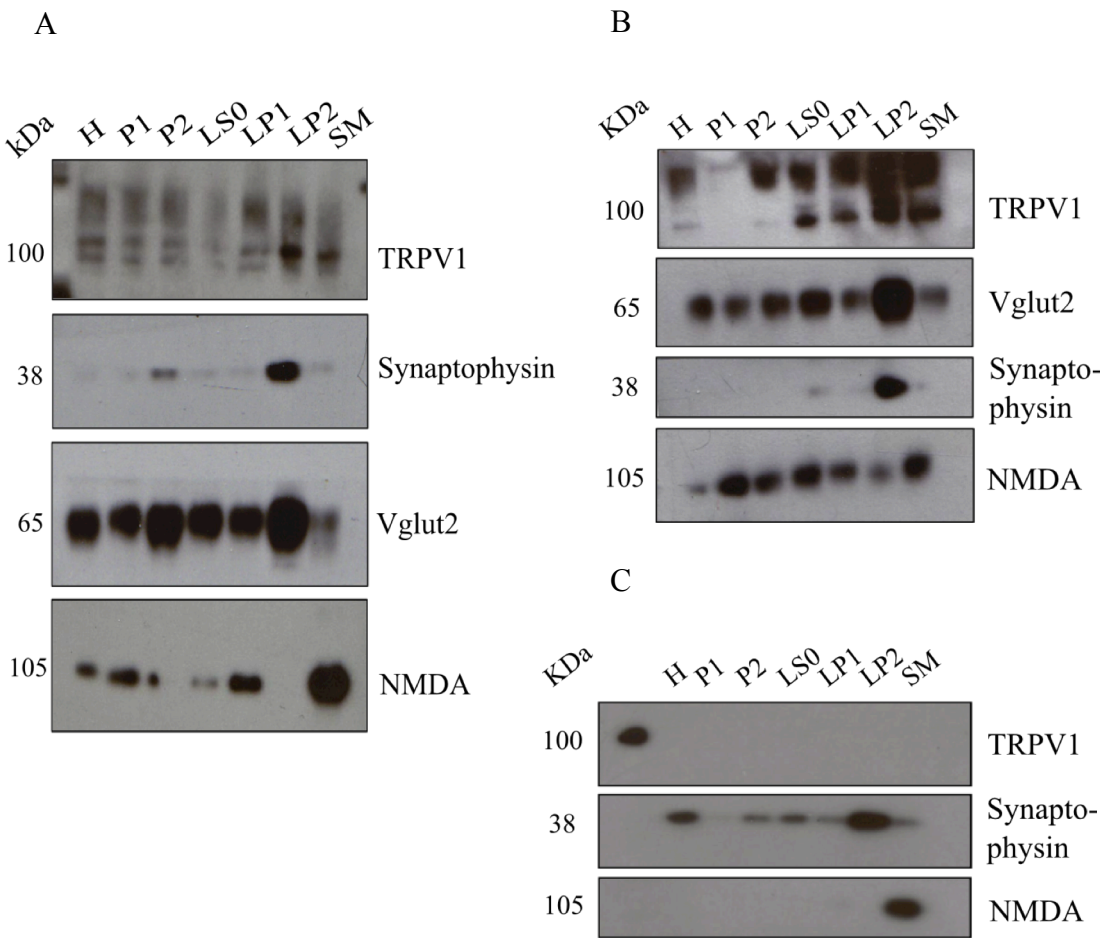

Figure 36: Sub-cellular fractionation of the mouse spinal cord

Crude synaptic vesicles were purified using established procedures, with the following fractions being analyzed: *Homogenate*; *P1*, crude nuclear pellet; *P2*, crude synaptosomes; *LS0*, hypo-osmotically shocked synaptosomes; *LP1*, pellet obtained after synaptosomal lysis; *LP2 (SV)*, crude synaptic vesicles; SM, synaptic membranes recovered after sucrose gradient. 5 µg protein per lane. Immunoblotting was carried out with antibodies as indicated. (A) Fractionation of spinal cords of SF-TRPV1 (low expresser), (B) wild type and (C) TRPV1 -/- mice

5.2.6. TRPV1 co-immunoisolates with Vglut2 purified vesicles

Thus far, the results indicate that TRPV1 and Vglut2 co-localize and physically associate. It is therefore possible that they are expressed on the same synaptic vesicle. Immunoisolation is an established method for investigating the protein content of specific organelles, such as synaptic vesicles. This method not only enables isolation of functional vesicles but also the isolation of specific synaptic vesicle subtypes. Therefore, immunoisolation experiments were performed to isolate Vglut2 positive vesicles from the LS0 fraction prepared from spinal cord and sciatic nerve of SF-TRPV1 BAC transgenic mice. Pan affinity beads were coupled with antibodies

against either Vglut2 or Flag. Beads without primary antibodies were subjected to the same procedure and used as control for nonspecifically bound material. Fig. 37A shows that TRPV1 co-immunoisolated with Vglut2 positive vesicles from the sciatic nerve. Importantly, Vglut2 also co-immunoisolated with Flag purified vesicles indicating that TRPV1 is present in Vglut2 containing vesicles. In the spinal cord the result was similar (Fig. 37B), except that TRPV1 bound nonspecifically to the beads while no nonspecific binding of Vglut2 was observed. The signal of TRPV1 in Vglut2 purified vesicles was much lower due to lower expression of TRPV1 in the spinal cord. As immunoisolations are performed without the addition of detergent, isolated synaptic vesicles are functionally intact and express other synaptic markers such as synaptophysin and synaptogyrin-1 (Fig. 37 A, B).

A

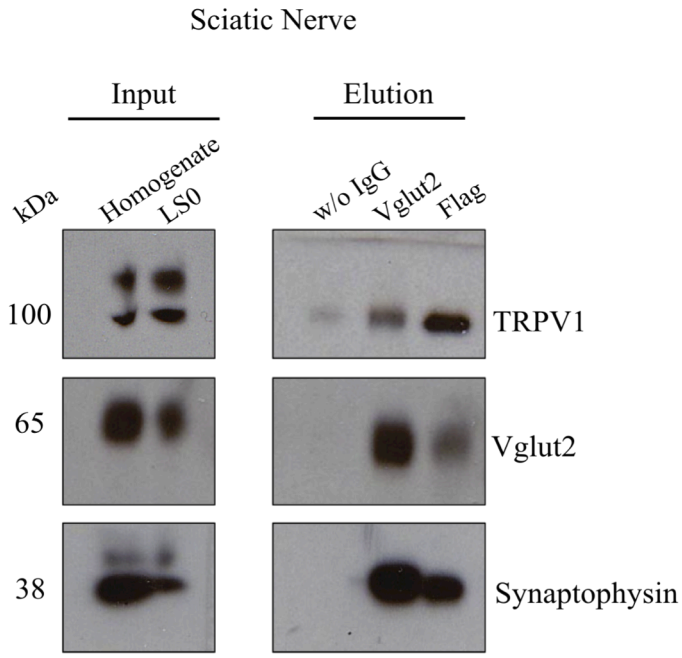

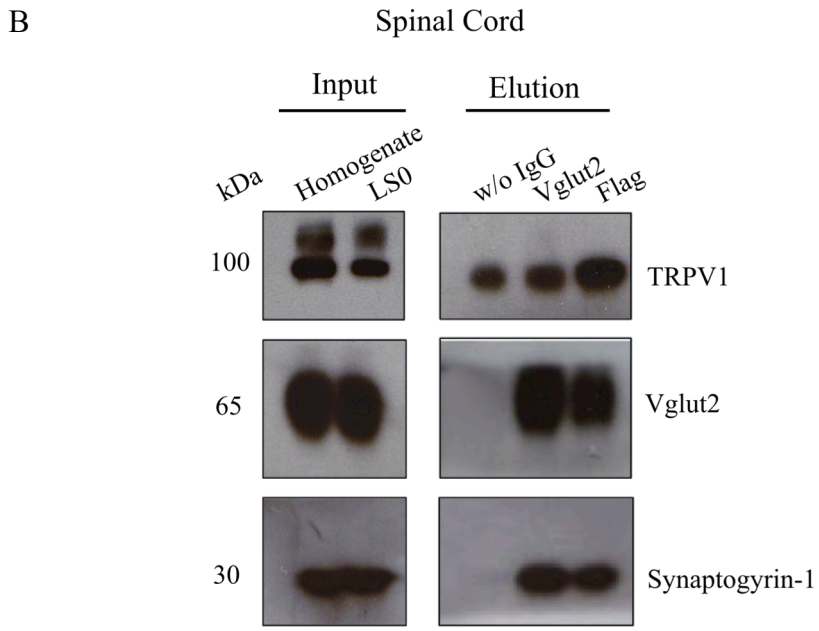

Figure 37: Immunoisolation of Vglut2 and Flag positive vesicles from spinal cord and sciatic nerve

(A) Vglut2 and Flag positive vesicles were purified from the LS0 fraction of the sciatic nerve. Synaptic vesicles are intact and express other synaptic markers such as synaptophysin. Flag positive vesicles also co-immunoisolated Vglut2. Beads without primary antibodies were subjected to the same procedure and used as control for nonspecifically bound material.

(B) Vglut2 and Flag positive vesicles were isolated from the spinal cord as in (A). TRPV1 bound to a large extent nonspecifically to the beads. Isolated vesicles were also positive for synaptogyrin-1.

5.2.7. Effect of TRPV1 activation and inhibition on glutamate uptake

VGLUTs use a proton gradient generated by a V-type H^+-ATPase to carry glutamate into the interior of the vesicle. ATP hydrolysis enables flow of protons into the vesicle interior making it more acidic. This generates a pH gradient across the vesicular membrane. At the same time, the vesicle interior becomes more positively charged, generating a corresponding membrane potential. Thus, VGLUTs are dependent on an electrochemical proton gradient for proper neurotransmitter loading (Fig. 38D). However, the regulatory mechanism of glutamate uptake into synaptic vesicles is still a central research theme.

To address the question of whether TRPV1 positive vesicles are capable of neurotransmitter loading, glutamate uptake assays of synaptic vesicle preparations from the spinal cord were performed. This assay is based on subcellular fractionation of the spinal cord to obtain a crude synaptic vesicle fraction that is incubated with tritium labeled glutamate. The amount of neurotransmitter uptake is determined by

scintillation counting. Because neurotransmitter uptake assays have been largely used to study brain synaptic vesicles, the assay had to first be established for the spinal cord. An important prerequisite is that a large quantity of synaptic vesicles is isolated in a functionally active form. For this reason, subcellular fractionation was carried out using rat spinal cord to obtain larger quantities of source material. To examine whether TRPV1 has a functional role in the vesicles, glutamate uptake was investigated using TRPV1 specific agonists and antagonists. Fig. 38 shows a scatter plot of the amount of radioactive glutamate (measured in dpm (decay/min)) that was taken up by the vesicles. Uptake was inhibited by the protonophore FCCP, which dissipates the synaptic vesicle proton gradient. Furthermore, the uptake was specifically blocked by the VGLUT inhibitor, trypan blue, validating efficient isolation of glutamatergic vesicles that were functionally intact. Capsaicin (10 µM) did not produce any effect (Fig. 38A) while two inhibitors, I-RTX (5 µM) and AMG9810 (10 µM), reduced glutamate uptake. The specificity of these two blockers was tested in uptake experiments of synaptic vesicles isolated from rat cerebellum, which is devoid of TRPV1 expression. Fig. 38B shows that neither blockers affected glutamate uptake, even at higher concentrations. However, when synaptic vesicles were purified from wild type and TRPV1 -/- mice and incubated with I-RTX, the reduction of glutamate uptake was also observed in the TRPV1 -/- mice, indicating a nonspecific effect of I-RTX (Fig. 38C). Thus, these data are inconclusive and do not provide evidence for a potential role of TRPV1 in synaptic vesicle loading.

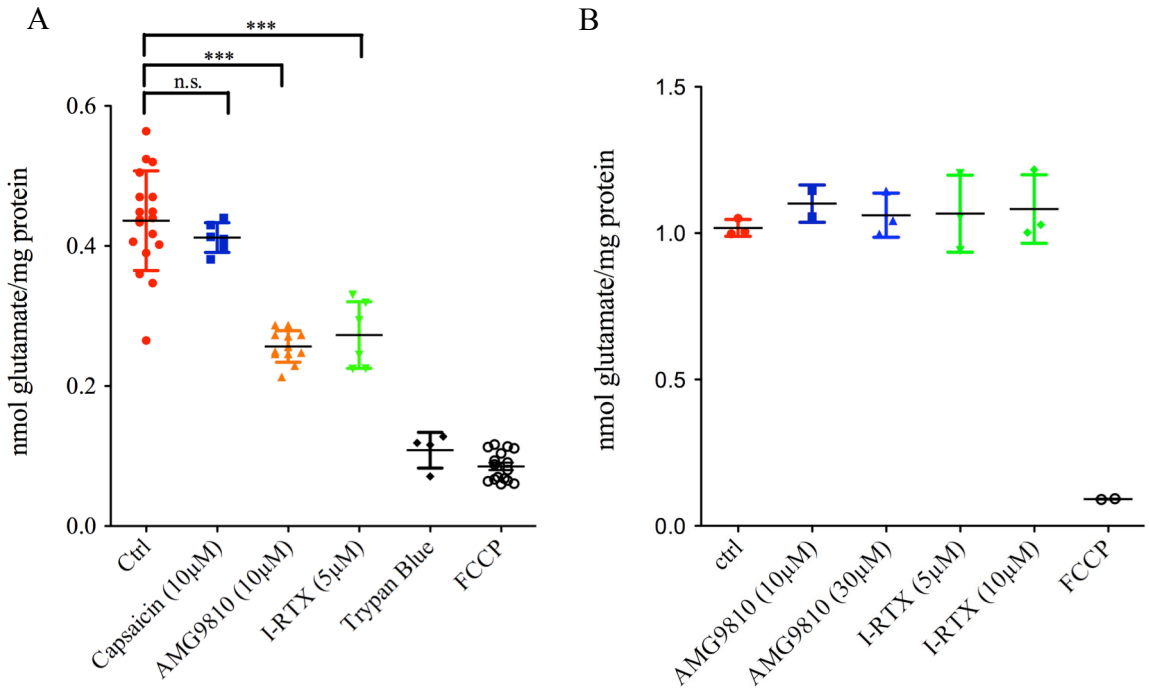

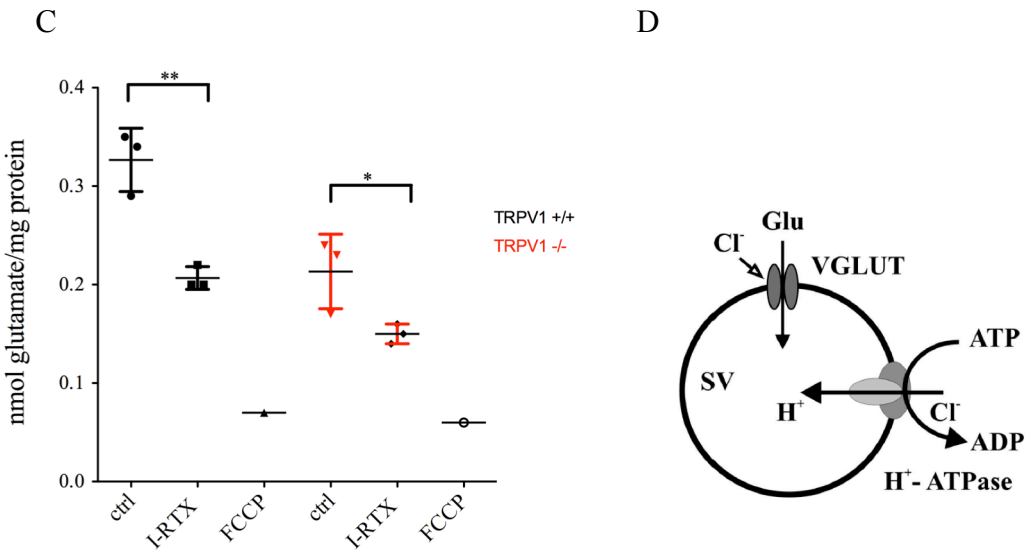

Figure 38: Effect of TRPV1 activation and inhibition on Glutamate uptake

Uptake is given in dpm (decay/min) and was normalized to protein concentration. Values represent the mean of three determinations ± SD (*Student's *t* test, $p < 0.05$). (A) represents at least three independent experiments and (C) a single experiment

(A) [^{3}H]-Glutamate uptake was performed using synaptic vesicles (LP2 fraction) purified from rat spinal cord. The presence of two TRPV1 blockers, I-RTX and AMG9810, reduced glutamate uptake while capsaicin did not produce any effect. Uptake was FCCP and Trypan blue sensitive.

(B) [^{3}H]-Glutamate uptake was performed using synaptic vesicles (LP2 fraction) purified from rat cerebellum. The presence of the two TRPV1 antagonists, AMG9810 (10, 30 µM) and I-RTX (5, 10 µM), had no effect on the uptake.

(C) [^{3}H]-Glutamate uptake was performed using synaptic vesicles (LP2 fraction) purified from spinal cord of C57Bl6 and TRPV1 -/- mice. I-RTX induced a reduction of glutamate uptake in both genotypes

(D) Loading of VGLUTs is achieved through a proton gradient generated by a H^+-ATPase. ATP hydrolysis generates a pH gradient across the vesicular membrane and a corresponding membrane potential. Chloride is needed by VGLUTs to function efficiently. Adapted from Liguz-Lecznar and Skangiel-Kramska, 2007

5.2.8. TRPV1 translocation is not affected in Vglut2 knockout mice

It is reasonable to assume that TRPV1 resides in Vglut2 vesicles to be transported to peripheral or central sites. To investigate whether Vglut2 is implicated in translocation of TRPV1, transverse sections of Vglut2 knockout embryos (E18) were stained for TRPV1. Vglut2 knockout mice die at birth (Moechars et al., 2006; Wallén-Mackenzie et al., 2010) because of its predominant expression during embryonic and early postnatal development. For this reason, embryos were used. Immunolabeling of TRPV1 was observed in the superficial laminae of the dorsal horn as well as in a subset of DRG neurons (Fig. 39A), indicating that TRPV1 is properly translocated in the absence of Vglut2. Wild type littermates were used as a positive control (Fig. 39B) and showed Vglut2 and TRPV1 co-localization in small- and medium-sized

DRG neurons as well as in the superficial laminae in the dorsal horn spinal cord. This is in agreement with other studies that reported a 94.2% overlap between TRPV1 and Vglut2 in the DRG (Liu et al., 2010). Moreover, TRPV1 function was assessed by calcium imaging experiments on cultured TG neurons prepared from Vglut2 knockout embryos (E18), using wild type embryos as a positive control. Fig. 39C shows the resulting fluorescence ratios plotted over time. Application of 1 µM capsaicin resulted in activation of TRPV1 expressing neurons. A high potassium solution was administered to select all neuronal cells. The responses of the neurons to capsaicin were similar in both genotypes, indicating that TRPV1 function in Vglut2 knockout embryos is not impaired.

A

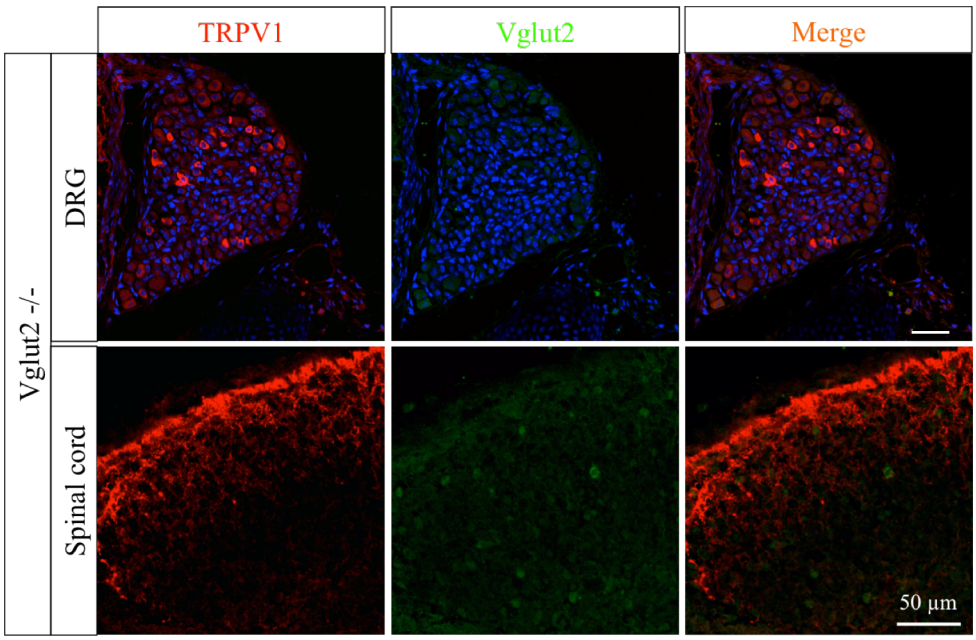

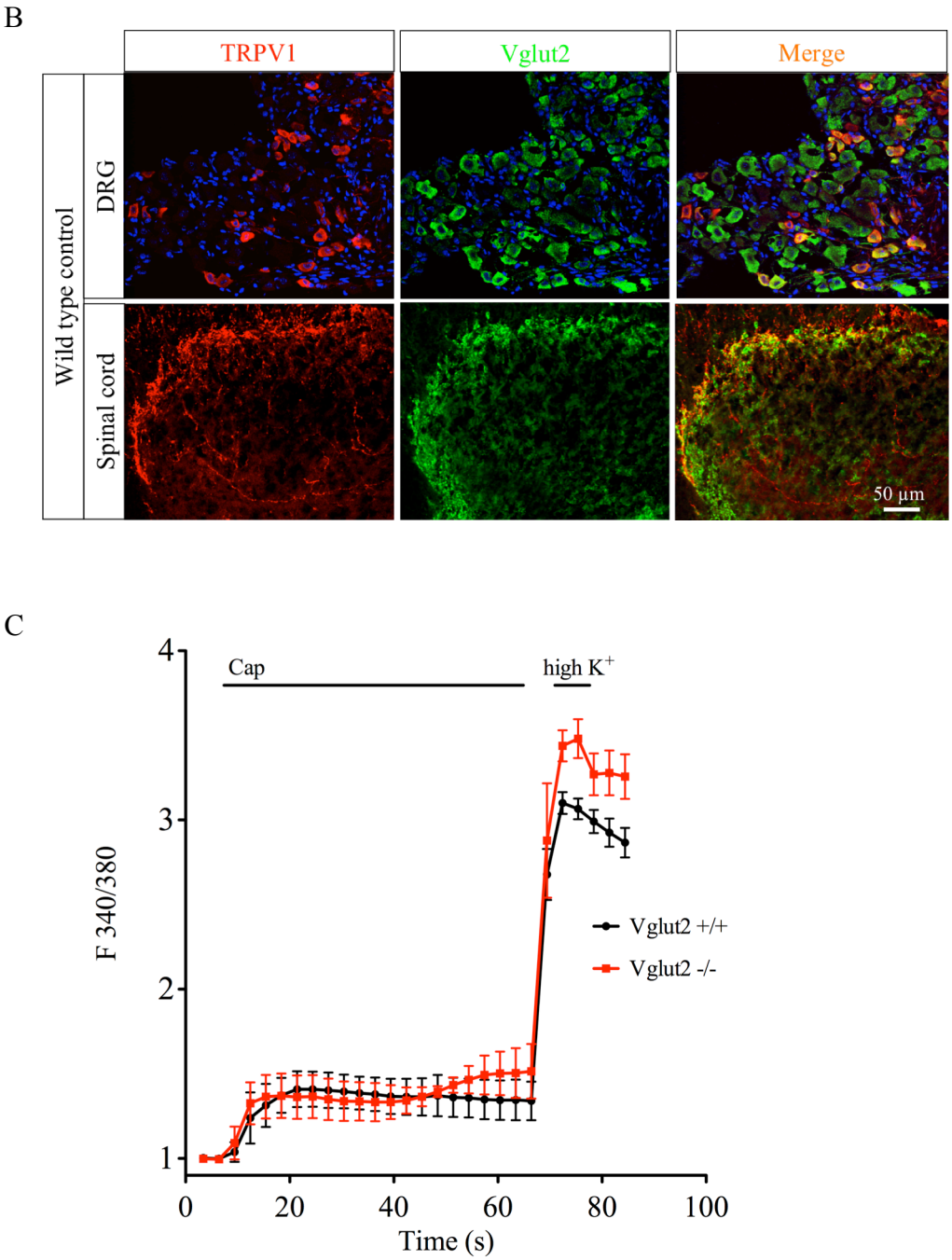

Figure 39: TRPV1 localization and activation are not impaired in Vglut2 deficient embryos

(A) TRPV1 and Vgut2 labeling in transverse sections of the spinal cord and DRG in Vglut2 -/- embryos. No labelling was detected for Vglut2. TRPV1 labeling was detected in a subset of DRG neurons as well as in the superficial laminae indicative of no defect in TRPV1 translocation.

(B) TRPV1 and Vglut2 co-labeling in Vglut2 +/+ mice. While TRPV1 was detected in small-and medium sized DRG neurons, Vglut2 expression was more widespread. In the spinal cord TRPV1 was only detected in laminae I and II overlapping with Vglut2 labeling. Overlap between TRPV1 and Vglut2 has been reported by other groups.

(C) Calcium imaging of cultured trigeminal ganglion neurons prepared from Vglut2 -/- and +/+ mice. TRPV1 activation was accessed by administration of 1 µM capsaicin. Similar responses were observed from TG neurons of Vglut2 +/+ and -/- mice. N=3

To summarize the results of this chapter, TRPV1 and Vglut2 showed co-expression in in transfected F11 cells, DRG neurons and the superficial layers of the spinal cord. The results of the subcellular fractionation and immunoisolations of Vglut2 - and TRPV1-containing vesicles suggest that a fraction of TRPV1 might be present on a Vglut2-expressing vesicular pool. To address the functional role of TRPV1 on these vesicles, glutamate uptake experiments were carried out but did not provide conclusive results, leaving the question of wheter TRPV1 is functional on vesicles open.

Contribution of other collegues to this thesis work:

- Jana Rossius generated the BAC transgenic SF-TRPV1 mice and did the southern blot analysis of the founder lines (Fig. 12B).
- Dr. Marieluise Kirchner (group Matthias Selbach) performed the mass spectrometry runs and analysis.
- Dr. Mirko Moroni carried out calcium imaging experiments on DRG cultures to test baclofen effects on TRPV1 function (Fig. 28 and Fig. 30A)

6. Discussion

By analogy to the first identified member of the TRP ion channel family in *Drosophila,* there is emerging evidence that mammalian TRP channels do not function as individual entities but rather depend on additional components that are necessary for their specific signaling. As directly or indirectly associated proteins can largely affect channel function and regulation, an understanding of signal transduction by ion channels requires comprehensive analysis of their molecular environment, So far, experimental procedures enabling unbiased and comprehensive access to the environment of TRPV1 have only begun to evolve. Therefore, this thesis work established a genetic and biochemical strategy for purifying TRPV1 protein complexes from sensory tissue of BAC transgenic SF-TRPV1 mice. High-resolution mass spectrometry was carried out on TRPV1 preparations from the DRG and the sciatic nerve to study protein constituents surrounding TRPV1 and to identify putative direct interaction partners.

6.1. Targeting SF-TRPV1 to sensory neurons using BAC transgenesis

Based on the fact that many current antibodies against TRPV1 do not immunoprecipitate well or lack sufficient specificity, an SF-tagged version of the receptor was generated and expressed in native sensory neurons using BAC transgenesis. The addition of an affinity tag to the N-terminus of TRPV1 did not affect its expression or functionality (Fig. 10), the prerequisite for the success of the purification of associated proteins. BAC transgenesis enabled expression of SF-tagged TRPV1 from the endogenous promoter, ensuring cell-type specific processing and regulation of SF-TRPV1. Compared with yeast-2-hybrid screens, the BAC strategy has the advantage that the fully processed and modified protein can serve as a bait and that protein interactions take place in their native environment and cellular location (Heintz, 2001; Aebersold and Mann, 2003).

Accurate expression and localization of SF-tagged TRPV1 in the transgenic mice was confirmed by immunohistochemisty of the DRG, dorsal horn of the spinal cord and the cornea (Fig. 14), demonstrating that SF-TRPV1 is expressed in small- and medium-sized DRG neurons as the native receptor and is transported into the central and peripheral nervous system. Importantly, the staining experiments also implied that there was no ectopic expression of SF-TRPV1, as it exhibited accurate wild type localization.

6.1.1. Considerations on the overexpressing founder

Due to the integration of different BAC copy numbers into the genome, differently expressing founder lines were obtained: one that expresses SF-TRPV1 at physiological levels (low expresser), and one that highly overexpresses SF-TRPV1 (over expresser), as shown by comparing TRPV1 expression levels of solubilized fractions from the DRG (Fig. 13). At the behavioral level, both founders showed comparable responses to acute thermal pain as wild type mice, indicating that under basal conditions, the BAC mice are indistinguishable from their wild type littermates. Interestingly, the overexpressing founder showed a much stronger sensitization and contralateral spread of heat hyperalgesia during neuropathic pain induced by unilateral chronic constriction injury (Fig. 16). Bilateral effects of unilateral injury or hind paw inflammation have been reported by many investigators (Koltzenburg et al., 1999; Sluka et al., 2001; 2002; Chen et al., 2000; Chacur et al., 2001) and depend on central sensitization and subsequent descending facilitation through supraspinal centers, notably through the Rostral Ventromedial Medulla (RVM) descending circuitry (Meeus and Nijs, 2007; Woolf, 2011; Wei et al., 2010; Chai et al., 2012). Furthermore, contralateral pain spread may be mediated by afferent fibers projecting to the contralateral dorsal horn or interposed interneurons (Culberson et al., 1979; Koltzenburg et al., 1999). In the over-expressing founder, these systems may be triggered and enhanced by the presence of a higher number of functional TRPV1 receptors in the spinal cord under pathological conditions.

Regarding the biochemistry, the “over expresser” was clearly advantageous for the purification of high amounts of TRPV1 from a small number of animals. This was critical as sensory tissue such as the DRG and the sciatic nerve provides only very limited source material and interaction partners might not be abundant. However, it is possible that due to high expression levels of the bait protein, protein localization and modification artifacts may occur, both of which could affect protein interactions (Berggård et al., 2007). The assembly of the protein complex may also not occur in a physiological and stoichiometric manner. For this reason, the “low expresser”, expressing SF-TRPV1 at near wild type levels, was beneficial and served to verify identified interactions by mass spectrometry and western blot analysis. Importantly, SF-TRPV1 receptors assemble with endogenous TRPV1 in these mice (Fig. 20C),

demonstrating recovery of heteromeric tagged and untagged molecules. This also circumvented the risk that tetramers composed of only untagged native TRPV1 compete for binding partners with SF-TRPV1.

6.2. Identification of TRPV1 interaction partners using MS-based proteomics

The identification of putative interaction partners depends largely on the proteomic strategy. Special biochemical considerations are required for the purification of membrane proteins, owing to their hydrophobic nature and association with a specific lipid environment. SF-tagged TRPV1 could be either purified using the Strep or the Flag tag. Two-step (tandem) affinity purifications have the advantage of decreasing background in subsequent label-free mass spectrometry runs (Rigaut et al., 1999; Gingras et al., 2007; Kaiser et al., 2008). However, immunoprecipitation procedures require speed and sensitivity for optimizing the identification of transient interaction partners. Therefore, single step purification using magnetic beads and bait recovery under physiological conditions provided the best experimental basis in terms of TRPV1 protein yield and complex integrity. Affinity purification of TRPV1 was achievable using both tags, however, Strep IPs showed poor TRPV1 depletion (Fig. 19, 20), possibly due to non-accessibility of the Strep tag due to steric constraints. Notably, TRPV1 could be detected in purified fractions from different tissue compartments: the DRG (soma), the sciatic nerve (peripheral) and the spinal cord (central) (Fig. 20, 21), providing the basis to also compare TRPV1 protein complex composition between different tissue compartments (i.e. peripheral versus central).

Mass spectrometric measurements of Flag-tag based purified fractions of TRPV1 were performed in a label-free manner. The difficulty of this approach is clearly to distinguish true interaction partners from background proteins that bind to the affinity matrix, an approach often associated with high false positive rates due to the complexity of the sample. Addressing high false positive rates had previously required tandem affinity purification – usually combined with gel electrophoresis – to obtain visually distinct protein bands, but this procedure requires large amounts of starting material (Rigaut et al., 1999; Collins and Choudhary, 2008; Fernández et al., 2009). However, label-free approaches, including new software tools, are being constantly improved to allow accurate protein quantification of tissue samples and have emerged to over-come the drawbacks associated with label-based approaches (Wong and Cagney, 2010; Lai et al., 2013; Megger et al., 2013).

To define true interactors, a "volcano-plot"-based strategy (Hubner and Mann, 2011) was employed which combines the significance value and the fold-change over the control (Fig. 22). TRPV1 was detected in the MS runs as the most abundant protein, confirming the efficiency of the affinity purification. Of the known interactors, calmodulin (Numazaki et al., 2003; Rosenbaum et al., 2004) and TRPV2 (Hellwig et al., 2005; Liapi and Wood, 2005; Rutter et al., 2005) were detected as highly enriched and therefore assigned as significant binders, validating the efficiency of the approach for isolating TRPV1 interacting proteins. Consistent with its known function as a calcium permeable ion channel, it was not surprising to detect a number of calcium binding proteins, such as S100 proteins. Calcium/Calmodulin binding domains are present on both intracellular domains. However, as TRPV1 plays a central role in sensitization processes and the development of inflammation, the main interest lay upon proteins that have a primary function in nociceptive signaling and sensitization. Essentially, two proteins, the $GABA_B$ receptor from the DRG affinity purification and Vglut2 from sciatic nerve purifications, were selected for further investigation to both verify a putative interaction with TRPV1 and evaluate any potential modulation of its function. Vglut2 was chosen, primarily due to its recent implication in thermal nociception (Lagerström et al., 2010). Importantly, both proteins were also identified as significant hits by Logopharm GmbH using a different MS approach, increasing the confidence of the assay results indicating them as potential interaction partners of TRPV1.

6.3. Association of TRPV1 with $GABA_B$ receptors

$GABA_B$ receptors mediate most inhibitory actions in the central and peripheral nervous system, and are involved also in the processing of nociceptive information. They belong to the family of metabotropic receptors and are composed of two subunits, $GABA_{B1}$ and $GABA_{B2}$, which need to be co-expressed to form a functional receptor (Kaupmann et al., 1998; Bettler et al., 2004). In TRPV1 pull-downs from the DRG, the $GABA_{B1a}$ receptor subunit, a splice variant of $GABA_{B1}$, was identified as significantly enriched. This is in agreement with the finding that in contrast to $GABA_{B1b}$, the $GABA_{B1a}$ variant is predominantly expressed in small DRG neurons (Towers et al., 2000; Charles et al., 2001). A physical association between TRPV1 and the $GABA_B$ receptor was verified by immunohistochemical and biochemical means. In consistency with other studies, $GABA_{B1}$ labeling was observed in the most

superficial laminae while $GABA_{B2}$ was more widely expressed (Calver et al., 2000; Towers et al., 2000; Charles et al., 2001), and both subunits showed high overlap with TRPV1 (Fig. 25). Similarly, in the DRG TRPV1 showed overlapping expression with $GABA_{B1a}$ and $GABA_{B2}$ (Fig. 24). There is disagreement as to the expression of $GABA_{B2}$ in DRG neurons, as a study by Engle did not detect any $GABA_{B2}$ protein in these cells (Engle et al., 2005). Interestingly, it was hypothesized that $GABA_{B1}$ subunits can form homodimers because mice lacking $GABA_{B2}$ have residual numbers of functional $GABA_B$ receptors in the hippocampus (Gassmann et al., 2004). Complementary to the MS results, endogenous $GABA_{B1}$ could be detected in Flag-tag based IPs of TRPV1 from the DRG on western blots (Fig. 26). Whether $GABA_{B2}$ is also present in the eluates is not clear at this point due to detection difficulties with the $GABA_{B2}$ antibody. MS analysis did not detect the $GABA_{B2}$ subunit in DRG IPs, while co-immunoprecipitation from transfected Hek293 cells demonstrated physical interaction of TRPV1 with $GABA_{B1}$ and $GABA_{B2}$ (Fig. 27). Thus, whether both subunits can actually bind to TRPV1 has to be further elucidated due to the possibility of an artifact based on over-expression of TRPV1 and the $GABA_B$ subunits in these cells.

6.3.1. Inhibition of TRPV1 sensitization by $GABA_B$ receptor activation

Co-localization of two proteins provides the physical basis for a functional association. TRPV1 and $GABA_B$ are both involved in nociceptive processing, even though they seem to have opposing functions. While TRPV1 sensitization by inflammatory mediators leads to hyperalgesia, $GABA_B$ activation results in inhibition of the spinal nociceptive pathway (Cho and Basbaum, 1991; Liu et al., 1992; Schuler et al., 2001; Bráz et al., 2012). In fact, $GABA_B$ knockout mice show pronounced thermal and mechanical hyperalgesia (Schuler et al., 2001; Magnaghi et al., 2008). The established $GABA_B$ specific agonist, baclofen, has anti-nociceptive effects in various animal models of inflammatory and neuropathic pain (Hao et al., 1992; Smith et al., 1994; Buritova et al., 1996; Takeda et al., 2004; Castro et al., 2006). In the dorsal horn, baclofen inhibits release of glutamate and Substance P from both large and small fibers (Patel et al., 2001). For this reason, intrathecal application of baclofen relieves central pain in chronic pain patients with spinal lesions or after cerebral strokes (Herman et al., 1992; Taira et al., 1995).

In agreement with a role of both receptors in inflammation, baclofen failed to activate TRPV1 *per se*, and did not affect TRPV1 currents when baclofen was co-applied with capsaicin or low pH (pH 5), indicating that $GABA_B$ activation does not affect TRPV1 acutely (unpublished data, Dr. Mirko Moroni). As a consequence, the effect of baclofen was tested on TRPV1 expressing DRG neurons during administration of several inflammatory mediators (Fig. 28, 30A). NGF, bradykinin and serotonin promote fast and prolonged hypersensitivity to capsaicin and heat stimuli, which is due to the sensitization of TRPV1 (Chuang et al., 2001; Zhang et al., 2005; Stein et al., 2006; Ohta et al., 2006) (Fig. 5). Interestingly, the presence of baclofen impaired the sensitization effect, as the neurons showed decreased responses to capsaicin stimulation after co-application of NGF and baclofen (Fig. 28, 30A). The same observation was made at the level of the whole animal. When thermal hyperalgesia was induced by injection of NGF, bradykinin or serotonin following unilateral adminstration of baclofen, a reduction of thermal pain sensitivity was observed in the ipsilateral hind paw, with no effect in the contralateral paw (Fig. 29, 30B, C). To test whether the baclofen-mediated reduction of sensitization is restricted to the PLC pathway, PGE_2 was included in the experiments because it mainly activates the cAMP/PKA signaling pathway (Bhave et al., 2002; Mohapatra et al., 2003). Interestingly, baclofen did not have any effect on PGE_2-induced thermal hypersensitivity (Fig. 31).

Heat hyperalgesia is a complex process to which several different mechanisms can contribute. Proinflammatory agents sensitize TRPV1 via channel phosphorylation through PKCε (Cesare et al., 1999; Premkumar and Ahern, 2000; Vellani et al., 2001 or cAMP-dependent PKA (Bhave et al., 2002; Mohapatra et al., 2003). NGF administration can have two consequences, either increased trafficking and insertion of TRPV1 into the membrane or activation of the PLC/PKC signaling pathway (Bonnington and McNaughton, 2003; Zhang et al., 2005; Huang et al., 2006) (Fig. 5). Since bradykinin and serotonin also activate the PLC-signaling pathway, it is possible that $GABA_B$ activation modulates the effect of PLC and thereby interferes with sensitization of TRPV1.

This could be mediated by a mechanism involving PIP_2. Activation of G_i-coupled $GABA_B$ receptors leads to dissociation of the heterotrimeric G protein into the Gα and Gβγ-subunit. While Gα inhibits AC and cAMP levels, resulting in inhibition of PKA, the Gβγ-protein subunit stimulates PLC-β to hydrolyze PIP_2. It has been widely described that upon PLC activation, the decrease in the concentration of PIP_2 sensitizes TRPV1 by relieving a tonic inhibition (Chuang et al., 2001; Stein et al., 2006; Lukacs et al., 2007; Klein et al., 2008). PIP_2 was also recently proposed to be a negative co-factor of TRPV1 (Jeske et al., 2011; Cao et al., 2013). However, an interesting study by Lukacs *et al*. showed that PIP_2 inhibits either the channel or the potentiating effect of PKC depending on changes in phosphoinositide levels (Lukacs et al., 2013), emphasizing that PIP_2 could play a role in diminishing sensitization of TRPV1.

$GABA_B$ receptors might also inhibit TRPV1 sensitization by modulating PKC, since baclofen did not diminish PGE_2-evoked hypersensitivity, which is largely based on the PKA/cAMP signaling pathway. Modulation of ion channels by PKC can occur through the activation of G_i or G_q- proteins (Strock and Diversé-Pierluissi, 2004). Calcium channels are, for instance, well known targets for inhibition by receptor-G protein pathways, as shown by the observation that pre-treatment of cells with pertussis toxin abolishes inhibition of calcium channels (Holz et al., 1986). G_q negatively modulates $Ca_v2.3$ channels by activation of muscarinic receptors via G_q and PKCδ (Bannister et al., 2004; Tedford and Zamponi, 2006). Similarly, M-type potassium currents are negatively regulated by $G_{i/q}$ protein-activated pathways (Passmore et al., 2003).

Gβγ subunits can also directly bind to and inhibit ion channels like $Ca_v2.2$ (Ikeda and Dunlap, 1999; Tedford and Zamponi, 2006; Currie, 2010), TRPM8 (Zhang et al., 2012) and TRPM1 (Shen et al., 2012). However, since TRPV1 currents *per se* are not affected by $GABA_B$ activation but only sensitization of the ion channel is attenuated by $GABA_B$ activation, it is unlikely that the G protein subunit directly binds to and closes the channel.

Interestingly, other GPCR-mediated pathways have already been shown to inhibit the activity of TRPV1. Activation of μ-opioid receptors, for example, indirectly inhibits TRPV1 via $G_{i/o}$ proteins and the PKA/cAMP pathway (Vetter et al., 2006; Endres-

Becker et al., 2007). Moreover, cannabinoids inhibit TRPV1 via calcineurin-mediated dephosphorylation (Jeske et al., 2006; Patwardhan et al., 2006). Whether dephosphorylation events by calcineurin play a role in the baclofen mediated reduction of TRPV1 sensitization seems unlikely, since it mainly counteracts PKA mediated phosphorylation (Mohamatra et al., 2005).

To summarize, these results reveal details on the mechanism of $GABA_B$ receptor-mediated induction of peripheral analgesia. It is conceivable that $GABA_B$ activation interferes with sensitization of TRPV1 via the PLC/PKCε-signaling pathway, which is the common main downstream signaling pathway of NGF and bradykinin even though serotonin and PGE_2 induced pain-related effects during inflammation may be mediated by both PKC and PKA (Sugiuar et al., 2004; Moriyama et al., 2005; Claudino et al, 2006; Villarreal et al., 2009). As a result of this, the pathways responsible for modulating the sensitization of TRPV1 by $GABA_B$ activation have to be still characterized by observing the effects of inhibitors on key members of the activated second-messenger cascades. Therefore, it will be of great interest when these findings can be reproduced in heterologous cells or oocytes where combinations of the $GABA_B$ subunits, G protein subunits as well as TRPV1 channels are expressed to dissect out the molecules mediating this effect. This will be accompanied by studies of TRPV1 function in DRG neurons obtained from $GABA_{B1}$ and $GABA_{B2}$ knockout mice to address the question whether the baclofen effect is mediated by $GABA_{B1}$ alone or if $GABA_{B2}$ is also involved. The biochemical data are so far inconclusive, albeit some $GABA_{B2}$ was co-purified in Hek293 cell overexpressing pull-downs. Yet, evidence for the existence of functional $GABA_{B1}$ receptor homodimers has been reported (Gassmann et al., 2004), emphasizing that $GABA_{B1}$ subunits could be functional by themselves.

6.3.2. Peripheral versus central $GABA_B$

There is controversy concerning the contribution of peripherally versus centrally expressed $GABA_B$ receptors to pain. When Gangadharan *et al.* analyzed conditional knockout mice lacking $GABA_B$ only in nociceptors, they claimed a redundant role for $GABA_B$ in the regulation of pain in the peripheral nervous system (Gangadharan et al., 2009). However, other studies have revealed that $GABA_B$ receptors have indeed a

peripheral function, as intraplantar baclofen administration produces local analgesic effects (Reis and Duarte, 2006; Whitehead et al., 2012). In agreement with the latter, unilateral baclofen injection did not reduce thermal hypersensitivity in the contralateral paw, suggesting a peripheral site of action (Fig. 29, 30B, C). There are two reasons for the discrepancy in the study of Gangadharan *et al.* First, the question of whether peripheral $GABA_B$ receptors can produce antinociceptive effects in the absence of central $GABA_B$ was not directly addressed in their study. This should be addressed using a central $GABA_B$ knockout mouse while leaving peripheral $GABA_B$ receptors intact. A second reason could be that they applied baclofen systemically, masking the peripheral effect of $GABA_B$ activation.

6.3.3. Conclusion and future perspectives

In conclusion, the contribution of $GABA_B$ receptor-mediated modulation of TRPV1 activity highlight the complexity of TRPV1 regulation and may provide a novel strategy to control and manipulate sensitization during inflammatory conditions. This is the first pathway describing the inhibition of TRPV1 sensitization while leaving intact acute activation of the receptor. TRPV1 antagonists have critical drawbacks in the clinics: core body temperature is increased and the threshold for detection of harmful heat is elevated which could lead to accidental burns (Vay et al., 2012). Therefore, it is of great interest to develop a TRPV1 antagonist whose analgesic property is separated from its thermoregulatory effects and basal heat sensitivity and only blocks sensitization by inflammatory mediators (Julius et al., 2013). This opens the possibility to develop selective GABAergic drugs for the treatment of chronic pain. Spinal $GABA_A$ receptor subtypes are already being promoted as novel analgesics to treat inflammatory and neuropathic pain (Knabl et al., 2008; Zeilhofer et al., 2009). This is based on findings that diminished inhibitory control is a major factor in chronic pain syndromes. $GABA_B$ selective drugs interfering only with peripheral sensitization could provide a therapeutic strategy by producing analgesia without many of the unwanted central side effects.

6.4. Association of TRPV1 with the Vesicular Glutamate Transporter 2

Mass spectrometry analysis of total TRPV1 eluates from the sciatic nerve revealed that TRPV1 receptors co-immunoprecipate specifically and abundantly Vglut2. Most primary afferents are glutamatergic and use the family of vesicular glutamate

transporters (VGLUT1-3) to package glutamate into vesicles. Vglut2 dominates in nociceptive primary afferents including peptidergic and nonpeptidergic (IB4 binding) C fibers (Brumovsky et al., 2007; Scherrer et al., 2010), which also express TRPV1 receptors (Liu et al., 2010; Scherrer et al., 2010). In agreement with these studies, co-localization of TRPV1 and Vglut2 was observed in the DRG (Fig. 39B) as well as in the superficial laminae of the spinal cord (Fig. 39B).

Co-assembly of TRPV1 and Vglut2 was further corroborated by forward and reverse affinity purification in transiently transfected F11 cells (Fig. 34). However, in heterologous cell systems artificial effects may occur due to overexpression of both proteins, as the proteins are not present at their native concentrations. For this reason, a proximity ligation assay was carried out and confirmed a physical association between these two proteins at the endogenous level in cultured DRG neurons (Fig. 33).

6.4.1. Presence of Vglut2 in peripheral nerves and its role in nociception

It was somewhat surprising that Vglut2 was so highly abundant in TRPV1 affinity purifications from the sciatic nerve. Yet, there is increasing evidence that Vglut2 is present in peripheral sensory tissues, supporting the idea that glutamate signaling is of functional relevance in the periphery. A number of different stimuli, including electrical, chemical or inflammatory stimulation, induce glutamate release from the skin, joints and peripheral nerve trunks. For instance, A and C fiber stimulation of the sciatic nerve and peripheral capsaicin treatment increase glutamate, but not aspartarte, levels in the rat hind paw extracellular space (deGroot et al., 2000). Interestingly, injection of capsaicin into a rat hind paw causes a 300% increase in interstitial glutamate that is suppressed by pre-administration of the TRPV1 antagonist capsazepine (Jin et al., 2009), pointing to a role of TRPV1 in glutamate release. Similarly, thermal stimulation of rat skin also produces subcutaneous glutamate release (Jin et al 2006). This suggests that glutamate is transported in peripheral nerves and that there is a specific mechanism for its release (Ibitokun and Miller 2010 a, b; Malet et al., 2013).

Most information regarding the functional importance of Vglut2 in nociceptors came from studies using conditional knockout mice lacking Vglut2 only in small-and

medium-sized DRG neurons. These mice showed decreased acute thermal pain sensitivity as well as reduced inflammatory pain (Lagerström et al., 2010; Liu et al., 2010; Scherrer et al., 2010; Lagerström et al., 2011). The heat pain deficit at higher temperatures as well as the absence of an acute response to intraplantar capsaicin injection in these mice is analogous to the phenotype seen in TRPV1 deficient mice (Caterina et al., 2000; Davis et al., 2000). Ablation of TRPV1 expressing DRG neurons or their central terminals produces a similar behavioral phenotype. These studies imply that Vglut2 is a key player in TRPV1 thermal nociception (Lagerström et al., 2010; Liu et al., 2010), pointing also to a possible functional link between these two proteins.

6.4.2. Co-existence of TRPV1 and Vglut2 in synaptic vesicles

It is conceivable that the use of mild solubilization conditions makes it possible to pull down incompletely solubilized membrane sheets and intact vesicles instead of solubilized protein complexes (le Maire et al., 2000; Schuck et al., 2003; Helbig et al., 2010). To rule out the possibility that the high abundance of Vglut2 is due to the low concentration of detergent in the purification procedure, higher detergent concentrations and different types of detergents such as Triton and RIPA buffer were included in the pull-downs. Importantly, Vglut2 was still specifically enriched in the samples even under harsher conditions (Fig. 35, Tab. 2). Based on these observations, it seemed likely that a fraction of TRPV1 resides in synaptic vesicles. Subcellular fractionation of the spinal cord was therefore carried out to purify and separate synaptic vesicles and membranes using established protocols (Varoqui et al., 2001). TRPV1 was found enriched in both, the synaptic membrane and vesicle, fractions (Fig. 36 A, B). Importantly, the same results were obtained using wild type and BAC transgenic SF-TRPV1 mice, emphasizing that the tagged version of TRPV1 behaves in a similar way and that localization to the synaptic vesicle fraction is not an artifact of the BAC transgenic mouse. This finding was supported by immunoisolations of TRPV1- and Vglut2 purified vesicles from the sciatic nerve and spinal cord (Fig. 37). These data suggest that, in addition to plasma membrane-bound TRPV1, there might be an additional localization of the receptor to Vglut2-containing synaptic vesicles. Supporting evidence for this observation comes from a recent study showing that TRPV1 expressing neurons in the Solitary Tract Nucleus (NTS) release additional

glutamate from a unique TRPV1-controlled vesicle pool that is temperature sensitive, calcium dependent and facilitated by NTS activity to generate asynchronous Excitatory Postsynaptic Potentials (EPSCs) (Peters et al., 2010). The presence of TRPV1 in synaptic structures and a possible involvement in synaptic transmission (Goswami et al., 2010) clearly enlarges the repertoire of TRPV1 function. Ion channels have been proposed to also function in synaptic vesicle membranes but evidence for their functional role is lacking. Most TRP channels are found at the plasma membrane where they promote cation influx. Interestingly, a subset of TRP channels, including three members of the TRPML family (Cheng et al., 2010), members of the TRPM family: TRPM1 (Oancea et al., 2009), TRPM7 (Krapivinsky et al., 2006; Brauchi et al., 2008), TRPM8 (Thebault et al., 2005) and TRPM2 (Lange et al., 2009), as well as TRPV5 (van de Graaf et al., 2006) are located in vesicular compartments. TRPY1, the only yeast TRP channel, is located in the yeast vacuole and mediates vacuolar calcium release, suggesting an ancient role for TRP channels in the regulation of vesicular ion exchange (Palmer et al., 2001; Denis and Cyert, 2002).

To address the function of TRPV1 in Vglut2-containing vesicles and to ask whether TRPV1 containing vesicles are capable of neurotransmitter loading, glutamate uptake experiments on synaptic vesicle fractions prepared from rat spinal cord were carried out but did not provide conclusive results (Fig. 38). Uptake was FCCP and trypan blue sensitive, validating functionality of the experiment. Pharmacological modulation of TRPV1 using capsaicin and two TRPV1 inhibitors, AMG9810 and I-RTX, showed that activation of TRPV1 did not affect glutamate uptake whereas inhibition resulted in reduction of uptake. However, the same result was obtained using synaptic vesicle preparations from TRPV1 deficient mice, indicating nonspecific effects of the blockers (Fig. 38C), which were absent in experiments using vesicle preparations from the rat cerebellum (Fig. 38B). It is unclear at this point why the inhibitors, both of which are very well characterized and exhibit very specific actions (Wahl et al., 2001; Seabrook et al., 2002; Gavva et al., 2005) have an effect in the TRPV1 knockout mice. Due to their lipophilic nature, they may block other components nonspecifically in the lipid bilayer by hydrophobic interactions, especially owing to the high concentrations that were used in this assay. A future and central aspect is therefore to characterize the TRPV1 vesicular pool in more detail and to elucidate if TRPV1 is principally functional on synaptic vesicles.

This characterization includes, for instance, studying localization of TRPV1 more precisely and visualize TRPV1-containing glutamatergic vesicles by electron microscopy (currently carried out in the laboratory). Reflection microscopy (TIRF) will be an alternative method to track mobility of fluorophore-labeled TRPV1-vesicles while they are close to the plasma membrane (Nofal et al., 2007).

Functional characterization of the TRPV1-vesicular pool is most essential and could be conducted by optical imaging of glutamate release using synapto-pHluorins (Miesenböck et al., 1998). These are pH-sensitive green fluorescent proteins that are fused to the luminal site of vesicular proteins. The system enables monitoring of vesicle exocytosis due to changes of the intracellular pH and resulting fluorescence inside the vesicles. As a matter of fact, a pHluorin-tagged TRPV1 construct was generated in the laboratory but rendered the receptor functionally inactive. A pHlourin-tagged Vglut2 (also generated in the lab) could be used instead to monitor glutamate release in neuronal cultures co-expressing TRPV1 in the presence or absence of TRPV1 antagonists.

Since exocytotic release of neurotransmitter depends on the presence of Ca^{2+} ions entering the neurons by depolarization, calcium accumulation by isolated synaptic vesicles (Gonçalves et al., 2000) provides another method to study TRPV1 functionality on synaptic vesicles. It has been reported that synaptic vesicles are able to take up calcium by an ATP-dependent process (Israël et al., 1980; Michaelson and Ophir, 1980) and that they have calcium binding properties (Kostyuk and Verkhratsky, 1994).

In conclusion, the biochemical data presented indicate co-existence of TRPV1 and Vglut2 on glutamatergic vesicles, yet the functional role of TRPV1 in these vesicles could not be solved in this thesis work, and thus leaves open questions that will be addressed in future studies.

6.4.3. Putative roles of TRPV1 in synaptic vesicles

The first evidence of an involvement of TRP channels in synaptic vesicles came from studies on TRPM7, which was found in intracellular acetylcholine-containing synaptic vesicles in sympathetic neurons and was shown to affect vesicle fusion and probability of neurotransmitter release (Krapivinsky et al., 2006; Brauchi et al., 2008). According to the ion exchange gel theory of synaptic vesicle fusion and

neurotransmitter release (Rahamimoff and Fernandez, 1997; Reigada et al., 2003), the matrix within synaptic vesicles may function as an ion-exchange resin that controls storage and release of ionic products in a counterion-dependent fashion, where counterions that are necessary for release of positively charged neurotransmitter are permeated by an unknown vesicular cation channel (Rahamimoff and Fernandez, 1997). In the case of TRPM7 containing vesicles, acetylcholine (positively charged) can only be released from this matrix (negatively charged) when a counterion, such as sodium or calcium (positively charged) enters the vesicle. It is conceivable that such a mechanism accounts for TRPV1 presence in the vesicles as well. The identity of an ion channel that permits ion exchange into glutamatergic vesicles has often been discussed but is at this point completely speculative. Synaptic membranes are devoid of PIP_2, but this lipid is abundant in the plasma membrane. For TRPM7, PIP_2 is critical for both vesicle-mediated exocytosis and activation of the channel. It is thought that TRPM7 only opens when the vesicle pH is low and PIP_2 in the plasma membrane binds cytoplasmic domains of TRPM7 (just before fusion). Opening of the channel would then allow ion exchange between the vesicle and cytoplasm. TRPV1 is similarly activated by low pH (Jordt et al., 2000) and is conductive for cations like calcium, sodium, potassium and even protons. It is possible that the receptor acts as a pH sensor; when the vesicular interiour acidifies, TRPV1 opens and thereby regulates glutamate loading or release. Based on the observation that cation influx into glutamatergic vesicles is directly coupled to proton exchange and that potassium ions increase glutamate uptake, the presence of cation/H^+ exchanger activity was recently discussed (Goh et al., 2011). Whether TRPV1 could account for a mechanism like this remains to be elucidated.

It is also possible, that TRPV1 is not regulating neurotransmitter uptake or release, but instead the interaction of TRPV1 with Vglut2 restrains some portion of the receptor to a vesicular pool that is readily insertable into the membrane upon nerve ending activation. Thereby, Vglut2 would act as a targeting vehicle that pulls a fraction of TRPV1 to synaptic vesicles and inserts it into the plasma membrane upon demand. This would be in agreement with results indicating that TRPV1 activation can modulate excitatory synaptic transmission and thereby modulating synaptic plasticity (Sikand and Premkumar, 2007; Gibson et al., 2008; Maione et al., 2009).

This mechanism would be slow enough to account for selective asynchronous release, as described by Peters (Peters et al., 2010).

This thesis work also addressed the question of whether TRPV1 is localized on Vglut2 positive vesicles for trafficking purposes. TRP channels must be targeted to specific locations in order to provide a high spatial and temporal regulation for the flow of sensory information. Vesicular translocation of TRP channels has been proposed as an important mechanism for TRP channel distribution and availability (Kanzaki et al., 1999; Cayouette and Boulay, 2007). Control of TRPV1 trafficking and delivery to its specific cellular compartments would therefore be an important step in regulating transduction of sensory stimuli. However, immunohistochemistry of DRG and spinal cord sections from Vglut2 knockout embryos demonstrated that TRPV1 does not depend on Vglut2 for proper localization of the receptor (Fig. 39A). Furthermore, functional TRPV1 receptors were present in TG cultures of Vglut2 knockout embryos as shown by calcium imaging (Fig. 39C). This is also in agreement with the reported observation that not all Vglut2 positive cells express TRPV1 (Liu et al., 2010), emphasizing Vglut2-independent distribution and activation of TRPV1 receptors.

6.4.4. Conclusion

The finding that Vglut2 was found in the sciatic nerve was interesting because it was recently discovered that Vglut2-mediated signaling exerts its function via the TRPV1 population (Lagerström et al., 2010). Immunohistochemistry demonstrated that Vglut2 and TRPV1 have overlapping distributions in DRG neurons, transfected F11 cells and the dorsal horn of the spinal cord. Importantly, subcellular fractionation of the spinal cord and immunoisolations of Vglut2 - and TRPV1-containing synaptic vesicles suggest that a subpopulation of TRPV1 is localized to a Vglut2-containing vesicular pool. These data are in agreement with other studies that reported an association of TRPV1 to synaptic structures and that suggested a role of the receptor in neurotransmission. However, the question of whether TRPV1 receptors are functional on synaptic vesicles could not be clarified in this work. The fact that TRPV1 is activated by low pH and is not dependent on lipids to be active are properties that may be also indicative of a function of the receptor in neurotransmitter

release. Thus, future work is needed to solve the question about the presence and function of TRPV1 channels in synaptic vesicles.

7. References

Aebersold, R., and Mann, M. (2003). Mass spectrometry-based proteomics. Nature *422*, 198–207.

Aihara, Y., Mashima, H., Onda, H., Hisano, S., Kasuya, H., Hori, T., Yamada, S., Tomura, H., Yamada, Y., Inoue, I., et al. (2000). Molecular cloning of a novel brain-type Na(+)-dependent inorganic phosphate cotransporter. J. Neurochem. *74*, 2622–2625.

Amaya, F., Shimosato, G., Nagano, M., Ueda, M., Hashimoto, S., Tanaka, Y., Suzuki, H., and Tanaka, M. (2004). NGF and GDNF differentially regulate TRPV1 expression that contributes to development of inflammatory thermal hyperalgesia. Eur. J. Neurosci. *20*, 2303–2310.

Andresen, M.C., Hofmann, M.E., and Fawley, J.A. (2012). The unsilent majority-TRPV1 drives "spontaneous" transmission of unmyelinated primary afferents within cardiorespiratory NTS. Am. J. Physiol. Regul. Integr. Comp. Physiol. *303*, R1207–R1216.

Ataka, T., Kumamoto, E., Shimoji, K., and Yoshimura, M. (2000). Baclofen inhibits more effectively C-afferent than Adelta-afferent glutamatergic transmission in substantia gelatinosa neurons of adult rat spinal cord slices. Pain *86*, 273–282.

Avelino, A., Cruz, C., Nagy, I., and Cruz, F. (2002). Vanilloid receptor 1 expression in the rat urinary tract. Neuroscience *109*, 787–798.

Balerio, G.N., and Rubio, M.C. (2002a). Baclofen analgesia: involvement of the GABAergic system. Pharmacol. Res. *46*, 281–286.

Balerio, G.N., and Rubio, M.C. (2002b). Pharmacokinetic-pharmacodynamic modeling of the antinociceptive effect of baclofen in mice. Eur J Drug Metab Pharmacokinet *27*, 163–169.

Bandell, M., Story, G.M., Hwang, S.W., Viswanath, V., Eid, S.R., Petrus, M.J., Earley, T.J., and Patapoutian, A. (2004). Noxious cold ion channel TRPA1 is activated by pungent compounds and bradykinin. Neuron *41*, 849–857.

Bannister, R.A., Melliti, K., and Adams, B.A. (2004). Differential modulation of CaV2.3 Ca2+ channels by Galphaq/11-coupled muscarinic receptors. Mol. Pharmacol. *65*, 381–388.

Basbaum, A.I., Bautista, D.M., Scherrer, G., and Julius, D. (2009). Cellular and molecular mechanisms of pain. Cell *139*, 267–284.

Bauer, M.B., Meller, S.T., and Gebhart, G.F. (1992). Bradykinin modulation of a spinal nociceptive reflex in the rat. Brain Res. *578*, 186–196.

Baumann, T.K., and Martenson, M.E. (2000). Extracellular protons both increase the activity and reduce the conductance of capsaicin- gated channels. J. Neurosci. *20*, RC80.

Bautista, D.M., Jordt, S.-E., Nikai, T., Tsuruda, P.R., Read, A.J., Poblete, J., Yamoah, E.N., Basbaum, A.I., and Julius, D. (2006). TRPA1 mediates the inflammatory actions of environmental irritants and proalgesic agents. Cell *124*, 1269–1282.

Bautista, D.M., Siemens, J., Glazer, J.M., Tsuruda, P.R., Basbaum, A.I., Stucky, C.L., Jordt, S.-E., and Julius, D. (2007). The menthol receptor TRPM8 is the principal detector of environmental cold. Nature *448*, 204–208.

Benham, C.D., Davis, J.B., and Randall, A.D. (2002). Vanilloid and TRP channels: a family of lipid-gated cation channels. Neuropharmacology *42*, 873–888.

Benke, D., and Zeilhofer, H.U. (2012). Divorce of obligatory partners in pain: disruption of GABA(B) receptor heterodimers in neuralgia. Embo J. *31*, 3234–3236.

Bennett, G.J., and Xie, Y.K. (1988). A peripheral mononeuropathy in rat that produces disorders of pain sensation like those seen in man. Pain *33*, 87–107.

Berggård, T., Linse, S., and James, P. (2007). Methods for the detection and analysis of protein-protein interactions. Proteomics *7*, 2833–2842.

Bettler, B., Kaupmann, K., Mosbacher, J., and Gassmann, M. (2004). Molecular structure and physiological functions of GABA(B) receptors. Physiol. Rev. *84*, 835–867.

Bevan, S., and Geppetti, P. (1994). Protons: small stimulants of capsaicin-sensitive sensory nerves. Trends Neurosci. *17*, 509–512.

Bhave, G., Hu, H.-J., Glauner, K.S., Zhu, W., Wang, H., Brasier, D.J., Oxford, G.S., and Gereau, R.W. (2003). Protein kinase C phosphorylation sensitizes but does not activate the capsaicin receptor transient receptor potential vanilloid 1 (TRPV1). Proc. Natl. Acad. Sci. U.S.a. *100*, 12480–12485.

Bhave, G., Zhu, W., Wang, H., Brasier, D.J., Oxford, G.S., and Gereau, R.W. (2002). cAMP-dependent protein kinase regulates desensitization of the capsaicin receptor (VR1) by direct phosphorylation. Neuron *35*, 721–731.

Bohlen, C.J., Priel, A., Zhou, S., King, D., Siemens, J., and Julius, D. (2010). A bivalent tarantula toxin activates the capsaicin receptor, TRPV1, by targeting the outer pore domain. Cell *141*, 834–845.

Bonnington, J.K., and McNaughton, P.A. (2003). Signalling pathways involved in the sensitisation of mouse nociceptive neurones by nerve growth factor. J. Physiol. (Lond.) *551*, 433–446.

Bowery, N.G., Bettler, B., Froestl, W., Gallagher, J.P., Marshall, F., Raiteri, M., Bonner, T.I., and Enna, S.J. (2002). International Union of Pharmacology. XXXIII. Mammalian gamma-aminobutyric acid(B) receptors: structure and function. Pharmacol. Rev. *54*, 247–264.

Brauchi, S., Krapivinsky, G., Krapivinsky, L., and Clapham, D.E. (2008). TRPM7 facilitates cholinergic vesicle fusion with the plasma membrane. Proc. Natl. Acad. Sci. U.S.a. *105*, 8304–8308.

Brauchi, S., Orta, G., Salazar, M., Rosenmann, E., and Latorre, R. (2006). A hot-sensing cold receptor: C-terminal domain determines thermosensation in transient receptor potential channels. J. Neurosci. *26*, 4835–4840.

Bráz, J.M., Nassar, M.A., Wood, J.N., and Basbaum, A.I. (2005). Parallel "pain" pathways arise from subpopulations of primary afferent nociceptor. Neuron *47*, 787–793.

Bráz, J.M., Sharif-Naeini, R., Vogt, D., Kriegstein, A., Alvarez-Buylla, A., Rubenstein, J.L., and Basbaum, A.I. (2012). Forebrain GABAergic neuron precursors integrate into adult spinal cord and reduce injury-induced neuropathic pain. Neuron *74*, 663–675.

Breese, N.M., George, A.C., Pauers, L.E., and Stucky, C.L. (2005). Peripheral inflammation selectively increases TRPV1 function in IB4-positive sensory neurons from adult mouse. Pain *115*, 37–49.

Bron, R., Klesse, L.J., Shah, K., Parada, L.F., and Winter, J. (2003). Activation of Ras is necessary and sufficient for upregulation of vanilloid receptor type 1 in sensory neurons by neurotrophic factors. Mol. Cell. Neurosci. *22*, 118–132.

Brumovsky, P., Watanabe, M., and Hökfelt, T. (2007). Expression of the vesicular glutamate transporters-1 and -2 in adult mouse dorsal root ganglia and spinal cord and their regulation by nerve injury. Neuroscience *147*, 469–490.

Btesh, J., Fischer, M.J.M., Stott, K., and McNaughton, P.A. (2013). Mapping the binding site of TRPV1 on AKAP79: implications for inflammatory hyperalgesia. J. Neurosci. *33*, 9184–9193.

Buritova, J., Chapman, V., Honoré, P., and Besson, J.M. (1996). The contribution of GABAB receptor-

mediated events to inflammatory pain processing: carrageenan oedema and associated spinal c-Fos expression in the rat. Neuroscience *73*, 487–496.

Calver, A.R., Medhurst, A.D., Robbins, M.J., Charles, K.J., Evans, M.L., Harrison, D.C., Stammers, M., Hughes, S.A., Hervieu, G., Couve, A., et al. (2000). The expression of GABA(B1) and GABA(B2) receptor subunits in the cNS differs from that in peripheral tissues. Neuroscience *100*, 155–170.

Cao, E., Cordero-Morales, J.F., Liu, B., Qin, F., and Julius, D. (2013). TRPV1 channels are intrinsically heat sensitive and negatively regulated by phosphoinositide lipids. Neuron *77*, 667–679.

Castro, A.R., Pinto, M., Lima, D., and Tavares, I. (2004). Nociceptive spinal neurons expressing NK1 and GABAB receptors are located in lamina I. Brain Res. *1003*, 77–85.

Castro, A.R., Pinto, M., Lima, D., and Tavares, I. (2006). Secondary hyperalgesia in the monoarthritic rat is mediated by GABAB and NK1 receptors of spinal dorsal horn neurons: a behavior and c-fos study. Neuroscience *141*, 2087–2095.

Caterina, M.J., Leffler, A., Malmberg, A.B., Martin, W.J., Trafton, J., Petersen-Zeitz, K.R., Koltzenburg, M., Basbaum, A.I., and Julius, D. (2000). Impaired nociception and pain sensation in mice lacking the capsaicin receptor. Science *288*, 306–313.

Caterina, M.J., Schumacher, M.A., Tominaga, M., Rosen, T.A., Levine, J.D., and Julius, D. (1997). The capsaicin receptor: a heat-activated ion channel in the pain pathway. Nature *389*, 816–824.

Cavanaugh, D.J., Chesler, A.T., Bráz, J.M., Shah, N.M., Julius, D., and Basbaum, A.I. (2011a). Restriction of transient receptor potential vanilloid-1 to the peptidergic subset of primary afferent neurons follows its developmental downregulation in nonpeptidergic neurons. J. Neurosci. *31*, 10119–10127.

Cavanaugh, D.J., Chesler, A.T., Jackson, A.C., Sigal, Y.M., Yamanaka, H., Grant, R., O'Donnell, D., Nicoll, R.A., Shah, N.M., Julius, D., et al. (2011b). Trpv1 reporter mice reveal highly restricted brain distribution and functional expression in arteriolar smooth muscle cells. J. Neurosci. *31*, 5067–5077.

Cavanaugh, D.J., Lee, H., Lo, L., Shields, S.D., Zylka, M.J., Basbaum, A.I., and Anderson, D.J. (2009). Distinct subsets of unmyelinated primary sensory fibers mediate behavioral responses to noxious thermal and mechanical stimuli. Proc. Natl. Acad. Sci. U.S.a. *106*, 9075–9080.

Cayouette, S., and Boulay, G. (2007). Intracellular trafficking of TRP channels. Cell Calcium *42*, 225–232.

Cesare, P., and McNaughton, P. (1996). A novel heat-activated current in nociceptive neurons and its sensitization by bradykinin. Proc. Natl. Acad. Sci. U.S.a. *93*, 15435–15439.

Cesare, P., Moriondo, A., Vellani, V., and McNaughton, P.A. (1999). Ion channels gated by heat. Proc. Natl. Acad. Sci. U.S.a. *96*, 7658–7663.

Chacur, M., Milligan, E.D., Gazda, L.S., Armstrong, C., Wang, H., Tracey, K.J., Maier, S.F., and Watkins, L.R. (2001). A new model of sciatic inflammatory neuritis (SIN): induction of unilateral and bilateral mechanical allodynia following acute unilateral peri-sciatic immune activation in rats. Pain *94*, 231–244.

Chai, B., Guo, W., Wei, F., Dubner, R., and Ren, K. (2012). Trigeminal-rostral ventromedial medulla circuitry is involved in orofacial hyperalgesia contralateral to tissue injury. Mol Pain *8*, 78.

Charles, K.J., Evans, M.L., Robbins, M.J., Calver, A.R., Leslie, R.A., and Pangalos, M.N. (2001). Comparative immunohistochemical localisation of GABA(B1a), GABA(B1b) and GABA(B2) subunits in rat brain, spinal cord and dorsal root ganglion. Neuroscience *106*, 447–467.

Chen, H.S., Chen, J., and Sun, Y.Y. (2000). Contralateral heat hyperalgesia induced by unilaterally intraplantar bee venom injection is produced by central changes: a behavioral study in the conscious

rat. Neurosci. Lett. *284*, 45–48.

Cheng, X., Shen, D., Samie, M., and Xu, H. (2010). Mucolipins: Intracellular TRPML1-3 channels. FEBS Lett. *584*, 2013–2021.

Chevesich, J., Kreuz, A.J., and Montell, C. (1997). Requirement for the PDZ domain protein, INAD, for localization of the TRP store-operated channel to a signaling complex. Neuron *18*, 95–105.

Cho, H.J., and Basbaum, A.I. (1991). GABAergic circuitry in the rostral ventral medulla of the rat and its relationship to descending antinociceptive controls. J. Comp. Neurol. *303*, 316–328.

Chuang, H.H., Prescott, E.D., Kong, H., Shields, S., Jordt, S.E., Basbaum, A.I., Chao, M.V., and Julius, D. (2001). Bradykinin and nerve growth factor release the capsaicin receptor from PtdIns(4,5)P2-mediated inhibition. Nature *411*, 957–962.

Clapham, D.E., Montell, C., Schultz, G., Julius, D., International Union of Pharmacology (2003). International Union of Pharmacology. XLIII. Compendium of voltage-gated ion channels: transient receptor potential channels. Pharmacol. Rev. *55*, 591–596.

Claudino, R.F., Kassuya, C.A.L., Ferreira, J., and Calixto, J.B. (2006). Pharmacological and molecular characterization of the mechanisms involved in prostaglandin E2-induced mouse paw edema. J. Pharmacol. Exp. Ther. *318*, 611–618.

Colburn, R.W., Lubin, M.L., Stone, D.J., Wang, Y., Lawrence, D., D'Andrea, M.R., Brandt, M.R., Liu, Y., Flores, C.M., and Qin, N. (2007). Attenuated cold sensitivity in TRPM8 null mice. Neuron *54*, 379–386.

Collins, M.O., and Choudhary, J.S. (2008). Mapping multiprotein complexes by affinity purification and mass spectrometry. Curr. Opin. Biotechnol. *19*, 324–330.

Cosens, D.J., and Manning, A. (1969). Abnormal electroretinogram from a Drosophila mutant. Nature *224*, 285–287.

Cox, J., Neuhauser, N., Michalski, A., Scheltema, R.A., Olsen, J.V., and Mann, M. (2011). Andromeda: a peptide search engine integrated into the MaxQuant environment. J. Proteome Res. *10*, 1794–1805.

Couture, R., Harrisson, M., Vianna, R.M., and Cloutier, F. (2001). Kinin receptors in pain and inflammation. Eur. J. Pharmacol. *429*, 161–176.

Cui, J.G., Meyerson, B.A., Sollevi, A., and Linderoth, B. (1998). Effect of spinal cord stimulation on tactile hypersensitivity in mononeuropathic rats is potentiated by simultaneous GABA(B) and adenosine receptor activation. Neurosci. Lett. *247*, 183–186.

Culberson, J.L., Haines, D.E., Kimmel, D.L., and Brown, P.B. (1979). Contralateral projection of primary afferent fibers to mammalian spinal cord. Exp. Neurol. *64*, 83–97.

Currie, K.P.M. (2010). G protein modulation of CaV2 voltage-gated calcium channels. Channels (Austin) *4*, 497–509.

Cuypers, E., Yanagihara, A., Karlsson, E., and Tytgat, J. (2006). Jellyfish and other cnidarian envenomations cause pain by affecting TRPV1 channels. FEBS Lett. *580*, 5728–5732.

Daniels, R.W., Collins, C.A., Chen, K., Gelfand, M.V., Featherstone, D.E., and DiAntonio, A. (2006). A single vesicular glutamate transporter is sufficient to fill a synaptic vesicle. Neuron *49*, 11–16.

Davis, J.B., Gray, J., Gunthorpe, M.J., Hatcher, J.P., Davey, P.T., Overend, P., Harries, M.H., Latcham, J., Clapham, C., Atkinson, K., et al. (2000). Vanilloid receptor-1 is essential for inflammatory thermal hyperalgesia. Nature *405*, 183–187.

de Bono, M., Tobin, D.M., Davis, M.W., Avery, L., and Bargmann, C.I. (2002). Social feeding in Caenorhabditis elegans is induced by neurons that detect aversive stimuli. Nature *419*, 899–903.

deGroot, J., S. Zhou and S. M. Carlton (2000). "Peripheral glutamate release in the hindpaw following low and high intensity sciatic stimulation." Neuroreport 11(3): 497-502.

Dedov, V.N., Tran, V.H., Duke, C.C., Connor, M., Christie, M.J., Mandadi, S., and Roufogalis, B.D. (2002). Gingerols: a novel class of vanilloid receptor (VR1) agonists. Br. J. Pharmacol. *137*, 793–798.

deGroot, J., Zhou, S., & Carlton, S. M. (2000). Peripheral glutamate release in the hindpaw following low and high intensity sciatic stimulation. *Neuroreport*, *11*(3), 497–502.

Denda, M., and Tsutsumi, M. (2011). Roles of transient receptor potential proteins (TRPs) in epidermal keratinocytes. Adv. Exp. Med. Biol. *704*, 847–860.

Denda, M., Fuziwara, S., Inoue, K., Denda, S., Akamatsu, H., Tomitaka, A., and Matsunaga, K. (2001). Immunoreactivity of VR1 on epidermal keratinocyte of human skin. Biochem. Biophys. Res. Commun. *285*, 1250–1252.

Denis, V., and Cyert, M.S. (2002). Internal Ca(2+) release in yeast is triggered by hypertonic shock and mediated by a TRP channel homologue. J. Cell Biol. *156*, 29–34.

Dhaka, A., Murray, A.N., Mathur, J., Earley, T.J., Petrus, M.J., and Patapoutian, A. (2007). TRPM8 is required for cold sensation in mice. Neuron *54*, 371–378.

Dinh, Q.T., Groneberg, D.A., Mingomataj, E., Peiser, C., Heppt, W., Dinh, S., Arck, P.C., Klapp, B.F., and Fischer, A. (2003). Expression of substance P and vanilloid receptor (VR1) in trigeminal sensory neurons projecting to the mouse nasal mucosa. Neuropeptides *37*, 245–250.

Dong, X.-P., Cheng, X., Mills, E., Delling, M., Wang, F., Kurz, T., and Xu, H. (2008). The type IV mucolipidosis-associated protein TRPML1 is an endolysosomal iron release channel. Nature *455*, 992–996.

Dray, A., and Perkins, M. (1993). Bradykinin and inflammatory pain. Trends Neurosci. *16*, 99–104.

Dray, A., Patel, I.A., Perkins, M.N., and Rueff, A. (1992). Bradykinin-induced activation of nociceptors: receptor and mechanistic studies on the neonatal rat spinal cord-tail preparation in vitro. Br. J. Pharmacol. *107*, 1129–1134.

Drew, L.J., and MacDermott, A.B. (2009). Neuroscience: Unbearable lightness of touch. Nature *462*, 580–581.

Endres-Becker, J., Heppenstall, P.A., Mousa, S.A., Labuz, D., Oksche, A., Schäfer, M., Stein, C., and Zöllner, C. (2007). Mu-opioid receptor activation modulates transient receptor potential vanilloid 1 (TRPV1) currents in sensory neurons in a model of inflammatory pain. Mol. Pharmacol. *71*, 12–18.

Engle, M.P., Gassman, M., Sykes, K.T., Bettler, B., and Hammond, D.L. (2005). Spinal nerve ligation does not alter the expression or function of GABA"B receptors in spinal cord and dorsal root ganglia of the rat. Neuroscience *138*, 11–11.

Fernández, E., Collins, M.O., Uren, R.T., Kopanitsa, M.V., Komiyama, N.H., Croning, M.D.R., Zografos, L., Armstrong, J.D., Choudhary, J.S., and Grant, S.G.N. (2009). Targeted tandem affinity purification of PSD-95 recovers core postsynaptic complexes and schizophrenia susceptibility proteins. Mol. Syst. Biol. *5*, 269.

Ferreira, S.H., Lorenzetti, B.B., and Poole, S. (1993). Bradykinin initiates cytokine-mediated inflammatory hyperalgesia. Br. J. Pharmacol. *110*, 1227–1231.

Ferrini, F., Salio, C., Vergnano, A.M., and Merighi, A. (2007). Vanilloid receptor-1 (TRPV1)-dependent activation of inhibitory neurotransmission in spinal substantia gelatinosa neurons of mouse. Pain *129*, 195–209.

Fischer, M.J.M., Btesh, J., and McNaughton, P.A. (2013). Disrupting sensitization of transient receptor potential vanilloid subtype 1 inhibits inflammatory hyperalgesia. J. Neurosci. *33*, 7407–7414.

Flockerzi, V. (2007). An introduction on TRP channels. Handb Exp Pharmacol 1–19.

Fremeau, R.T., Kam, K., Qureshi, T., Johnson, J., Copenhagen, D.R., Storm-Mathisen, J., Chaudhry, F.A., Nicoll, R.A., and Edwards, R.H. (2004). Vesicular glutamate transporters 1 and 2 target to functionally distinct synaptic release sites. Science *304*, 1815–1819.

Fremeau, R.T., Troyer, M.D., Pahner, I., Nygaard, G.O., Tran, C.H., Reimer, R.J., Bellocchio, E.E., Fortin, D., Storm-Mathisen, J., and Edwards, R.H. (2001). The expression of vesicular glutamate transporters defines two classes of excitatory synapse. Neuron *31*, 247–260.

Fürst, S. (1999). Transmitters involved in antinociception in the spinal cord. Brain Res. Bull. *48*, 129–141.

Galvez, T., Duthey, B., Kniazeff, J., Blahos, J., Rovelli, G., Bettler, B., Prézeau, L., and Pin, J.P. (2001). Allosteric interactions between GB1 and GB2 subunits are required for optimal GABA(B) receptor function. Embo J. *20*, 2152–2159.

Gangadharan, V., Agarwal, N., Brugger, S., Tegeder, I., Bettler, B., Kuner, R., and Kurejova, M. (2009). Conditional gene deletion reveals functional redundancy of GABAB receptors in peripheral nociceptors in vivo. Mol Pain *5*, 68.

García-Sanz, N., Valente, P., Gomis, A., Fernández-Carvajal, A., Fernández-Ballester, G., Viana, F., Belmonte, C., and Ferrer-Montiel, A. (2007). A role of the transient receptor potential domain of vanilloid receptor I in channel gating. J. Neurosci. *27*, 11641–11650.

Gassmann, M., Shaban, H., Vigot, R., Sansig, G., Haller, C., Barbieri, S., Humeau, Y., Schuler, V., Müller, M., Kinzel, B., et al. (2004). Redistribution of GABAB(1) protein and atypical GABAB responses in GABAB(2)-deficient mice. J. Neurosci. *24*, 6086–6097.

Gaudet, R. (2008). TRP channels entering the structural era. J. Physiol. (Lond.) *586*, 3565–3575.

Gaudet, R. (2009). Divide and conquer: high resolution structural information on TRP channel fragments. J. Gen. Physiol. *133*, 231–237.

Gavva, N.R., Tamir, R., Qu, Y., Klionsky, L., Zhang, T.J., Immke, D., Wang, J., Zhu, D., Vanderah, T.W., Porreca, F., et al. (2005). AMG 9810 [(E)-3-(4-t-butylphenyl)-N-(2,3-dihydrobenzo[b][1,4] dioxin-6-yl)acrylamide], a novel vanilloid receptor 1 (TRPV1) antagonist with antihyperalgesic properties. J. Pharmacol. Exp. Ther. *313*, 474–484.

Geppetti, P., Nassini, R., Materazzi, S., and Benemei, S. (2008). The concept of neurogenic inflammation. BJU Int. *101 Suppl 3*, 2–6.

Gibson, H.E., Edwards, J.G., Page, R.S., Van Hook, M.J., and Kauer, J.A. (2008). TRPV1 channels mediate long-term depression at synapses on hippocampal interneurons. Neuron *57*, 746–759.

Gingras, A.-C., Gstaiger, M., Raught, B., and Aebersold, R. (2007). Analysis of protein complexes using mass spectrometry. Nat. Rev. Mol. Cell Biol. *8*, 645–654.

Gloeckner, C.J., Boldt, K., and Ueffing, M. (2009a). Strep/FLAG tandem affinity purification (SF-TAP) to study protein interactions. Curr Protoc Protein Sci *Chapter 19*, Unit19.20.

Gloeckner, C.J., Boldt, K., Schumacher, A., and Ueffing, M. (2009b). Tandem affinity purification of

protein complexes from mammalian cells by the Strep/FLAG (SF)-TAP tag. Methods Mol. Biol. *564*, 359–372.

Goh, G.Y., Huang, H., Ullman, J., Borre, L., Hnasko, T.S., Trussell, L.O., and Edwards, R.H. (2011). Presynaptic regulation of quantal size: K+/H+ exchange stimulates vesicular glutamate transport. Nat. Neurosci. *14*, 1285–1292.

Gonçalves, P.P., Meireles, S.M., Neves, P., and Vale, M.G. (2000). Methods for analysis of Ca(2+)/H(+) antiport activity in synaptic vesicles isolated from sheep brain cortex. Brain Res. Brain Res. Protoc. *5*, 102–108.

Goswami, C., Rademacher, N., Smalla, K.-H., Kalscheuer, V., Ropers, H.-H., Gundelfinger, E.D., and Hucho, T. (2010). TRPV1 acts as a synaptic protein and regulates vesicle recycling. J. Cell. Sci. *123*, 2045–2057.

Goswami, C., Dreger, M., Jahnel, R., Bogen, O., Gillen, C., and Hucho, F. (2004). Identification and characterization of a Ca2+ -sensitive interaction of the vanilloid receptor TRPV1 with tubulin. J. Neurochem. *91*, 1092–1103.

Goswami, C., Dreger, M., Otto, H., Schwappach, B., and Hucho, F. (2006). Rapid disassembly of dynamic microtubules upon activation of the capsaicin receptor TRPV1. J. Neurochem. *96*, 254–266.

Grandl, J., Kim, S.E., Uzzell, V., Bursulaya, B., Petrus, M., Bandell, M., and Patapoutian, A. (2010). Temperature-induced opening of TRPV1 ion channel is stabilized by the pore domain. Nat. Neurosci. *13*, 708–714.

Gras, C., Herzog, E., Bellenchi, G.C., Bernard, V., Ravassard, P., Pohl, M., Gasnier, B., Giros, B., and Mestikawy, El, S. (2002). A third vesicular glutamate transporter expressed by cholinergic and serotoninergic neurons. J. Neurosci. *22*, 5442–5451.

Gu, Q., Kwong, K., and Lee, L.-Y. (2003). Ca2+ transient evoked by chemical stimulation is enhanced by PGE2 in vagal sensory neurons: role of cAMP/PKA signaling pathway. J. Neurophysiol. *89*, 1985–1993.

Gunthorpe, M.J., Harries, M.H., Prinjha, R.K., Davis, J.B., and Randall, A. (2000). Voltage- and time-dependent properties of the recombinant rat vanilloid receptor (rVR1). J. Physiol. (Lond.) *525 Pt 3*, 747–759.

Gunthorpe, M.J., Benham, C.D., Randall, A., and Davis, J.B. (2002). The diversity in the vanilloid (TRPV) receptor family of ion channels. Trends Pharmacol. Sci. *23*, 183–191.

Guo, A., Vulchanova, L., Wang, J., Li, X., and Elde, R. (1999). Immunocytochemical localization of the vanilloid receptor 1 (VR1): relationship to neuropeptides, the P2X3 purinoceptor and IB4 binding sites. Eur. J. Neurosci. *11*, 946–958.

Hao, J.X., Xu, X.J., Yu, Y.X., Seiger, A., and Wiesenfeld-Hallin, Z. (1992). Baclofen reverses the hypersensitivity of dorsal horn wide dynamic range neurons to mechanical stimulation after transient spinal cord ischemia; implications for a tonic GABAergic inhibitory control of myelinated fiber input. J. Neurophysiol. *68*, 392–396.

Hardie, R.C., and Minke, B. (1992). The trp gene is essential for a light-activated Ca2+ channel in Drosophila photoreceptors. Neuron *8*, 643–651.

Hardie, R.C., and Raghu, P. (2001). Visual transduction in Drosophila. Nature *413*, 186–193.

Hargreaves, K., Dubner, R., Brown, F., Flores, C., and Joris, J. (1988). A new and sensitive method for measuring thermal nociception in cutaneous hyperalgesia. Pain *32*, 77–88.

Heintz, N. (2001). BAC to the future: the use of bac transgenic mice for neuroscience research. Nat. Rev. Neurosci. *2*, 861–870.

Helbig, A.O., Heck, A.J.R., and Slijper, M. (2010). Exploring the membrane proteome--challenges and analytical strategies. J Proteomics *73*, 868–878.

Helliwell, R.J., McLatchie, L.M., Clarke, M., Winter, J., Bevan, S., and McIntyre, P. (1998). Capsaicin sensitivity is associated with the expression of the vanilloid (capsaicin) receptor (VR1) mRNA in adult rat sensory ganglia. Neurosci. Lett. *250*, 177–180.

Hellwig, N., Albrecht, N., Harteneck, C., Schultz, G., and Schaefer, M. (2005). Homo- and heteromeric assembly of TRPV channel subunits. J. Cell. Sci. *118*, 917–928.

Hellwig, N., Plant, T.D., Janson, W., Schäfer, M., Schultz, G., and Schaefer, M. (2004). TRPV1 acts as proton channel to induce acidification in nociceptive neurons. J. Biol. Chem. *279*, 34553–34561.

Herman, R.M., D'Luzansky, S.C., and Ippolito, R. (1992). Intrathecal baclofen suppresses central pain in patients with spinal lesions. A pilot study. Clin J Pain *8*, 338–345.

Herzog, E., Takamori, S., Jahn, R., Brose, N., and Wojcik, S.M. (2006). Synaptic and vesicular co-localization of the glutamate transporters VGLUT1 and VGLUT2 in the mouse hippocampus. J. Neurochem. *99*, 1011–1018.

Holz, G.G., Rane, S.G., and Dunlap, K. (1986). GTP-binding proteins mediate transmitter inhibition of voltage-dependent calcium channels. Nature *319*, 670–672.

Hsu, Y.-J., Hoenderop, J.G.J., and Bindels, R.J.M. (2007). TRP channels in kidney disease. Biochim. Biophys. Acta *1772*, 928–936.

Huang, J., Zhang, X., and McNaughton, P.A. (2006). Inflammatory pain: the cellular basis of heat hyperalgesia. Curr Neuropharmacol *4*, 197–206.

Huber, A., Sander, P., and Paulsen, R. (1996a). Phosphorylation of the InaD gene product, a photoreceptor membrane protein required for recovery of visual excitation. J. Biol. Chem. *271*, 11710–11717.

Huber, A., Sander, P., Bähner, M., and Paulsen, R. (1998). The TRP Ca2+ channel assembled in a signaling complex by the PDZ domain protein INAD is phosphorylated through the interaction with protein kinase C (ePKC). FEBS Lett. *425*, 317–322.

Huber, A., Sander, P., Gobert, A., Bähner, M., Hermann, R., and Paulsen, R. (1996b). The transient receptor potential protein (Trp), a putative store-operated Ca2+ channel essential for phosphoinositide-mediated photoreception, forms a signaling complex with NorpA, InaC and InaD. Embo J. *15*, 7036–7045.

Hubner, N.C., Bird, A.W., Cox, J., Splettstoesser, B., Bandilla, P., Poser, I., Hyman, A., and Mann, M. (2010). Quantitative proteomics combined with BAC TransgeneOmics reveals in vivo protein interactions. J. Cell Biol. *189*, 739–754.

Hubner, N.C., and Mann, M. (2011). Extracting gene function from protein-protein interactions using Quantitative BAC InteraCtomics (QUBIC). Methods *53*, 453–459.

Hunt, S.P., and Mantyh, P.W. (2001). The molecular dynamics of pain control. Nat. Rev. Neurosci. *2*, 83–91.

Huttner, W.B., Schiebler, W., Greengard, P., and De Camilli, P. (1983). Synapsin I (protein I), a nerve terminal-specific phosphoprotein. III. Its association with synaptic vesicles studied in a highly purified synaptic vesicle preparation. J. Cell Biol. *96*, 1374–1388.

Hwang, S.J., and Valtschanoff, J.G. (2003). Vanilloid receptor VR1-positive afferents are distributed differently at different levels of the rat lumbar spinal cord. Neurosci. Lett. *349*, 41–44.

Ikeda, S.R., and Dunlap, K. (1999). Voltage-dependent modulation of N-type calcium channels: role of G protein subunits. Adv. Second Messenger Phosphoprotein Res. *33*, 131–151.

Inoue, K., Koizumi, S., Fuziwara, S., Denda, S., Inoue, K., and Denda, M. (2002). Functional vanilloid receptors in cultured normal human epidermal keratinocytes. Biochem. Biophys. Res. Commun. *291*, 124–129.

Israël, M., Manaranche, R., Marsal, J., Meunier, F.M., Morel, N., Frachon, P., and Lesbats, B. (1980). ATP-dependent calcium uptake by cholinergic synaptic vesicles isolated from Torpedo electric organ. J. Membr. Biol. *54*, 115–126.

Jeske, N.A., Patwardhan, A.M., Gamper, N., Price, T.J., Akopian, A.N., and Hargreaves, K.M. (2006). Cannabinoid WIN 55,212-2 regulates TRPV1 phosphorylation in sensory neurons. J. Biol. Chem. *281*, 32879–32890.

Jeske, N.A., Patwardhan, A.M., Ruparel, N.B., Akopian, A.N., Shapiro, M.S., and Henry, M.A. (2009). A-kinase anchoring protein 150 controls protein kinase C-mediated phosphorylation and sensitization of TRPV1. Pain *146*, 301–307.

Jeske, N.A., Por, E.D., Belugin, S., Chaudhury, S., Berg, K.A., Akopian, A.N., Henry, M.A., and Gomez, R. (2011). A-kinase anchoring protein 150 mediates transient receptor potential family V type 1 sensitivity to phosphatidylinositol-4,5-bisphosphate. J. Neurosci. *31*, 8681–8688.

Ji, R.-R., Samad, T.A., Jin, S.-X., Schmoll, R., and Woolf, C.J. (2002). p38 MAPK activation by NGF in primary sensory neurons after inflammation increases TRPV1 levels and maintains heat hyperalgesia. Neuron *36*, 57–68.

Jin, X., Morsy, N., Winston, J., Pasricha, P.J., Garrett, K., and Akbarali, H.I. (2004). Modulation of TRPV1 by nonreceptor tyrosine kinase, c-Src kinase. Am. J. Physiol., Cell Physiol. *287*, C558–C563.

Jin, X., Touhey, J., and Gaudet, R. (2006). Structure of the N-terminal ankyrin repeat domain of the TRPV2 ion channel. J. Biol. Chem. *281*, 25006–25010.

Jin, Y.-H., Yamaki, F., Takemura, M., Koike, Y., Furuyama, A., and Yonehara, N. (2009). Capsaicin-induced glutamate release is implicated in nociceptive processing through activation of ionotropic glutamate receptors and group I metabotropic glutamate receptor in primary afferent fibers. J. Pharmacol. Sci. *109*, 233–241.

Jones, K.A., Borowsky, B., Tamm, J.A., Craig, D.A., Durkin, M.M., Dai, M., Yao, W.J., Johnson, M., Gunwaldsen, C., Huang, L.Y., et al. (1998). GABA(B) receptors function as a heteromeric assembly of the subunits GABA(B)R1 and GABA(B)R2. Nature *396*, 674–679.

Jordt, S.E., Tominaga, M., and Julius, D. (2000). Acid potentiation of the capsaicin receptor determined by a key extracellular site. Proc. Natl. Acad. Sci. U.S.a. *97*, 8134–8139.

Jordt, S.-E., Bautista, D.M., Chuang, H.-H., McKemy, D.D., Zygmunt, P.M., Högestätt, E.D., Meng, I.D., and Julius, D. (2004). Mustard oils and cannabinoids excite sensory nerve fibres through the TRP channel ANKTM1. Nature *427*, 260–265.

Julius, D. (2013). TRP Channels and Pain. Annu. Rev. Cell Dev. Biol. *29*, 355–384.

Julius, D., and Basbaum, A.I. (2001). Molecular mechanisms of nociception. Nature *413*, 203–210.

Jung, J., Shin, J.S., Lee, S.-Y., Hwang, S.W., Koo, J., Cho, H., and Oh, U. (2004). Phosphorylation of vanilloid receptor 1 by Ca2+/calmodulin-dependent kinase II regulates its vanilloid binding. J. Biol. Chem. *279*, 7048–7054.

Kaiser, P., Meierhofer, D., Wang, X., and Huang, L. (2008). Tandem affinity purification combined with mass spectrometry to identify components of protein complexes. Methods Mol. Biol. *439*, 309–326.

Kanzaki, M., Zhang, Y.Q., Mashima, H., Li, L., Shibata, H., and Kojima, I. (1999). Translocation of a calcium-permeable cation channel induced by insulin-like growth factor-I. Nat. Cell Biol. *1*, 165–170.

Kato, S., Aihara, E., Nakamura, A., Xin, H., Matsui, H., Kohama, K., and Takeuchi, K. (2003). Expression of vanilloid receptors in rat gastric epithelial cells: role in cellular protection. Biochem. Pharmacol. *66*, 1115–1121.

Kaupmann, K., Huggel, K., Heid, J., Flor, P.J., Bischoff, S., Mickel, S.J., McMaster, G., Angst, C., Bittiger, H., Froestl, W., et al. (1997). Expression cloning of GABA(B) receptors uncovers similarity to metabotropic glutamate receptors. Nature *386*, 239–246.

Kaupmann, K., Malitschek, B., Schuler, V., Heid, J., Froestl, W., Beck, P., Mosbacher, J., Bischoff, S., Kulik, A., Shigemoto, R., et al. (1998). GABA(B)-receptor subtypes assemble into functional heteromeric complexes. Nature *396*, 683–687.

Kedei, N., Szabo, T., Lile, J.D., Treanor, J.J., Olah, Z., Iadarola, M.J., and Blumberg, P.M. (2001). Analysis of the native quaternary structure of vanilloid receptor 1. J. Biol. Chem. *276*, 28613–28619.

Khasar, S.G., Lin, Y.H., Martin, A., Dadgar, J., McMahon, T., Wang, D., Hundle, B., Aley, K.O., Isenberg, W., McCarter, G., et al. (1999). A novel nociceptor signaling pathway revealed in protein kinase C epsilon mutant mice. Neuron *24*, 253–260.

Kim, A.Y., Tang, Z., Liu, Q., Patel, K.N., Maag, D., Geng, Y., and Dong, X. (2008). Pirt, a phosphoinositide-binding protein, functions as a regulatory subunit of TRPV1. Cell *133*, 475–485.

Kim, S.E., Patapoutian, A., and Grandl, J. (2013). Single residues in the outer pore of TRPV1 and TRPV3 have temperature-dependent conformations. PLoS ONE *8*, e59593.

Klein, R.M., Ufret-Vincenty, C.A., Hua, L., and Gordon, S.E. (2008). Determinants of molecular specificity in phosphoinositide regulation. Phosphatidylinositol (4,5)-bisphosphate (PI(4,5)P2) is the endogenous lipid regulating TRPV1. J. Biol. Chem. *283*, 26208–26216.

Knabl, J., Witschi, R., Hösl, K., Reinold, H., Zeilhofer, U.B., Ahmadi, S., Brockhaus, J., Sergejeva, M., Hess, A., Brune, K., et al. (2008). Reversal of pathological pain through specific spinal GABAA receptor subtypes. Nature *451*, 330–334.

Kollarik, M., and Undem, B.J. (2004). Activation of bronchopulmonary vagal afferent nerves with bradykinin, acid and vanilloid receptor agonists in wild-type and TRPV1-/- mice. J. Physiol. (Lond.) *555*, 115–123.

Koltzenburg, M., Wall, P.D., and McMahon, S.B. (1999). Does the right side know what the left is doing? Trends Neurosci. *22*, 122–127.

Kostyuk, P., and Verkhratsky, A. (1994). Calcium stores in neurons and glia. Neuroscience *63*, 381–404.

Krapivinsky, G., Mochida, S., Krapivinsky, L., Cibulsky, S.M., and Clapham, D.E. (2006). The TRPM7 ion channel functions in cholinergic synaptic vesicles and affects transmitter release. Neuron *52*, 485–496.

Kuner, R., Köhr, G., Grünewald, S., Eisenhardt, G., Bach, A., and Kornau, H.C. (1999). Role of heteromer formation in GABAB receptor function. Science *283*, 74–77.

Laffray, S., Bouali-Benazzouz, R., Papon, M.-A., Favereaux, A., Jiang, Y., Holm, T., Spriet, C., Desbarats, P., Fossat, P., Le Feuvre, Y., et al. (2012). Impairment of GABAB receptor dimer by endogenous 14-3-3ζ in chronic pain conditions. Embo J. *31*, 3239–3251.

Lagerström, M.C., Rogoz, K., Abrahamsen, B., Lind, A.-L., Olund, C., Smith, C., Mendez, J.A., Wallén-Mackenzie, A., Wood, J.N., and Kullander, K. (2011). A sensory subpopulation depends on vesicular glutamate transporter 2 for mechanical pain, and together with substance P, inflammatory

pain. Proc. Natl. Acad. Sci. U.S.a. *108*, 5789–5794.

Lagerström, M.C., Rogoz, K., Abrahamsen, B., Persson, E., Reinius, B., Nordenankar, K., Olund, C., Smith, C., Mendez, J.A., Chen, Z.-F., et al. (2010). VGLUT2-dependent sensory neurons in the TRPV1 population regulate pain and itch. Neuron *68*, 529–542.

Lai, X., Wang, L., and Witzmann, F.A. (2013). Issues and applications in label-free quantitative mass spectrometry. Int J Proteomics *2013*, 756039.

Landry, M., Bouali-Benazzouz, R., Mestikawy, El, S., Ravassard, P., and Nagy, F. (2004). Expression of vesicular glutamate transporters in rat lumbar spinal cord, with a note on dorsal root ganglia. J. Comp. Neurol. *468*, 380–394.

Lange, I., Yamamoto, S., Partida-Sanchez, S., Mori, Y., Fleig, A., and Penner, R. (2009). TRPM2 functions as a lysosomal Ca2+-release channel in beta cells. Sci Signal *2*, ra23.

Lawson, J.J., McIlwrath, S.L., Woodbury, C.J., Davis, B.M., and Koerber, H.R. (2008). TRPV1 unlike TRPV2 is restricted to a subset of mechanically insensitive cutaneous nociceptors responding to heat. J Pain *9*, 298–308.

le Maire, M., Champeil, P., and Moller, J.V. (2000). Interaction of membrane proteins and lipids with solubilizing detergents. Biochim. Biophys. Acta *1508*, 86–111.

Lee, H., and Caterina, M.J. (2005). TRPV channels as thermosensory receptors in epithelial cells. Pflugers Arch. *451*, 160–167.

Leo, S., Moechars, D., Callaerts-Vegh, Z., D'Hooge, R., and Meert, T. (2009). Impairment of VGLUT2 but not VGLUT1 signaling reduces neuropathy-induced hypersensitivity. Eur J Pain *13*, 1008–1017.

Lepage, P.K., and Boulay, G. (2007). Molecular determinants of TRP channel assembly. Biochem. Soc. Trans. *35*, 81–83.

Lewin, G.R., Ritter, A.M., and Mendell, L.M. (1993). Nerve growth factor-induced hyperalgesia in the neonatal and adult rat. J. Neurosci. *13*, 2136–2148.

Li, H.S., and Montell, C. (2000). TRP and the PDZ protein, INAD, form the core complex required for retention of the signalplex in Drosophila photoreceptor cells. J. Cell Biol. *150*, 1411–1422.

Liang, Y.F., Haake, B., and Reeh, P.W. (2001). Sustained sensitization and recruitment of rat cutaneous nociceptors by bradykinin and a novel theory of its excitatory action. J. Physiol. (Lond.) *532*, 229–239.

Liapi, A., and Wood, J.N. (2005). Extensive co-localization and heteromultimer formation of the vanilloid receptor-like protein TRPV2 and the capsaicin receptor TRPV1 in the adult rat cerebral cortex. Eur. J. Neurosci. *22*, 825–834.

Liguz-Lecznar, M., and Skangiel-Kramska, J. (2007). Vesicular glutamate transporters (VGLUTs): the three musketeers of glutamatergic system. Acta Neurobiol Exp (Wars) *67*, 207–218.

Lishko, P.V., Procko, E., Jin, X., Phelps, C.B., and Gaudet, R. (2007). The ankyrin repeats of TRPV1 bind multiple ligands and modulate channel sensitivity. Neuron *54*, 905–918.

Liu, H., Llewellyn-Smith, I.J., Pilowsky, P., and Basbaum, A.I. (1992). Ultrastructural evidence for GABA-mediated disinhibitory circuits in the spinal cord of the cat. Neurosci. Lett. *138*, 183–187.

Liu, Y., Abdel Samad, O., Zhang, L., Duan, B., Tong, Q., Lopes, C., Ji, R.-R., Lowell, B.B., and Ma, Q. (2010). VGLUT2-dependent glutamate release from nociceptors is required to sense pain and suppress itch. Neuron *68*, 543–556.

Luche, S., Santoni, V., and Rabilloud, T. (2003). Evaluation of nonionic and zwitterionic detergents as membrane protein solubilizers in two-dimensional electrophoresis. Proteomics *3*, 249–253.

Lukacs, V., Thyagarajan, B., Varnai, P., Balla, A., Balla, T., and Rohacs, T. (2007). Dual regulation of TRPV1 by phosphoinositides. J. Neurosci. *27*, 7070–7080.

Lukacs, V., Yudin, Y., Hammond, G.R., Sharma, E., Fukami, K., and Rohacs, T. (2013). Distinctive changes in plasma membrane phosphoinositides underlie differential regulation of TRPV1 in nociceptive neurons. J. Neurosci. *33*, 11451–11463.

Lumpkin, E.A., and Caterina, M.J. (2007). Mechanisms of sensory transduction in the skin. Nature *445*, 858–865.

Maccarrone, M., Rossi, S., Bari, M., De Chiara, V., Fezza, F., Musella, A., Gasperi, V., Prosperetti, C., Bernardi, G., Finazzi-Agrò, A., et al. (2008). Anandamide inhibits metabolism and physiological actions of 2-arachidonoylglycerol in the striatum. Nat. Neurosci. *11*, 152–159.

Macpherson, L.J., Geierstanger, B.H., Viswanath, V., Bandell, M., Eid, S.R., Hwang, S., and Patapoutian, A. (2005). The pungency of garlic: activation of TRPA1 and TRPV1 in response to allicin. Curr. Biol. *15*, 929–934.

Magnaghi, V., Ballabio, M., Camozzi, F., Colleoni, M., Consoli, A., Gassmann, M., Lauria, G., Motta, M., Procacci, P., Trovato, A.E., et al. (2008). Altered peripheral myelination in mice lacking GABAB receptors. Mol. Cell. Neurosci. *37*, 599–609.

Maione, S., Cristino, L., Migliozzi, A.L., Georgiou, A.L., Starowicz, K., Salt, T.E., and Di Marzo, V. (2009). TRPV1 channels control synaptic plasticity in the developing superior colliculus. J. Physiol. (Lond.) *587*, 2521–2535.

Malan, T.P., Mata, H.P., and Porreca, F. (2002). Spinal GABA(A) and GABA(B) receptor pharmacology in a rat model of neuropathic pain. Anesthesiology *96*, 1161–1167.

Malet, M., Vieytes, C.A., Lundgren, K.H., Seal, R.P., Tomasella, E., Seroogy, K.B., Hökfelt, T., Gebhart, G.F., and Brumovsky, P.R. (2013). Transcript expression of vesicular glutamate transporters in lumbar dorsal root ganglia and the spinal cord of mice - Effects of peripheral axotomy or hindpaw inflammation. Neuroscience *248C*, 95–111.

Malin, S.A., Davis, B.M., Koerber, H.R., Reynolds, I.J., Albers, K.M., and Molliver, D.C. (2008). Thermal nociception and TRPV1 function are attenuated in mice lacking the nucleotide receptor P2Y2. Pain *138*, 484–496.

Marchand, F., Perretti, M., and McMahon, S.B. (2005). Role of the immune system in chronic pain. Nat. Rev. Neurosci. *6*, 521–532.

Margeta-Mitrovic, M., Jan, Y.N., and Jan, L.Y. (2001a). Function of GB1 and GB2 subunits in G protein coupling of GABA(B) receptors. Proc. Natl. Acad. Sci. U.S.a. *98*, 14649–14654.

Margeta-Mitrovic, M., Jan, Y.N., and Jan, L.Y. (2001b). Ligand-induced signal transduction within heterodimeric GABA(B) receptor. Proc. Natl. Acad. Sci. U.S.a. *98*, 14643–14648.

Marmigère, F., and Ernfors, P. (2007). Specification and connectivity of neuronal subtypes in the sensory lineage. Nat. Rev. Neurosci. *8*, 114–127.

Marsch, R., Foeller, E., Rammes, G., Bunck, M., Kössl, M., Holsboer, F., Zieglgänsberger, W., Landgraf, R., Lutz, B., and Wotjak, C.T. (2007). Reduced anxiety, conditioned fear, and hippocampal long-term potentiation in transient receptor potential vanilloid type 1 receptor-deficient mice. J. Neurosci. *27*, 832–839.

McNamara, F.N., Randall, A., and Gunthorpe, M.J. (2005). Effects of piperine, the pungent component of black pepper, at the human vanilloid receptor (TRPV1). Br. J. Pharmacol. *144*, 781–790.

McNamara, C.R., Mandel-Brehm, J., Bautista, D.M., Siemens, J., Deranian, K.L., Zhao, M., Hayward, N.J., Chong, J.A., Julius, D., Moran, M.M., et al. (2007). TRPA1 mediates formalin-induced pain. Proc. Natl. Acad. Sci. U.S.a. *104*, 13525–13530.

Meeus, M., and Nijs, J. (2007). Central sensitization: a biopsychosocial explanation for chronic widespread pain in patients with fibromyalgia and chronic fatigue syndrome. Clin. Rheumatol. *26*, 465–473.

Megger, D.A., Bracht, T., Meyer, H.E., and Sitek, B. (2013). Label-free quantification in clinical proteomics. Biochim. Biophys. Acta *1834*, 1581–1590.

Mery, L., Strauss, B., Dufour, J.F., Krause, K.H., and Hoth, M. (2002). The PDZ-interacting domain of TRPC4 controls its localization and surface expression in HEK293 cells. J. Cell. Sci. *115*, 3497–3508.

Michael, G.J., and Priestley, J.V. (1999). Differential expression of the mRNA for the vanilloid receptor subtype 1 in cells of the adult rat dorsal root and nodose ganglia and its downregulation by axotomy. J. Neurosci. *19*, 1844–1854.

Michaelson, D.M., and Ophir, I. (1980). Sidedness of (calcium, magnesium) adenosine triphosphatase of purified Torpedo synaptic vesicles. J. Neurochem. *34*, 1483–1490.

Miesenböck, G., De Angelis, D.A., and Rothman, J.E. (1998). Visualizing secretion and synaptic transmission with pH-sensitive green fluorescent proteins. Nature *394*, 192–195.

Minke, B., Wu, C., and Pak, W.L. (1975). Induction of photoreceptor voltage noise in the dark in Drosophila mutant. Nature *258*, 84–87.

Misgeld, U., Bijak, M., and Jarolimek, W. (1995). A physiological role for GABAB receptors and the effects of baclofen in the mammalian central nervous system. Prog. Neurobiol. *46*, 423–462.

Moechars, D., Weston, M.C., Leo, S., Callaerts-Vegh, Z., Goris, I., Daneels, G., Buist, A., Cik, M., van der Spek, P., Kass, S., et al. (2006). Vesicular glutamate transporter VGLUT2 expression levels control quantal size and neuropathic pain. J. Neurosci. *26*, 12055–12066.

Mohapatra, D.P., and Nau, C. (2003). Desensitization of capsaicin-activated currents in the vanilloid receptor TRPV1 is decreased by the cyclic AMP-dependent protein kinase pathway. J. Biol. Chem. *278*, 50080–50090.

Molliver, D.C., Radeke, M.J., Feinstein, S.C., and Snider, W.D. (1995). Presence or absence of TrkA protein distinguishes subsets of small sensory neurons with unique cytochemical characteristics and dorsal horn projections. J. Comp. Neurol. *361*, 404–416.

Molliver, D.C., Wright, D.E., Leitner, M.L., Parsadanian, A.S., Doster, K., Wen, D., Yan, Q., and Snider, W.D. (1997). IB4-binding DRG neurons switch from NGF to GDNF dependence in early postnatal life. Neuron *19*, 849–861.

Montell, C. (1999). Visual transduction in Drosophila. Annu. Rev. Cell Dev. Biol. *15*, 231–268.

Montell, C. (2005). TRP channels in Drosophila photoreceptor cells. pp. 45–51.

Montell, C., and Rubin, G.M. (1989). Molecular characterization of the Drosophila trp locus: a putative integral membrane protein required for phototransduction. Neuron *2*, 1313–1323.

Montell, C., Birnbaumer, L., and Flockerzi, V. (2002). The TRP channels, a remarkably functional family. Cell *108*, 595–598.

Morenilla-Palao, C., Planells-Cases, R., García-Sanz, N., and Ferrer-Montiel, A. (2004). Regulated exocytosis contributes to protein kinase C potentiation of vanilloid receptor activity. J. Biol. Chem. *279*, 25665–25672.

Moriyama, T., Higashi, T., Togashi, K., Iida, T., Segi, E., Sugimoto, Y., Tominaga, T., Narumiya, S., and Tominaga, M. (2005). Sensitization of TRPV1 by EP1 and IP reveals peripheral nociceptive mechanism of prostaglandins. Mol Pain *1*, 3.

Moriyama, T., Iida, T., Kobayashi, K., Higashi, T., Fukuoka, T., Tsumura, H., Leon, C., Suzuki, N., Inoue, K., Gachet, C., et al. (2003). Possible involvement of P2Y2 metabotropic receptors in ATP-induced transient receptor potential vanilloid receptor 1-mediated thermal hypersensitivity. J. Neurosci. *23*, 6058–6062.

Morris, J.L., König, P., Shimizu, T., Jobling, P., and Gibbins, I.L. (2005). Most peptide-containing sensory neurons lack proteins for exocytotic release and vesicular transport of glutamate. J. Comp. Neurol. *483*, 1–16.

Musella, A., De Chiara, V., Rossi, S., Prosperetti, C., Bernardi, G., Maccarrone, M., and Centonze, D. (2009). TRPV1 channels facilitate glutamate transmission in the striatum. Mol. Cell. Neurosci. *40*, 89–97.

Müller, C.S., Haupt, A., Bildl, W., Schindler, J., Knaus, H.-G., Meissner, M., Rammner, B., Striessnig, J., Flockerzi, V., Fakler, B., et al. (2010). Quantitative proteomics of the Cav2 channel nano-environments in the mammalian brain. Proc. Natl. Acad. Sci. U.S.a. *107*, 14950–14957.

Ni, B., Rosteck, P.R., Nadi, N.S., and Paul, S.M. (1994). Cloning and expression of a cDNA encoding a brain-specific Na(+)-dependent inorganic phosphate cotransporter. Proc. Natl. Acad. Sci. U.S.a. *91*, 5607–5611.

Niemeyer, B.A., Suzuki, E., Scott, K., Jalink, K., and Zuker, C.S. (1996). The Drosophila light-activated conductance is composed of the two channels TRP and TRPL. Cell *85*, 651–659.

Nilius, B., and Mahieu, F. (2006). A road map for TR(I)Ps. pp. 297–307.

Nilius, B., Owsianik, G., Voets, T., and Peters, J.A. (2007). Transient receptor potential cation channels in disease. Physiol. Rev. *87*, 165–217.

Nishikawa, M., Hirouchi, M., and Kuriyama, K. (1997). Functional coupling of Gi subtype with GABAB receptor/adenylyl cyclase system: analysis using a reconstituted system with purified GTP-binding protein from bovine cerebral cortex. Neurochem. Int. *31*, 21–25.

Nofal, S., Becherer, U., Hof, D., Matti, U., and Rettig, J. (2007). Primed vesicles can be distinguished from docked vesicles by analyzing their mobility. J. Neurosci. *27*, 1386–1395.

Numazaki, M., Tominaga, T., Takeuchi, K., Murayama, N., Toyooka, H., and Tominaga, M. (2003). Structural determinant of TRPV1 desensitization interacts with calmodulin. Proc. Natl. Acad. Sci. U.S.a. *100*, 8002–8006.

Numazaki, M., Tominaga, T., Toyooka, H., and Tominaga, M. (2002). Direct phosphorylation of capsaicin receptor VR1 by protein kinase Cepsilon and identification of two target serine residues. J. Biol. Chem. *277*, 13375–13378.

Oancea, E., Vriens, J., Brauchi, S., Jun, J., Splawski, I., and Clapham, D.E. (2009). TRPM1 forms ion channels associated with melanin content in melanocytes. Sci Signal *2*, ra21.

Ohta, T., Ikemi, Y., Murakami, M., Imagawa, T., Otsuguro, K.-I., and Ito, S. (2006). Potentiation of transient receptor potential V1 functions by the activation of metabotropic 5-HT receptors in rat primary sensory neurons. J. Physiol. (Lond.) *576*, 809–822.

Oliveira, A.L.R., Hydling, F., Olsson, E., Shi, T., Edwards, R.H., Fujiyama, F., Kaneko, T., Hökfelt, T., Cullheim, S., and Meister, B. (2003). Cellular localization of three vesicular glutamate transporter mRNAs and proteins in rat spinal cord and dorsal root ganglia. Synapse *50*, 117–129.

Owsianik, G., D'hoedt, D., Voets, T., and Nilius, B. (2006). Structure-function relationship of the TRP

channel superfamily. Rev. Physiol. Biochem. Pharmacol. *156*, 61–90.

Padgett, C.L., and Slesinger, P.A. (2010). GABAB receptor coupling to G-proteins and ion channels. Adv. Pharmacol. *58*, 123–147.

Palmada, M., Poppendieck, S., Embark, H.M., van de Graaf, S.F.J., Boehmer, C., Bindels, R.J.M., and Lang, F. (2005). Requirement of PDZ domains for the stimulation of the epithelial Ca2+ channel TRPV5 by the NHE regulating factor NHERF2 and the serum and glucocorticoid inducible kinase SGK1. Cell. Physiol. Biochem. *15*, 175–182.

Palmer, C.P., Zhou, X.L., Lin, J., Loukin, S.H., Kung, C., and Saimi, Y. (2001). A TRP homolog in Saccharomyces cerevisiae forms an intracellular Ca(2+)-permeable channel in the yeast vacuolar membrane. Proc. Natl. Acad. Sci. U.S.a. *98*, 7801–7805.

Pandey, A., and Mann, M. (2000). Proteomics to study genes and genomes. Nature *405*, 837–846.

Passmore, G.M., Selyanko, A.A., Mistry, M., Al-Qatari, M., Marsh, S.J., Matthews, E.A., Dickenson, A.H., Brown, T.A., Burbidge, S.A., Main, M., et al. (2003). KCNQ/M currents in sensory neurons: significance for pain therapy. J. Neurosci. *23*, 7227–7236.

Patel, K.N., Liu, Q., Meeker, S., Undem, B.J., and Dong, X. (2011). Pirt, a TRPV1 modulator, is required for histamine-dependent and -independent itch. PLoS ONE *6*, e20559.

Patel, S., Naeem, S., Kesingland, A., Froestl, W., Capogna, M., Urban, L., and Fox, A. (2001). The effects of GABA(B) agonists and gabapentin on mechanical hyperalgesia in models of neuropathic and inflammatory pain in the rat. Pain *90*, 217–226.

Patwardhan, A.M., Jeske, N.A., Price, T.J., Gamper, N., Akopian, A.N., and Hargreaves, K.M. (2006). The cannabinoid WIN 55,212-2 inhibits transient receptor potential vanilloid 1 (TRPV1) and evokes peripheral antihyperalgesia via calcineurin. Proc. Natl. Acad. Sci. U.S.a. *103*, 11393–11398.

Peng, J., and Li, Y.-J. (2010). The vanilloid receptor TRPV1: role in cardiovascular and gastrointestinal protection. Eur. J. Pharmacol. *627*, 1–7.

Perez-Reyes, E. (2010). G protein-mediated inhibition of Cav3.2 T-type channels revisited. Mol. Pharmacol. *77*, 136–138.

Perl, E.R. (2007). Ideas about pain, a historical view. Nat. Rev. Neurosci. *8*, 71–80.

Peters, J.H., McDougall, S.J., Fawley, J.A., and Andresen, M.C. (2011). TRPV1 marks synaptic segregation of multiple convergent afferents at the rat medial solitary tract nucleus. PLoS ONE *6*, e25015.

Peters, J.H., McDougall, S.J., Fawley, J.A., Smith, S.M., and Andresen, M.C. (2010). Primary afferent activation of thermosensitive TRPV1 triggers asynchronous glutamate release at central neurons. Neuron *65*, 657–669.

Phillips, A.M., Bull, A., and Kelly, L.E. (1992). Identification of a Drosophila gene encoding a calmodulin-binding protein with homology to the trp phototransduction gene. Neuron *8*, 631–642.

Pinto, M., Sousa, M., Lima, D., and Tavares, I. (2008). Participation of mu-opioid, GABA(B), and NK1 receptors of major pain control medullary areas in pathways targeting the rat spinal cord: implications for descending modulation of nociceptive transmission. J. Comp. Neurol. *510*, 175–187.

Premkumar, L.S., Agarwal, S., and Steffen, D. (2002). Single-channel properties of native and cloned rat vanilloid receptors. J. Physiol. (Lond.) *545*, 107–117.

Premkumar, L.S., and Ahern, G.P. (2000). Induction of vanilloid receptor channel activity by protein kinase C. Nature *408*, 985–990.

Premkumar, L.S., Qi, Z.-H., Van Buren, J., and Raisinghani, M. (2004). Enhancement of potency and efficacy of NADA by PKC-mediated phosphorylation of vanilloid receptor. J. Neurophysiol. *91*, 1442–1449.

Prescott, E.D., and Julius, D. (2003). A modular PIP2 binding site as a determinant of capsaicin receptor sensitivity. Science *300*, 1284–1288.

Przesmycki, K., Dzieciuch, J.A., Czuczwar, S.J., and Kleinrok, Z. (1998). An isobolographic analysis of drug interaction between intrathecal clonidine and baclofen in the formalin test in rats. Neuropharmacology *37*, 207–214.

Qamar, S., Vadivelu, M., and Sandford, R. (2007). TRP channels and kidney disease: lessons from polycystic kidney disease. Biochem. Soc. Trans. *35*, 124–128.

Rahamimoff, R., and Fernandez, J.M. (1997). Pre- and postfusion regulation of transmitter release. Neuron *18*, 17–27.

Rappsilber, J., Ishihama, Y., and Mann, M. (2003). Stop and go extraction tips for matrix-assisted laser desorption/ionization, nanoelectrospray, and LC/MS sample pretreatment in proteomics. Anal. Chem. *75*, 663–670.

Reeh, P.W., and Steen, K.H. (1996). Tissue acidosis in nociception and pain. Prog. Brain Res. *113*, 143–151.

Reigada, D., Díez-Pérez, I., Gorostiza, P., Verdaguer, A., Gómez de Aranda, I., Pineda, O., Vilarrasa, J., Marsal, J., Blasi, J., Aleu, J., et al. (2003). Control of neurotransmitter release by an internal gel matrix in synaptic vesicles. Proc. Natl. Acad. Sci. U.S.a. *100*, 3485–3490.

Reis, G.M.L., and Duarte, I.D.G. (2006). Baclofen, an agonist at peripheral GABAB receptors, induces antinociception via activation of TEA-sensitive potassium channels. Br. J. Pharmacol. *149*, 733–739.

Rigaut, G., Shevchenko, A., Rutz, B., Wilm, M., Mann, M., and Séraphin, B. (1999). A generic protein purification method for protein complex characterization and proteome exploration. Nat. Biotechnol. *17*, 1030–1032.

Roberts, J.C., Davis, J.B., and Benham, C.D. (2004). [3H]Resiniferatoxin autoradiography in the CNS of wild-type and TRPV1 null mice defines TRPV1 (VR-1) protein distribution. Brain Res. *995*, 176–183.

Rogoz, K., Lagerström, M.C., Dufour, S., and Kullander, K. (2012). VGLUT2-dependent glutamatergic transmission in primary afferents is required for intact nociception in both acute and persistent pain modalities. Pain *153*, 1525–1536.

Rohacs, T. (2007). Regulation of TRP channels by PIP(2). Pflugers Arch. *453*, 753–762.

Rosenbaum, T., Gordon-Shaag, A., Munari, M., and Gordon, S.E. (2004). Ca2+/calmodulin modulates TRPV1 activation by capsaicin. J. Gen. Physiol. *123*, 53–62.

Rutter, A.R., Ma, Q.-P., Leveridge, M., and Bonnert, T.P. (2005). Heteromerization and colocalization of TrpV1 and TrpV2 in mammalian cell lines and rat dorsal root ganglia. Neuroreport *16*, 1735–1739.

Salas, M.M., Hargreaves, K.M., and Akopian, A.N. (2009). TRPA1-mediated responses in trigeminal sensory neurons: interaction between TRPA1 and TRPV1. Eur. J. Neurosci. *29*, 1568–1578.

Schaefer, M. (2005). Homo- and heteromeric assembly of TRP channel subunits. Pflugers Arch. *451*, 35–42.

Schäfer, M.K.-H., Varoqui, H., Defamie, N., Weihe, E., and Erickson, J.D. (2002). Molecular cloning and functional identification of mouse vesicular glutamate transporter 3 and its expression in subsets of

novel excitatory neurons. J. Biol. Chem. *277*, 50734–50748.

Scherrer, G., Low, S.A., Wang, X., Zhang, J., Yamanaka, H., Urban, R., Solorzano, C., Harper, B., Hnasko, T.S., Edwards, R.H., et al. (2010). VGLUT2 expression in primary afferent neurons is essential for normal acute pain and injury-induced heat hypersensitivity. Proc. Natl. Acad. Sci. U.S.a. *107*, 22296–22301.

Schnizler, K., Shutov, L.P., Van Kanegan, M.J., Merrill, M.A., Nichols, B., McKnight, G.S., Strack, S., Hell, J.W., and Usachev, Y.M. (2008). Protein kinase A anchoring via AKAP150 is essential for TRPV1 modulation by forskolin and prostaglandin E2 in mouse sensory neurons. J. Neurosci. *28*, 4904–4917.

Schuck, S., Honsho, M., Ekroos, K., Shevchenko, A., and Simons, K. (2003). Resistance of cell membranes to different detergents. Proc. Natl. Acad. Sci. U.S.a. *100*, 5795–5800.

Schuler, V., Lüscher, C., Blanchet, C., Klix, N., Sansig, G., Klebs, K., Schmutz, M., Heid, J., Gentry, C., Urban, L., et al. (2001). Epilepsy, hyperalgesia, impaired memory, and loss of pre- and postsynaptic GABA(B) responses in mice lacking GABA(B(1)). Neuron *31*, 47–58.

Schulte, U., Müller, C.S., and Fakler, B. (2011). Ion channels and their molecular environments--glimpses and insights from functional proteomics. Semin. Cell Dev. Biol. *22*, 132–144.

Schwenk, J., Harmel, N., Brechet, A., Zolles, G., Berkefeld, H., Müller, C.S., Bildl, W., Baehrens, D., Hüber, B., Kulik, A., et al. (2012). High-resolution proteomics unravel architecture and molecular diversity of native AMPA receptor complexes. Neuron *74*, 621–633.

Schwenk, J., Harmel, N., Zolles, G., Bildl, W., Kulik, A., Heimrich, B., Chisaka, O., Jonas, P., Schulte, U., Fakler, B., et al. (2009). Functional proteomics identify cornichon proteins as auxiliary subunits of AMPA receptors. Science *323*, 1313–1319.

Schwenk, J., Metz, M., Zolles, G., Turecek, R., Fritzius, T., Bildl, W., Tarusawa, E., Kulik, A., Unger, A., Ivankova, K., et al. (2010). Native GABA(B) receptors are heteromultimers with a family of auxiliary subunits. Nature *465*, 231–235.

Seabrook, G.R., Sutton, K.G., Jarolimek, W., Hollingworth, G.J., Teague, S., Webb, J., Clark, N., Boyce, S., Kerby, J., Ali, Z., et al. (2002). Functional properties of the high-affinity TRPV1 (VR1) vanilloid receptor antagonist (4-hydroxy-5-iodo-3-methoxyphenylacetate ester) iodo-resiniferatoxin. J. Pharmacol. Exp. Ther. *303*, 1052–1060.

Seal, R.P., Akil, O., Yi, E., Weber, C.M., Grant, L., Yoo, J., Clause, A., Kandler, K., Noebels, J.L., Glowatzki, E., et al. (2008). Sensorineural deafness and seizures in mice lacking vesicular glutamate transporter 3. Neuron *57*, 263–275.

Seal, R.P., Wang, X., Guan, Y., Raja, S.N., Woodbury, C.J., Basbaum, A.I., and Edwards, R.H. (2009). Injury-induced mechanical hypersensitivity requires C-low threshold mechanoreceptors. Nature *462*, 651–655.

Shen, Y., Rampino, M.A.F., Carroll, R.C., and Nawy, S. (2012). G-protein-mediated inhibition of the Trp channel TRPM1 requires the Gβγ dimer. Proc. Natl. Acad. Sci. U.S.a. *109*, 8752–8757.

Shieh, B.H., and Zhu, M.Y. (1996). Regulation of the TRP Ca2+ channel by INAD in Drosophila photoreceptors. Neuron *16*, 991–998.

Sidi, S., Friedrich, R.W., and Nicolson, T. (2003). NompC TRP channel required for vertebrate sensory hair cell mechanotransduction. Science *301*, 96–99.

Siemens, J., Zhou, S., Piskorowski, R., Nikai, T., Lumpkin, E.A., Basbaum, A.I., King, D., and Julius, D. (2006). Spider toxins activate the capsaicin receptor to produce inflammatory pain. Nature *444*, 208–212.

Sikand, P., and Premkumar, L.S. (2007). Potentiation of glutamatergic synaptic transmission by protein kinase C-mediated sensitization of TRPV1 at the first sensory synapse. J. Physiol. (Lond.) *581*, 631–647.

Silos-Santiago, I., Greenlund, L.J., Johnson, E.M., and Snider, W.D. (1995). Molecular genetics of neuronal survival. Curr. Opin. Neurobiol. *5*, 42–49.

Sluka, K.A. (2002). Stimulation of deep somatic tissue with capsaicin produces long-lasting mechanical allodynia and heat hypoalgesia that depends on early activation of the cAMP pathway. J. Neurosci. *22*, 5687–5693.

Sluka, K.A., Kalra, A., and Moore, S.A. (2001). Unilateral intramuscular injections of acidic saline produce a bilateral, long-lasting hyperalgesia. Muscle Nerve *24*, 37–46.

Smith, G.D., Gunthorpe, M.J., Kelsell, R.E., Hayes, P.D., Reilly, P., Facer, P., Wright, J.E., Jerman, J.C., Walhin, J.-P., Ooi, L., et al. (2002). TRPV3 is a temperature-sensitive vanilloid receptor-like protein. Nature *418*, 186–190.

Smith, G.D., Harrison, S.M., Birch, P.J., Elliott, P.J., Malcangio, M., and Bowery, N.G. (1994). Increased sensitivity to the antinociceptive activity of (+/-)-baclofen in an animal model of chronic neuropathic, but not chronic inflammatory hyperalgesia. Neuropharmacology *33*, 1103–1108.

Smith, J.A., Davis, C.L., and Burgess, G.M. (2000). Prostaglandin E2-induced sensitization of bradykinin-evoked responses in rat dorsal root ganglion neurons is mediated by cAMP-dependent protein kinase A. Eur. J. Neurosci. *12*, 3250–3258.

Snider, W.D., and McMahon, S.B. (1998). Tackling pain at the source: new ideas about nociceptors. Neuron *20*, 629–632.

Sokal, D.M., and Chapman, V. (2003). Inhibitory effects of spinal baclofen on spinal dorsal horn neurones in inflamed and neuropathic rats in vivo. Brain Res. *987*, 67–75.

Song, X., Zhao, Y., Narcisse, L., Duffy, H., Kress, Y., Lee, S., and Brosnan, C.F. (2005). Canonical transient receptor potential channel 4 (TRPC4) co-localizes with the scaffolding protein ZO-1 in human fetal astrocytes in culture. Glia *49*, 418–429.

Stein, A.T., Ufret-Vincenty, C.A., Hua, L., Santana, L.F., and Gordon, S.E. (2006). Phosphoinositide 3-kinase binds to TRPV1 and mediates NGF-stimulated TRPV1 trafficking to the plasma membrane. J. Gen. Physiol. *128*, 509–522.

Strock, J., and Diversé-Pierluissi, M.A. (2004). Ca2+ channels as integrators of G protein-mediated signaling in neurons. Mol. Pharmacol. *66*, 1071–1076.

Stucky, C.L., and Lewin, G.R. (1999). Isolectin B(4)-positive and -negative nociceptors are functionally distinct. J. Neurosci. *19*, 6497–6505.

Sugiuar, T., Bielefeldt, K., and Gebhart, G.F. (2004). TRPV1 function in mouse colon sensory neurons is enhanced by metabotropic 5-hydroxytryptamine receptor activation. J. Neurosci. *24*, 9521–9530.

Szallasi, A., Cortright, D.N., Blum, C.A., and Eid, S.R. (2007). The vanilloid receptor TRPV1: 10 years from channel cloning to antagonist proof-of-concept. Nat Rev Drug Discov *6*, 357–372.

Szolcsányi, J., Joó, F., and Jancsó-Gábor, A. (1971). Mitochondrial changes in preoptic neurons after capsaicin desensitization of the hypothalamic thermodetectors in rats. Nature *229*, 116–117.

Taira, T., Kawamura, H., Tanikawa, T., Iseki, H., Kawabatake, H., and Takakura, K. (1995). A new approach to control central deafferentation pain: spinal intrathecal baclofen. Stereotact Funct Neurosurg *65*, 101–105.

Takamori, S., Holt, M., Stenius, K., Lemke, E.A., Grønborg, M., Riedel, D., Urlaub, H., Schenck, S., Brügger, B., Ringler, P., et al. (2006). Molecular anatomy of a trafficking organelle. Cell *127*, 831–846.

Takeda, M., Tanimoto, T., Ikeda, M., Kadoi, J., and Matsumoto, S. (2004). Activaton of GABAB receptor inhibits the excitability of rat small diameter trigeminal root ganglion neurons. Neuroscience *123*, 491–505.

Tang, Y., Tang, J., Chen, Z., Trost, C., Flockerzi, V., Li, M., Ramesh, V., and Zhu, M.X. (2000). Association of mammalian trp4 and phospholipase C isozymes with a PDZ domain-containing protein, NHERF. J. Biol. Chem. *275*, 37559–37564.

Tedford, H.W., and Zamponi, G.W. (2006). Direct G protein modulation of Cav2 calcium channels. Pharmacol. Rev. *58*, 837–862.

Thebault, S., Lemonnier, L., Bidaux, G., Flourakis, M., Bavencoffe, A., Gordienko, D., Roudbaraki, M., Delcourt, P., Panchin, Y., Shuba, Y., et al. (2005). Novel role of cold/menthol-sensitive transient receptor potential melastatine family member 8 (TRPM8) in the activation of store-operated channels in LNCaP human prostate cancer epithelial cells. J. Biol. Chem. *280*, 39423–39435.

Thilo, F., Liu, Y., Schulz, N., Gergs, U., Neumann, J., Loddenkemper, C., Gollasch, M., and Tepel, M. (2010). Increased transient receptor potential vanilloid type 1 (TRPV1) channel expression in hypertrophic heart. Biochem. Biophys. Res. Commun. *401*, 98–103.

Tominaga, M. (2007). Nociception and TRP channels. Handb Exp Pharmacol 489–505.

Tominaga, M., and Tominaga, T. (2005). Structure and function of TRPV1. Pflugers Arch. *451*, 143–150.

Tominaga, M., Caterina, M.J., Malmberg, A.B., Rosen, T.A., Gilbert, H., Skinner, K., Raumann, B.E., Basbaum, A.I., and Julius, D. (1998). The cloned capsaicin receptor integrates multiple pain-producing stimuli. Neuron *21*, 531–543.

Tominaga, M., Numazaki, M., Iida, T., Moriyama, T., Togashi, K., Higashi, T., Murayama, N., and Tominaga, T. (2004). Regulation mechanisms of vanilloid receptors. Novartis Found. Symp. *261*, 4–12–discussion12–8–47–54.

Tominaga, M., Wada, M., and Masu, M. (2001). Potentiation of capsaicin receptor activity by metabotropic ATP receptors as a possible mechanism for ATP-evoked pain and hyperalgesia. Proc. Natl. Acad. Sci. U.S.a. *98*, 6951–6956.

Towers, S., Princivalle, A., Billinton, A., Edmunds, M., Bettler, B., Urban, L., Castro-Lopes, J., and Bowery, N.G. (2000). GABAB receptor protein and mRNA distribution in rat spinal cord and dorsal root ganglia. Eur. J. Neurosci. *12*, 3201–3210.

Tóth, A., Boczán, J., Kedei, N., Lizanecz, E., Bagi, Z., Papp, Z., Edes, I., Csiba, L., and Blumberg, P.M. (2005). Expression and distribution of vanilloid receptor 1 (TRPV1) in the adult rat brain. Brain Res. Mol. Brain Res. *135*, 162–168.

Trevisani, M., Smart, D., Gunthorpe, M.J., Tognetto, M., Barbieri, M., Campi, B., Amadesi, S., Gray, J., Jerman, J.C., Brough, S.J., et al. (2002). Ethanol elicits and potentiates nociceptor responses via the vanilloid receptor-1. Nat. Neurosci. *5*, 546–551.

Tsunoda, S., Sierralta, J., Sun, Y., Bodner, R., Suzuki, E., Becker, A., Socolich, M., and Zuker, C.S. (1997). A multivalent PDZ-domain protein assembles signalling complexes in a G-protein-coupled cascade. Nature *388*, 243–249.

Tusher, V.G., Tibshirani, R., and Chu, G. (2001). Significance analysis of microarrays applied to the ionizing radiation response. Proc. Natl. Acad. Sci. U.S.a. *98*, 5116–5121.

Ufret-Vincenty, C.A., Klein, R.M., Hua, L., Angueyra, J., and Gordon, S.E. (2011). Localization of the

PIP2 sensor of TRPV1 ion channels. J. Biol. Chem. *286*, 9688–9698.

van de Graaf, S.F.J., Hoenderop, J.G.J., and Bindels, R.J.M. (2006). Regulation of TRPV5 and TRPV6 by associated proteins. Am. J. Physiol. Renal Physiol. *290*, F1295–F1302.

van Huizen, R., Miller, K., Chen, D.M., Li, Y., Lai, Z.C., Raab, R.W., Stark, W.S., Shortridge, R.D., and Li, M. (1998). Two distantly positioned PDZ domains mediate multivalent INAD-phospholipase C interactions essential for G protein-coupled signaling. Embo J. *17*, 2285–2297.

Varoqui, H., Schäfer, M.K.-H., Zhu, H., Weihe, E., and Erickson, J.D. (2001). Identification of the differentiation-associated Na+/PI transporter as a novel vesicular glutamate transporter expressed in a distinct set of glutamatergic synapses. J. Neurosci. *22*, 142–155.

Vay, L., Gu, C., and McNaughton, P.A. (2012). The thermo-TRP ion channel family: properties and therapeutic implications. Br. J. Pharmacol. *165*, 787–801.

Vellani, V., Mapplebeck, S., Moriondo, A., Davis, J.B., and McNaughton, P.A. (2001). Protein kinase C activation potentiates gating of the vanilloid receptor VR1 by capsaicin, protons, heat and anandamide. J. Physiol. (Lond.) *534*, 813–825.

Vennekens, R., Hoenderop, J.G., Prenen, J., Stuiver, M., Willems, P.H., Droogmans, G., Nilius, B., and Bindels, R.J. (2000). Permeation and gating properties of the novel epithelial Ca(2+) channel. J. Biol. Chem. *275*, 3963–3969.

Vennekens, R., Prenen, J., Hoenderop, J.G., Bindels, R.J., Droogmans, G., and Nilius, B. (2001). Pore properties and ionic block of the rabbit epithelial calcium channel expressed in HEK 293 cells. J. Physiol. (Lond.) *530*, 183–191.

Vetter, I., Wyse, B.D., Monteith, G.R., Roberts-Thomson, S.J., and Cabot, P.J. (2006). The mu opioid agonist morphine modulates potentiation of capsaicin-evoked TRPV1 responses through a cyclic AMP-dependent protein kinase A pathway. Mol Pain *2*, 22.

Villarreal, C.F., Funez, M.I., Figueiredo, F., Cunha, F.Q., Parada, C.A., and Ferreira, S.H. (2009). Acute and persistent nociceptive paw sensitisation in mice: the involvement of distinct signalling pathways. Life Sci. *85*, 822–829.

Vlachová, V., Teisinger, J., Susánková, K., Lyfenko, A., Ettrich, R., and Vyklický, L. (2003). Functional role of C-terminal cytoplasmic tail of rat vanilloid receptor 1. J. Neurosci. *23*, 1340–1350.

Voets, T., Talavera, K., Owsianik, G., and Nilius, B. (2005). Sensing with TRP channels. Nat. Chem. Biol. *1*, 85–92.

Vulcu, S.D., Liewald, J.F., Gillen, C., Rupp, J., and Nawrath, H. (2004). Proton conductance of human transient receptor potential-vanilloid type-1 expressed in oocytes of Xenopus laevis and in Chinese hamster ovary cells. Neuroscience *125*, 861–866.

Wahl, P., Foged, C., Tullin, S., and Thomsen, C. (2001). Iodo-resiniferatoxin, a new potent vanilloid receptor antagonist. Mol. Pharmacol. *59*, 9–15.

Walker, R.G., Willingham, A.T., and Zuker, C.S. (2000). A Drosophila mechanosensory transduction channel. Science *287*, 2229–2234.

Wallén-Mackenzie, A., Wootz, H., and Englund, H. (2010). Genetic inactivation of the vesicular glutamate transporter 2 (VGLUT2) in the mouse: what have we learnt about functional glutamatergic neurotransmission? Ups. J. Med. Sci. *115*, 11–20.

Wang, S., Dai, Y., Fukuoka, T., Yamanaka, H., Kobayashi, K., Obata, K., Cui, X., Tominaga, M., and Noguchi, K. (2008). Phospholipase C and protein kinase A mediate bradykinin sensitization of TRPA1: a molecular mechanism of inflammatory pain. Brain *131*, 1241–1251.

Ward, S.M., Bayguinov, J., Won, K.-J., Grundy, D., and Berthoud, H.R. (2003). Distribution of the vanilloid receptor (VR1) in the gastrointestinal tract. J. Comp. Neurol. *465*, 121–135.

Warming, S., Costantino, N., Court, D.L., Jenkins, N.A., and Copeland, N.G. (2005). Simple and highly efficient BAC recombineering using galK selection. Nucleic Acids Res. *33*, e36.

Waxman, S.G., Cummins, T.R., Dib-Hajj, S.D., and Black, J.A. (2000). Voltage-gated sodium channels and the molecular pathogenesis of pain: a review. J Rehabil Res Dev *37*, 517–528.

Wei, F., Dubner, R., Zou, S., Ren, K., Bai, G., Wei, D., and Guo, W. (2010). Molecular depletion of descending serotonin unmasks its novel facilitatory role in the development of persistent pain. J. Neurosci. *30*, 8624–8636.

Wells, C.A., Betke, K.M., Lindsley, C.W., and Hamm, H.E. (2012). Label-free detection of G protein-SNARE interactions and screening for small molecule modulators. ACS Chem Neurosci *3*, 69–78.

Wes, P.D., Xu, X.Z., Li, H.S., Chien, F., Doberstein, S.K., and Montell, C. (1999). Termination of phototransduction requires binding of the NINAC myosin III and the PDZ protein INAD. Nat. Neurosci. *2*, 447–453.

White, J.P.M., Urban, L., and Nagy, I. (2011). TRPV1 function in health and disease. Curr Pharm Biotechnol *12*, 130–144.

Whitehead, R.A., Puil, E., Ries, C.R., Schwarz, S.K.W., Wall, R.A., Cooke, J.E., Putrenko, I., Sallam, N.A., and MacLeod, B.A. (2012). GABA(B) receptor-mediated selective peripheral analgesia by the non-proteinogenic amino acid, isovaline. Neuroscience *213*, 154–160.

Wilson, N.R., Kang, J., Hueske, E.V., Leung, T., Varoqui, H., Murnick, J.G., Erickson, J.D., and Liu, G. (2005). Presynaptic regulation of quantal size by the vesicular glutamate transporter VGLUT1. J. Neurosci. *25*, 6221–6234.

Wojcik, S.M., Rhee, J.S., Herzog, E., Sigler, A., Jahn, R., Takamori, S., Brose, N., and Rosenmund, C. (2004). An essential role for vesicular glutamate transporter 1 (VGLUT1) in postnatal development and control of quantal size. Proc. Natl. Acad. Sci. U.S.a. *101*, 7158–7163.

Wong, J.W.H., and Cagney, G. (2010). An overview of label-free quantitation methods in proteomics by mass spectrometry. Methods Mol. Biol. *604*, 273–283.

Woolf, C.J., and Ma, Q. (2007). Nociceptors--noxious stimulus detectors. Neuron *55*, 353–364.

Woolf, C.J. (2011). Central sensitization: implications for the diagnosis and treatment of pain. Pain *152*, S2–S15.

Wu, Z.-Z., Chen, S.-R., and Pan, H.-L. (2004). Differential sensitivity of N- and P/Q-type Ca2+ channel currents to a mu opioid in isolectin B4-positive and -negative dorsal root ganglion neurons. J. Pharmacol. Exp. Ther. *311*, 939–947.

Xu, H., Blair, N.T., and Clapham, D.E. (2005). Camphor activates and strongly desensitizes the transient receptor potential vanilloid subtype 1 channel in a vanilloid-independent mechanism. J. Neurosci. *25*, 8924–8937.

Xu, X.Z., Chien, F., Butler, A., Salkoff, L., and Montell, C. (2000). TRPgamma, a drosophila TRP-related subunit, forms a regulated cation channel with TRPL. Neuron *26*, 647–657.

Xu, X.Z., Choudhury, A., Li, X., and Montell, C. (1998). Coordination of an array of signaling proteins through homo- and heteromeric interactions between PDZ domains and target proteins. J. Cell Biol. *142*, 545–555.

Yang, B.H., Piao, Z.G., Kim, Y.-B., Lee, C.-H., Lee, J.K., Park, K., Kim, J.S., and Oh, S.B. (2003).

Activation of vanilloid receptor 1 (VR1) by eugenol. J. Dent. Res. *82*, 781–785.

Yang, K., Kumamoto, E., Furue, H., and Yoshimura, M. (1998). Capsaicin facilitates excitatory but not inhibitory synaptic transmission in substantia gelatinosa of the rat spinal cord. Neurosci. Lett. *255*, 135–138.

Yoon, E.-J., Gerachshenko, T., Spiegelberg, B.D., Alford, S., and Hamm, H.E. (2007). Gbetagamma interferes with Ca2+-dependent binding of synaptotagmin to the soluble N-ethylmaleimide-sensitive factor attachment protein receptor (SNARE) complex. Mol. Pharmacol. *72*, 1210–1219.

Yue, L., Peng, J.B., Hediger, M.A., and Clapham, D.E. (2001). CaT1 manifests the pore properties of the calcium-release-activated calcium channel. Nature *410*, 705–709.

Zander, J.-F., Münster-Wandowski, A., Brunk, I., Pahner, I., Gómez-Lira, G., Heinemann, U., Gutiérrez, R., Laube, G., and Ahnert-Hilger, G. (2010). Synaptic and vesicular coexistence of VGLUT and VGAT in selected excitatory and inhibitory synapses. J. Neurosci. *30*, 7634–7645.

Zeilhofer, H.U., Möhler, H., and Di Lio, A. (2009). GABAergic analgesia: new insights from mutant mice and subtype-selective agonists. Trends Pharmacol. Sci. *30*, 397–402.

Zhang, X., Huang, J., and McNaughton, P.A. (2005). NGF rapidly increases membrane expression of TRPV1 heat-gated ion channels. Embo J. *24*, 4211–4223.

Zhang, X., Li, L., and McNaughton, P.A. (2008). Proinflammatory mediators modulate the heat-activated ion channel TRPV1 via the scaffolding protein AKAP79/150. Neuron *59*, 450–461.

Zhang, X., Mak, S., Li, L., Parra, A., Denlinger, B., Belmonte, C., and McNaughton, P.A. (2012). Direct inhibition of the cold-activated TRPM8 ion channel by Gαq. Nat. Cell Biol. *14*, 851–858.

Zhou, X.-L., Batiza, A.F., Loukin, S.H., Palmer, C.P., Kung, C., and Saimi, Y. (2003). The transient receptor potential channel on the yeast vacuole is mechanosensitive. Proc. Natl. Acad. Sci. U.S.a. *100*, 7105–7110.

Zolles, G., Wenzel, D., Bildl, W., Schulte, U., Hofmann, A., Müller, C.S., Thumfart, J.-O., Vlachos, A., Deller, T., Pfeifer, A., et al. (2009). Association with the auxiliary subunit PEX5R/Trip8b controls responsiveness of HCN channels to cAMP and adrenergic stimulation. Neuron *62*, 814–825.

Zygmunt, P.M., Petersson, J., Andersson, D.A., Chuang, H., Sørgård, M., Di Marzo, V., Julius, D., and Högestätt, E.D. (1999). Vanilloid receptors on sensory nerves mediate the vasodilator action of anandamide. Nature *400*, 452–457.

Zylka, M.J., Rice, F.L., and Anderson, D.J. (2005). Topographically distinct epidermal nociceptive circuits revealed by axonal tracers targeted to Mrgprd. Neuron *45*, 17–25.

8. Acknowledgements

Scientific Acknowledgements

I would like to thank my group leader Prof. Dr. Jan Siemens for giving me the opportunity to work on this project, for his advices, support, engagement and supervision throughout the years.

I also thank all the people that I have been working with: Mirko Moroni, Jana Rossius, Kun Song, Henning Kuich and Sonja Winkler.

Special thanks go to Jana Rossius who generated the BAC transgenic SF-TRPV1 mice and to Dr. Mirko Moroni who did the calcium imaging for the $GABA_B$ project. Their data are included in this thesis for completeness.

Furthermore, I would like to thank colleagues and collaborators of other labs for technical support and helpful discussions: Dr. Marieluise Kirchner (group Prof. Matthias Selbach, MDC) for the mass spectrometry, Dr. Christiane Wetzel (group Prof. Gary Lewin, MDC) for help with mouse behavioral work and Dr. Johannes Friedrich Zander (group Prof. Gudrun Ahnert-Hilger, Charité) for teaching me glutamate uptake assays.

Finally, I would like to thank my university supervisors Prof. Dr. Gary Lewin and Prof. Dr. Constanze Scharff for the official supervision of my PhD project.

Personal Acknowledgements

Besonders danke ich meinen Eltern, dass sie mir durch ihre persönliche und finanzielle Unterstützung diese Doktorarbeit möglich gemacht haben.

Ich danke den vielen lieben Doktoranden und Postdocs am MDC, ganz besonders Philip und Florian (AG Rathjen) für die lustigen Kaffeepausen und beer sessions, und Stephen Marino (AG Daumke) für seine wertvollen biochemischen Weisheiten.

Der größte Dank geht an Matteo für die letzten wunderbaren Jahre und für seine Unterstützung während der Doktorarbeit.

9. Erklärung

Hiermit versichere ich, Christina Hanack, dass ich die vorgelegte Dissertation mit dem Titel "Proteomics reveal insights into TRPV1 function " selbstständig und ohne unerlaubte Hilfe angefertigt habe.

Ort, Datum

10. Appendix

10.1. Control stainings

Immunolabeling was performed with only the secondary antibodies to confirm labeling specificity of the primary antibodies.

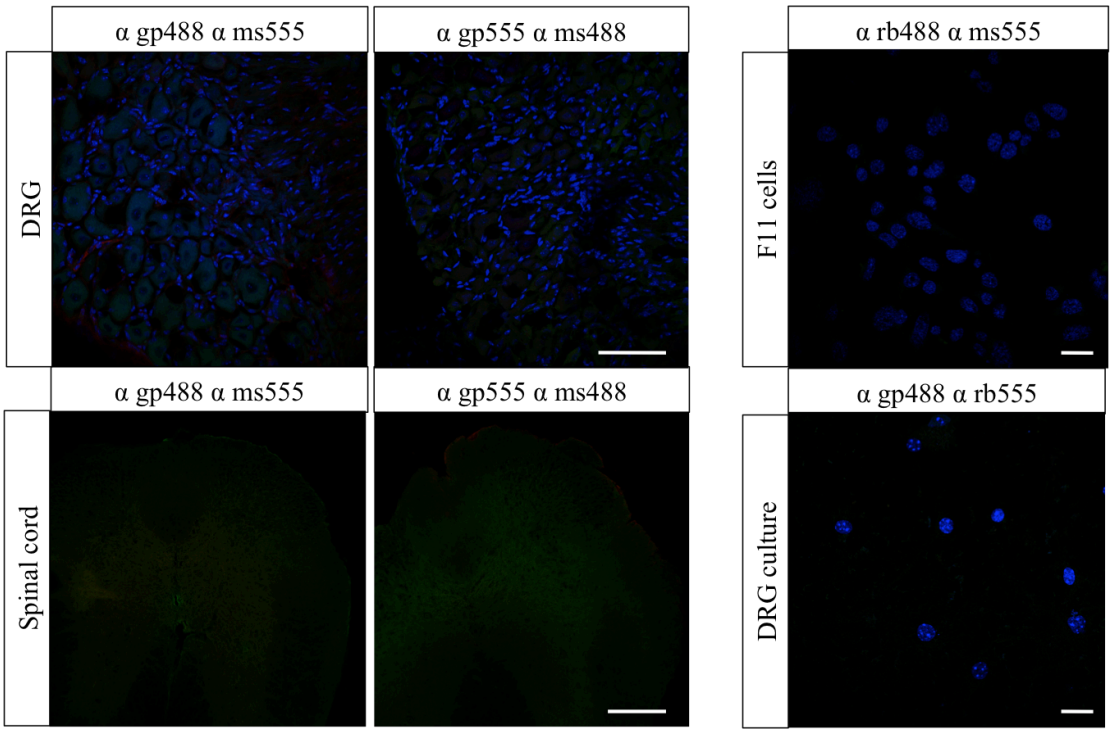

Figure 40: Control staining experiments to confirm labeling specificity

Immunohistochemistry of mouse DRG and spinal cord sections (left) as well as cultured DRG and transfected F11 cells (right). Labeling was performed using secondary antibodies against the indicated species. Left scale bar = 50 µM, right scale bar = 10 µM

10.2. Mass spectrometry results of TRPV1 purifications from the DRG and sciatic nerve

The tables list identified proteins with log2 ratios > 2 of a representative mass spectrometry run.

Protein Name	DRG Ratio Flag/wt control
TRPV1	14.06572
Erlin-2	7.97359
60S ribosomal protein L4	7.270174
Dolichyl-diphosphooligosaccharide--protein glycosyltransferase 63 kDa subunit	7.174485
60S ribosomal protein L5	6.876945
Bifunctional aminoacyl-tRNA synthetase	6.828121
Isoleucine--tRNA ligase	6.540192
60S ribosomal protein L13	6.452223
Dolichyl-diphosphooligosaccharide--protein glycosyltransferase 48 kDa subunit	6.421251
Lysyl hydroxylase 3	6.27738
60S ribosomal protein L13a	6.271766
Basic transcription factor 3-like 4	6.193616
Uncharacterized protein KIAA0090	5.991731
Sodium channel voltage-gated type VII alpha	5.887917
Calcium/calmodulin-dependent protein kinase type II subunit alpha	5.872499
Elongation factor p18	5.870461
Gamma-aminobutyric acid type B receptor subunit 1	5.84519
Thioredoxin 1	5.770335
SEC22 vesicle-trafficking protein homolog B	5.745583
TRPV2	5.723862
40S ribosomal protein S15	5.589052
60S ribosomal protein L28	5.57913
60S ribosomal protein L27	5.512504
1-phosphatidylinositol-4,5-bisphosphate phosphodiesterase delta-4	5.48753
40S ribosomal protein S18	5.479719
Dolichyl-diphosphooligosaccharide--protein glycosyltransferase 67 kDa subunit	5.479277
RAS-related C3 botulinum substrate 1	5.403835
Decaprenyl pyrophosphate synthase subunit 2	5.391245
Gamma-glutamyltransferase 7	5.385009
Dihydrolipoamide acetyltransferase component of pyruvate dehydrogenase complex	5.36774
Ras-related protein Rab-2A	5.337629
Cathepsin D, isoform CRA_a	5.29218
MCG18601	5.287918
Protein S100-A13	5.277575
Calnexin-T	5.216681
ELAV (Embryonic lethal, abnormal vision, Drosophila)-like 2 (Hu antigen B)	5.198704
Fragile X mental retardation syndrome-related protein 1	5.198622
Calcium/calmodulin-dependent protein kinase type II subunit gamma	5.162958

60S ribosomal protein L34	5.119701
Leucine-rich repeat-containing protein 59	5.10457
Intracellular hyaluronan-binding protein 4	5.102943
Dihydrolipoamide dehydrogenase	5.074197
AU-specific RNA-binding enoyl-CoA hydratase	5.054584
60S ribosomal protein L6	5.029243
Zinc finger ZZ-type and EF-hand domain-containing protein 1	5.016453
Calmodulin-dependent calcineurin A subunit alpha isoform	4.96145
Plasma membrane Ca++ transporting ATPase 4 splice variant b	4.905636
Cellular glutathione peroxidase	4.872281
Aminoacyl tRNA synthase complex-interacting multifunctional protein 2	4.857098
Protein S100-A11	4.840776
ATP synthase subunit epsilon, mitochondrial	4.840765
Serine (Or cysteine) peptidase inhibitor, clade B, member 6a, isoform CRA_a	4.834977
Protein phosphatase 1 regulatory subunit 11	4.808995
2-arachidonoylglycerol hydrolase	4.798229
Protein sel-1 homolog 1;Suppressor of lin-12-like protein 1	4.790906
60S ribosomal protein L19	4.775677
Tripeptidyl aminopeptidase	4.766551
BM88 antigen	4.756827
Membrane protein, palmitoylated 6 (MAGUK p55 subfamily member 6), isoform CRA_b;Mpp6 protein	4.755085
Complex III subunit 8	4.749458
63 kDa membrane protein	4.710586
Endoplasmic reticulum lipid raft-associated protein 1;Erlin-1;Protein KE04 homolog;Stomatin-prohibitin-flotillin-HflC/K domain-containing protein 1	4.69025
3-ketoacyl-CoA thiolase, mitochondrial	4.671722
60S ribosomal protein L21	4.656963
Myelin expression factor 2	4.643327
Beta-1 metal-binding globulin	4.622141
ATP-dependent RNA helicase eIF4A-2	4.603557
60S ribosomal protein L26	4.490191
Membrane magnesium transporter 1	4.483568
38 kDa FK506-binding protein	4.477815
60S ribosomal protein L8	4.465585
Sodium/potassium-dependent ATPase subunit beta-3	4.4577
Protein OS-9	4.45486
DEAD box protein 46	4.453121
UPF0670 protein C8orf55 homolog	4.42718
60S ribosomal protein L35	4.408187
Basolateral Na-K-Cl symporter	4.397059
Ras-related protein Rab-18	4.339368
Probable saccharopine dehydrogenase	4.337026
Cytochrome b5 outer mitochondrial membrane isoform	4.332969
Ufm1-specific protease 2	4.322038
C-myc binding protein	4.305542
MCG140066	4.284773
DnaJ homolog subfamily A member 1	4.268282

Creatine kinase, muscle	4.259291
33 kDa VAMP-associated protein	4.256092
Macropain epsilon chain	4.246581
Alpha-coat protein;Coatomer subunit alpha	4.245555
40S ribosomal protein S21	4.230611
Histone H1.3	4.219267
EH domain-containing protein 2	4.152058
Complement component 1, q subcomponent binding protein	4.145009
Phosphatidate cytidylyltransferase	4.138003
Transmembrane emp24 domain trafficking protein 2	4.131705
Electron transferring flavoprotein, alpha polypeptide	4.130466
Elastase-2;Leukocyte elastase	4.129835
Endonuclease/exonuclease/phosphatase family domain-containing protein 1	4.12886
60S ribosomal protein L10a	4.114745
Alpha-1,3-mannosyltransferase ALG2	4.10866
47 kDa heat shock protein	4.106911
RNA binding motif protein 3	4.105685
Thioredoxin domain containing 13	4.079258
UDP--Glc:glycoprotein glucosyltransferase	4.073082
Myosin heavy chain 3	4.060732
Heme oxygenase 2	4.042922
Novel protein similar to human ubiquinol-cytochrome C reductase complex 7.2 kDa protein UQCR10	4.041927
Anoctamin-10	4.012815
Elongation factor 2	4.008687
40S ribosomal protein S3a	3.999888
Anion exchange protein 1	3.961849
Ribosomal protein S5	3.937901
Tight junction protein ZO-2	3.929485
Neural cell adhesion molecule L1	3.90858
Calcium/calmodulin-dependent protein kinase II, beta	3.896931
Aspartate--tRNA ligase	3.891847
Ecto-ADP-ribosyltransferase 3	3.88115
Cell adhesion molecule 4	3.875323
Nucleoside diphosphate kinase B	3.871355
RNA binding motif protein, X chromosome retrogene	3.870526
Arginyl-tRNA synthetase, cytoplasmic	3.845374
Rho-guanine nucleotide exchange factor	3.824953
Proteasome (Prosome, macropain) 26S subunit, non-ATPase, 7	3.810899
Voltage-dependent calcium channel subunit alpha-2/delta-1	3.809999
Fibronectin receptor subunit beta;Integrin beta-1	3.809595
Tropomyosin alpha-4 chain	3.806823
17-beta-hydroxysteroid dehydrogenase 12	3.803135
DEAD (Asp-Glu-Ala-Asp) box polypeptide 17, isoform CRA_a	3.776843
Tetratricopeptide repeat protein 35	3.771374
Small nuclear ribonucleoprotein F	3.746529
Eukaryotic translation initiation factor 3 subunit 8	3.712837
Phenylalanyl-tRNA synthetase alpha chain	3.697526
Copine III	3.692136

Branched-chain acyl-CoA oxidase	3.688754
26S protease regulatory subunit 4	3.686583
26S proteasome non-ATPase regulatory subunit 1	3.673881
Lin-7 homolog C (C. elegans)	3.628582
Dehydrogenase/reductase (SDR family) member 8, isoform CRA_b	3.599379
Solute carrier family 27 (Fatty acid transporter), member 4	3.536387
Histone H2A	3.506866
60S ribosomal protein L10	3.505534
CD44 antigen	3.471048
Glycosyltransferase 25 family member 1	3.464647
Cellular thyroid hormone-binding protein	3.449514
40S ribosomal protein S23	3.444857
60S ribosomal protein L14	3.441199
DEAH box protein 15	3.430175
Microsomal signal peptidase 25 kDa subunit	3.422061
Malectin	3.418487
Beta-2-microglobulin	3.409155
26S proteasome non-ATPase regulatory subunit 3	3.406635
Ras-related protein Rab-11B	3.401883
Protein S100-A6	3.387655
60S ribosomal protein L27a	3.357033
Molecule associated with JAK3 N-terminus	3.349319
40S ribosomal protein S19	3.34675
60S ribosomal protein L24	3.340546
Peripherin	3.318243
CDGSH iron sulfur domain-containing protein 3, mitochondrial	3.311332
Loss of heterozygosity 11 chromosomal region 2 gene A protein homolog	3.299009
DnaJ homolog subfamily A member 2	3.297006
Aminoacyl tRNA synthase complex-interacting multifunctional protein 1	3.280271
Phosphatidylinositide phosphatase SAC1	3.279285
PP2A subunit A isoform PR65-alpha	3.278976
100 kDa coactivator	3.277481
Aldehyde dehydrogenase family 18 member A1	3.271659
Coiled-coil-helix-coiled-coil-helix domain-containing protein 3, mitochondrial	3.271394
Calgranulin-B	3.26534
Eukaryotic translation initiation factor 1A, Y-linked	3.265028
Calcium/calmodulin-dependent protein kinase type II subunit delta	3.25691
hnRNP associated with lethal yellow protein	3.232787
Syntaxin-7	3.220203
Receptor expression-enhancing protein 1	3.198452
Membrane-associated progesterone receptor component 2	3.181985
Transmembrane emp24 protein transport domain containing 9, isoform CRA_b	3.1727
40S ribosomal protein S27	3.171839
Heterogeneous nuclear ribonucleoprotein A/B	3.152125
Tax1 (Human T-cell leukemia virus type I) binding protein 3	3.13848
Coatomer subunit beta	3.135547
Diaphorase-1	3.126965

Apoptosis-inducing factor, mitochondrion-associated 1	3.121419
40S ribosomal protein S28	3.114708
Atlastin-3	3.10297
Thioredoxin domain containing 4 (Endoplasmic reticulum)	3.088939
Histone H2B type 1-F/J/L	3.085897
Activity-dependent neuroprotective protein	3.031467
Diacylglycerol kinase epsilon	3.031141
C-protein, skeletal muscle fast isoform	3.028589
Butyrate-induced protein 1	3.019914
Endothelial differentiation-related factor 1	3.010689
60S ribosomal protein L18a	3.008582
26S protease regulatory subunit 10B	3.008298
Putative uncharacterized protein	3.00524
Transmembrane protein 85	3.003022
A10;D-3-phosphoglycerate dehydrogenase	2.990187
Annexin A7	2.982847
Ras-related protein Rab-35	2.980297
Actin-binding protein 280	2.966967
26S protease regulatory subunit 6B	2.960881
Cathepsin B	2.945405
Small nuclear ribonucleoprotein E	2.934918
Fox-1 homolog B	2.917435
Basal cell adhesion molecule	2.91532
Glutathione peroxidase	2.91397
Neural visinin-like protein 3	2.901918
Glyoxalase I	2.901886
Alpha glucosidase 2 alpha neutral subunit	2.89594
Integral membrane protein 2B	2.888674
Putative uncharacterized protein Nucb1	2.866593
NAC-alpha domain-containing protein 1	2.846331
Carnitine O-palmitoyltransferase 1, liver isoform	2.831146
Prolactin regulatory element binding, isoform CRA_c	2.822372
Solute carrier family 25 (Mitochondrial carrier, citrate transporter), member 1	2.815476
60S ribosomal protein L23a	2.800808
60S ribosomal protein L7	2.780524
Cytochrome c oxidase subunit 7A1, mitochondrial	2.775616
VAMP-associated protein 33b	2.774768
Mammalian ependymin-related protein 1	2.766402
Stomatin-like protein 2	2.75227
Ig kappa chain V-V region K2	2.751661
Reticulon 1	2.749731
Serine/threonine kinase receptor associated protein	2.739051
Calreticulin	2.717033
EH-domain containing 4	2.708728
Transketolase	2.703695
60S ribosomal protein L17	2.703068
Adapter-related protein complex 3 mu-1 subunit	2.701445
Endonuclease domain-containing 1 protein	2.688651
60S ribosomal protein L32	2.687492

39S ribosomal protein L14, mitochondrial	2.671333
Calcium pump 2	2.654795
Myosin-Ib	2.6523
A kinase (PRKA) anchor protein (Gravin) 12	2.642762
Farnesyl-diphosphate farnesyltransferase	2.637617
Adapter-related protein complex 3 mu-2 subunit	2.633422
Dodecenoyl-Coenzyme A delta isomerase (3,2 trans-enoyl-Coenyme A isomerase)	2.613855
40S ribosomal protein S27-like	2.583855
Hyperpolarization-activated cation channel	2.569413
Microfibril-associated glycoprotein 4	2.564356
BAG family molecular chaperone regulator 2	2.563978
Transmembrane protein 111	2.55949
Pyruvate carboxylase, mitochondrial	2.552222
Histone H1	2.54681
Calpain-5	2.543916
Macropain subunit C5	2.520885
Dimethylargininase-1;N(G),N(G)-dimethylarginine dimethylaminohydrolase 1	2.517762
Ras-related protein Rab-7a	2.51529
Atlastin-1	2.515101
Protein kinase C, alpha	2.507678
Developmentally-regulated GTP-binding protein 1	2.484977
LYR motif-containing protein 4	2.474811
B6dom1 antigen	2.469888
MCG3543, isoform CRA_a	2.460191
40S ribosomal protein S14	2.441137
Microsomal glutathione S-transferase 1	2.429928
Hepatoma-derived growth factor	2.406019
Diazepam binding inhibitor, splice form 1b;MCG17804, isoform CRA_b	2.400009
Alpha-NAC, muscle-specific form	2.38902
Alpha-actinin cytoskeletal isoform	2.382214
Coiled-coil domain-containing protein 109A	2.381525
Low molecular mass protein 3	2.368614
Calcium-activated neutral proteinase small subunit	2.359337
Membrane-organizing extension spike protein	2.315287
Membrane glycoprotein SFA-1	2.312176
Eukaryotic translation initiation factor 2, subunit 3, structural gene X-linked	2.30886
Autophagy-related protein LC3 A	2.308138
Conventional kinesin heavy chain	2.307296
Synaptic glycoprotein SC2	2.30477
Guanine nucleotide binding protein (G protein), alpha inhibiting 1	2.303185
Melanoma inhibitory activity protein 3	2.295516
52 kDa ribonucleoprotein autoantigen Ro/SS-A	2.294472
ATP synthase subunit f, mitochondrial	2.280929
Lens epithelium-derived growth factor	2.275519
TRM112-like protein	2.266568
Small nuclear ribonucleoprotein Sm D1	2.237221
Cytosol aminopeptidase	2.22935

Apolipoprotein J	2.222962
[Acyl-carrier-protein] S-acetyltransferase	2.203518
Cold shock domain-containing protein E1	2.201385
Low molecular mass protein 19	2.186768
Influenza virus NS1A-binding protein homolog	2.169805
Glycophorin-C	2.169717
Heterogeneous nuclear ribonucleoprotein U	2.164323
H-2 class I histocompatibility antigen, D-B alpha chain	2.13753
FXYD domain-containing ion transport regulator 2	2.137086
140 kDa Ca(2+)-binding protein	2.135396
NADH dehydrogenase [ubiquinone] iron-sulfur protein 5	2.133685
Transmembrane protein 33	2.133433
Myeloperoxidase	2.130334
Eukaryotic translation initiation factor 2A	2.11955
Hsc70-interacting protein;	2.118846
Procollagen C-endopeptidase enhancer protein	2.113965
Damage-specific DNA-binding protein 1	2.112316
MCG13498, isoform CRA_d;Mitochondrial carrier homolog 2 (C. elegans)	2.10564
Centrosomin	2.104515
Apolipoprotein A4	2.100176
Putative uncharacterized protein S100a4	2.099201
Cleft lip and palate transmembrane protein 1 homolog	2.088917
Integrin beta-4	2.087397
Tight junction protein 1	2.084974
Novel protein (2810405J04Rik)	2.07044
OCIA domain-containing protein 1	2.070423
Dipeptidyl aminopeptidase-like protein 6	2.053332
Protein RUFY3;Rap2-interacting protein x	2.048285
BAG family molecular chaperone regulator 3	2.035685
Nerve growth factor receptor (TNFR superfamily, member 16)	2.033313
Microtubule-associated protein 4	2.023058
Membrane glycoprotein gp42	2.007681
Endoplasmic reticulum resident protein 46	2.007631
Eukaryotic translation elongation factor 1 gamma	2.006362
Novel protein (2310003F16Rik)	2.005737
Growth factor receptor bound protein 2	2.001648
Oxysterol-binding protein	2.001548

Tab. 3: Mass spectrometry results of a representative run of TRPV1 purifications from the DRG. Shown are identified proteins with a log2 ratio (ratio Flag/wt control) > 2

Protein Name	Nerve Ratio Flag/wt control
TRPV1	10.3298022
CD9 antigen	6.417505582
Asp (Abnormal spindle)-like, microcephaly associated (Drosophila	6.30374368
Tripeptidyl aminopeptidase	3.935315132
Importin subunit beta-1	3.862293561
Ciliary neurotrophic factor	3.669302622
Glycerol-3-phosphate dehydrogenase, mitochondrial	3.540314356
ATP-grasp domain-containing protein 1	3.434890429

Dimethylargininase-1	3.403739929
Keratan sulfate proteoglycan lumican	3.281757037
UPF0493 protein KIAA1632	3.216431936
Tax interaction protein 1	3.101343473
Flavoprotein subunit of complex II	3.097756386
Microtubule-associated protein 2	2.886883443
ATPase inhibitor, mitochondrial	2.847003301
Sodium/potassium-dependent ATPase subunit beta-3	2.807219505
Alpha-tubulin 1	2.806165059
Guanine nucleotide-binding protein alpha-q	2.802647909
26 kDa cell surface protein TAPA-1	2.59375
3-ketoacyl-CoA thiolase, mitochondrial	2.582313855
[Acyl-carrier-protein] S-acetyltransferase	2.582027753
Guanine nucleotide-binding protein G(o) subunit alpha	2.573239962
Mimecan	2.521315257
Tropomodulin-2	2.584675221
Alpha T-catenin	2.512056669
Tetraspanin-9	2.511130015
Cytoplasmic dynein 1 heavy chain 1	2.503421741
Protein phosphatase 1C catalytic subunit	2.502336502
Thy-1 membrane glycoprotein	2.456354777
Citrate synthase, mitochondrial	2.43272082
Complex I-30kD	2.416609128
Dynactin subunit 1	2.416793232
Peripherin	2.405795097
Synaptic vesicle membrane protein VAT-1 homolog	2.386101723
CapZ alpha-2	2.326163292
Acidic-type mitochondrial creatine kinase	2.325819333
EH domain-containing protein 2	2.293447177
Vesicular glutamate transporter 2	2.274166044
Medium-chain specific acyl-CoA dehydrogenase, mitochondrial	2.269789696
Gamma-synuclein	2.240861893
Ras-related protein Rab-5C	2.231398582
Cytosolic NADP-isocitrate dehydrogenase	2.196002324
Myelin P2 protein	2.178702672
Eukaryotic translation initiation factor 3 subunit 2	2.159476598
ATP synthase subunit delta, mitochondrial	2.147540092
Ecto-ADP-ribosyltransferase 3	2.128956477
Pyruvate carboxylase, mitochondrial	2.070031484
Complex I subunit B13;Complex I-13kD-B	2.065882683
Long-chain acyl-CoA synthetase 1	2.060798963
3-methylcrotonyl-CoA carboxylase 1	2.049775124
Actin-related protein 1B	2.024033864
Neural cell adhesion molecule 1	2.022345722
Uncharacterized protein C3orf24 homolog	2.022154808
NADH dehydrogenase [ubiquinone] 1 beta subcomplex subunit 4	2.022082965

Tab. 4: Mass spectrometry results of a representative run of TRPV1 purifications from the sciatic nerve. Shown are identified proteins with a log2 ratio (ratio Flag/wt control) > 2